# A Lean Approach to System Design and the Development of a Multi-Stage Dredging System for Commercial Applications

by

Caleb Brian Dyck

A thesis submitted in partial fulfillment of the requirements for the degree of

Master of Science

in

Engineering Management

Department of Mechanical Engineering
University of Alberta

# Abstract

The development of any technology requires that a balance must be struck between meeting requirements and dealing with constraints. This thesis presents a lean approach to the initial design and development of a complex, multi-physics system for industrial implementation, undertaken due to constraints on resources and time, to manage economic, human, and technical risks associated with the project's requirements. Through this method, we identify and explain the major effects on the system which should be investigated in further study to reduce or retire risks in implementation.

A case study and a descriptive system design are presented for a novel dredge technology that utilizes a cable-driven propulsion system to position a dredge head along a predetermined path. To date, this dredge system has provided adequate performance. Improving the system's automatic controller is the next step in the system's development. The design case simplifies component models to identify system parameters that show high sensitivity, and to identify areas of the system that require particular care in future study. Because engineering analysis cannot make accurate predictions for these models, some of the simplified models were tested through a lean experimental design. Three parameters were tested: (1) dredge head velocity; (2) depth of the dredge head; and (3) rotational speed of the dredge pump. Both dredge head velocity and dredge head depth show a positive relationship to dredge production within the simplified system model.

The lean approach is an initial design step to provide the engineer with an understanding of system behavior related to key requirements in a way that can be used to target areas of key interest in a later, more comprehensive design study. This initial lean approach is typically used

in organizations with limited resources as it is focused on reducing design costs and risks associated with complex system design.

# Acknowledgements

I would like to extend my deepest expression of thanks to my academic supervisor, Dr. Michael Lipsett, who continuously supported and provided guidance for this research. Although the journey took longer than initially anticipated, there was continuous encouragement throughout. I appreciated the high-quality feedback along with technical and non-technical discussions throughout. Thank you, Dr. Lipsett, for your confidence in me.

An expression of thanks to Jeremy Leonard, the owner of the sponsor company, Canada Pump and Power. Jeremy Leonard has provided continued guidance, financial support, and a great deal of expert knowledge in the dredging process. Jeremy, thank you for introducing me to the dredging world and giving me the opportunity to grow and learn within the field of dredging.

Some of the information presented within this research is based on empirical corporate knowledge provided by colleagues at Canada Pump and Power; but, wherever possible, references have been provided. I greatly appreciate and have benefited from the cooperation of dredge operators, field supervisors and the engineering team at Canada Pump and Power. This includes all of those who provided me with access to operating equipment, feedback on the operational dredge process and help in the overall design of the dredge technology developed for this study. Specifically, Jeff Young for his expert knowledge in the form of discussions and information based on many years of dredge experience. Danny Carlson who assisted in dredge system component drawings, design and selection, system control, and software implementation. Curtis Richie who assisted in gathering of empirical data and analysis of data for the dredge system. Jake Davidson who developed the control software implemented for the dredge system of interest. Thank you for your contributions to my work.

I would also like to express my appreciation and thanks to Dr. Robyn Braun for her feedback and technical edits. I would also like to acknowledge the efforts of the members of my committee and their constructive feedback on my research.

Lastly, I am grateful for the love and support of my family. My wife Alyesha Dyck, who encouraged me to finish my research while advancing in my career and raising our new daughter Ayla-Maze, the greatest joy of my life. Thank you Alyesha for your patience, support, and continued love throughout the last fifteen years.

# Table of Contents

# List of Tables

# List of Figures

# List of Symbols

| Term | Description |
|---|---|
| $G$ | Global coordinate system |
| $L$ | Local coordinate system of the dredge cage, dredge pump, and dredge cage attachment points |
| $x, y, z$ | Cartesian Coordinates |
| $\boldsymbol{l_i}$ | Cable Lengths, Positioning Winches {$i$ =1, 2, 3,4} |
| $\boldsymbol{w_i}$ | Coordinates, Positioning Winches {$i$ =1, 2, 3,4} |
| $\boldsymbol{a_i}$ | Dredge Head, Cage Attachments Points {$i$ =1,2,3,4} |
| $\boldsymbol{p}$ | Origin, Dredge Head |
| $x$-$z$ | Plane, Local Cartesian Coordinates |
| $x$-$y$ | Plane, Local Cartesian Coordinates |
| $y$-$z$ | Plane, Local Cartesian Coordinates |
| $\boldsymbol{R_{sh}}$ | Total Resistance, Barge Ship |
| $\boldsymbol{R_{f(sh)}}$ | Friction Resistance, Barge Ship |
| $\boldsymbol{R_{r(sh)}}$ | Residual Resistance, Barge Ship |
| $\rho_{f(sh)}$ | Density of Fluid, Barge Ship |
| $\boldsymbol{v}$ **or** $\boldsymbol{\dot{x}}$ | Velocity, Barge Ship & Dredge Head |
| $\boldsymbol{R_{a(sh)}}$ | Air Resistance, Barge Ship |
| $\boldsymbol{F_{D(sh)}}$ | Drag Force, Barge Ship |
| $\boldsymbol{F_{l(sh)}}$ | Lift Force, Barge Ship |

| | |
|---|---|
| $\boldsymbol{W_{sh}}$ | Weight, Barge Ship |
| $\boldsymbol{m_{sh}}$ | Mass, Barge Ship |
| $\boldsymbol{g}$ | Gravity Force |
| $\boldsymbol{B_{sh}}$ | Buoyancy Force, Barge Ship |
| $V_{sh}$ | Volume of Water Displaced, Barge Ship |
| $\boldsymbol{F_i}$ | Inertia Force, Barge Ship $\{i = 1,2,3,4\}$ |
| $\boldsymbol{a}$ **or** $\boldsymbol{\ddot{x}}$ | Acceleration, Barge Ship & Dredge Head |
| $\boldsymbol{F_t}$ | Tension Force, Barge Ship |
| $\boldsymbol{F_{sh}}$ | Net External Forces, Barge Ship |
| $\boldsymbol{I_m}$ | Rotational Matrix of Inertia, Positioning Winch $\{m = 1,2,3,4\}$ |
| $\boldsymbol{q}$ | Vector Winch Drum Angles, Positioning Winch |
| $\boldsymbol{T_f}$ | Motor Viscous Damping Friction Coefficients, Winch $\{f = 1,2,3,4\}$ |
| $r$ | Radius of the Pulley/Winch Drum, Positioning Winch |
| $\boldsymbol{\tau}$ | Torques exerted by the winch motors, $\tau_i$ |
| $\boldsymbol{F_c}$ | Force Applied to the Winch, Positioning Winch $\{c = 1,2,3,4\}$ |
| $D_{\emptyset}$ | Matrix of Angles $\emptyset_{d,i}$ at which the cable enters drum $\{i = 1,2,3,4\}$ |
| $\boldsymbol{d_s}$ | Distance, Centreline of winch drum to centreline of pulley $\{s = 1,2,3,4\}$ |
| $\boldsymbol{l_i}$ | Cable Lengths, Positioning Winch $\{i = 1,2,3,4\}$ |
| $\boldsymbol{\eta_i}$ | Normalized Cable Length, Positioning Winch $\{i = 1,2,3,4\}$ |
| $\boldsymbol{A}$ | Structured Matrix, Positioning Winch |
| $\boldsymbol{\eta_{ix}}, \boldsymbol{\eta_{iy}}, \boldsymbol{\eta_{iz}}$ | Vector Components of Winch Force, Positioning Winch $\{i = 1,2,3,4\}$ |
| $\boldsymbol{R_{T(DH)}}$ | Total Resistance, Dredge Head |

| | |
|---|---|
| $\dot{\boldsymbol{l}}_i$ | Velocity of cable lengths $\{i=1,2,3,4\}$ |
| $\ddot{\boldsymbol{l}}_{\boldsymbol{i}}$ | Acceleration of cables $\{i=1,2,3,4\}$ |
| $\boldsymbol{R}_{\boldsymbol{f}(\boldsymbol{DH})}$ | Frictional Resistance, Dredge Head |
| $\boldsymbol{N}_{(\boldsymbol{DH})}$ | Normal Force, Dredge Head |
| $\boldsymbol{R}_{\boldsymbol{R}(\boldsymbol{DH})}$ | Residual Resistance, Dredge Head |
| $\boldsymbol{F}_{\boldsymbol{D}(\boldsymbol{DH})}$ | Drag Force, Dredge Head |
| $\boldsymbol{F}_{\boldsymbol{L}(\boldsymbol{DH})}$ | Lift Force, Dredge Head |
| $\boldsymbol{W}_{(\boldsymbol{DH})}$ | Weight, Dredge Head |
| $\boldsymbol{W}_{\boldsymbol{cage}}$ | Weight, Dredge Cage |
| $\boldsymbol{W}_{\boldsymbol{pump}}$ | Weight, Dredge Pump |
| $\boldsymbol{B}_{(\boldsymbol{DH})}$ | Buoyancy Force, Dredge Head |
| $V_{(DH)}$ | Volume of Water Displaced, Dredge Head |
| $\boldsymbol{R}_{\boldsymbol{DH}}$ | Cutting Forces, Dredge Head |
| $\rho_{f(DH)}$ | Density of Fluid, Dredge Head |
| $C_c$ | Coefficient, Cutting Force, Dredge Head |
| $h_c$ | Thickness, Cutting Ring, Dredge Head |
| $\boldsymbol{F}_{(\boldsymbol{sl})}$ | Momentum Force, Slurry, Dredge Head |
| $\dot{\boldsymbol{m}}$ | Mass flow rate in the discharge pipe |
| $\boldsymbol{V}$ | Velocity of the slurry flow |
| $m_{(DH)}$ | Mass, Dredge Head |
| $\boldsymbol{f}_{\boldsymbol{wi}}$ | Tension Winch Cables $\{i=1,2,3,4\}$ |

| | |
|---|---|
| $\boldsymbol{F}_{(\boldsymbol{DH})}$ | Net External Forces, Dredge Head |
| $\boldsymbol{F}_{\boldsymbol{I}(\boldsymbol{DH})}$ | Net Inertia Force, Dredge Head |
| $\boldsymbol{f}_{\boldsymbol{bx}}$ | Sum of external forces and inertia applied to system, x-direction |
| $\boldsymbol{f}_{\boldsymbol{by}}$ | Sum of external forces and inertia applied to system, y-direction |
| $\boldsymbol{f}_{\boldsymbol{bz}}$ | Sum of external forces and inertia applied to system, z-direction |
| $\boldsymbol{w}$ | $\begin{bmatrix} \boldsymbol{f}_{\boldsymbol{bx}} \\ \boldsymbol{f}_{\boldsymbol{by}} \\ \boldsymbol{f}_{\boldsymbol{bz}} \end{bmatrix}$ |
| $\boldsymbol{f}$ | $\begin{bmatrix} \boldsymbol{f}_{\boldsymbol{w1}} \\ \boldsymbol{f}_{\boldsymbol{w2}} \\ \boldsymbol{f}_{\boldsymbol{w3}} \\ \boldsymbol{f}_{\boldsymbol{w4}} \end{bmatrix}$ |
| $I$ | Identity Matrix |
| $M$ | $m_{(DH)}\ x\ I$ |
| $\boldsymbol{A}_{\boldsymbol{iy}}$ | Pulley $y$-coordinate {i =1,2,3,4} |
| $\boldsymbol{A}_{\boldsymbol{ix}}$ | Pulley $x$-coordinate {i =1,2,3,4} |
| $\Delta P_{loss}$ | Pressure loss, Pipeline |
| $\Delta P_{ph}$ | Horizontal Resistance, Pipeline |
| $\Delta P_{pi}$ | Inclined Resistance, Pipeline |
| $a_p$ | $8\frac{\rho_w L_p}{\pi^2 D^5}$ |
| $b_p$ | $b_p = \pi \frac{D^2}{4}\ L_p$ |
| $L_p$ | Length of Pipe, Pipeline |
| $\lambda_f$ | Coefficient of friction for water, Pipeline |

| | |
|---|---|
| $\rho_f$ | Density of Fluid, Pipeline |
| $D_p$ | Diameter of the Pipe, Pipeline |
| $S_{kt}$ | Coefficient solid's effect, Pipeline |
| $\beta_p$ | Angle, Pipeline |
| $\boldsymbol{V_c}$ | Critical Deposition Velocity, Pipeline |
| $\rho_s$ | Density, Solids |
| $\rho_w$ | Density, Water |
| $S$ | $\rho_s/\rho_w$ |
| $d$ | Solids Particle Diameter Pipeline, Pipeline |
| $C_s$ | Solid Particle Volume Fraction, Pipeline |
| $\mu_m$ | Mixture Fluid Viscosity, Pipeline |
| $\mu_\omega$ | Water Viscosity, Pipeline |
| $b$ | Rotation Speed of the Pump Shaft, Production |
| $h$ | External Diameter of the Pump's Impeller, Production |
| $Q_p$ | Average Production Rate of homogeneous mixture in pipeline, Production |
| $Q_m$ | Average Mixture Flow, Production |
| $C_v$ | Concentration of the Mixture, by Volume, Production |
| $\rho_m$ | Density of the mixture, Production |
| $H_r$ | Head Reduction Ratio, Production |
| $H_m$ | Head of Mixture, Production |
| $H_w$ | Head of Water, Production |
| $\eta_r$ | Efficiency Reduction Ratio, Production |

| | |
|---|---|
| $\eta_m$ | Efficiency of Mixture, Production |
| $\eta_w$ | Efficiency of Water, Production |
| $R_H$ | Correction Factor, Head Reduction, Solids Effects, Production |
| $HR_{15\%}$ | Head Reduction with constant $C_v$ of 15%, Production |
| $R_\eta$ | Reduction of Pump Efficiency |
| $P_m$ | Measured Pump Power |
| $d_{50}$ | Median Diameter of Solid Particles, Production |
| $P_0$ | Maximum Flow Rate and Corresponds to $C_v$ = 0% |
| $Q_0$ | Flow Rate corresponds to P0 |
| $Q_m$ | Operating Flow Rate of Mixture |
| $Q'$ | Selected Pump Flow Rate |
| $H_w'$ | Pump Head, related to $Q'$ |
| $C_v'$ | Concentration that corresponds to $H_w'$ and $Q'$ |
| TDH | Total Dynamic Head |
| $H_{pm}'$ | Total Dynamic Head Pressure at the Pressure Sensor |
| $P_s$ | Pressure Measured by the Sensor |
| $V'$ | Mixture Velocity at the Pressure Sensor |
| $D_s$ | Pipe Diameter at the Pressure Sensor |
| $\rho'$ | Mixture density, Algorithm |
| $C_{vm}$ | Calculated concentration of mixture based on Hw' and Q' |
| $Eff_w'$ | Efficiency that corresponds to $H_w'$ and $Q'$ |
| $\dot{E}_D$ | Excavation Rate, Excavation |

| | |
|---|---|
| $w_{cr}$ | Width of the Dredge Head Cutting Ring, Excavation |
| $h_d$ | Depth of the Cutting Ring into the Material, Excavation |
| $\rho_{si}$ | In-situ Soil Density, Excavation |
| $k_s$ | Spillage at Excavation, Excavation |
| $\boldsymbol{K}_p$ | Matrixes of constants |
| $\boldsymbol{K}_v$ | Matrixes of constants |
| $\dot{\boldsymbol{q}}$ | Angular Velocity |
| $\ddot{\boldsymbol{q}}$ | Angular Acceleration |
| $\boldsymbol{u}$ | Vector of motor torques, Control Method Bruckmann et al. [1,2] |
| $\boldsymbol{f_d}$ | Force required to move the end effector from the existing location to the new desired location |
| $r_i$ | Rope length radius |
| $\boldsymbol{d^G}$ | Hoist Rope Length |
| $D_{j,k}$ | Distance between two circle centres |
| $n_i$ | Initial rope exit position |
| $\Delta d_i$ | Change in the ropes exist position relative the initial position |
| $r_d$ | Radius of the bare winch drum |
| $d_e$ | Distance from winch centreline, $d_e = f(n_i + \Delta d_i)$ |
| $d_i$ | Centreline of the winch drum |
| $rev_{cap}$ | Drum wrap capacity |
| $d_w$ | Drum length (inside flange to inside flange) |
| $d_{th}$ | Thickness of winch rope |

| | |
|---|---|
| $n$ | Rope layers on drum |
| $rev_{int}$ | Initial number of revolutions or rope wraps on the drum |
| $n_{capcity}$ | Maximum number of allowable rope layers for the winch system |
| $r^*$ | Corrected radius of winch drum based on number of cable wraps |
| $\Delta L_i$ | Total change in rope length {$i$ =1,2,3,4} |
| $l_s$ | Length of rope from exit position on winch to first pulley |
| $\boldsymbol{f_{min}}$ | Minimum winch force |
| $\boldsymbol{f_{max}}$ | Maximum winch force |
| $c_i$ | Cable stiffness coefficient {i =1,2,3,4} |
| $d_i$ | Cable dampening coefficient {i =1,2,3,4} |
| $\Delta \boldsymbol{d^G}_i$ | Change in length due to elasticity {i =1,2,3,4} |
| A | Cross section of the cable |
| E | Young's modulus |
| $\boldsymbol{d^G}_{i,0}$ | Untensed cable length {i =1,2,3,4} |
| $d^G{}_i$ | Length of the tensed cable {i =1,2,3,4} |
| $\varepsilon_i$ | $\frac{\Delta d^G{}_i}{d^G{}_i}$ |
| $\Delta l_i$ | Change in cable lengths, first pulley to dredge head {i =1,2,3,4} |
| $\boldsymbol{A_i}$ | Fixed shaft/pulley location {i =1,2,3,4} |
| $\boldsymbol{L_i}$ **and** $\boldsymbol{\theta_i}$ | Length and angle of each cable respectively |
| $r$ | Cable pulley radii which is identical for all four pulleys {$r = r_{1,}\, r_{2,}\, r_{3,}\, r_4$} |
| $C$ | Winch Viscous damping coefficients, $C = Diag\ \{C_1, C_2, C_3, C_4\}$ |

| | |
|---|---|
| $\boldsymbol{J}$ | Rotational inertia of the lumped pulley/motor shaft, $\boldsymbol{J} = Diag\ \{\boldsymbol{J_1}, \boldsymbol{J_2}, \boldsymbol{J_3}, \boldsymbol{J_4}\}$ |
| $\boldsymbol{T}$ | Vector of cable tensions, $\tau_i$ |
| $\boldsymbol{\beta}$ | Vector of pulley cables, $\boldsymbol{\beta_i}$. $\boldsymbol{\beta_i} = 0$ when the dredge head is located at the origin and a positive angle $\boldsymbol{\beta}_i$ on one pulley results in a change in cable length $\Delta\boldsymbol{L_i} = \boldsymbol{L_i} - \Delta\boldsymbol{L_{0i}} = -\boldsymbol{\beta_i}r$ |
| $Q_{man}$ | Manufacturer's pump flow rate at specified pressure |
| $Q_{test}$ | Measured pump flow rate at specified pressure |
| $Q_{Err_1}$ | Error between test data and manufacturer published data |
| $Q_{Avg}$ | Average measured flow rate for the trial |
| $Q_{pred}$ | Average predicted flow rate for the trial |
| $Q_{Err_2}$ | Error between the measured and predicted flow rates per trial |
| $C_{v(Err)}$ | Error between the measured and predicted solids concentrations per trial |
| $C_{v(Trial)}$ | Average measured concentration for the trial |
| $C_{v(pred)}$ | Average predicted flow rate for the trial |
| $k_{(meas)}$ | Measured K factor for the trial |
| $k_{(pred)}$ | Predicted K factor for the trial |
| $k_{(err)}$ | Mean absolute error between, $k_s$ |

# Chapter 1: Introduction

### A Lean Approach to Early System Modeling

Product innovations are developed in response to discrete events, specific problems, and new technological opportunities [1]. Innovators are often creative, forward-thinking individuals who focus on ways to solve problems using non-conventional tools. They are influenced by operational experience, systems' behaviors, and other knowledge, such as organizational, social, and economic structures, as well as marketing considerations [2]. Once the need for a product is realized, the speed at which the product is designed, developed, tested, and brought to market is critical for securing market space. However, speed must be balanced with product quality and cost [3].

While innovators are important to the realization of the early product [2], the complete design, understanding, and optimization of a system often requires scientific modeling and verification by design engineers. Design engineers focus on the in-depth understanding of the system and its behavior so that engineering principles can be applied to the system design to improve its performance, durability, and manufacturing cost. This process includes understanding aspects such as the physics that govern the system's behavior, the components that make up the system, and how these components interact with one another. The engineering design process allows the design to be modeled, tested, and verified by others within the scientific or engineering community. A detailed and comprehensive engineering design process which identifies all aspects of the system can be costly and time-consuming and is not always worthwhile in the early stages of system design.

It is important to introduce a new technology to market as soon as possible. Late entry results in higher development and manufacturing costs, lower profit margins, and a lowering of the firm's market value [4]. However, if a product is introduced before it is ready, there may be quality and safety problems, followed by customer dissatisfaction. Organizations use technology readiness levels [5], standardized technology maturity assessment tools, to help engineers manage the risks associated with early product introduction [6].

When dealing with limited resources and time there are tradeoffs between schedule, spending, scope, and quality. As a design becomes more complex, the design engineer must deal with the major risks in uncertainty upfront to best manage and minimize the potential consequences later in the engineering design. Some major areas of uncertainty can be dealt with early in the project lifecycle though initial system prototyping and simplification. This early identification through modeling, prototyping, and testing can assist the engineer in gaining knowledge and information that may help with key decisions related to risk and the development of a robust project management framework for final product design. Managing and controlling these risks involves identification and assessment of risks, and the implementation of measures to eliminate, mitigate or in some cases accept the risk.

Simplification, in most instances, risks model accuracy; developing models of complex system can lead to a high degree of uncertainty, and these complex models can be difficult to analyze or even understand due to the sheer number of system interactions [7]. The engineer must strike a delicate balance between simplicity and accuracy in the development of a useful model. The model must be developed so that no behaviours lead to significant deviations from requirements, or severe failure modes.

This work presents a lean approach to modeling, prototyping, and testing in the early stages of the design and development of a complex multi-physics system. We emphasize the simplification of the otherwise complex system to develop an early baseline understanding of the system and its behavior. This baseline understanding can then be used to identify and investigate the influences of key parameters on the simplified model. Moreover, this approach focuses on revealing aspects of important design variables and system parameters that highlight sensitive responses in the model. What's more, for many engineering design problems, developing a complete understanding of the entire system is not required [8], as long as the system behavior is well understood. This lean approach is intended to provide system knowledge for the engineer that may be used in a future, more comprehensive study, where complex system models and improved experimental design can be developed based on the findings of this initial lean approach.

Design creates a product's success [9], and its waste, which is a primary reason that companies use lean production from the start [10]. A significant risks of comprehensive design early on, especially when dealing with complex systems, is developing system models that function well in a laboratory environment but do not perform well in practical industrial applications [11]. In these cases, significant early investment may not benefit the organization. Figure 1.1 illustrates the lean approach which focuses on (1) model simplification, (2) early protype testing and (3) iterations to improve knowledge and identify problematic parameters. The lean approach applies early and frequent iterations, through a minimal viable prototype, to complete initial testing and improve knowledge.

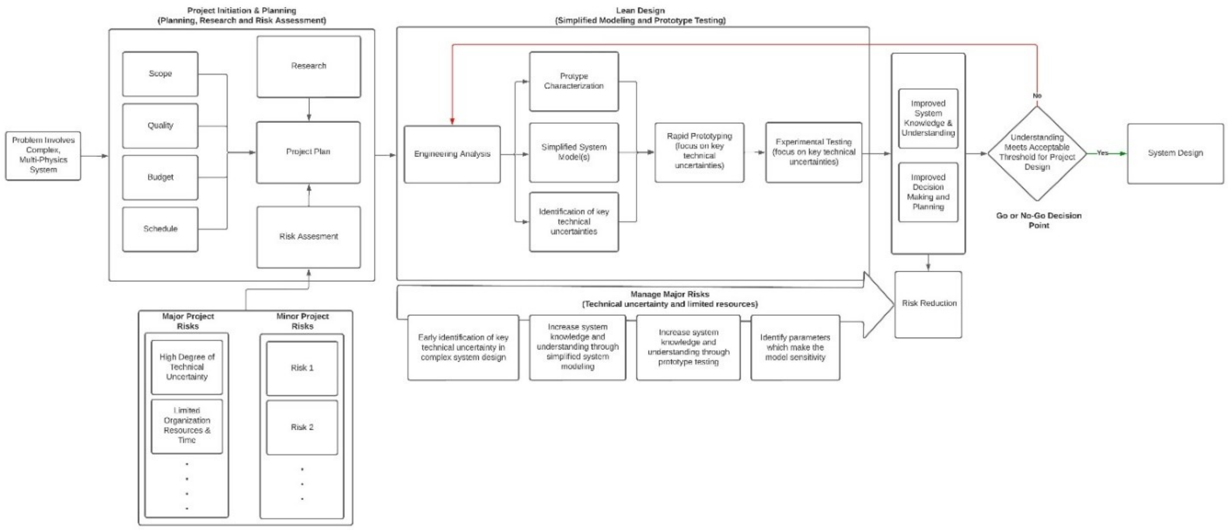


Figure 1.1: Lean Approach, Initial Design Understanding with Limited Resources and Time

The simplified models of a lean approach do not encompass all system aspects but manage early design risks associated with areas of high uncertainty and gaps in knowledge. These simplified models can be reworked through iteration and testing until they meet a minimum threshold, reducing the level of uncertainty associated with simplification. As a result, this lean approach will reduce or retire major risks in design, prototyping and experimental verification early on.

The present work considers the modeling of an automatic cable-driven dredge system using a lean approach. The system involves many interacting subcomponents, as well as the excavation and hydro-transport of solids, and the interaction of the system with many influencing parameters. The approach provides a study of scope, rather than a full parametric analysis of the entire multi-physics system. It results in a preliminary understanding of the system and important physics but does not provide a complete parametric model. The work splits the system into a set of sub-systems and develops a framework of their interaction. The initial results from this case study may be used as the basis for future complex modeling, experimental design, and optimization of the system.

Through this lean approach we developed a reasonable, baseline understanding of a complex system and identify areas of significant potential technical risks that can inform decision makers on additional investigation into the physics. The work does not contain or provide the standard reproducible scientific results typically found in a structured design of experiments methodology. Instead, it attempts to identify and explain the major workings of the system, which can then be investigated in further study and used to reduce or retire risks in implementation.

**What is Dredging?**

Dredging involves removing settled, or suspended, solids from aquatic environments such as ponds, lakes, oceans, and rivers [12]. Dredging is conducted for a variety of reasons, including environmental remediation, aggregate and mining applications, tailings and reclamation, overgrowth applications, waterway, and beach maintenance. The major activities of dredging involve in-situ excavation or erosion, transportation of materials, and redistribution of materials. Appendix A provides more details on dredging methods along with example figures of dredgers.

Hydraulic dredgers pump fluid, typically water, into the soil, to erode and suspend a solid-fluid mixture, and to induce a pressure gradient within the soil that creates flow over the bed of materials. The flow mixes with loose solids to develop a solid-fluid mixture known as a slurry or dredgeate. As a slurry is developed, the mixture is conveyed through a connecting pipeline, via hydraulic transport, sometimes called hydro-transport. For most dredge projects, the goal is to reduce the water and energy inputs while maximizing the volume of solids moved. To increase the solids concentration in the slurry, many hydraulic dredge systems include some form of excavation. However, with increased concentration of the solids, friction losses during transport also increase which reduces the flow. Moreover, if the flow rate drops below a critical velocity threshold, specific to the solids being transported, solids can settle, and plug the discharge line. For these reasons, it is critical to control the dredge system to maintain conditions above the minimum deposition velocity for the slurry concentration and the available dredge system power. Instrumentation such as flow meters, density meters and pressure sensors provide operators with production data that is used to manipulate the dredge equipment controls and increase or decrease production rate.

**Problem Definition**

The primary aim of modeling and simulating the dredging processes and systems is to estimate the behaviour of a dredging process or system, without costly research or prototype tests [13]. However, with the modeling and development of any system, comes a certain amount of risk. The level of acceptable risk in design for industry varies depending on the organization and design requirements. The elimination, mitigation, or acceptance of identified risks are based on the nature of the risks and potential outcomes. Risk acceptance determines the experimentation required for engineering verification and testing of the physical prototype. For organizations with limited resources there simply may not be the resources available to complete a full parametric system model and comprehensive experimental design, especially when dealing with a complex, multi-physics system. Although this lean approach leaves some risks unmanaged, the knowledge and improved understanding of the system behavior can be used in future, more comprehensive study, to manage key risks when developing a parametric model and experimental design for system control and optimization.

## Thesis Scope and Objectives

This thesis proposes an economical method for product development that relies on highly simplified models of system physics to design, develop, and test a prototype system. This work focuses on a case study and descriptive system design of a novel dredge technology that utilizes a cable-driven propulsion system to position the dredge head along a predetermined path. The case study shows how simplified models of the dredge system components were developed, considers the parts and their interactions, verifies several models in small-scale lab testing, and critiques the design in the context of design requirements and operational considerations. The early design process will be considered in the context of managing uncertainty and risk in complex, multi-physics design.

The main objectives were as follows.

1. Identify the main processes for a cable-driven dredge system.
2. Developed simplified system models that can be used to investigate influencing system parameters as a lean approach to industrial modeling and design.
3. Identify key system parameters and test their influence on the system.
4. Verify the system models through small scale lab testing that can be used to develop a more comprehensive model and optimized controller in future work.
5. Identify key parameters that make the system sensitive through small scale lab testing to reduce uncertainty and risk in future work such as complex modeling, experimental design, and development of an improved system controller.

## Organization

This introduction is followed by a literature review of project management methods, uncertainty, risk and lean systems in the context of engineering design. Chapter 2 also provides an overview and literature review of dredging component models and cable-driven robots. Chapter 3 is an overview of components for the novel dredge system studied. Chapter 4 establishes simplified component models for the dredge system and examines some of the limitations of the models developed. Chapter 5 describes the lean approach to prototype development and initial testing. Chapter 6 discusses the results of the simplified models, prototype testing and influence of three parameters. Finally, Chapter 7 discusses lessons learned and areas of further study.

# Chapter 2: Literature Review

Organizations competing for market share are continuously trying to manage resources while developing new products that provide a competitive edge. Designing new products becomes especially challenging when the designs involve complex systems; where knowledge is limited, and uncertainty is high. This challenge is further compounded when an organization's resources and time are limited. Therefore, organizations with limited resources must carefully manage these design projects and implement strategies to reduce system uncertainty while improving system knowledge.

In this chapter, we start by reviewing the project management process and providing a brief overview of each of the process phases and project knowledge areas. Next, we review both the predictive and adaptive project management approaches while identifying some of their characteristics and properties. A brief overview of design in industry and complex multi-physics systems is presented, followed by a consideration of the links between uncertainty and risk, and how they are managed in the project management life cycle. The project management review concludes with a summary of the term "lean" in the context of project management and design work.

This chapter also provides an overview of the literature reviewed on the dredge process and overall system models which make up the dredge system, as well as of the dredge system subcomponents: centrifugal pump models, pipeline models, and ship dynamics. Lastly, this section covers wire-driven robots and various methods developed by researchers for modeling and controlling large-scale systems. Due to the broad spectrum of topics covered here, please note that this literature review presents only a small sample of available work and is not intended to be all inclusive of all topics.

## Project Management, Design and Methodology

Researchers use engineering design to guide systematic observation and experimentation, inductive and deductive reasoning, and the formation and testing of hypotheses to produce theories testable by observation [14]. Engineering design for industry usually involves a mixture of scientific method and intuitive creativity [15], and is often motivated by profit or a need to improve processes or optimize systems. Most researchers and organizations use some form of project management to oversee an engineering design project where the primary focus of the management is to increase a project's success. There are a wide array of engineering design models and management strategies, many of which are tailored to specific project conditions. Risk management is integral to all engineering project management strategies.

## Project

The Project Management Institute defines a project as "a temporary endeavor undertaken to create a unique product, service or result" [16]. Juran considers a project as a positive or negative problem with a scheduled solution [17]. A project is unique, has a start and a finish (schedule) and considers costs (budget), scope (magnitude of work to be done) and quality (performance requirements) [18]. The project's schedule, budget, scope and quality are considered its framework [19], which can be mapped onto the project management and engineering design process.

## Project Management

The Project Management Institute defines project management as the "the application of knowledge, skills, tools, and techniques to project activities to meet the project requirements." [16]. The traditional project management life cycle includes five phases: initiation; planning; execution; monitoring and controlling; and closure [20]. Initiation involves identifying stakeholders, developing a project charter, project scope and project objectives. Planning provides an estimation of the resources required, develops a schedule, identifies tasks, estimates budget, and assesses project risks. Execution involves executing the planned sequence of tasks from the planning stage. Monitoring and controlling occurs throughout the project management life cycle [21], and is meant to provide the project with continuous checks to ensure the overall project stays within the planned framework. Closure or project termination involves feedback that helps the team evaluate the process and technical success [18]. It is widely accepted that there are ten knowledge areas in project management [16]: integration; scope; time management; cost management; quality; human resources; communications; risk; procurement; stakeholders. Project management is important throughout a project life cycle as it provides a framework that can be implemented to improve a project's success [22].

Project management methodologies range between a predictive and an adaptive approach. The traditional or predictive project management develops schedule from a known scope and then manages the implementation of the project in accordance with the schedule [23]. Predictive project management emphasizes early planning, estimation and risk identification based on available project knowledge and understanding. This structure provides a linear framework of sequential tasks that can be planned, executed, monitored, and controlled throughout the entire project life cycle. Due to the emphasis on early planning, predictive project management can influence design costs early on [24, 25] and is well suited for sequential or procedural design projects [26] with predictable environments [27].

Alternatively, adaptive project management thinking is commonly used for projects that are subject to high rates of change and uncertainty [28]. The high level of uncertainty, especially early on, makes it difficult to predict project schedule, costs, scope, and quality. To deal with the uncertainty, adaptive project management uses an iterative approach [29], and utilizes the feedback from each iteration to drive project development. The adaptive method commonly uses short intervals to plan, execute/create and review strategy, with each interval having a go/no-go decision structure [30]. This short interval framework allows project teams to better manage high levels of uncertainty as the team can systematically test assumptions and strategies [31]. The adaptive approach is commonly utilized in software and IT industries and is referred to as "agile" software development [32]. In addition to the predictive and adaptive methods, several other hybrid methods have been developed that combine a portion of the predictive and adaptive project management methods to deal with more specific project characteristics [33-35].

**Waterfall Design Methodology**

The engineering design process is an iterative decision-making process that applies engineering principles while using resources to meet an objective [36]. Traditionally, the engineering design process has followed a waterfall design methodology [37]. The waterfall design methodology involves information and deliverables that flow in sequence from one step to the next, much like how water flows from one rock to another as it progresses down a waterfall. The linear progression of the waterfall design methodology occurs from the project start to its completion, with each step or phase relying on deliverables from the previous step. To be effective, the waterfall design methodology requires predictability [27] so that the engineer can properly estimate the project cost and schedule. Therefore, when uncertainty and risk are high, the waterfall design methodology is not ideal [30] and a more iterative, agile, and collaborative approach to engineering design must be taken [28].

Below are brief summaries of well-known agile methods including Scrum, Dynamic Systems Development Model, Crystal Methods, Feature-Driven Development, Lean Development, Extreme Programming, and Adaptive Software Development.

- Scrum involves short sprints, typically between two- and eight-weeks of highly collaborative teamwork. At the beginning of each sprint there is a planning stage, followed by activity, and a review at the end where progress is demonstrated, and a go or no-go decision made.
- Dynamic Systems Development Method includes three time-boxed, iterative phases: Functional Model; Design-and-Build; Implementation. The Functional Model phase consists of gathering functional and non-functional requirements. The design-and-build phase focuses on meeting the requirements by engineering and prototyping. Lastly, implementation involves training, review, and feedback of the system by users in their environment.
- Crystal Methods also involves incremental cycles of up to four months. This method values improved interactions between people, community, skills, talents, and communications. Within this method, communication, and criticality with project priorities in a matrix help to select the appropriate methodology. Elements of the methodology and project priorities are divided up into thirteen categories (roles, skills, teams, techniques, activities, process, milestones, work products, standards, tools, personality, quality, and team values) which are each considered when tailoring the adaptive methodology to a project.
- Feature-Driven Development (FDD) involves short, feature-driven iterations with process guidelines. FDD involves five processes: feature modeling; features list; planning feature; designing feature; and building feature. The design feature and building feature stages includes high iterations and customer feedback. Once complete, the features are integrated to the whole system.

- Lean Development focuses on providing value to the customer through collaborative interactions and customer feedback. Lean Development includes a start-up phase (feasibility), steady state phase (iterative analysis, design, testing), and renewal phase (knowledge transfer) where emphasis is place on technical foundation, policies, and guidelines to manage the effort within these stages.
- Extreme Programming encourages collaborative, face-to-face, creative interactions with teams that have aligned values. It emphasizes the team's alignment with five central values including communication, simplicity, feedback, courage, and quality work.
- Lastly, Adaptive Software Development (ASD) uses principles much like the agile framework with an emphasis on fast, iterative development cycles, especially in projects with high uncertainty. It includes five stages: project initiation; adaptive cycle planning; plan by feature; design by feature; and build by feature. ASD focusses on collaborative work environments in the plan-by-feature phase, and iterative feedback from the design-by-feature to adaptive cycle planning phase. ASD includes six characteristics: mission-focused; feature-based; iterative; time-boxed; risk-driven; and change-tolerant. It is highly focused on adaptability over optimization.

In addition to software development, there are examples of agile approaches in hardware development projects. One example is Rothman [38], who organizes projects by functional teams, each with specific knowledge domains. These functional teams work in an integrated, collaborative environment which provides alignment and understanding of the cross-function interdependencies. To verify system design parameters and understanding of system interdependencies, Rothman encourages iterative cycles of prototyping, modeling, and mock-ups.

**Industrial Engineering Design and Complex Multi-Physics Systems**

Industrial product improvements and innovation are critical for organizations competing for market share. Engineering design and the application of project management allows organizations to improve competing products and processes. Industrial engineering design has many driving factors, such as curiosity, markets, consumers, organizational needs, competition, ascetics, reliability, materials, cost, and efficiency [39]. As a result, there is a wide range of industrial engineering design approaches, one generalized approach is shown in Figure 2.1 [39].

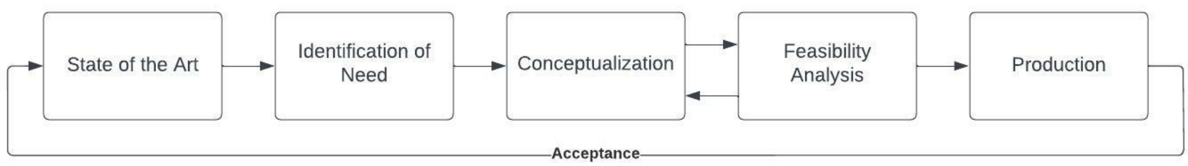


Figure 2.1: Design Process [39]

The product development process balances speed, quality and costs, where some research indicates that product development speed tends to have the greatest influence on product success [40]. However, it is also critical for producers to improve product quality while reducing product costs at the initial design stage, as optimizing product design in the early stages leads to a significant reduction in costs and improved quality [10]. Industrial engineering design can also be applied to wide range of application. Some of these design applications are predictable and involve principles and behaviors which are well understood. Alternatively, some designs are more complex which often involve multi- disciplines, less predictability and principles and behaviors which are not well understood.

One design technique used to accelerate the understanding of a complex system is to decompose the system into functional or physical subcomponents to levels that can be individually evaluated [41]. However, if not properly integrated, this strategy may result in emergent properties [42], or interactions, which can in turn create behaviours that were not predicted from the analysis of the subsystems alone. Another strategy for understanding complex system is model order-reduction, which lowers the computation complexity of mathematical models in numerical simulations that would not otherwise be feasible [43]. A subset of model order-reduction is simplified physics-based or operational-based reduction methods. Both approach model development through simplification. Order-reduction models incorporate the modeling parameters as free parameters, but also approximate the input–output behavior of the full-order model for any parameter value within the domain of interest [44]. Although model simplification methods exist, engineering design with limited personnel resources, tight budgets and time constraints must be especially thoughtful in their approach to model simplification.

Alternatively, Systems Engineering uses discipline-specific teams, with specialized knowledge, to complete subsystems [45] with useful functions for the whole system. The function of Systems Engineering is to guide the engineering of complex systems where technical and human-centred disciplines overlap [46]. Historically, Systems Engineering has been applied to industries such as aerospace, consumer electronics and telecommunications [47]. Although Systems Engineering has many benefits, its structure is characterized by significant resources, large project teams, and extended timelines [30]. Therefore, investigation into alternative techniques is warranted for organization with limited resources and time.

**Uncertainty and Risk**

Uncertainty is defined by Kreye et al. as a "potential deficiency in any phase or activity of the process which can be characterized as not definite, not known or not reliable" [48]. The engineering design process involves uncertainty and risk throughout the project lifecycle. For systems that are complex, the uncertainty in the design is increased [49]. In engineering design, managing risk due to uncertainty is essential and can have a significant impact on the likelihood of a project's success [50]. Moreover, some research shows that uncertainty affects how people act during engineering design [51], which can make activities and decisions during design more challenging [52-54] and lead to negative impacts on product performance. Therefore, there has been significant research dealing with project uncertainty in technical systems, design information [55], as well as methods for managing uncertainty [56-58]. The analysis of risk considers the probability that a negative or positive event may occur [59]. Negative risks pose a threat to the project success or stakeholders whereas positive risks provide the opportunity to improve the project success or positive impact on the stakeholders. Risks management deals with the systematic identification, analysis, and assessment of risks [60] from project initiation to closure.

In project management, an initial risk assessment is completed during project planning and then continuously revisited in the subsequent stages. Risks identified are stored in a risk registry and managed throughout the project lifecycle. Risk assessments consider the probability of a risk event occurring in combination with the potential consequence of such an event, typically evaluated in a matrix form. As a project progresses and evolves, risks may evolve and their probability and consequences may change [61]. Therefore, project risks must be continuously revaluated for their probability and consequence. Negative project risks can be eliminated, mitigated, or tolerated depending on their potential to occur, their consequence and the project risk tolerance. Alternatively, positive project risks can be exploited, enhanced, or accepted [62].

Risk management typically decomposes risks into categories, often considering internal or external risks to a project [63]. Internal risks, or source-oriented risks, stem from the execution of a project and include project areas such as cost, schedule, quality, and scope. As the name suggests, external risks are external to the project and involve areas such as market, environment, legal and many others external influences on the project. Internal risks are more easily controlled by the project team, whereas external project risk mainly are outside of the project teams' control [64].

Uncertainty in engineering design due to the lack of knowledge introduces project risks that may impact the outcome and execution of a design [65]. Levels of uncertainty, much like risk, can be managed or accepted if they are properly identified. However, in complex designs, where knowledge may be limited, it is difficult for the engineer to realize, adequately analyze, or properly manage the risks associated with uncertainty. Therefore, developing techniques for early identification of risks and uncertainty will provide the engineer greater control over de-risking the technology.

For many organizations, the risks associated with complete product design are reduced through modeling, prototyping and experimental design. Initial product models and prototypes are often smaller in physical size than the final product design, which reduces costs. Even so, complex multi-physics systems often involve significant resources, multiple disciplines, large costs, and significant time. Many organizations cannot afford the costly and often lengthy experimental process required for the development of these multi-physics, complex systems.

While some organizations may be able to tolerate the time and costs associated with a comprehensive design process, for those with limited resources and strict time constraints, a lean approach to industrial design is often required. To manage reduced resources and time, while lowering some risk, this approach must balance a basic system understanding with the knowledge that other risks remain. The goal of this lean industrial design approach is the development of a reasonable framework for understanding a system's behavior and the initial identification of system vulnerabilities. The lean approach provides an initial, intentionally simplified, model of a complex system to provide a better framework for future complex modeling and a full parametric design. The intent of a lean industrial design approach is to create value for customers by assessing risk early and eliminating waste in the product development process [10].

**Lean Design**

Lean manufacturing, developed by Sakichi Toyoda, Kiichiro Toyoda, and Taiichi Ohno, and best known from Toyota's "lean" production systems [66], focuses on elimination of waste and improving customer satisfaction [67]. Many researchers have since developed "lean designs" by maintaining an agile design framework and continuous customer feedback [68]. Lean design in project management focuses on eliminating waste while making a product better, faster, and more cost effective [69]. Project costs are a function of a project's objectives, time, and scope [70] and a lean agile design in the early stages of a project life cycle can help identify and retire waste associated with the high degree of uncertainty in complex, multi-physics design.

**Summary**

Engineering design and project management are often considered two separate streams of engineering. However, for organization with limited resources, engineering design and project management are often completed by a few or even one individual. For these organization, project management and engineering design not only intersect but are often acted on as if they were one and the same. As this study focuses on a case study of a complex, multi-physics design with limited resources and time, we consider here both project management and engineering design to be the same.

Throughout the project life cycle, engineering principles are applied to meet or exceed the needs and expectations of the stakeholders [71]. It is the experience of the author that project management and the engineering design process involves significant elements of business, which are dynamic and quickly changing. Customer and stakeholder expectations can change as further understanding and precision of the problem is developed through the project lifecycle. As a result, there is significant cost to the project to incorporate design changes during the later stages. Therefore, organization with limited resources and time must utilize methods to gain precision early in the design stages to reduce or retire large project risks associated uncertainty or limited knowledge.

**Dredging Overview**

Dredging is an industrial process for removing solid materials from bodies of water [11]. Prior to the introduction of centrifugal pumps, dredged materials were mainly transported by mechanical means, such as buckets. In the subsequent decades, a variety of dredge approaches have been developed including the suction hopper dredge, a range of cutterhead dredges and deep-sea dredges [72]. Historically, dredge production relied on specialized operators who used manual controls based on experience and instrumentation [73]. Hiring specialized dredge operators with experience continues to be a challenge, and researchers have found that manual control of dredge production through inexperienced operators results in low production and poor efficiency [74]. The difficulties of dredge operations are mainly attributed to the extremely complicated underwater environment [75]. With recent advances in computing, automating the dredge process and system control to reduce the reliance on operators is an area of active research by scholars and manufacturers [76-79]. The dredging industry has recently seen improvements in dredge control [80-82], and emerging technologies have shifted the industry focus towards semi-automated and fully automated dredge systems [83]. However, more than 95% of large dredge systems are still operated manually [74].

**Dredging Process & Modeling**

The complete dredge process involves multi-physics and a diverse set of parameters. This includes the hydraulic transport of solids, including the pump and pipeline process, the dredge hull dynamics, and the dredge head movement plus excavation process [11]. Much of the literature reviewed, such as work by de Bree, 1977 [22]; Miedema, 1987 [84]; Matousek, 1997 [85]; and van Rhee, 2002 [21], tends to focus on individual dredge processes. The development of simulation dredge models has been introduced by the CLAMSHELL program [86], the result of field experience, mathematical modeling, and physical research. A model for bucketwheel dredge has also been developed that simulates the combination of cutting and hydraulic transport of tin-ore [87]. A trailing suction hopper dredge system has also been modeled that focuses on the complete dredge cycle using first principles; the model developed is used to validate actual data and the performance of the dredger through the implementation of a model predictive controller (MPC) [11]. In other works, the soil cutting process and the fundamental laws governing hydraulic transport were used to develop a computer model that simulated the bucket wheel dredge for deep water tin-ore applications [86, 88]. Other dredge models developed in the literature use partial differential equations (PDE). However these PDE models become overly complex to use in most practical applications and only perform well in laboratory environments [11].

**Centrifugal Slurry Pumps & Modeling**

Centrifugal slurry pumps are used in a variety of process industries for the transportation of solid-liquid mixtures [89] and are primarily used for dredging applications. Researchers [90-

93] have performed several experimental studies to model the effects of solids on pump performance and flow field. Empirical correlations have been proposed [90-95] that estimate the effect of solids on the pump performance. However, due to the variation in pump design and slurry characteristics [89], a large number of different correlations exist. Currently, computational fluid dynamics (CFD) is another method being used by researchers to model the solid-liquid flow in slurry handling components [90-95]. The advantage of the CFD-based approach, over empirical correlations, is that it allows a wider range of operating conditions to be analyzed. Two common models used in CFD-based approach are Eulerian-Eulerian and Mixture [89].

**Dredge Pipeline Process & Modeling**

Modeling of the pipeline process, the effects of solids on pump performance and the effects of solids transport in a pipeline has been studied extensively [85, 96-100]. The models mainly focus on predicting flow rate, based on pump speed and a given mixture density. These models have been developed from empirical correlations that can be easily calibrated to data [11]. One of the common approaches correlates empirical data in combination with semi-theoretical reasoning [101]. Other approaches are based on theory, such as Wilson [102, 103], Wilson & Pugh [104] and Televantos et al. [105], or other analyses such as those of Roco & Shook [106], and Hsu et al. [107]. Furboter [11, 98], Worster and Denny [108] have developed simplified pressure loss models for slurry flowing in a pipeline. However, both theory-based and empirical correlation model approaches have their limitations. The empirical correlations are limited by their range of applicability and the theoretical models are challenging to implement in most practical applications [109]. Like centrifugal slurry pump modeling, computational fluid dynamics (CFD), which has the advantages of analyzing a wider range of operating conditions, is being used to investigate the solid-liquid flow in a pipeline [110].

**Ship Dynamics & Modeling**

Extensive research and modeling have been conducted on ship dynamics. Davidson and Schiff [111] developed a mathematical model that describes the ship's steering dynamics. Subsequently Nomoto developed first or second order transfer functions [112] that are still widely used for guidance and control design because of its simple and effective structure and easy-understanding [113]. A model using Taylor-series expansions has been developed by Abkowitz [114] that describes ship dynamics and accounts for the surge and sway forces and yaw moments acting on a ship in three degrees of freedom. Other researchers [115-118] have made simplifications to this model based on sensitivity analysis that reduced coefficients based on low sensitivity [113]. Other works [119] look at the cross-flow drag formulations applying lateral forces on a ship during maneuvering.

**Cable-Driven Robots**

Parallel mechanisms have many advantages, such as increased robustness, faster speed, and higher efficiency, when compared to open-kinematic chain mechanisms [120]. For example, cable-driven robots are extensions of parallel mechanisms that use flexible cables to pull an end effector [121]. There are two main disadvantages of cable-driven robots, when compared to the rigid links of single actuated robots. The first is their inability to push the end effector. The second is the additional complexity of design, planning and control [122-124]. Although cable-driven robots cannot push the end effector due to the flexibility in the cables, these robots are more practical for use in large applications [125-127], in handling heavy materials and [128], in access to remote hazardous environments [129].

Cable-driven robots have several advantages when applied to large scale applications, including the robot's ability to span and work over large spaces while keeping the heavy components stationary. What's more, the system's components are easy to build, reconfigure and maintain [127]. Another advantage is the system's ability to adapt to changing working conditions while dealing with fast dynamics [124]. Two examples of well-known cable robots are Intelligent Spreader Bar [130, 131] and the NIST RoboCrane [131].

Suspended cable-driven robots have up to six degrees of freedom [122, 130] whereas planar robots, a subcategory that works on a single plane, can have up to three degrees of freedom, depending on rotation. A method of controlling a four-cable, suspended planar robot with three degrees freedom has been developed by Jin and Randall [132]. This method uses a laser scanner at the end effector as an additional sensor for determining its position. Other research has focused on the cable tension to determine the size of the motors and cables [120]. More recently, researchers have developed hybrid open kinematic chains that have cable sections in tension, as well as conventional links and lower pair joints. Some literature focuses on the modeling and control of underwater cable-driven robots [133-135]. An underwater cable-driven dredge system is designed, and a control scheme is simulated to move the end effector along a predetermined path [135].

**Summary**

Extensive research has been completed on dredge systems. However, much of the research tends to focus on specific dredge subcomponents [84, 85, 88, 96, 136]. Of the dredge system models developed that look at the entire dredge process, many are black-box models [137-139] or simplified physical models that capture only the main dynamic behaviors of the system [11]. Moreover, the literature reviewed does not consider the combination of a cable-driven system with hydraulic production modeling.

Substantial work has been done on modeling individual dredge processes, complete dredge processes, and a variety of control techniques along with system optimization. However, none of the projects in the literature reviewed addressed the combination of a cable-driven dredge system, hydrodynamics, excavation, and production of a complete dredge system. In additional, the literature reviewed does not consider the practical challenges associated with dredging and the level of sensitivity of the system parameters. The real-world dredge process is complex, involves a high level of variability and often a great degree of uncertainty. As a result, this thesis develops and examines the simplified dynamics of a cable-driven dredge to evaluate the sensitivity of the influencing parameters as a streamlined approach in the development of complete multi-physics system model.

One of the main challenges of complete dredge modeling, and one of the drivers of simplified or black box models, is the difficulties in integrating rigid body dynamics, hydrodynamics, soil-tool interaction, and propulsion of vessels that are in contact with the solid media. Therefore, new dredge technology development requires not only simplified modelling but also empirical investigations to determine how novel subsystems interact.

# Chapter 3: Cable-driven Dredge, System Description

The cable-driven dredge comprises a set of separate subsystems, including the barge ship, dredge head, positioning winches, and controls system, connected as modular components. This chapter provides a brief overview of these system components as part of the complete cable-driven dredge system. As shown in Figure 3.1, the dredge system studied here uses a network of cables to move a dredge head and connecting pipe.

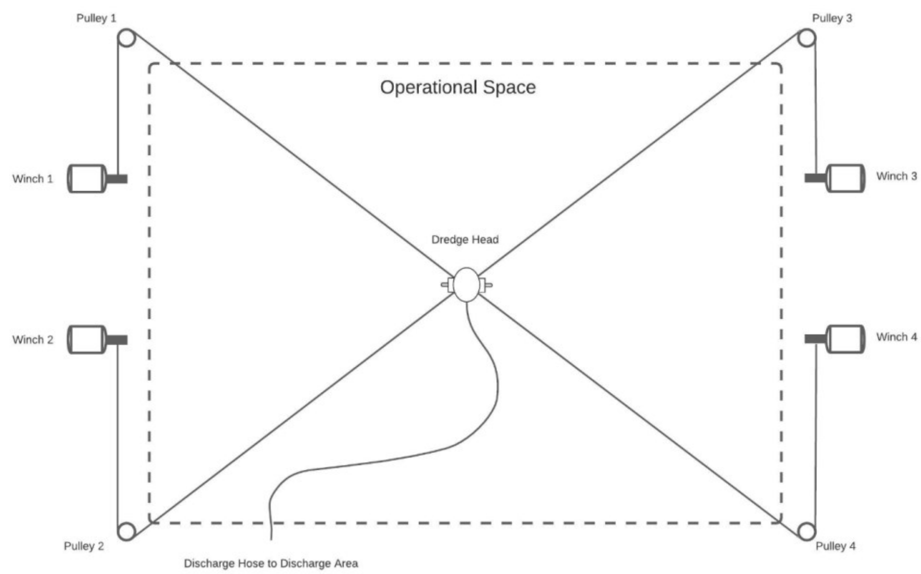


Figure 3.1: Cable-driven Dredge System

**Dredge System Components**

The dredge system is made up of the following components.

1. Barge Ship, Hoist and Controller
2. Dredge Head
3. Position Winches, Controllers (Variable Frequency Drive), Pulley and Ropes
4. Dredge Pump and Discharge Pipe
5. Control System

The cable-driven dredge system has a barge ship, which is connected to the dredge head through a hoist and rope. The barge ship supports the weight of the dredge head and controls its vertical position and applied force against the material bed. The barge ship consists of three modular barge sections in a u-shaped configuration and supports the dredge head, gantry, hoist, hoist controller, global positioning system, and communications antenna. The general assembly of the barge ship for the cable-driven dredge is shown in Figure 3.2.

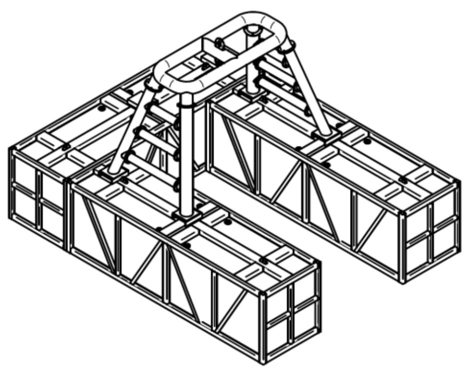

Figure 3.2: Dredge Ship, Gantry & Hoist

Unlike conventional hydraulic dredgers, the barge ship does not have its own propulsion system. Instead, the movement of the barge ship is coupled to the movement and position of the dredge head. A wire rope connects the barge ship and the dredge head.

The dredge head consists of the dredge pump and dredge cage, rigidly connected to one another. The dredge head connects to the four positioning winch cables along a thin disc at the base of the dredge cage, as shown in Figure 3.3.

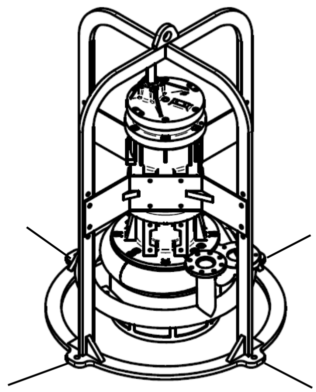

Figure 3.3: Dredge Head

The dredge pump excavates solids as it moves through the workspace. The dredge cage is both a protective mechanism for the dredge head and the structural connection point for the hoist and positioning winch cables.

The cable-driven dredge uses four positioning winches to coordinate the movement of the end effector, dredge pump and discharge pipe. The four winches are each mounted on a rigid, mobile steel skid, as shown in Figure 3.4. The mobile winch skids are anchored at designated positions along an application's shoreline.

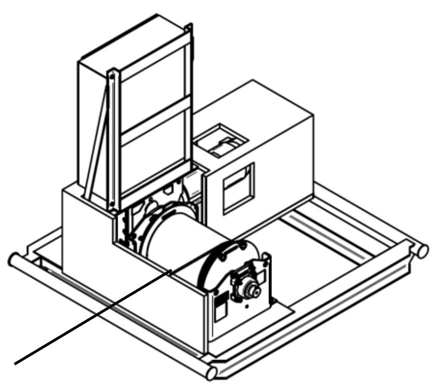

Figure 3.4: Positioning Winch and Controller

Winches connect to the dredge head through ropes that run through an initial pulley at shore. Each winch includes a variable frequency drive controller connected to the main dredge controller and power source. Winch torques apply tension to the cables and position the dredge head along a predetermined path. The movement of the cable-driven dredge is coordinated by the four winch controllers and the main cable-driven dredge controller.

The dredge pump excavates solids through erosion and transfers energy to the liquid for hydraulic transport of the solids-fluid mixture. Because of the hydraulic transport process, the dredge pump is considered a separate component, even though it is part of the dredge head. The cable-driven dredge pump is a submersible centrifugal dredge pump, with an induction motor controlled through a non-submersible variable frequency drive controller and the main dredge controller. The dredge pump motor and its controller are connected through a submersible power cable, affixed to the floating discharge pipe.

The main function of the cable-driven dredge is to position the dredge head within the workspace while maintaining a target production rate. To do this, the system controls the dredge head position, velocity, and acceleration along a predetermined path. The controller uses instrumentation to provide feedback to the main controller including the following: the three-dimensional position of the dredge head; the weight of the dredge head and corresponding applied force on the application bottom; the cable forces applied to the dredge head; discharge pressure and flow in the pipeline; and the input power to the dredge pump. A communication network relays these details from the main controller to the corresponding winch motor controllers, pump motor controller and hoist controller.

Since each dredge application is unique, an experienced dredge operator will set the initial system parameter targets. Using these initial target inputs, the main controller coordinates the cable-driven dredge system to move within the control space and produce consistent, targeted solids production. Figure 3.5 shows the user interface and dredge path pattern and Figure 3.6 shows the general communication network for the dredge controller.

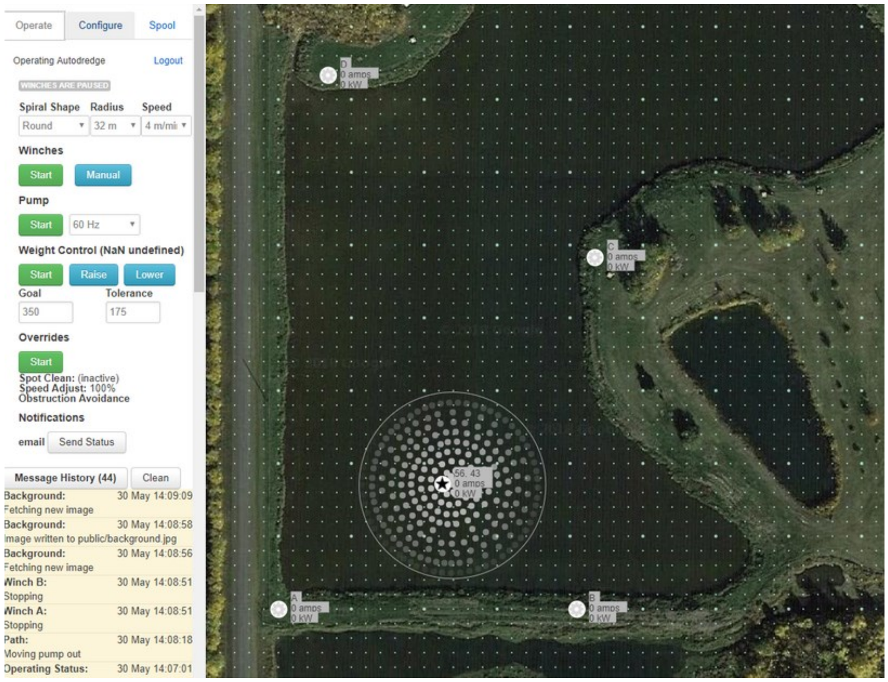


Figure 3.5: User Interface

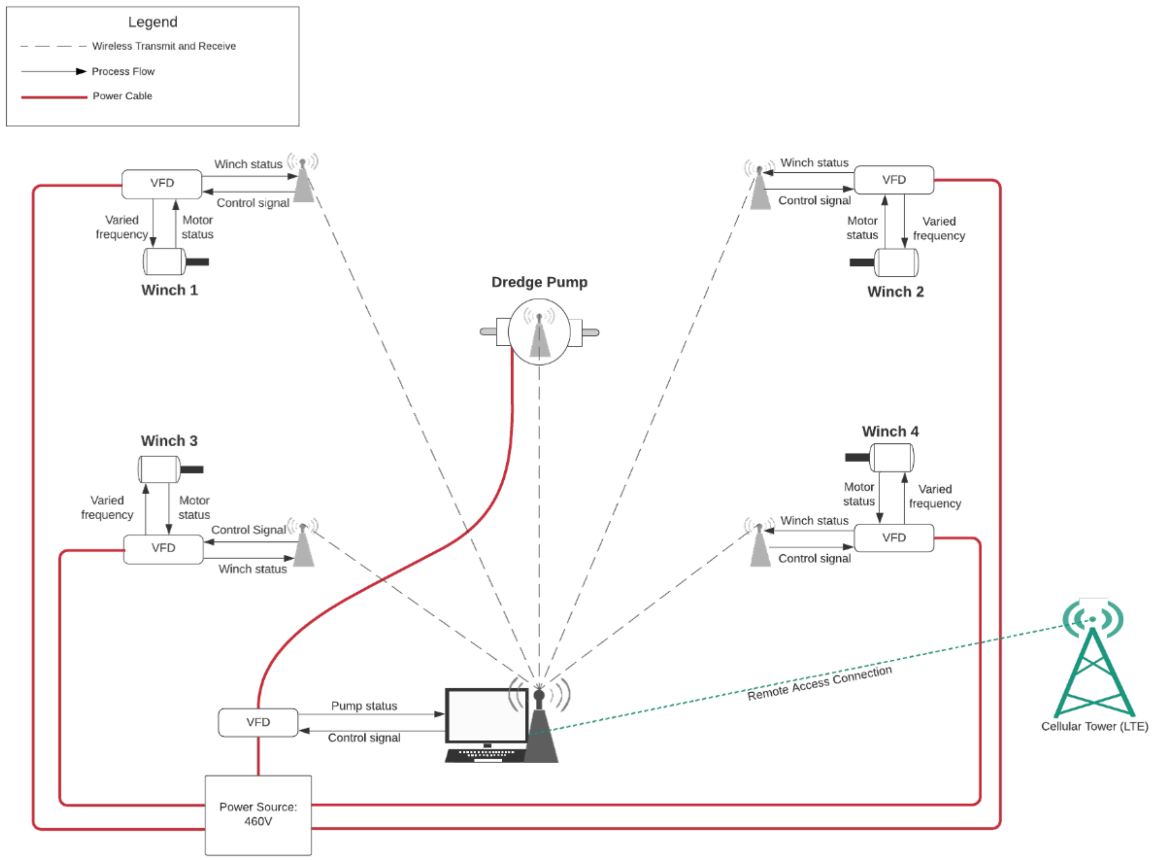


Figure 3.6: Communication Network, Cable-driven Dredge System

**Process Modeling of Complex Dredging**

The dredge system under study here is an introductory platform technology. That is, no previous models have been developed that describe the entire system. In Chapter 4, simplified dynamic models are developed for initial insight into component behavior and the associated forces. Often, more comprehensive system models are further developed based on partial differential equations (PDE). However, these PDE models can result in complex equations with system parameters that are difficult to measure [88] and the PDE models can therefore be difficult to implement in many practical applications. Instead of further developing a model for the cable-driven dredge based on PDE, we initially use first principles to model the system behavior and identify how the complete cable-driven dredge system functions and how the dredge components relate to the production output.

Five main functions of the dredge system have been identified as part of the system process model.

*Power*

Several of the cable-driven dredge components require a power supply. The main power source is a shore-mounted diesel generator. The main system components that require power are: four positioning winches; dredge pump; barge ship hoist winch; main system controller; winch motor controllers; and pump motor controller.

*Control System*

The main control system for the cable-driven dredge is made up of the following components: one main system controller; four winch controllers; one hoist controller; one dredge pump controller; and component instrumentation. The main controller for the cable-driven dredge interprets input parameters from the commissioning operator and data from the system instrumentation. Using these input parameters, the main controller adjusts the movement of the dredge system through each of the component controllers.

*Dynamic Positioning*

The dynamic positioning of the dredge system throughout the workspace is executed by four shore-mounted winches and their respective motor controllers. The vertical control of the dredge head is done through a winch hoist and controller.

*Excavation*

The dredge cage is designed with a cutting disk at its base to excavate solids. As the system moves, the cutting disk excavates a loose layer of material surrounding the inlet of the dredge pump. This process allows the passing fluid to erode loose solids and entrain them in the fluid traveling to the pump inlet. The cable-driven dredge barge ship is connected to the dredge head through a hoist rope. By adjusting the length of the hoist rope, the dredge system controls the depth of the dredge into the material and the applied force on the application bed.

*Hydraulic-Transport*

The hydraulic transport process involves the solid-fluid mixture traveling through the dredge pump and discharge pipeline to a designated discharge area. The overall dredge system processes are shown as a block scheme in Figure 3.7, with each of the main components identified as a block. Each component block is categorized into one or more of the five main system functions and connected to other system component blocks. These relationships and overall functions are discussed in more detail in the following section.

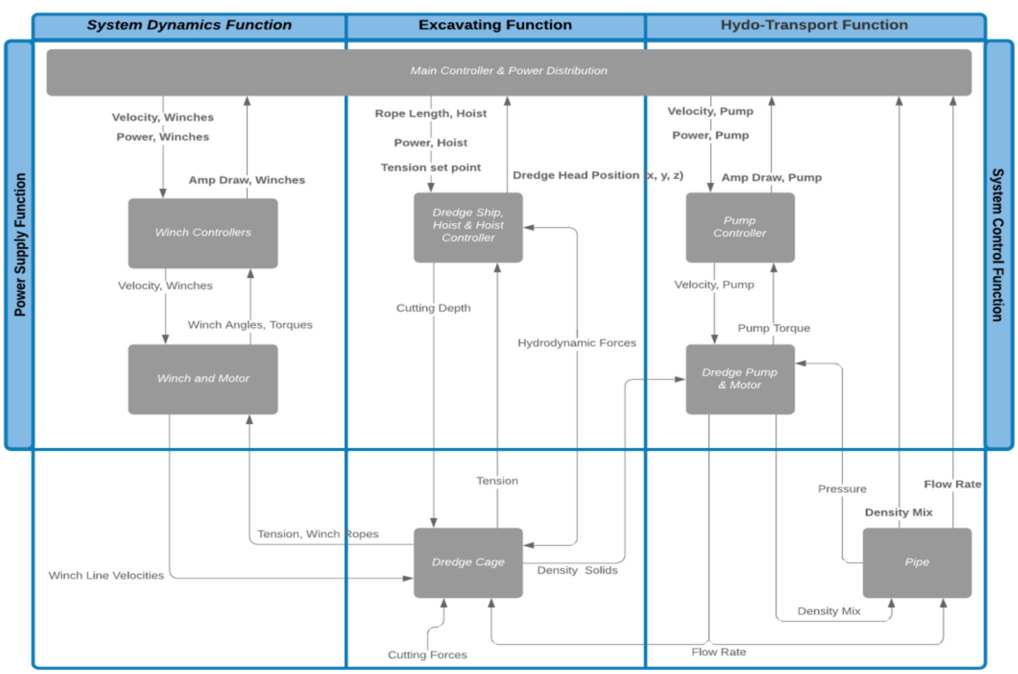


Figure 3.7: Main Dredge System Process

**Dredge Component Processes**

There are eight major components identified for the cable-driven dredge. Each of these components and their relation to the five system functions are shown in Table 3.1.

Table 3.1: Components and Main Dredge Functions

| **Component Description** | **Main Dredge Function(s)** |
| --- | --- |
| Power Source & Main Controller | Power Supply, Control System, System Dynamics, Excavation and Hydro-Transport |
| Winch Motor Controllers | Power Supply, Control System, and System Dynamics |
| Winch and Motors | Power Supply, Control System and System Dynamics |
| Dredge Ship, Hoist and Controller | Power Supply, Control System and Excavation |
| Dredge Cage | Excavation |
| Pump Controller | Power Supply, Control System and Hydro-Transport |
| Dredge Pump and Motor | Power Supply, Control System and Hydro-Transport |
| Discharge Pipe | Hydro-Transport |

*Power Source*

Many conventional dredge systems have a local power source aboard the barge ship. These power systems typically consist of diesel generators, which provide power to the ship's positioning system and hydraulic dredge components. The cable-driven dredge does not have a power source or propulsion system aboard the barge ship. Instead, the cable-driven dredge power source and propulsion system are shore-based. Moving the power source and propulsion system from the ship to the shore allows the dredge ship to be more compact. Furthermore, shore-based components are easier to access and service. The shore-based power source for the cable-driven dredge is a diesel generator. However, alternative power sources may be utilized when available.

The gauge size of each electrical cable is dependent on the component distance from the power source and the required power draw. When the distance between the components and a power supply is too great, the power source may be split into multiple sources that supply power to individual clusters of system components. Alternatively, the voltage being supplied by the power source may be increased to reduce the required amperage demand over long distances. For simplicity, the dredge system's power source model is generalized to a single source. It is assumed that the main power supply does not limit production. As highlighted in Figure 3.8, the power supply function is independent of other system functions and overall production. Details of the power generation and distribution are not further explored.

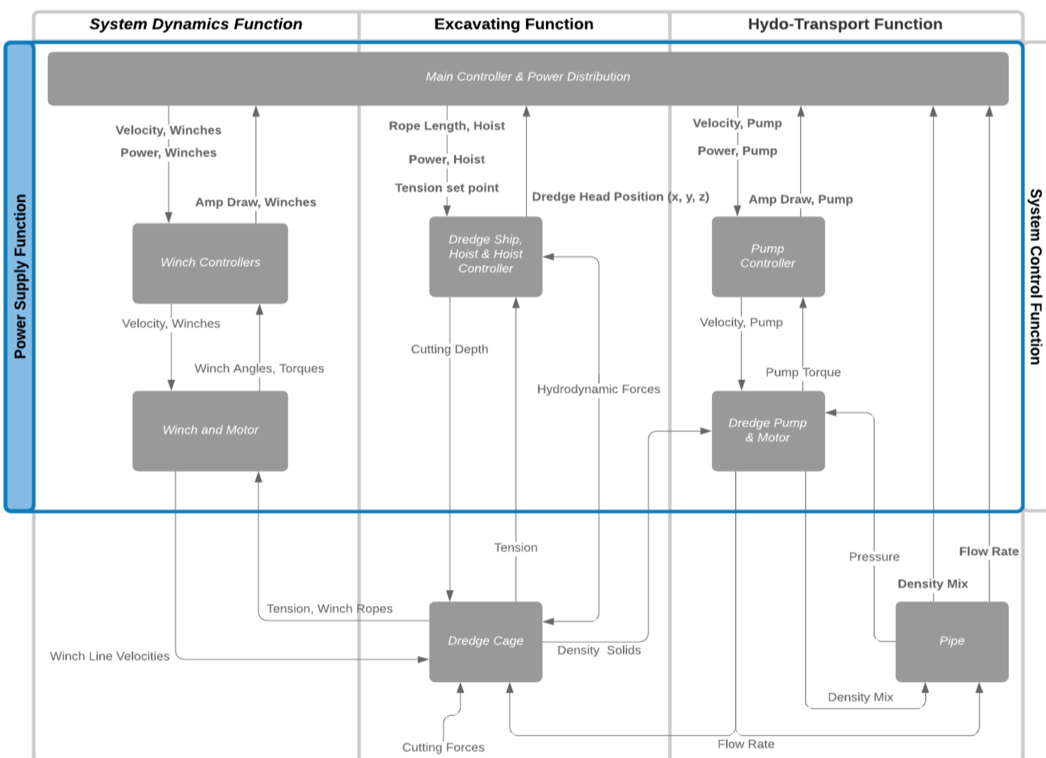


Figure 3.8: Power Supply Function

*Motor Controllers for Winches*

Motor controllers for the positioning winches are an important part of the overall control function for the cable-driven dredge. Each winch system has its own motor controller consisting of a variable frequency drive (VFD). By altering the frequency of the voltage being supplied to the winch induction motors, these drives control the angular speed of the motor and connecting winch drum. Each motor controller connects directly to the power source, main controller, and winch motor. Each of the winch controllers are installed on a steel baseplate alongside the electric winch. Installing the winch controller close to the motor reduces the potential for signal distortions that could influence the output signal and resulting system control.

In addition to their control system function, the winch controllers are responsible for the dynamic positioning function of the cable-driven dredge. The winch controllers adjust the position, velocity, and acceleration of the winch over a set period. In turn, this controls the winch rope length, velocity, and acceleration. The winch rotation changes the length of the winch line, which in turn controls the dredge head dynamics. The winch controllers and their relation to the main functions are highlighted in Figure 3.9.

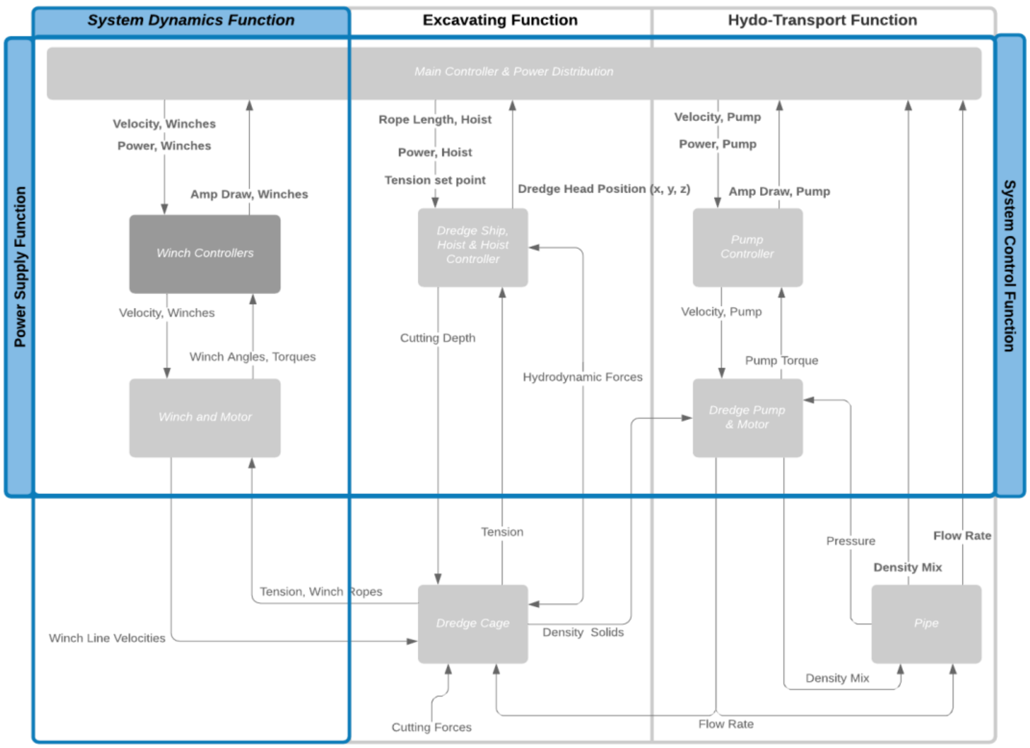


Figure 3.9: Winch Motor Control Functions

Each winch controller receives power inputs from the distribution source. The input power to each winch controller is supplied by an electrical cable carrying a constant sine wave. The position, velocity, and acceleration input from the main control system are secondary inputs to each winch controller. This input is based on the calculated change in rope length that will coordinate the dredge system's movement through the space over a planned period.

Each winch controller includes a closed loop feedback system. This system provides an estimated torque, calculated based on the winch amperage draw and applied load. This feedback loop and control allow us to set the upper limits of the applied winch torque. This prevents the winches from exceeding a load limit, possibly resulting in component failure. The secondary feedback loop is an encoder that provides the position and angle of the winch drum and can be used to determine the change in winch rope lengths.

*Position Winches and Rope*

The four position winches and their associated ropes are the main mechanism for the dynamic positioning function. Figure 3.10 highlights the four-winch system and the relationship of the winch system to the other components and functions of the cable-driven dredge.

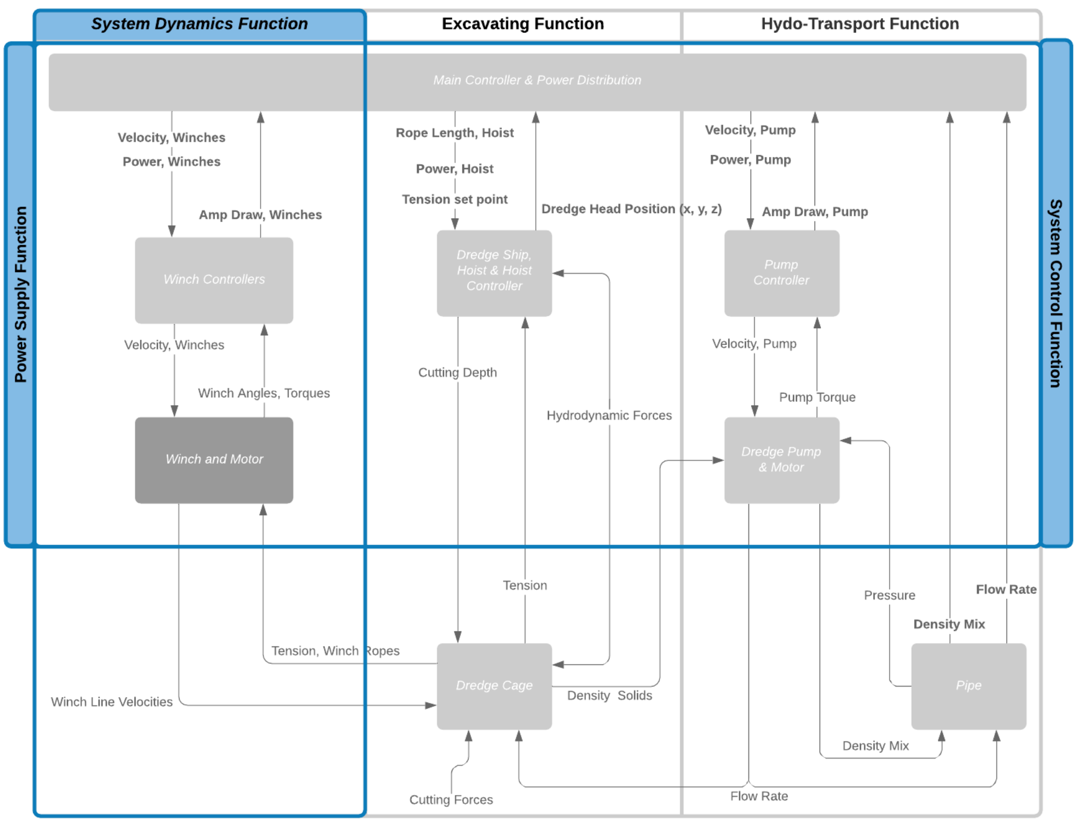


Figure 3.10: Winch and Motor

Figure 3.10 includes the main input and output parameters for the positing winches. As illustrated, each winch receives input from the winch controller.[1] Each of the winch motors apply torque to their corresponding winch drum. This changes the winch drum's rotational speed, and the speed of the winch rope, resulting in movement of the dredge head. This coordinated control of the four positing winches enables the dynamic positioning of the dredge head.

*Barge Ship and Hoist*

For conventional dredges, the ship influences serval system functions, such as powering, sailing, and excavating. In contrast, the cable-driven dredge's barge ship does not support powering or sailing and only functions as a mechanism to influence the rate of excavation. The cable-driven dredge barge ship comprises of three sectional barges pinned together. The barge ship supports a gantry and a hoist that is responsible for controlling the cutting depth of the dredge head and the applied force against the sediment bed. The ship and hoist are involved in the power supply, control system and excavating functions of the dredge system, highlighted in Figure 3.11.

[1] Only the velocity input is shown as the adjustment and control of the dredge head velocity is the main control goal. However, it should be noted that position, velocity, and acceleration are all inputs.

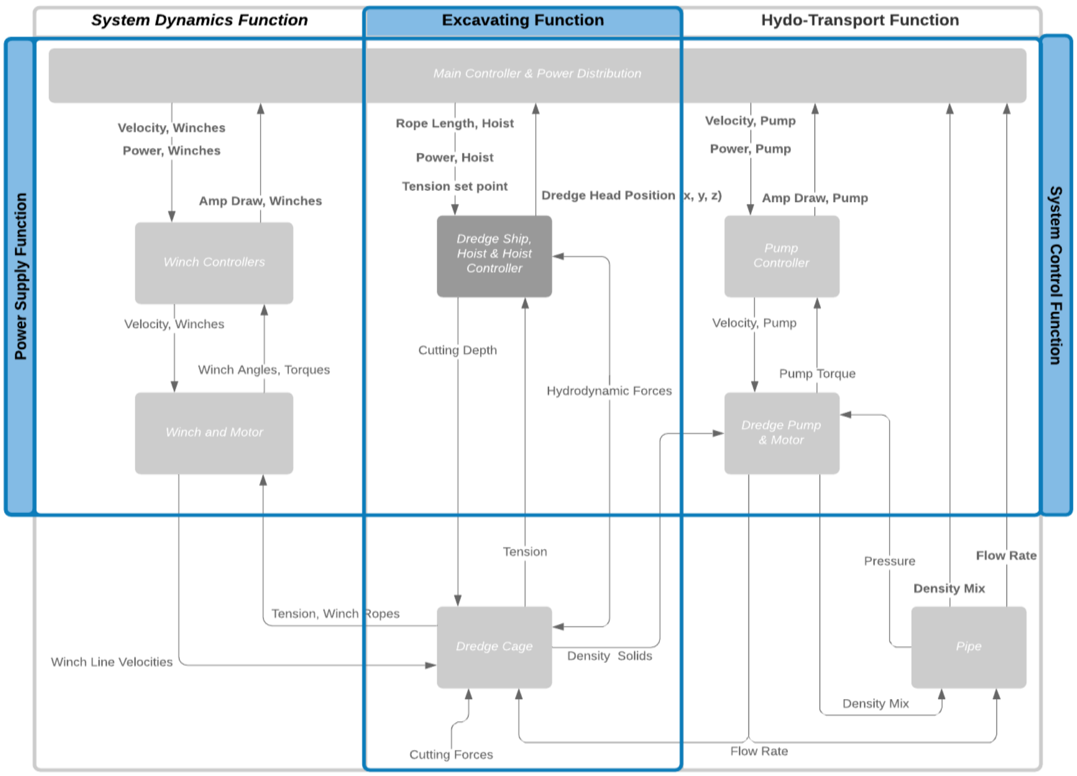


Figure 3.11: Dredge Ship, Hoist and Controller

The ship and hoist maintain a constant line tension as the dredge head moves through the workspace. To account for uneven bottom profiles within the application, the dredge hoist controller has a load cell measure the line tension so that the hoist can adjusts the winch line length to maintain a constant applied force. The main inputs for the ship and hoist are the power supply, tension set point and the hoist rope length. The main outputs of the dredge hoist are the cutting depth. The feedback from the dredge head to the ship is the applied line tension. The dredge ship and hoist also form an important part of the control system insofar as an onboard global positioning system relays the position of the dredge head in three dimensions back to the main controller. The controller uses this information to correct for line length error that may have propagated over a long period of operating time.

*Dredge Cage*

The dredge cage is an important aspect of the dredge system's model since it is the main component of the system's excavation function. As the dredge cage moves through the workspace, the cage excavates the bottom layer of loose solids. This excavation activity breaks up the sediment bonds, so the solids are more easily entrained within the surrounding carrier fluid. The solid-fluid mixture travels to the inlet of the dredge pump and initiates the hydraulic transport process. Compared to erosion from the pump flow only, the excavation of material has a much greater influence on the dredge system's overall production rate [140]. The relationship of the dredge cage model and the interconnecting variables are highlighted in Figure 3.12.

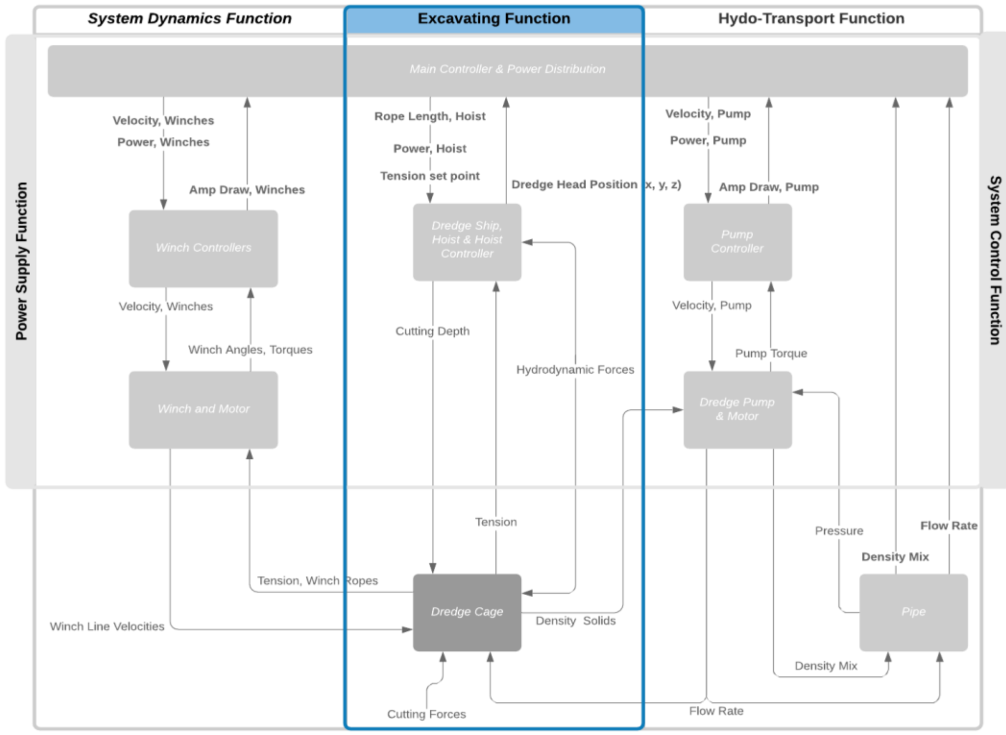


Figure 3.12: Dredge Cage

The two main forces applied to the dredge cage are cutting forces and hydrodynamic forces. The cutting forces are dependent on the in-situ material density and cohesive bonds of the soil. As the sediment bonds are broken up, the surrounding fluid penetrates the open voids created between the solid grains. The excavation process induces a pressure difference across the material, increasing cutting force [11]. The hydrodynamic forces are dependent on the system's movement through the fluid.

The force applied by the dredge head determines how deeply the dredge cage will penetrate the sediment layer. This force is influenced by the weight of the dredge head, which is controlled by the ship hoist tension force. This tension force is measured by an internal load cell and control loop system. The input weight set by the system is dependent on the properties of the in-situ materials.

*Motor Controller, Dredge Pump*

The dredge pump motor controller is a VFD motor controller, like those in the winch motor controllers. The dredge pump motor controller varies the frequency of the output voltage supplied to the dredge pump motor to control the pump impeller position, velocity, and acceleration. As highlighted in Figure 3.13, the pump motor controller is part of the dredge system's main control function.[2]

[2] Velocity is shown as this is the primary focus of the pump.

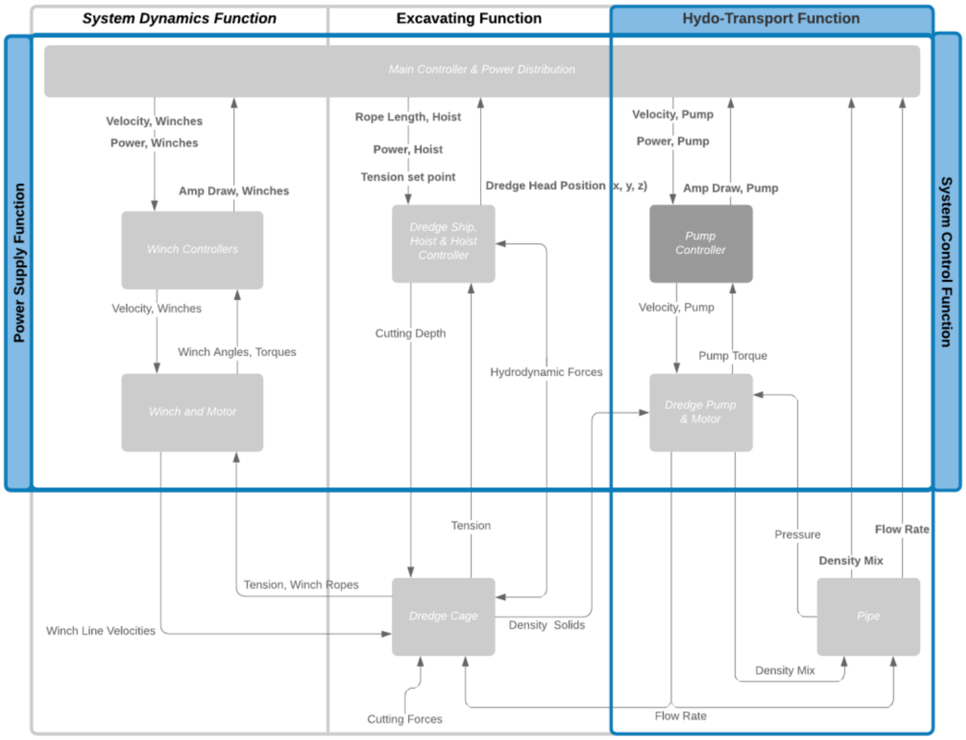


Figure 3.13: Pump Controller

Because the dredge pump motor is submerged, the dredge pump motor controller is remote from the submersible dredge pump motor and connected by an electrical cable. This separation creates the risk of noise on the signal. Therefore, inline filters are installed that slow the pulse of the change in voltage over time and reduces mode noise and currents.

The volume flow rate of the centrifugal dredge pump is directly proportional to the angular velocity of the motor and coupled pump. The pump motor controllers adjust flow through the dredge pump's rotational motor speed and regulates the production rate. Like the winch motor controllers, the pump motor controller has a closed loop system with torque control that estimates the applied torque based on amperage draw and impeller loading.

Based on field observation and operator experience, we expect that the applied load on the pump can be used as a measure of the instantaneous mass flow rate or production rate of the cable-driven dredge system. As the applied load increases due to the increased fluid density, the power and associated amperage draw are expected to increase. The measured amperage draw can then be used as a feedback mechanism to the main cable-driven dredge controller to adjust the dredge head movement to improve the control and system production.

*Dredge Pump & Pipe*

The primary purpose of the dredge pump is to transfer energy to kinetic fluid energy for hydraulic solids transport. The dredge pump’s main functions of excavating, and fluid-transport process are shown in Figure 3.14.

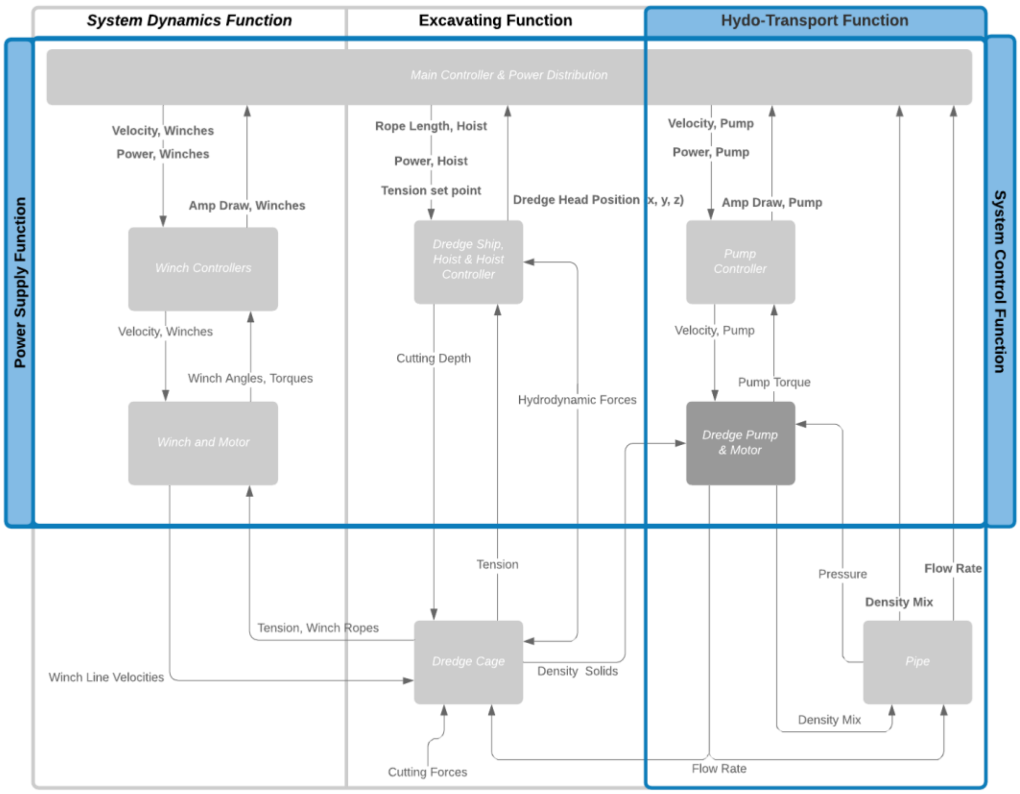


Figure 3.14: Dredge Pump and Motor

When the dredge pump is stationary in an application, erosion is the main mechanism for excavating the surrounding material. As fluid is drawn to the inlet of the pump, the lift forces associated to the movement of fluid past the solids suspends the loose sediment to be entrained in the flow and drawn to the dredge pump. The rate at which the erosion process occurs depends on the fluid velocity, density of solids, compactness, cohesive bonds, and shape of the in-situ solids. Excavation by the dredge cage is the second mechanism that influences production rate. The pump's output flow rate also influences the excavation rate of the system.

The main inputs of the dredge pump are the angular speed of the impeller and the density of the solids at the inlet. Other important inputs on the dredge pump are the fluid dynamics and losses in the discharge pipeline. As the density of the mixture increases in the discharge pipeline, the pressure at the discharge of the pump will increase. The increase in discharge pressure affects the pump flow rate. The system's discharge pressure and flow rate will eventually balance at a new operating point until the mixture density changes again due to the change in input solids concentration. The main outputs of the dredge pump and pipeline, as shown in Figure 3.15, are the density of the mixture and the flow rate.

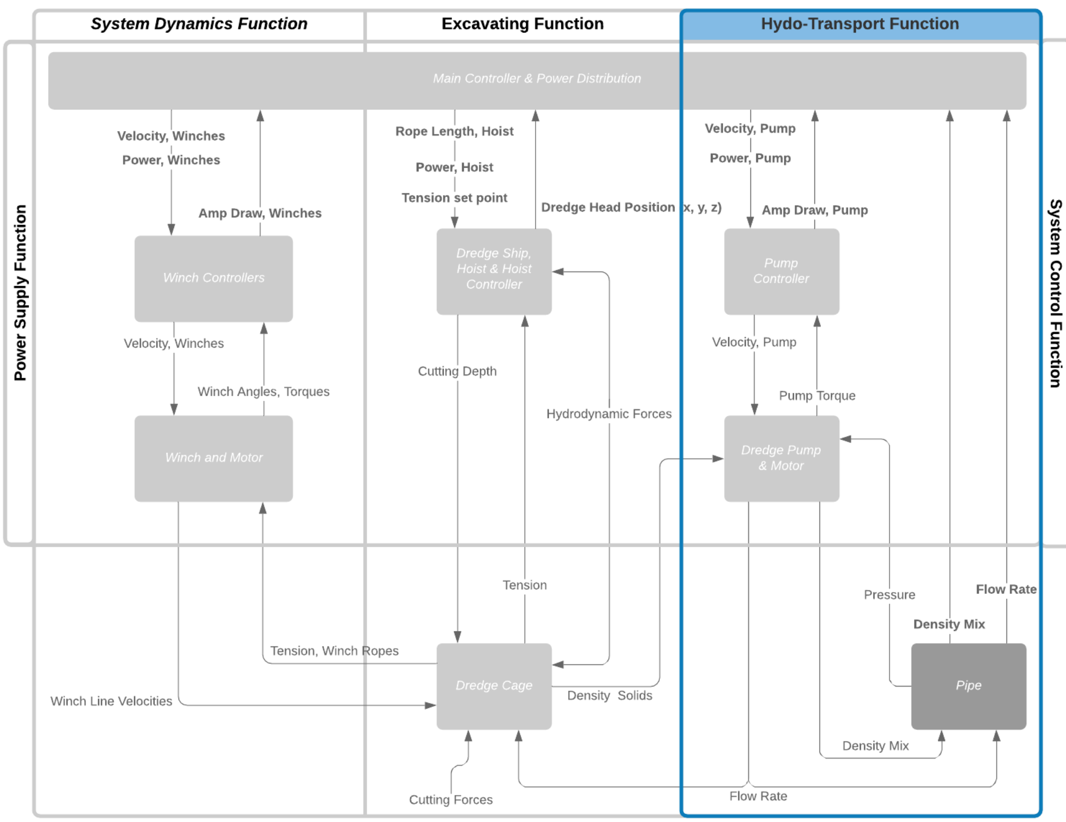


Figure 3.15: Pipe

The process model developed for our dredge system provides an initial basic framework for understanding the interaction of the interconnected dredge components. However, further investigation is required into key physical system processes, structural design, and system dynamics to develop an engineering model.

# Chapter 4: Simplified Dredge System Dynamics

### Cable-driven Dredge System Dynamics

Here, simplified dynamical equations for the cable-driven dredge system components are developed and further simplified through the initial assumptions. This simplification is intentional within the lean approach framework. The simplified equations will be used as the initial framework for future study and development of complete parametrized equations of motion. Moreover, the equations developed are used to detect parameters with high levels of sensitivity that required careful attention in future study. The barge ship, the dredge head, the position winches, the dredge pump, and the discharge pipeline are discussed. Figure 4.1 shows the local coordinate system at the dredge head where the inertial coordinate frame, $z$, points out of the page in the positive direction. The local coordinate system, L, relates to the local space of the dredge cage, dredge pump, and dredge cage attachment points.

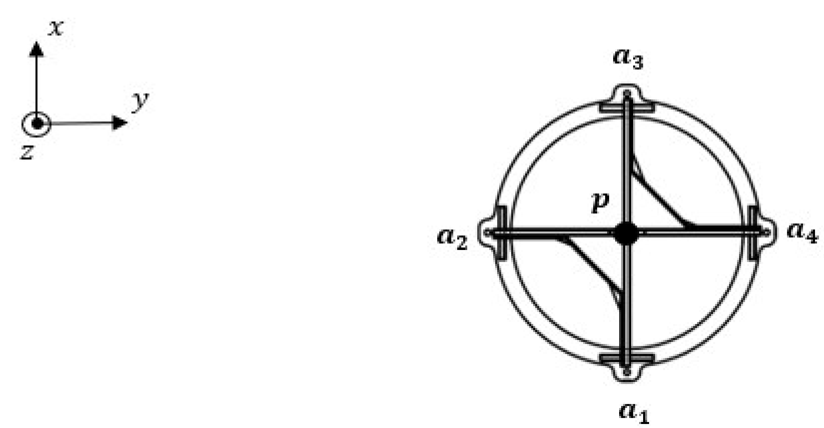


Figure 4.1: Dredge Cage, Local Coordinate System

The origin and centre of mass for the dredge head is $\boldsymbol{p} = \boldsymbol{p}(\boldsymbol{x}, \boldsymbol{y}, \boldsymbol{z})$, and $\{\boldsymbol{a_1}, \boldsymbol{a_2}, \boldsymbol{a_3}, \boldsymbol{a_4}\}$ are the set of $x$, $y$, and $z$ coordinates for each dredge cage attachment point. In addition to the local coordinate system, a global coordinate system, G, is defined. The global coordinate system relates to the dredge application global workspace. The dredge workspace includes the area in which the dredge system can move. This workspace is contained by the perimeter of the four position winches. The global coordinate system is illustrated in Figure 4.2. Where $\{\boldsymbol{w_1}, \boldsymbol{w_2}, \boldsymbol{w_3}, \boldsymbol{w_4}\}$ are the set of fixed positions in *x*, *y,* and *z* directions for each of the four positioning winches, and $\{\boldsymbol{l_1}, \boldsymbol{l_2}, \boldsymbol{l_3}, \mathbf{l_4}\}$ are the four rope lengths joining the dredge head and the positioning winches.

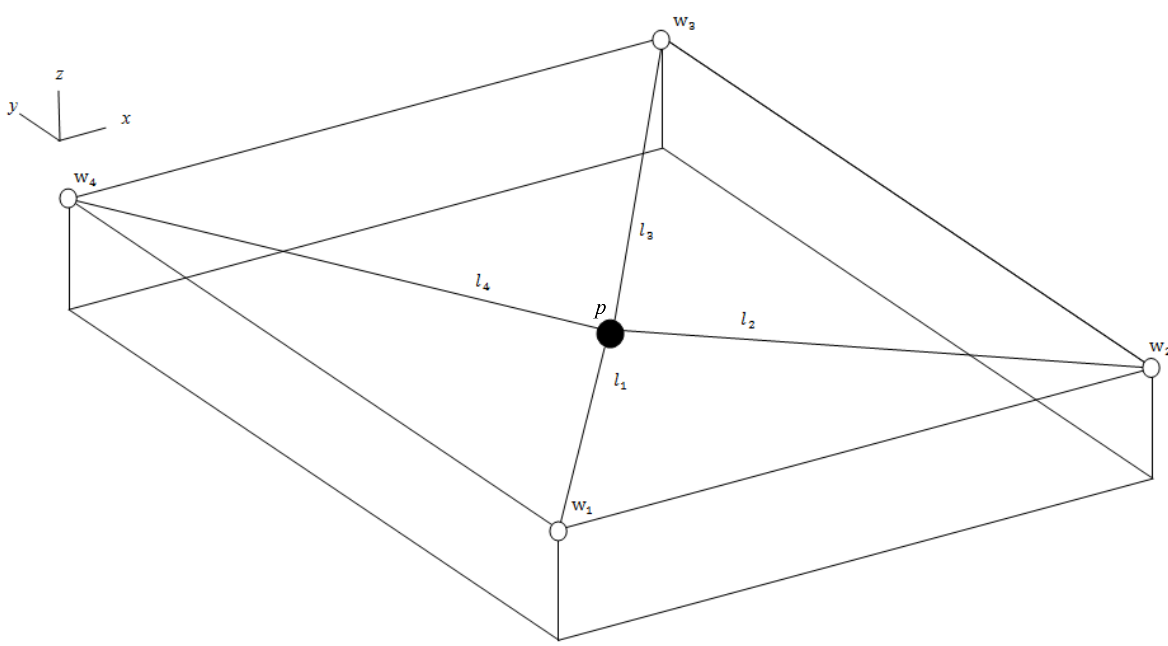


Figure 4.2: Global Coordinate System

The global and local coordinate systems are related through Eq. (1):

$$\boldsymbol{p} = \boldsymbol{a_i^G} - \boldsymbol{a_i^L} \tag{1}$$

where $\boldsymbol{a_i} = \{\boldsymbol{a_1}, \boldsymbol{a_2}, \boldsymbol{a_3}, \boldsymbol{a_4}\}$ and the $G$ and $L$ superscripts differentiate between the global and local coordinate systems, respectively. If no superscript is present, then the vector is assumed to be expressed with respect to the local coordinate system.

**Barge Ship Dynamics**

This section briefly describes the forces applied to the barge ship. However, the barge ship dynamics are not covered in depth in this study and will be an area of future study. A free body diagram of the barge ship is shown in Figure 4.3. Here we describe the associated forces with the barge ship's movement to investigate parameters that influence the overall dredge system. For the cable-driven dredge, the barge ship consists of three modular sections, a gantry frame, hoist winch and controls. The hoist system contains a controller and load cell which measures the tension applied to the hoist rope. To get a basic understanding of the system, the ship's dynamics are evaluated in a single plane and in the ship's direction of motion. It is assumed that the dominant effects will be captured in the ship direction of motion. A localized, *x-z* coordinate is used for this simplified two-dimensional evaluation.

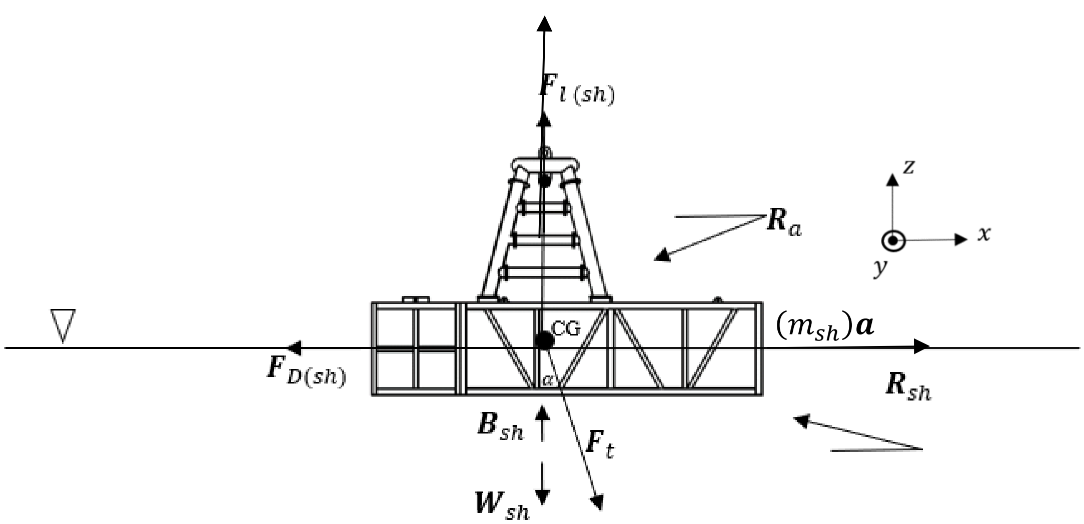


Figure 4.3: FBD, Barge Ship

For this analysis several simplifying assumptions have been made.

1. Velocity and acceleration of the ship are only in the *x*-direction.
2. Velocity of the ship is less than one meter per minute.
3. For the simplified analysis of the barge ship, it is assumed the dominant forces act through the ship's centre of gravity resulting in negligible rotation.
4. The vertical component associated with the resistance forces is negligible.
5. The dredge head velocity and acceleration are equal to the ship's velocity and acceleration. This assumes an ideal transmission between the connecting cable of the dredge head and ship. This assumption is made based on the short distance between the barge ship and dredge head and a large diameter connecting cable that is stiff.
6. External factors influencing the drag and lift force are the relative velocity of the surrounding water and wind (i.e., current and wind gusts). Although high velocity currents and extreme weather can happen, for the purposes of this analysis, it is assumed that the body of water is calm, and there is no current or extreme weather. This assumption is based on typical operating conditions for the dredge system which are small bodies of waters that are inland and sheltered from extreme weather.

*Resistance Forces*

The total resistance of the ship, $\boldsymbol{R_{sh}}$, can be divided into three main categories: friction; residual; and air resistance. The total resistance of the ship, at different velocities, can be experimentally determined by measuring the resistance force of the ship in a towing tank.

*Friction Resistance of the Ship*

The friction resistance due to the fluid is dependent on the ship's wetted area, and the coefficient of friction. The frictional resistance of the ship is denoted as $\boldsymbol{R_{f(sh)}}$.

*Residual Resistance of the Ship*

The residual resistance of the ship is dependent on the wave resistance and the eddy resistance. The residual resistance of the ship is denoted as $\boldsymbol{R_{r(sh)}}$.

*Air Resistance of the Ship*

The air resistance of the ship is dependent on the ship's velocity and cross-sectional area above the waterline. The air resistance of the ship is denoted as $\boldsymbol{R_{a(sh)}}$.

*Drag Force*

As the ship moves through a fluid with a velocity, $\boldsymbol{v}$, the fluid will apply a drag force opposite to the ship's relative motion. The drag force of the ship is denoted as $\boldsymbol{F_{D(sh)}}$.

*Lift Force*

As the ship moves through the fluid at a velocity, $\boldsymbol{v}$, the fluid applies a lift force on the ship, perpendicular to the ship's relative motion. The lift force applied to the ship is denoted as $\boldsymbol{F_{l(sh)}}$.

*Weight of Ship*

The weight of the ship is described in Eq. (2).

$$\boldsymbol{W_{sh}} = m_{sh}\boldsymbol{g} \tag{2}$$

where, $m_{sh}$ is the mass of the ship, and $\boldsymbol{g}$ is the gravitational force.

*Buoyancy Force*

The buoyancy force applied by the displaced volume of water is described by Eq. (3).

$$\boldsymbol{B_{sh}} = \rho_{f(sh)} V_{sh}\boldsymbol{g} \tag{3}$$

where, $V_{sh}$ is the volume of fluid displaced by the ship and $\rho_{f(sh)}$ is the density of the fluid on which the ship floats.

*Rope Drag and Transmission between Ship and Dredge Head*

The ship is connected to the dredge cage through a hoist and connecting rope. It is assumed that the drag force associated with the rope moving through the water is negligible for the system dynamics. For this simplified analysis, we also assume that the hoist rope between the dredge head and ship has an ideal transmission with negligible elongation and mass. This assumption is based on the rope length between the ship and the dredge head being short and any vertical hoist adjustment of the dredge head being done when the dredge system is static. However, for dynamic hoist adjustments and for deeper applications with longer rope lengths this assumption will need to be re-evaluated. The tension force on the ship is a result of the forces applied by dredge head.

*Inertia Force*

The inertia force of the ship, $\boldsymbol{F_{i(sh)}}$, is related to the acceleration of the ship and described by Eq. (4). It is assumed that the ship's inertia acts only in the horizontal direction and any vertical component is negligible. This assumption is based on negligible wave action, no vertical adjustment of the applied tension in the ship hoist rope during the dredge movement and the cuboid shape of the ship. Moreover, it is assumed that the ship has no rotation around the *z*-axis. This assumption is based on the simplified planar analysis for this initial study. Further three-dimensional analysis will be required to understand the effects and influence of rotation on the system.

$$\boldsymbol{F_{i(sh)}} = (m_{sh})\boldsymbol{a} \tag{4}$$

where, $\boldsymbol{a}$ is the acceleration of the dredge ship and dredge head and equal to $\boldsymbol{\ddot{x}}$.

*Resolving the Tension Force*

Assuming that the ship's vertical acceleration is negligible, and the hoist tension is adjusted independent of the system's horizontal motion, and no rotation of the system we solve for the tension force.

We start by subtracting the inertia forces, $\boldsymbol{F}_{\boldsymbol{i(sh)}}$, from the net external forces applied to the ship, $\boldsymbol{F}_{\boldsymbol{sh}}$, and equate the difference to zero, as shown in Eq. (5).

$$\sum(\boldsymbol{F}_{\boldsymbol{sh}} - \boldsymbol{F}_{\boldsymbol{i(sh)}}) = 0 \tag{5}$$

Solving 5 in the ship's direction of motion we get:

$$\boldsymbol{F}_{\boldsymbol{t_x}} sin\alpha = \boldsymbol{R}_{\boldsymbol{a(sh)}_x} + \boldsymbol{R}_{\boldsymbol{(sh)}_x} + \boldsymbol{F}_{\boldsymbol{D(sh)}_x} + (m_{sh})\ddot{\boldsymbol{x}}_{\boldsymbol{x}} \tag{6}$$

where, α is the angle formed between the dredge head and the ship.

Solving 5, in the perpendicular direction of the ship's direction of motion we get:

$$\boldsymbol{F}_{\boldsymbol{t_z}} cos\alpha = \boldsymbol{F}_{\boldsymbol{l(sh)}_z} - \boldsymbol{W}_{\boldsymbol{sh}} + \boldsymbol{B}_{\boldsymbol{sh}} \tag{7}$$

**Winch and Cable Dynamics**

This section describes the winch system dynamics as a component of the entire dredge. For the dredge system under consideration here, there are four shore-mounted winches, each with their own motor controller, as shown in Figure 4.4. The dredge system also includes a hoist on the dredge ship. The hoist receives feedback from a load cell, which maintains a target force. The hoist system controls the weight of the dredge head against the bed of material and the vertical position of the dredge head. For this model, the hoist is considered fixed and independent of the four shore-mounted winches. The bed of material is considered homogeneous and isotropic. Therefore, the rope length of the hoist does not change during dredge system motion.

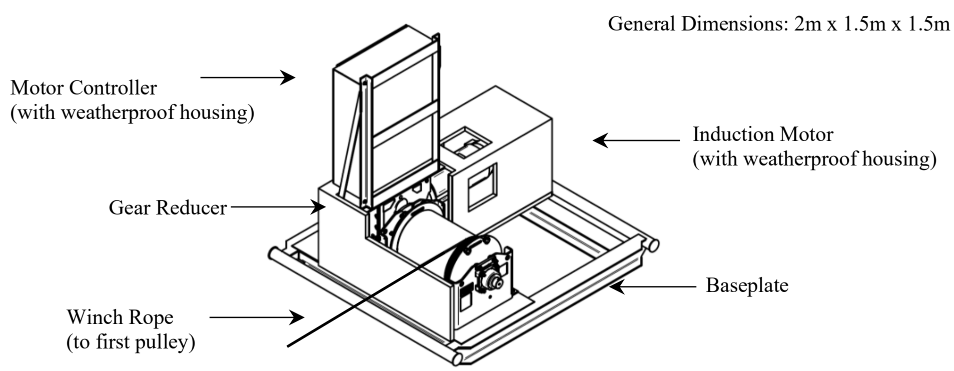


Figure 4.4: Winch & Baseplate, General Layout

Each of the shore-mounted winches connect via ropes to the centralized dredge head. The four winch ropes connect at the base of the dredge cage at the cutting ring. The cutting ring connection points are ninety-degrees from their neighbours, as shown in Figure 4.5.

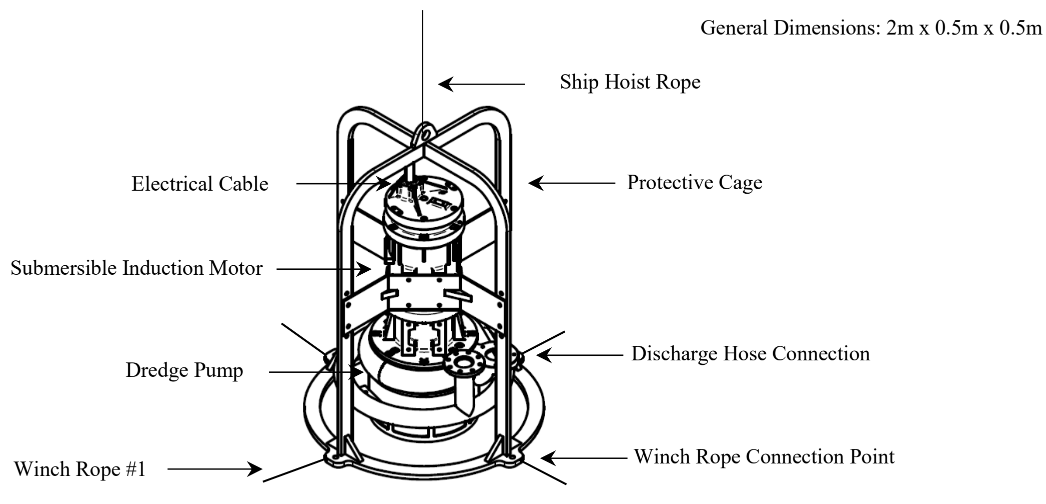


Figure 4.5: Dredge Cage, Connection Pins

Between the winch and dredge head connection points, each winch rope runs through an initial pulley. Each pulley is set a minimum distance away from the centreline of the winch drum to maintain the required fleet angle. Each position winch and associated pulley is anchored at a fixed shore location. The drum and first pulley are illustrated in Figure 4.6.

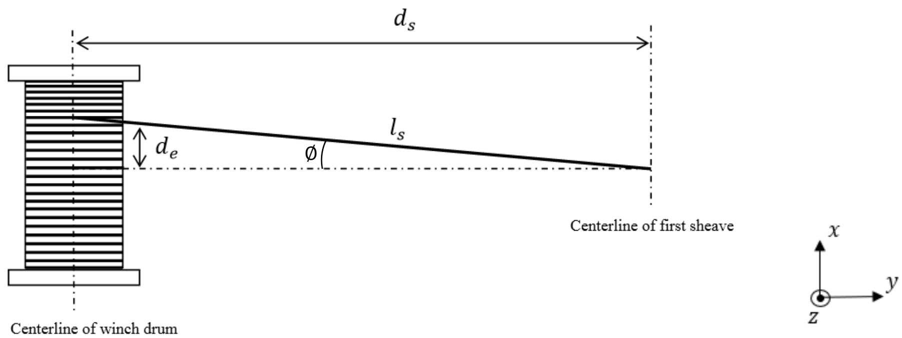


Figure 4.6: Winch Drum, Top View

Assuming the multiple rope layers that accumulate on each wrap of the drum are not a source of displacement (i.e., the radius of the winch drum, $r_d$, stays constant), and the weight of the rope is negligible, the simplified dynamic equation for the four position winches is described by Eq. (8) [135]. It is assumed that the winch is rotating slowly enough that the rotation with respect to the vertical may be neglected.

$$\boldsymbol{I_m}\ddot{\boldsymbol{q}} + \boldsymbol{T_f}\dot{\boldsymbol{q}} + r_d\boldsymbol{F_c} = \boldsymbol{\tau} \tag{8}$$

where, $\boldsymbol{\tau}$ is the vector of motor torques, $\boldsymbol{q}$ is the vector of winch drum angles, and $\boldsymbol{I_m}$ is the rotational inertia for the combined motor shaft and cable pulley,

$$\boldsymbol{I_m} = \begin{bmatrix} \boldsymbol{I_1} & 0 & 0 & 0 \\ 0 & \boldsymbol{I_2} & 0 & 0 \\ 0 & 0 & \boldsymbol{I_3} & 0 \\ 0 & 0 & 0 & \boldsymbol{I_4} \end{bmatrix}$$

$\boldsymbol{T_f}$ is the rotational matrix of motor viscous damping friction coefficients,

$$\boldsymbol{T_f} = \begin{bmatrix} \boldsymbol{t_1} & 0 & 0 & 0 \\ 0 & \boldsymbol{t_2} & 0 & 0 \\ 0 & 0 & \boldsymbol{t_3} & 0 \\ 0 & 0 & 0 & \boldsymbol{t_4} \end{bmatrix}$$

$r_d$ is the radius of the pulley/winch drum, and $\boldsymbol{F_c}$ is the force applied to the winch and equal to $D_\emptyset \boldsymbol{f_{wi}}$ where $D_\emptyset$ is the matrix that describes the angle at which the cable enters the drum and $\boldsymbol{f_{wi}}$ is the total tension force in the winch rope.

$$D_{\emptyset} = \begin{bmatrix} Cos\emptyset_{d,1} & 0 & 0 & 0 \\ 0 & Cos\emptyset_{d,2} & 0 & 0 \\ 0 & 0 & Cos\emptyset_{d,3} & 0 \\ 0 & 0 & 0 & Cos\emptyset_{d,4} \end{bmatrix}$$

$$Cos\emptyset_{d,i} = \frac{d_s}{l_s}$$

where, $d_s$ is the distance between the centreline of the winch drum and centreline of the first pulley, $l_s$ is the length of rope from exit position on winch to first pulley, and $\emptyset$ is the angle formed by the exit position of the winch rope and centreline.

*Winch Cable Dynamics*

It is assumed that the winch cables behave as a linear spring model. For large wire driven robots, that use heavy steel cables with stretch, this assumption is not reasonable. However, for the cable-driven dredge, the positioning winch cables are made of a synthetic material with a specific gravity which is like that of water. As a result, it is assumed that entire section of rope from the winch to dredge head is equally supported by the surrounding fluid resulting in negligible effect of a catenary. Moreover, the taught winch cable weight, relative to the dredge head mass, is considered negligible when evaluating the system's motion.

The linear spring model of the cable stretch is approximated through Eq. (9) [135]

$$\boldsymbol{f_{wi}} = c_i \Delta d^G{}_i + d_i \Delta d^G{}_i \tag{9}$$

where, $c_i$ is the stiffness coefficient, $d_i$ the dampening coefficient and $\Delta d^G{}_i$ denotes the length change due to elasticity.

$$\Delta d^G{}_i = d^G{}_i - d^G{}_{i,0} \tag{10}$$

where, $d^G{}_i$ is the length of the tensed cable and $d^G{}_{i,0}$ is the untensed cable.

$$c_i = \frac{EA}{d^G{}_{i,0}} = \frac{EA}{d^G{}_i\,(1-\varepsilon_i)}, \qquad \varepsilon_i = \frac{\Delta d^G{}_i}{d^G{}_i} \tag{11}$$

where, A is the cross section of the cable and E is Young's modulus. However, Papazoglou et al. [135] has shown that the dampening effects are negligible and the dominant term in underwater cables is the stiffness, which results in Eq. (12) [135],

$$\Delta l_i = \frac{\boldsymbol{f_{wi}}}{c_i} = \frac{\boldsymbol{f_{wi}} d^G{}_i(1-\frac{\Delta d^G{}_i}{d^G{}_i})}{EA} \longrightarrow \Delta l_i = \frac{\boldsymbol{f_{wi}} d^G{}_i}{EA+\boldsymbol{f_{wi}}} \tag{12}$$

Each of the positioning winch cable lengths from the first sheave to the dredge head can be described as vectors. The winch cable length vectors are shown in Eq. (13).

$$\boldsymbol{l_i} = \boldsymbol{w_i^G} - \boldsymbol{a_i^G} = \boldsymbol{w_i^G} - (\boldsymbol{p} + \boldsymbol{a_i^L}) \tag{13}$$

where $\boldsymbol{w_i^G}$ are the set of *x*, *y,* and *z* global coordinates for each of the four winch positions, $\boldsymbol{a_i^G}$ is the set of *x, y,* and *z* global coordinates for the connection points on the dredge head cage, and $\boldsymbol{p}$ is the centre of mass of the dredge head. Taking the magnitude of each vector results in Eq. (14),

$$\|\boldsymbol{l_i}\| = \|\boldsymbol{w_i^G} - (\boldsymbol{p} + \boldsymbol{a_i^L})\| \tag{14}$$

Each of the vectors can then be normalized using Eq. (15).

$$\boldsymbol{\eta_i} = \frac{\boldsymbol{l_i}}{||\boldsymbol{l_i}||} \tag{15}$$

where,

$$\boldsymbol{\eta_i} = [\, \boldsymbol{\eta_{ix}}, \boldsymbol{\eta_{iy}}, \boldsymbol{\eta_{iz}} \,] = \frac{\boldsymbol{l_i}}{||\boldsymbol{l_i}||}$$

Considering the system of cable lengths results in the matrix shown in Eq. (16).

$$\boldsymbol{A} = [\,\boldsymbol{\eta}_1\,\boldsymbol{\eta}_2\,\boldsymbol{\eta}_3\,\boldsymbol{\eta}_4] = \begin{bmatrix} \eta_{1x} & \eta_{2x} & \eta_{3x} & \eta_{4x} \\ \eta_{1y} & \eta_{2y} & \eta_{3y} & \eta_{4y} \\ \eta_{1z} & \eta_{2z} & \eta_{3z} & \eta_{4z} \end{bmatrix} \tag{16}$$

The Jacobian matrix can then be used for the transformation between the velocity of point $\boldsymbol{p}$, and the velocity of the positioning system cable lengths (where the velocity of point $\boldsymbol{p}$ is equal to the dredge head velocity, $\dot{\boldsymbol{x}}$) as shown in Eq. (17).

$$\begin{bmatrix} \dot{l}_1 \\ \dot{l}_2 \\ \dot{l}_3 \\ \dot{l}_4 \end{bmatrix} = \boldsymbol{A}^T\dot{\boldsymbol{x}} = \begin{bmatrix} \eta_{1x} & \eta_{1y} & \eta_{1z} \\ \eta_{2x} & \eta_{2y} & \eta_{2z} \\ \eta_{3x} & \eta_{3y} & \eta_{3z} \\ \eta_{4x} & \eta_{4y} & \eta_{4z} \end{bmatrix} \begin{bmatrix} \dot{x}_x \\ \dot{x}_y \\ \dot{x}_z \end{bmatrix} \tag{17}$$

*Acceleration Relationship between Cable Lengths and Dredge Head*

To determine the acceleration of point $\boldsymbol{p}$, the time derivative of Eq. (17) can be taken. $\boldsymbol{A}^T$ and $\dot{\boldsymbol{x}}$ are both dependent on time. Therefore, the derivative of Eq. (18) becomes

$$\begin{bmatrix} \ddot{l}_1 \\ \ddot{l}_2 \\ \ddot{l}_3 \\ \ddot{l}_4 \end{bmatrix} = \boldsymbol{A}^T\ddot{\boldsymbol{x}} + \dot{\boldsymbol{A}}^T\dot{\boldsymbol{x}} \tag{18}$$

**Dredge Head Dynamics**

This section describes the dredge head dynamics as a component of the entire dredge system. For the dredge system of interest, the dredge head consists of the dredge cage and pump. The dredge cage has four connection points at its base located ninety degrees from their closest neighbours. These connections are the attachment points for the four winch ropes that apply the main force for the dredge head movement. At the top of the cage, there is a single lifting point that connects the dredge head to the ship's hoist rope. The dredge pump is rigidly connected to the centre of the dredge cage. Discharge from the dredge pump runs through the discharge pipeline to shore. The discharge pipe weight is assumed to be completely supported by pipe floats.

For this preliminary work it is assumed that the main external forces acting on the dredge head act within the plane of the system's motion. This assumption will need to be further investigated in future work. To develop a reasonable estimate for the equations of motion, and the main influential forces applied to the system, we consider the dredge head in one plane. A free body diagram of the dredge head, without the pump or discharge hose, is shown in Figure 4.7.

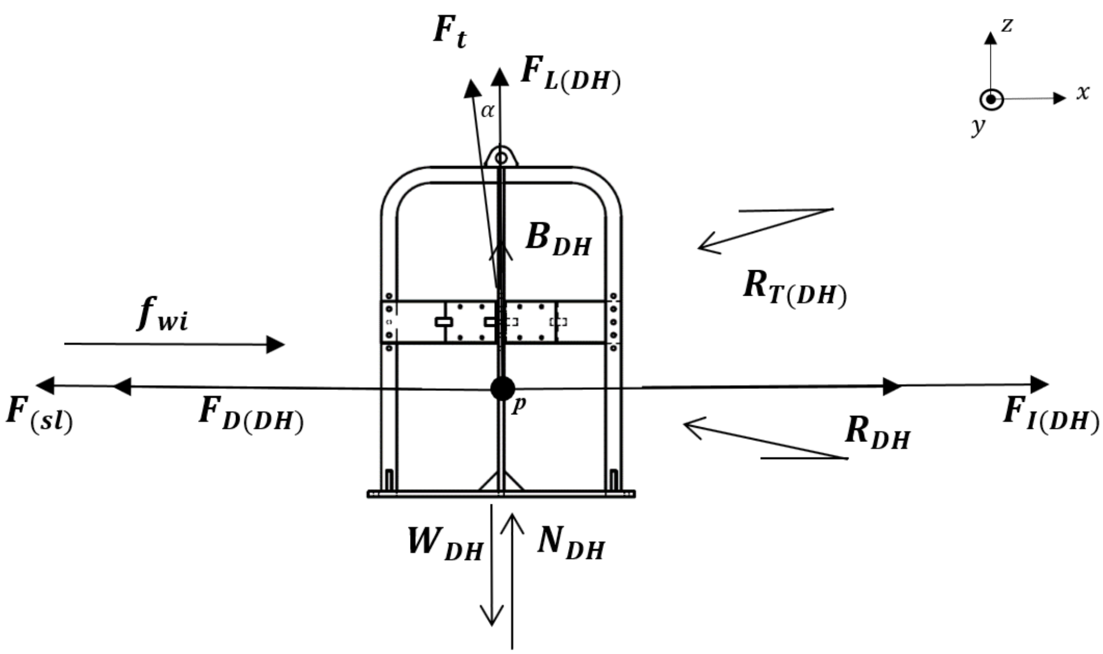


Figure 4.7: FBD, Dredge Head (with dredge pump removed)

For this analysis, several simplifying assumptions have been made.

1. Velocity and acceleration of the dredge head are only in the *x*-direction.
2. Velocity of the dredge head are less than one meter per minute.

3. For the simplified analysis of the dredge head, it is assumed the dominant forces act through the dredge head's centre of gravity resulting in negligible rotation.
4. The dredge head velocity and acceleration are equal to the ship's velocity and acceleration. This assumes an ideal transmission between the connecting cable of the dredge head and ship.
5. The dredge head is positioned on a horizontal plan within the workspace. Vertical adjustments of the dredge head are done while the system is static. Based on the dredge head movement on a horizontal plane, it is assumed that the major effects of the resistance forces act on the dredge system opposite the dredge head motion with a negligible resistance force acting in the vertical direction.
6. External factors influencing the drag and lift force are the relative velocity of the surrounding water and wind (i.e., current and wind gusts). Although high velocity currents and extreme weather can happen, for the purposes of this analysis, it is assumed that the body of water is calm, and there is no current or extreme weather. This assumption is based on typical operating conditions for the dredge system on small bodies of waters that are inland and sheltered from extreme weather.

The total resistance, drag and lift forces applied to the dredge head are not covered in depth in this study as these forces will be obtained empirically within a tow tank in future work. The following section provides a brief overview of the forces involved and their influence on the dredge head as part of this simplified analysis.

*Resistance Forces*

The total resistance of the dredge head, $\boldsymbol{R}_{\boldsymbol{T}(\boldsymbol{DH})}$, can be divided into frictional and residual resistance.

*Frictional Resistance of the Dredge Head*

The frictional resistance associated with the dredge head is caused by the interaction of the dredge head with both the fluid and the application surface (soil properties and the surface area of the dredge cutting ring). The frictional resistance for the dredge head is denoted by $\boldsymbol{R_{f(DH)}}$.

*Residual Resistance of the Dredge Head*

The residual resistance of the dredge head is dependent on wave and eddy resistance of the fluid. The residual resistance of the dredge head is denoted by $\boldsymbol{R_{R(DH)}}$.

*Drag Force*

As the dredge cage moves through a fluid at a velocity, $\boldsymbol{v}$, the fluid will apply a drag force on the dredge head opposite its relative motion. The drag force is denoted by $\boldsymbol{F_{D(DH)}}$.

*Lift Force*

As the dredge head moves through the fluid at a velocity, $\boldsymbol{v}$, the fluid will apply a lift force on the dredge cage perpendicular to its relative motion. The lift force is denoted by $\boldsymbol{F_{L(DH)}}$.

*Dredge Head Weight*

The dredge head is made up of the dredge cage and the dredge pump. Therefore, the overall weight of the dredge head $\boldsymbol{W_{(DH)}}$ consists of the dredge cage weight $\boldsymbol{W_{cage}}$, plus the dredge pump weight $\boldsymbol{W_{pump}}$. The dredge head weight force acts through the centre of gravity located at point $\boldsymbol{p}$, as shown in Figure 4.7. The total dredge head weight force is shown by Eq. (19).

$$\boldsymbol{W}_{(\boldsymbol{DH})} = \boldsymbol{W}_{\boldsymbol{cage}} + \boldsymbol{W}_{\boldsymbol{pump}} \tag{19}$$

*Buoyancy*

The buoyancy force applied by the displaced volume of water is described by Eq. (20).

$$\boldsymbol{B}_{(\boldsymbol{DH})} = \rho_{f(DH)} V_{(DH)} \boldsymbol{g} \tag{20}$$

where, $\boldsymbol{V}_{(\boldsymbol{DH})}$ is the total volume of fluid displaced by the dredge head and $\rho_{f(DH)}$ is the density of the fluid around the dredge head.

*Cutting Force*

The dredge head encounters a cutting force, $\boldsymbol{R}_{\boldsymbol{DH}}$, caused by the interaction of the dredge cage cutting ring, and the pond floor, as shown in Figure 4.7. We assume that the dredge pump excavates the soil as it moves through the mudline. Therefore, the buildup of material in front of the dredge head and the associated force is considered negligible. The cutting force acts in the opposite direction of the dredge cage motion and is described in Eq. (21).

Assuming the cutting forces only acts in the direction opposite of the dredge head, Miedema [84] has described the cutting force as follows.

$$\boldsymbol{R}_{\boldsymbol{DH}} = C_c \boldsymbol{v} h_c^2 \tag{21}$$

where, $C_c$ is the coefficient of cutting force which depends on the soil properties, and $h_c$ is the thickness of the cutting ring.

The depth of the material cut is dependent on the hoist rope length, soil properties, the horizontal area of the cutting ring, and the normal force applied to the base of the dredge head.

*Normal Force*

A normal force, $\boldsymbol{N}_{(\boldsymbol{DH})}$, is applied to the base of the dredge head and is equal to the dredge head weight applied to the soil plus any vertical component associated with the interaction of the soil and the dredge head.

*Tension Force Applied by Hoist*

The tension force in the wire rope connection between the ship gantry and the dredge head were developed in the ship dynamics section. The equal and opposite tension force is applied to the dredge head connection point. The tension forces applied to the dredge head are summarized in Eqs. (6) and (7).

*Force Applied by the Discharge Hose*

Between the dredge head and the shore, the discharge hose is installed in a serpentine configuration along the water's surface, as shown in Figure 4.8.

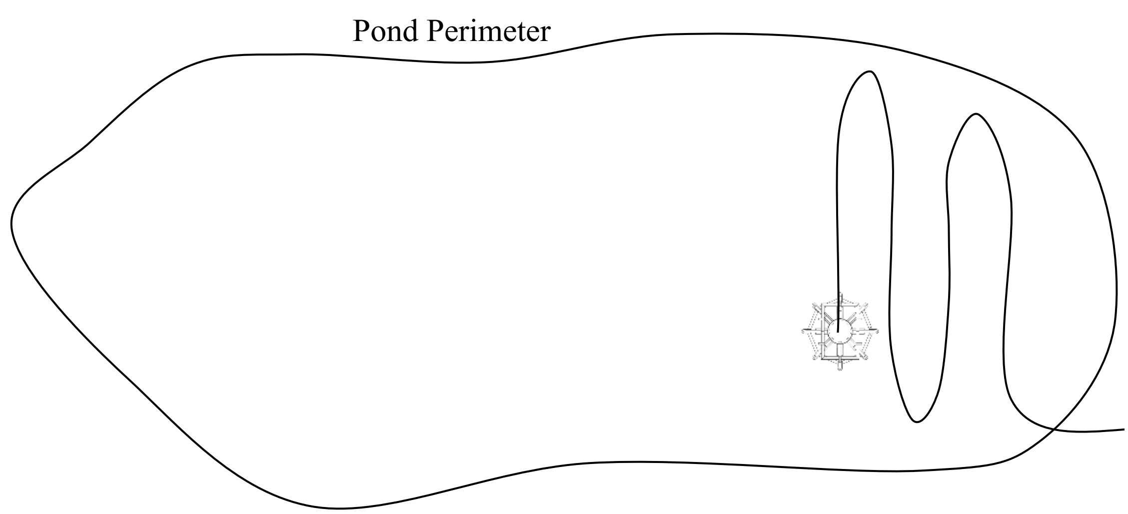


Figure 4.8: General Overview, Serpentine Discharge Hose

The serpentine configuration hose is modeled as a flexible rope, supported by floats at the water's surface. The flexible discharge hose and floats are shown in Figure 4.9.

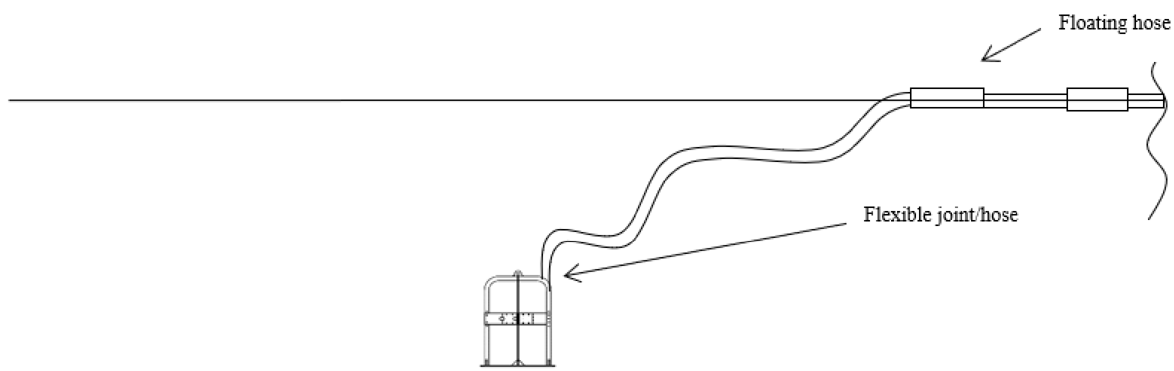


Figure 4.9: Flexible Discharge Hose

Since the discharge hose is modeled as a flexible rope, it is assumed to apply no compression force on the dredge head. We further assume that sufficient hose length is available so that the tension force applied to the dredge head is negligible.

*Momentum Force of Slurry*

We also consider the force generated by the change in momentum of slurry existing the dredge head. This force is described by Eq. (24).

$$\begin{aligned} \boldsymbol{F}_{(sl)_x} &= [(\dot{m}\boldsymbol{V})_{out} - (\dot{m}\boldsymbol{V})_{in}]_x \\ \boldsymbol{F}_{(sl)_y} &= [(\dot{m}\boldsymbol{V})_{out} - (\dot{m}\boldsymbol{V})_{in}]_y \end{aligned} \tag{24}$$

where, $\dot{m}$ is the mass flow rate concentration in the discharge pipe, and $\boldsymbol{V}$ is the measured velocity of the slurry flow.

*Inertia Force*

The inertia force is related to the acceleration of the dredge head as it moves through the water. The total inertia force is described by Eq. (25).

$$\boldsymbol{F}_{\boldsymbol{I}(\boldsymbol{DH})} = \left(m_{(DH)}\right)\boldsymbol{a} \tag{25}$$

where, $m_{(DH)}$ is the mass of the dredge head.

*Propulsion Force Applied by the Positioning Winches*

Four shore-mounted winches apply a coordinated force to the dredge head to move it along a predetermined path. Each of the four winch drums is connected to the dredge head through a corresponding winch rope. The shore-mounted winches are used to position the dredge head within the operating area. The force applied by each of the positioning winches acts in three dimensions. However, for this simplified analysis we have only considered the dredge head motion to act in a two-dimensional plane.

The winch rope forces applied to the dredge head are summarized below:

$\boldsymbol{f}_{\boldsymbol{w1}}$ is the force applied to the dredge head by winch 1;

$\boldsymbol{f}_{\boldsymbol{w2}}$ is the force applied to the dredge head by winch 2;

$\boldsymbol{f}_{\boldsymbol{w3}}$ is the force applied to the dredge head by winch 3;

$\boldsymbol{f}_{\boldsymbol{w4}}$ is the force applied to the dredge head by winch 4.

*Dredge Head, Motion Equations*

For Eq. (26), we assume the dredge head's vertical acceleration is negligible, the dredge surface area is flat, and the hoist tension is adjusted independently of the dredge head motion.

$$\sum\left(\boldsymbol{F}_{(DH)} - \boldsymbol{F}_{I(DH)}\right) = 0 \tag{26}$$

where, $\boldsymbol{F}_{(\boldsymbol{DH})}$ is the net external forces applied to the dredge head, and $\boldsymbol{F}_{\boldsymbol{I}(\boldsymbol{DH})}$ is the inertia force.

**Planar Cable-driven Dredge Dynamics**

After looking at the equations and influencing forces for each of the dredge system components, we now consider the interaction of the cable-driven system. This is done to refine the system dynamics, based on the assumptions made. This allows us to see which aspects of the system need to be included because they are found to contribute significantly to the governing equations, and which of the operating conditions are constrained such that they can be ignored.

We consider the cable-driven dredge to have three degrees of freedom, with negligible rotation around its centre of mass. The assumption of negligible rotation may not be reasonable. However, this assumption was necessary as part of the lean approach in this initial investigation. Further studies will need to include the influence of rotation on the system to understand the influence when developing a complete system controller. The cable-driven dredge uses a four-winch positioning system, as illustrated in Figure 4.10.

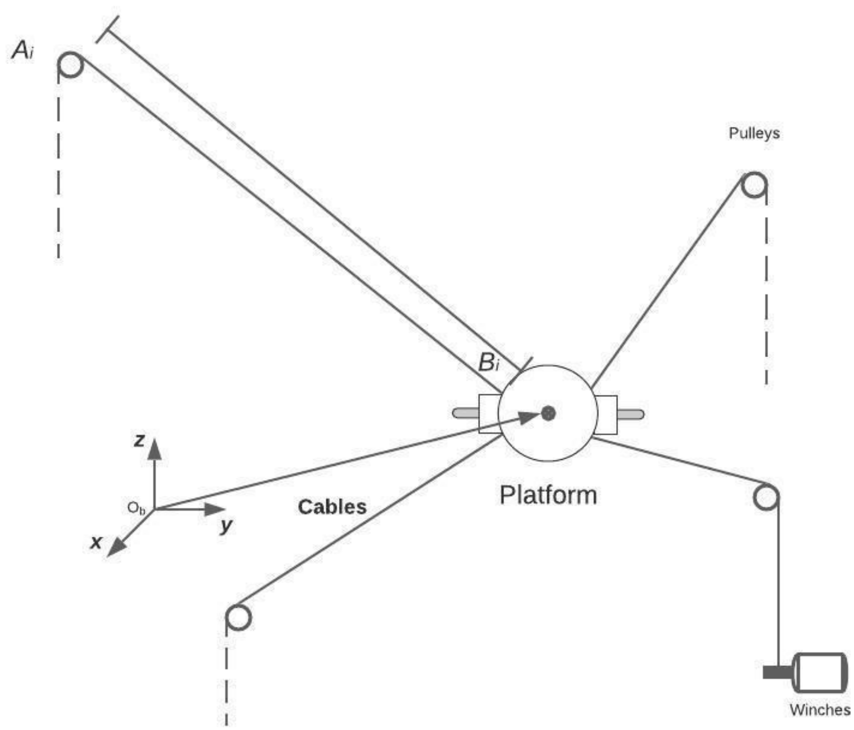


Figure 4.10: The Cable-driven Robot and Its Components [141]

For simplification, it is assumed that the winches and dredge head work on the same two-dimensional plane and each actuator and pulley are combined as a lumped mass. The dredge system is illustrated in Figure 4.11 and the lumped motor shaft and cable pulley are illustrated in Figure 4.12

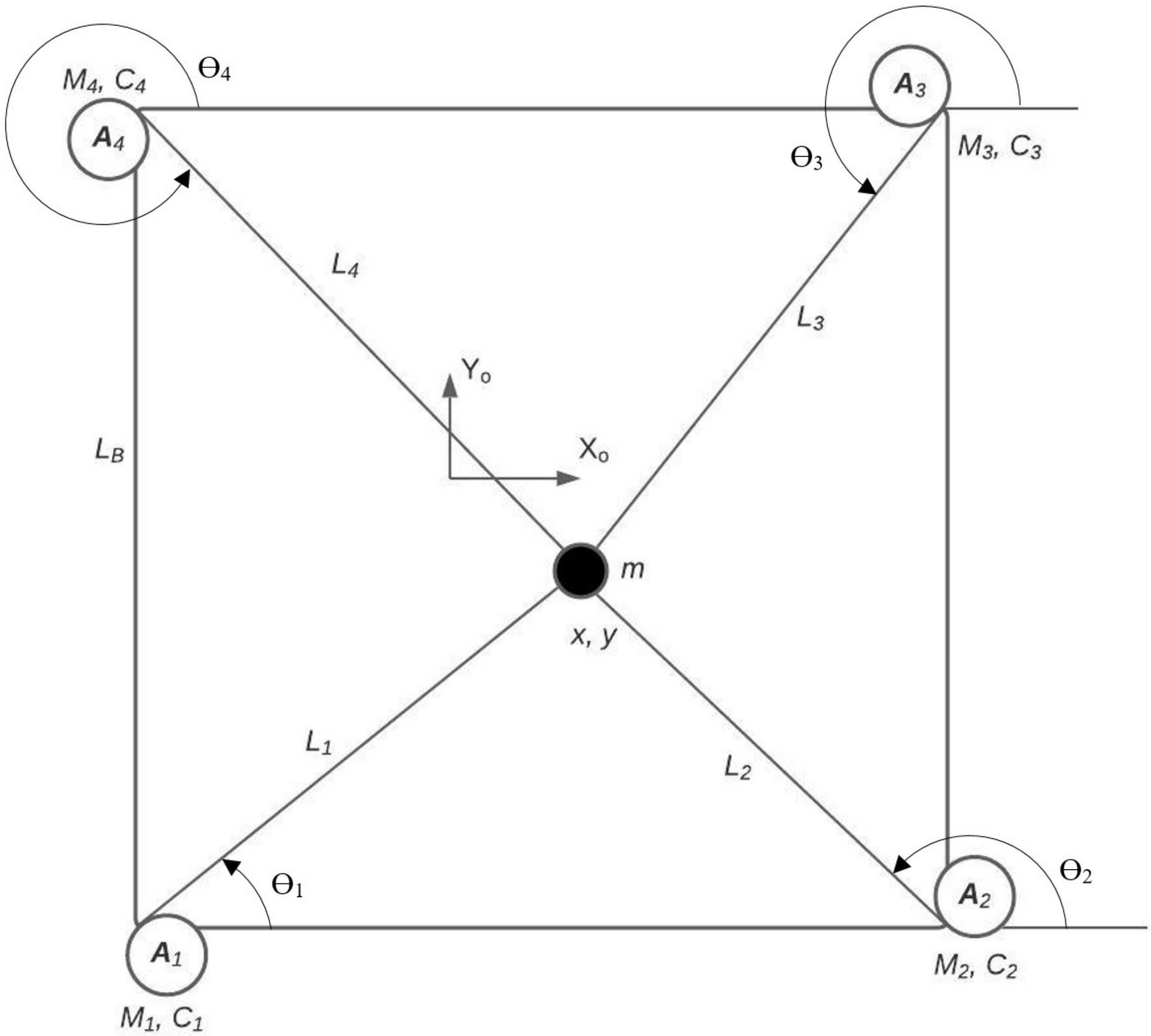


Figure 4.11: Four Cable, Planar System with Rectangular Configuration of Winches [142, 143]

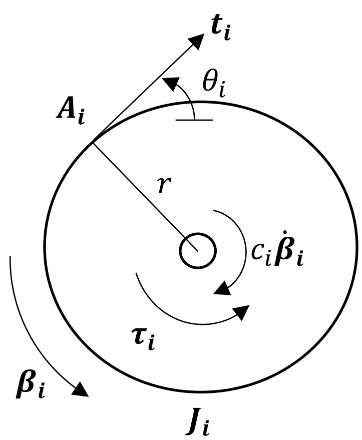


Figure 4.12: Free body diagram of the *i*[th] shaft/pulley [142, 143]

If the dredge head is considered a lumped mass, with no rotation, and the connecting cables between the winches and the dredge head are considered to have constant tension, with no elongation, then Gallina et al. [142] describe the dynamic equation by Eq. (27).

$$M\ddot{\boldsymbol{X}} = \boldsymbol{F} \tag{27}$$

where, $\boldsymbol{X} = \{x, y\}$ in Cartesian coordinates, $M = m\ x\ I$, where $m$ is the lumped mass of the of the system and $I$ is the identity matrix, and $\boldsymbol{F}$ is the resultant of the cable forces acting on the dredge head.

Considering a force balance on the dredge head in Figure 4.11 we get Eq. (28) [142].

$$\boldsymbol{F} = S\boldsymbol{T} \tag{28}$$

where, $\boldsymbol{T} \in \mathbb{R}^n$ is the vector of cable tensions, $t_i$, and

$$S = \begin{bmatrix} -cos\ \theta_1, & cos\ \theta_2, & cos\ \theta_{3,} & -cos\ \theta_4 \\ -sin\ \theta_1, & -sin\ \theta_2, & sin\ \theta_3 & sin\ \theta_4 \end{bmatrix}.$$

Next, we considering the dynamics of the pulley/motor shaft from the free body diagram shown in Figure 4.12 [142]. We consider a lumped mass rotational inertia for the shaft and cable pulley of each actuator as described by Eq. (29) [142].

$$\boldsymbol{J\ddot{\beta}} + C\boldsymbol{\dot{\beta}} + r\boldsymbol{T} = \boldsymbol{\tau} \tag{29}$$

where,

$\boldsymbol{A_i} = \{\boldsymbol{A_{ix}}, \boldsymbol{A_{iy}}\}^T$ is the fixed shaft/pulley location

$L_i$ and $\theta_i$ are the length and angle of each cable respectively,

$r = r_{1,} r_{2,} r_{3,} r_4$ is the cable pulley radii which is identical for all four pulleys,

$C = Diag\ \{C_1, C, C_3, C_4\}$ are the rotational viscous damping coefficients.

$\boldsymbol{J} = Diag\ \{\boldsymbol{J_1}, \boldsymbol{J_2}, \boldsymbol{J_3}, \boldsymbol{J_4}\}$ and is the rotational inertia of the lumped pulley/motor shaft

$\boldsymbol{\tau} \in \mathbb{R}^n$ is the torques exerted by the winch motors, $\tau_i$

$\boldsymbol{\beta} \in \mathbb{R}^n$ is the vector of pulley cables, $\boldsymbol{\beta_i}$. $\boldsymbol{\beta_i} = 0$ when the dredge head is located at the origin and a positive angle $\boldsymbol{\beta}_i$ on one pulley results in a change in cable length $\Delta\boldsymbol{L_i} = \boldsymbol{L_i} - \Delta\boldsymbol{L_{0i}} = -\boldsymbol{\beta}_i r$

where,

$$\boldsymbol{L_i} = \sqrt{(\boldsymbol{x} - \boldsymbol{A_{ix}})^2 + (\boldsymbol{y} - \boldsymbol{A_{iy}})^2}$$ is the general winch cable lengths and

$$\boldsymbol{L_{0i}} = \sqrt{(\boldsymbol{A_{ix}})^2 + (\boldsymbol{A_{iy}})^2}$$ is the initial winch cable length.

$$\boldsymbol{\beta} = \begin{bmatrix} \boldsymbol{\beta_1}(\boldsymbol{X}) \\ \vdots \\ \boldsymbol{\beta_4}(\boldsymbol{X}) \end{bmatrix} = \frac{1}{r} \begin{bmatrix} \boldsymbol{L_1} - \sqrt{(\boldsymbol{x} - \boldsymbol{A_{1x}})^2 + (\boldsymbol{y} - \boldsymbol{A_{1y}})^2} \\ \vdots \\ \boldsymbol{L_n} - \sqrt{(\boldsymbol{x} - \boldsymbol{A_{4x}})^2 + (\boldsymbol{y} - \boldsymbol{A_{4y}})^2} \end{bmatrix}$$

Taking the time derivative of $\boldsymbol{\beta}(\boldsymbol{X})$ and substituting into Eq. (30) [142] we obtain,

$$\boldsymbol{J}\left(\frac{d}{dt}\frac{\partial\boldsymbol{\beta}}{dX}\dot{\boldsymbol{X}} + \frac{\partial\boldsymbol{\beta}}{dX}\ddot{\boldsymbol{X}}\right) + C\frac{\partial\boldsymbol{\beta}}{dX}\dot{\boldsymbol{X}} = \boldsymbol{\tau} - \boldsymbol{T}r \tag{30}$$

where,

$$\frac{\partial\boldsymbol{\beta}}{dX} = -\frac{1}{r}\begin{bmatrix} \frac{x-\boldsymbol{A_{1x}}}{\boldsymbol{L_1}}, & \frac{y-\boldsymbol{A_{1y}}}{\boldsymbol{L_1}} \\ & \vdots \\ \frac{\boldsymbol{x}-\boldsymbol{A_{4x}}}{\boldsymbol{L_1}}, & \frac{\boldsymbol{y}-\boldsymbol{A_{4y}}}{L_4} \end{bmatrix}$$

Combining equations 30, 29 and 28 the standard form of the dynamical equation for the cable-driven dredge are described through Eq. (31) [142].

$$M_{eq}(X)\ddot{\boldsymbol{X}} + \boldsymbol{N}(X,\dot{X}) = \boldsymbol{S}(X)\boldsymbol{\tau} \tag{31}$$

where,

$$M_{eq} = rM + \boldsymbol{S}(X)\boldsymbol{J}\frac{\partial\boldsymbol{\beta}}{dX}$$

$$\boldsymbol{N}(X,\dot{X}) = \boldsymbol{S}(X)\left(\boldsymbol{J}\frac{d}{dt}\frac{\partial\boldsymbol{\beta}}{dX} + C\frac{\partial\boldsymbol{\beta}}{dX}\right)\dot{\boldsymbol{X}}$$

**S** is a function of X since the relationship between the angle of the winches $\theta_i$ is

$$\theta_i = \tan^{-1}\left(\frac{\boldsymbol{y}-\boldsymbol{A_{iy}}}{\boldsymbol{x}-\boldsymbol{A_{ix}}}\right)$$

**Discharge Pipe Model**

To estimate the pressure loss in pipe we use Furboter's model [79, 98] in combination with Worster and Denny [108] modeling the vertical section of the pipe.

$$\Delta P_{loss} = \Delta P_{ph} + \Delta P_{pi} \tag{32}$$

where, $\Delta P_{ph}$ is the horizontal resistance in the pipeline, and $\Delta P_{pi}$ is the pressure loss in the inclined section of the pipeline.

$$\Delta P_{ph} = \lambda_f a_p Q_m^2 + \frac{\rho_w \, g \, S_{kt} b_p C_t}{Q_m} \tag{33}$$

$$\Delta P_{pi} = \lambda_f a_p Q_m^2 + \frac{\rho_w \, g \, S_{kt} b_p C_t}{Q_m} \cos \beta_p \tag{34}$$

where,

$a_p = 8 \frac{\rho_w L_p}{\pi^2 {D_p}^5}$,

$b_p = \pi \frac{D^2}{4} L_p$,

$C_t$ is the transport concentration

$Q_m$ is the mixture flow rate

$\lambda_f$ is the coefficient of friction for water,

$\rho_w$ is the density of water,

$D_p$ is the diameter of the pipe,

$S_{kt}$ is the coefficient for the solids,

$L_p$ is the pipe length,

$g$ is the gravitational constant,

$\beta_p$ is the angle of the pipe.

*Deposition Velocity*

Once the mixture enters the discharge pipeline, there are four common flow regimes: homogeneous; pseudo-homogeneous; heterogeneous, partly stratified; heterogeneous, fully stratified [144]. One of the factors governing the rate of production is the critical deposition velocity of the solids being transported. Critical velocity is dependent on the solid particle size, particle shape, density, and percent of solids in the mixture. If a minimum velocity is not met, the particles will fall out of suspension and begin to settle in the pipeline. As a result of this deposition, the dredge system may experience a restriction or line plugging resulting in a total loss of fluid flow. If, however, the velocity of the slurry fluid is too high, energy is wasted through additional frictional losses and mixing, with little to no dredge production benefits [144]. A heterogeneous mixture is the most economical for solids transport [145].

With Newtonian fluids, the critical deposition velocity, $\boldsymbol{V_c}$, is described by [146]

$$\boldsymbol{V_c} = \begin{cases} 21{D_p}^{0.11}(S-1)^{0.37}(\mu_\omega/\rho_w)^{0.26} & for\ d_{50} \leq 100\ \mu m \\ 6.32{D_p}^{0.468}d^{0.168}{C_s}^{0.356}(S-1)^{0.545}(\rho_\omega/\mu_\omega)^{0.09} & for\ d_{50} \leq 100\ \mu m \end{cases} \quad (35)$$

where,

$D_p$ is the pipe diameter,

$S$ is equal to $\frac{\rho_s}{\rho_w}$,

$\mu_\omega$ is the viscosity of water,

$d$ is the particle diameter,

$\rho_f$ is the density of the fluid,

$C_s$ is the solid particle volume fraction, and

$\mu_m$ is the viscosity of mixture

**Pump and Production Model**

*Pump Characteristics*

A characteristics curve for each dredge pump is developed based on manufacturer's data. However, affinity laws serve as a useful way of scaling the characteristics curve data based on different impeller diameters and rotational speeds. The affinity laws [147], for flow $Q$, head $H$, and base horse power $P$ are shown in Eqs. (36), (37), and (38), respectively:

$$Q_2 = Q_1 \left(\frac{b_2}{b_1}\right)\left(\frac{h_2}{h_1}\right) \tag{36}$$

$$H_2 = H_1 \left(\frac{b_2}{b_1}\right)^2 \left(\frac{h_2}{h_1}\right)^2 \tag{37}$$

$$P_2 = P_1 \left(\frac{b_2}{b_1}\right)^3 \left(\frac{h_2}{h_1}\right)^3 \tag{38}$$

where, *b* is the rotation speed of the pump shaft, and *h* is the external diameter of the pump's impeller.

*Dredge Production*

Using water as the carrier fluid for solids transport, the average production rate $Q_p$ of a of a homogenous mixture, with no slip, can be described by Eq. (39):

$$Q_p = Q_m C_v \tag{39}$$

where,

$C_v = \frac{\rho_m - \rho_w}{\rho_s - \rho_w}$ is the concentration of the mixture, by volume,

$\rho_s$ is density of solid,

$\rho_m$ is density of the mixture.

As solids are introduced to a dredge system, the mixture influences the pump head characteristics and efficiency. The head and efficiency reduction ratios [148] are shown in Eq. (40) and (41).

$$H_r = \frac{H_m}{H_w} \tag{40}$$

where, $H_m$ is the head of mixture and $H_w$ is the head of water.

$$\eta_r = \frac{\eta_m}{\eta_w} \quad (41)$$

where, $\eta_m$ is the pump's efficiency with a mixture and $\eta_w$ is the pump's efficiency with water.

The exact ratios are specific and unique, and dependent not only on the pump, but also the mixture characteristics. However, researchers have gathered head ratio and efficiency ratio data for a variety of applications. Using the test data provided by Wilson et. al. [148], the head ratio and efficiency ratio have been generalized so an estimate of these ratios can be determined based on the average particle size and impeller diameter.

The test data presented by Wilson, K. et. al. [148] are based on solids with a specific gravity equal to 2.65 and a constant volume concentration of the mixture being 15%. Correction factors are presented for different mixture concentrations up to 20% which is a realistic range for practical dredge applications. The correction factor [148] for different concentrations is shown by Eq. (42).

$$R_H = HR_{15\%} \frac{C_v}{0.15} \quad (42)$$

where, $HR_{15\%}$ is the head reduction based on empirical test data at a constant $C_v$ of 15% and $H_r = 1 - R_H$.

For concentration with solids specific gravity equal to 2.65, average particle size of 425 µm and impeller diameter of 152 mm $R_H \cong C_v$ [148].

$$R_H \cong C_v \quad (43)$$

The efficiency reduction for a slurry mixture is also shown through experimental data in Eq. (44) [148],

$$\eta_r = 1 - R_\eta \tag{44}$$

where, $R_\eta$ is the reduction of pump efficiency, $R_H = R_\eta$ (assumed for small pumps) [148].

The power required to move a mixture is described by Eq. (45).

$$P_m = \frac{\rho_m \, g \, H_m \, Q_m}{\eta_m} \tag{45}$$

Substituting terms from Eqs. (40), (41), (42), and (44) into (45) and rearranging, we get Eq. (46).

$$C_v = \frac{\left(\frac{P_m \, \eta_w}{g \, Q_m H_w}\right) - \rho_w}{\rho_s - \rho_w} \tag{46}$$

At constant pump speed and flow rate for a given mixture through a pipeline, the head and efficiency values are always equal to, or lower than, water [148]. Therefore, we can use a convergence of a unique solution to Eq. (46) to satisfy through an iterative error reduction algorithm to solve for a predicted solids concentration and mixture flow rate.

**Production Algorithm**

The following assumptions are made in the development of the algorithm.

- The dredge pump operates at a steady state.
- The dredge pump power draw and discharge pressure are measured quantities.
- The dredge pump water curve data (manufacturers data) is known.
- The power consumption curve for the dredge pump has positive slope for the range of flow rates.
- The carrier fluid is water.
- The solids density of the mixture is greater than that of water.

- The solids are finely graded sands of density S = 2650 kg/m³, with $d_{50}$ = 425µm.
- The mixture flow is heterogeneous.

A generic production diagram is shown in Figure 4.13 and illustrates the steps of the algorithm.

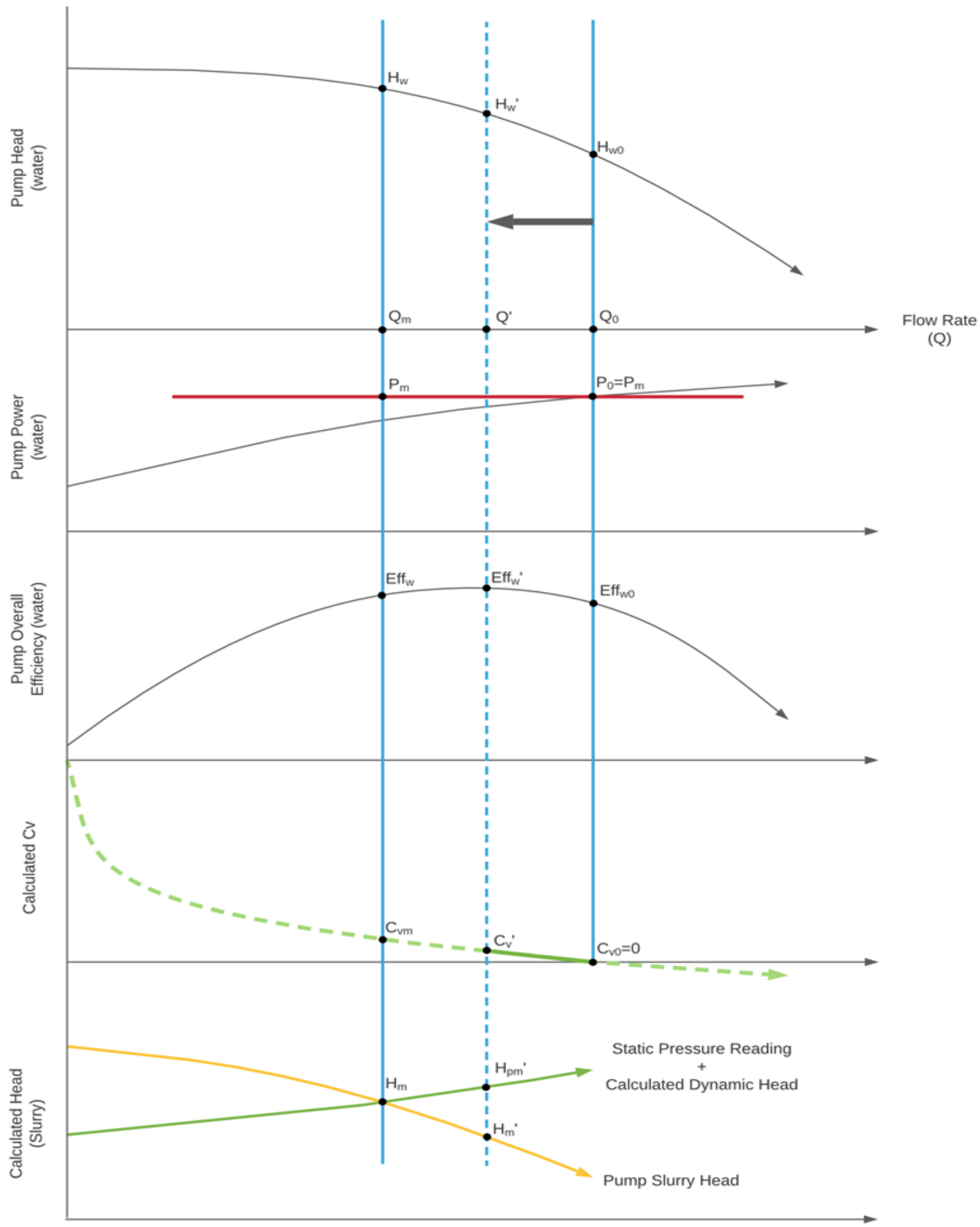


Figure 4.13: Generic Production Diagram

*Algorithm Steps*

1) When pumping clear water, plot the measured system power input, $P_m$, as a horizontal line across the range of pump flow rates. The intersection of the horizontal line with the pump's power curve for water (point $P_0$) marks the maximum possible flow rate and corresponds to $C_v = 0\%$. The operating flow rate $Q_m$ must be less than $Q_0$.
   a) This is the maximum possible flow rate because this is the power required to pump clean water based on a pump's characteristic curve on water.
   b) This maximum flow value and input power should be verified for different site conditions and equipment configurations by operating the pump in clean water while connected to the complete system. The pump input power, discharge head, and flow rate on clean water must always match the published curve or calculation error will result.
   c) If $P_m$ is greater than all points of the power curve, set $Q_0$ to the maximum pump flow rate.
2) Choose an arbitrary flow rate $Q'$. The corresponding head on water $H_w'$ and efficiency on water $Eff_w'$ is read from the pump characteristic curve.
3) $C_v'$ is calculated using Eq. (46).
4) Using the $C_v'$ and Eq. (42), (40), $H_w'$ is reduced to $H_m'$ accounting for the head reduction caused by the solid particles in the slurry mixture.
5) The static pressure sensor reading is then converted to Total Dynamic Head (TDH) of slurry using $Q'$ and $C_v'$ in Eqs. (47), (48), (49).

$$H_{pm}' = \frac{P_s}{\rho' g} + \frac{V'^2}{2g} \tag{47}$$

$$V' = \frac{4Q'}{\pi D_s} \tag{48}$$

$$\rho' = \rho_w + C_v' \left(\rho_s - \rho_w\right) \tag{49}$$

where,

$H_{pm}'$ is the Total Dynamic Head at the pressure sensor,

$P_s$ is the pressure measured by the sensor,

$V'$ is the mixture velocity at the pressure sensor,

$D_s$ is the pipe diameter at the pressure sensor,

$\rho'$ is the mixture density.

1) While $H_{pm}'$ is greater than $H_m'$, decrease $Q'$ until convergence as shown by Figure 4.13. If $H_{pm}'$ is less than $H_m'$, $Q'$ must be increased.
2) At convergence, $Q_m$ is equal to $Q'$, $C_{vm}$ is equal to $C_v'$.

Limitation of the production algorithm[3] and Eq. (46) are as follows.

- $0\% < C_v < 20\%$.
- For small pumps, $R_H = R_\eta$ [148]
- Particles in the mixture under 40 µm are assumed to be negligible.
- Solids SG of 2.65.

**Excavation Model**

The compactness of the in-situ solids influences dredge production. The solid's shape, size, and density are the main factors which influence the ability of the passing fluid to generate enough lift so that the solid may be suspended in the fluid and transported to the inlet of the dredge system. Compacted solids must be broken up for effective fluid transport to occur. The

[3] Note: Correction factors for the above conditions have been provided by Wilson et. Al [148] K. Wilson, G. Addie, A. Sellgreen, and R. Clift, *Slurry Transport using Centrifugal Pumps*. New York: Springer Science, 2006. However, these corrections were not used in this model verification.

erosion generated by the inlet flow of the dredge pump is insufficient to fluidize compacted material [11]. For compacted soils, a mechanical agitator is required to break up these bonds before the solids may be fluidized. For loosely compacted solids, such as coarse sands, a high-pressure waterjet may be sufficient[4]. For loose, free-flowing solids, such as fine particles, the solids may be held in suspension as a slurry and will tend to migrate toward the inlet of the dredge pump. As the percentage of solids increase, the slurry density increases which requires more power input to transport the mixture.

To maintain a consistent excavation rate, the cable-driven dredge in this study continuously moves along a path. As it moves, the dredge cage ring excavates a layer of sediment, as illustrated in Figure 4.14.

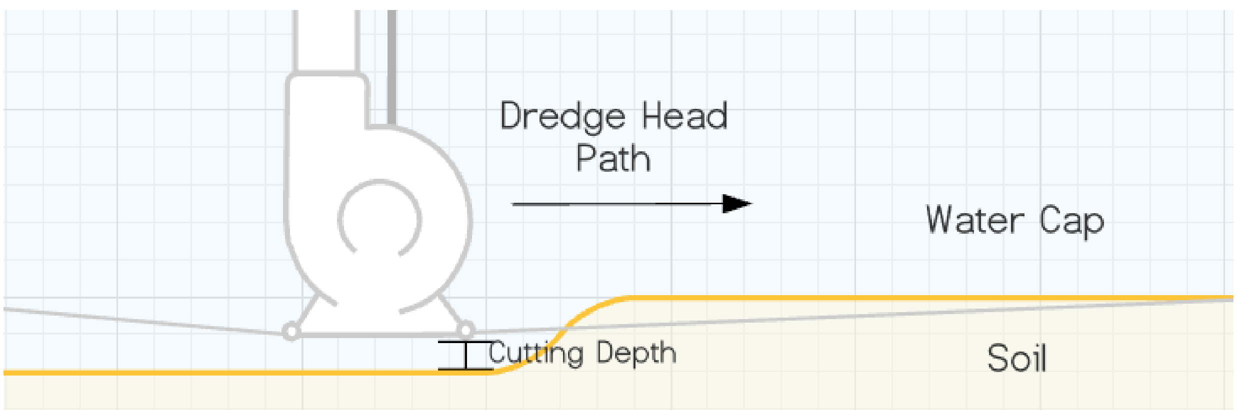


Figure 4.14: Dredge Head Cut and Path

We assume that the dredge head penetrates the saturated sediment bed, and the connecting ropes to the barge ship and positioning winches are taught. This assumption is based on (1) the dredge head weight and (2) the erosion effects around the pump during operation. The

[4] The rate at which the solids are excavated may be influenced by a form of agitation. However, agitation methods on production are not considered in this work.

estimated rate at which the dredge system excavates the solid layer, as the system moves, is described by Eq. (50).

$$\dot{E}_D = k_s \, w_{cr} \boldsymbol{v} \, h_d \rho_{si} \tag{50}$$

where,

$w_{cr}$ is the width of the dredge cage cutting ring,

$\boldsymbol{v}$ is the velocity of the dredge head,

$h_d$ is the depth of the cutting ring into the material,

$\rho_{si}$ is the in-situ density of the solids before being excavated,

$k_s$ is the spillage or excess material being transported to the inlet of the pump.

Once the solids enter the dredge pump and pipeline, there are upper limits for the production rate. If the mixture density increases and the flow remains the same, the required power to move the mixture increases. If the dredge pump has insufficient power to meet the energy demands of the dredge setup, the flow rate and pressure will decrease to an operating point that satisfies the system conditions and power constraints.

**Dredge Head Position Control**

Control is all about modifying the natural dynamics of the system to achieve some preferred output, subject to the limitations of performance. However, at this preliminary stage the understanding of the dynamics is limited, and therefore so is the potential to control the system. The following section provides a brief overview of the cable-driven dredge control methods, as well as the system's control limitations and the boundary conditions. However, it is not the goal of this thesis to develop a control system nor to optimize the process at this preliminary stage.

The control hierarchy for the cable-driven dredge is shown in Figure 4.15.

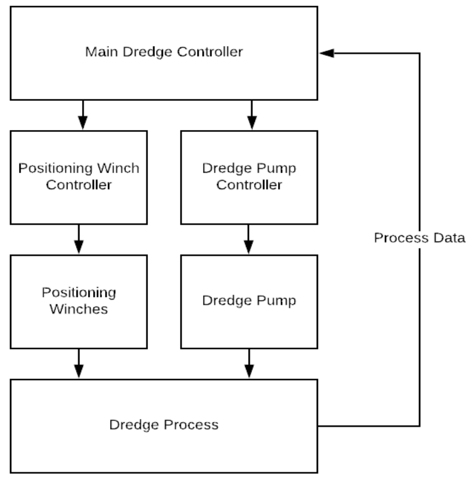


Figure 4.15: Dredge System Hierarchy Control

*Method for System Control*

We consider a method proposed by Bruckmann et al. [149, 150] to control the dredge system's movement along a predetermined path. This solution [149] provides control of the end effector in operational space which allows an otherwise non-linear equation to be linearized through feedback. It is important to note that this solution does not consider rotation. The non-iterative solution presented by Bruckmann et al. [149] provides continuous solutions and is differentiable at all points there is a solution [135].

The nonlinear control solution is shown in Eq. (51) [149].

$$\boldsymbol{u} = \boldsymbol{K}_p(\boldsymbol{q_d} - \boldsymbol{q}) + \boldsymbol{K}_v(\dot{\boldsymbol{q}}_{\boldsymbol{d}} - \dot{\boldsymbol{q}}) + \boldsymbol{M_m}\ddot{\boldsymbol{q}}_{\boldsymbol{d}} + \boldsymbol{T_f}\dot{\boldsymbol{q}}_{\boldsymbol{d}} + r\boldsymbol{D}\boldsymbol{f_{wi}} \tag{51}$$

where,

$\boldsymbol{K}_p$ and $\boldsymbol{K}_v$ and are matrices of constants,

$\dot{\boldsymbol{q}}$ is the angular velocity,

$\ddot{\boldsymbol{q}}$ is the angular acceleration,

$\boldsymbol{M_m}$ is the rotational inertia,

$\boldsymbol{T_f}$ is the is the matrix of motor viscous friction coefficients,

$r$ is the radius of the drum,

$\boldsymbol{D}$ is the matrix that describes the angles $\theta_{d,i}$ at which the rope is entering the drum,

$\boldsymbol{f_{wi}}$ is the forces in the ropes,

$\boldsymbol{u}$ is the vector of motor torques.

The dynamics of the system can be expressed as [149]:

$$\boldsymbol{M_p}\,\ddot{\boldsymbol{p}} - \boldsymbol{g_E} + \left(\boldsymbol{M_m}\ddot{\boldsymbol{q}}_{\boldsymbol{d}} + \boldsymbol{T_f}\dot{\boldsymbol{q}}_{\boldsymbol{d}}\right)\frac{\boldsymbol{A^T D^{-1}}}{r} = \boldsymbol{u}\frac{\boldsymbol{A^T D^{-1}}}{r} \tag{52}$$

$$\begin{bmatrix} \dot{\boldsymbol{l}}_1 \\ \dot{\boldsymbol{l}}_2 \\ \dot{\boldsymbol{l}}_3 \\ \dot{\boldsymbol{l}}_4 \end{bmatrix} = \begin{bmatrix} \dot{\boldsymbol{q}}_1 \\ \dot{\boldsymbol{q}}_2 \\ \dot{\boldsymbol{q}}_3 \\ \dot{\boldsymbol{q}}_4 \end{bmatrix} r = \boldsymbol{A^T}\dot{\boldsymbol{p}} \tag{53}$$

$$\begin{bmatrix} \ddot{\boldsymbol{l}}_1 \\ \ddot{\boldsymbol{l}}_2 \\ \ddot{\boldsymbol{l}}_3 \\ \ddot{\boldsymbol{l}}_4 \end{bmatrix} = \begin{bmatrix} \ddot{\boldsymbol{q}}_1 \\ \ddot{\boldsymbol{q}}_2 \\ \ddot{\boldsymbol{q}}_3 \\ \ddot{\boldsymbol{q}}_4 \end{bmatrix} r = \boldsymbol{A^T}\ddot{\boldsymbol{p}} + \dot{\boldsymbol{A}}^{\boldsymbol{T}}\dot{\boldsymbol{p}} \tag{54}$$

Combining Eqs (52), (53) and (54) we get

$$\underbrace{\boldsymbol{M}_p + \frac{\boldsymbol{A}^T\boldsymbol{D}^{-1}\boldsymbol{M_m}\boldsymbol{A}}{r^2}}_{\boldsymbol{M_{eq}}}\ddot{p} + \underbrace{\boldsymbol{g}_E + \frac{\boldsymbol{A}^T\boldsymbol{D}^{-1}\boldsymbol{M_m}\dot{\boldsymbol{A}}}{r^2}\dot{\boldsymbol{p}} + \frac{\boldsymbol{A}^T\boldsymbol{D}^{-1}\boldsymbol{M_m}\boldsymbol{T_f}\dot{\boldsymbol{p}}}{r}}_{\boldsymbol{N}} = \underbrace{\boldsymbol{u}\frac{\boldsymbol{A}^T\boldsymbol{D}^{-1}}{r}}_{\boldsymbol{f_d}} \tag{55}$$

The final global linearization is shown by Eq. (56),

$$\boldsymbol{f_d} = M_{eq}\boldsymbol{v} + \boldsymbol{N} \tag{56}$$

where, $\boldsymbol{v} = \ddot{\boldsymbol{p}}$.

The final desired force is shown in Eq. (57) [149] incorporates the difference between the desired term and the feedback term of the velocity and position.

$$\boldsymbol{f_d} = \boldsymbol{M_{eq}}\left(\ddot{\boldsymbol{p}}_{\boldsymbol{d}} + \boldsymbol{K}_p(\boldsymbol{p_d} - \boldsymbol{p}) + \boldsymbol{K}_d(\dot{\boldsymbol{p}}_{\boldsymbol{d}} - \dot{\boldsymbol{p}})\right) + \boldsymbol{N} \tag{57}$$

where, $\boldsymbol{f_d}$ is the force required to move the end effector from the existing location to the new desired location.

Once the desired force $\boldsymbol{f_d}$ is determined, it can be used to determine the desired motor torques for the winches. However, because the dynamic model rarely contains all mechanical factors [135], we instead used a trajectory generation for the overdetermined kinematic system over the proposed force control method.

*Trajectory Generation/Positioning Control*

Using the winch rope lengths, in combination with the hoist rope length, the dredge head position can be determined within the workspace. As described by Jacobsen [135], the end effector's positioning can be determined through triangulation of the dredge head and reflection into a two-dimensional plane. This method [135] is briefly described below.

Using Eq. (58), the winch rope lengths can be reflected into the *x-y* plane providing the rope length radius $r_i$.

$$r_i = \sqrt{{l_i}^2 - {d^G}^2} \tag{58}$$

where, $d^G$ is the depth of the dredge head and equal to the ship's hoist-rope length.

The dredge barge ship is assumed to operate on the same flat plane as the winches. Otherwise, a correction factor will need to be added.

Four circle radii can then be defined within the workspace through Eq. (59),

$$r_i{}^2 = (x - x_i)^2 + (y - y_i)^2 \tag{59}$$

The distance between any of the two circle centres is then calculated using Eq. (60).

$$D_{j,k} = \sqrt{\left(x_k - x_j\right)^2 + \left(y_k - y_j\right)^2} \tag{60}$$

where, $(j, k) \in \{\{1,2\}, \{2,3\}, \{3,4\}, \{4,1\}\}$.

Using one of the intersection points and two centre points of adjacent circles, the area, *A*, formed by the three points can be calculated in Eq. (61). If *A* > 0, the circles are intersecting.

$$A = \frac{1}{4}\sqrt{\left(D + r_j + r_k\right)\left(D + r_j - r_k\right)\left(D - r_j + r_k\right)\left(-D + r_j + r_k\right)} \tag{61}$$

The dredge head *x-y* plane coordinates of the workspace can then be found through the intersection of the points in Eqs. (62) and (63).

$$x_{1,2} = \frac{x_j + x_k}{2} + \frac{\left(x_k + x_j\right)\left(r_j^2 - r_k^2\right)}{2D^2} \pm 2A\frac{y_j - y_k}{D^2} \tag{62}$$

$$y_{1,2} = \frac{y_j + y_k}{2} + \frac{\left(y_k + x_j\right)\left(r_j^2 - r_k^2\right)}{2D^2} \pm 2A\frac{x_j - x_k}{D^2} \tag{63}$$

We determine the position of the dredge head in three-dimensions within the operating space using Eqs. (62) and (63), in combination with the hoist rope length. Through the control method and position feedback, the dredge head can be positioned along a path as illustrated in Figure 4.16.

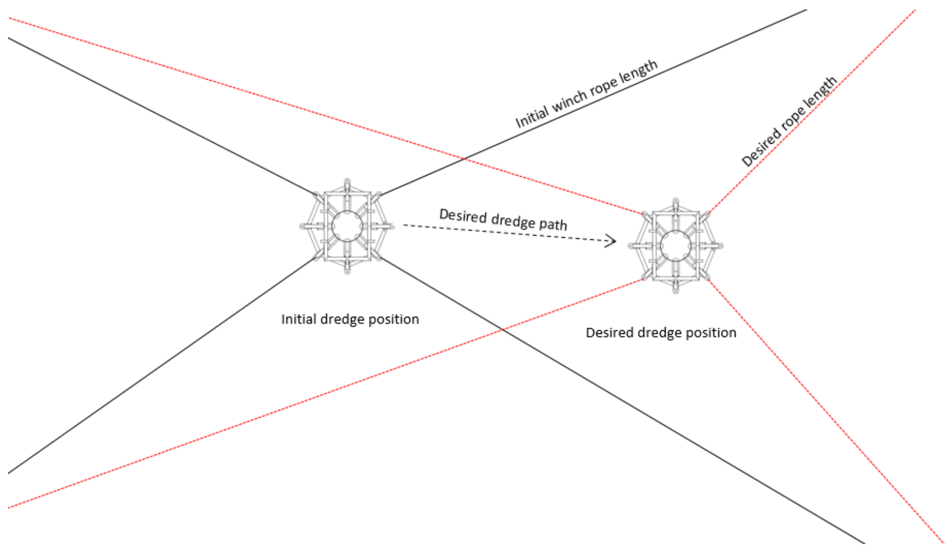


Figure 4.16: Dredge Head Path

**Error Considerations and Limitations of System**

The dredge system and the components modeled in this lean approach have been idealized and several sources of error are considered here.

*Winch Fleet Angles*

Each winch must maintain a fleet angle [151] for the winch ropes to spool along the winch drum in a consistent and predictable manner, without a specialized guide. The fleet angle is shown below in Figure 4.17.

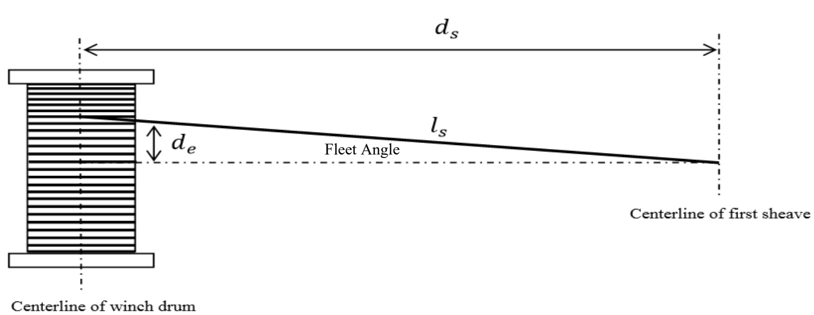


Figure 4.17: Winch and Fleet Angle

Using Eq. (64), the minimum distance $d_s$ to the first sheave can be calculated.

$$d_s = \frac{0.5 * length\ of\ winch\ drum}{1.5} \tag{64}$$

The distance between the winch and first pulley is fixed. However, the length of the rope changes depending on the rope's exit position along the length of the winch drum through Eq. (65) [135].

$$l_s = \sqrt{{d_e}^2 + {d_s}^2} \tag{65}$$

where, $d_e = f(n_i + \Delta d_i)$ and is a function that is dependent on the initial rope exit position $n_i$, plus the change in the ropes exit position relative to the initial position $\Delta d_i$. $\Delta d_i$ is based on the thickness of rope being used for the application and the change in winch motor angle $\Delta q_i$. $d_e$ is a measured quantity.

*Encoder*

The dredge head is positioned within the operating area through careful measurement of the length of winch rope spooling onto or off the drum. To measure the rope lengths, we utilize motor encoders that measure the change in winch motor angle. Multiplying the change in winch motor angle $\Delta q_i$, by the radius of the winch drum, $r_d$, we calculate the arc length or the change in total winch rope length. The total length of rope required to reach the perimeter of the application may require several layers along the winch drum. The total number of rope layers at a given time will vary as the dredge head moves through the operating space. Therefore, the radius used to calculate the change in rope length will vary as a function of the number of layers on the winch drum. Each new rope layer added to or removed from the winch drum effects the radius when calculating the changing rope lengths. To define the number of layers on each winch drum, the number of revolutions to reach the winch drum wrap capacity per layer is defined and shown in Eq. (66).

$$rev_{cap} = d_w / d_{th} \tag{66}$$

where,

$d_w$ is the drum length (inside flange to inside flange),

$d_{th}$ is the thickness of the rope being used for the application.

Using the winch angle provided by the encoder, the total change in winch drum revolutions is calculated using Eq. (67).

$$\Delta rev = \frac{\Delta q_i}{2\pi} \tag{67}$$

By adding to the initialized number of revolutions, $rev_{int}$, the number, $n$, of layers on the drum can be determined.

$$\begin{gathered} n = 0, (rev_{int} + \Delta rev) \leq rev_{cap} \\ n = 1, 1rev_{cap} < (rev_{int} + \Delta rev) \leq 2rev_{cap} \\ n = 2,\ 2rev_{cap} < (rev_{int} + \Delta rev) \leq 3rev_{cap} \\ . \\ . \\ n_{capcity} \end{gathered} \tag{68}$$

where, $n_{capcity}$ is the maximum number of allowable rope layers for the winch system.

Using Eq. (68) to determine the number of layers on the drum, a correction factor for the radius, $r^*$, is defined to calculate the total change in rope length, $\Delta L_i$, as shown in Eq. (69) and Eq. (70).

$$r^* = r_d + n d_{th} \tag{69}$$

$$\Delta L_i = \Delta q_i \cdot r^* \tag{70}$$

Using Eq. (70), the change in length between the first pulley and the dredge head, $\Delta l_i$, can be calculated using Eq. (71).

$$\Delta l_i = \Delta L_i - \Delta l_s \tag{71}$$

*Mass of Winch Rope; Catenary Effect*

Large-scale, wire-driven robots use large heavy cables that span long distances. Due to the cable mass and distance, the effects of elongation and sag become pronounced [152]. The model for the cable-driven dredge uses a synthetic rope with a specific gravity like that of water. As a result, the rope used with the cable-driven dredge is uniformly supported between the winches and end effector.[5]

*Rope Stretch*

For fully constrained cable-driven robots, the dominant dynamics are the longitudinal vibration [153, 154]. Therefore, the simplified spring model considered here for the evaluation of the cable dynamics needs to be further explored and evaluated in a future study.

*Vibrations*

One of the main complexities of large-scale wire robots is that they are susceptible to vibrations due to the elasticity in the cables [153]. The vibrations in large-scale cable-driven robot platforms have been shown to perform complex coupled 6D oscillations, particularly in the case when motion changes abruptly [125, 155]. A control framework and method to increase the system's stiffness, proposed by Radojicic et al. [125], to deal with these complex and coupled oscillations over-constrains the system with additional cables. However, increasing the number

[5] This model neglects the effects of the catenary since the system uses a synthetic rope with a specific gravity like that of water.

of winches and associated cables has practical implications in a working dredge environment. The addition of cables increases the system complexity and as a result reduces the system's reliability and increases its total cost. What's more, the motions of the cable-driven dredge are assumed to be slow and the effects due to vibration are considered negligible for this simplified analysis. Elements of energy storage and dissipation have not been accessed as part of this study. Because a modal analysis of the lumped parameter system requires knowledge of all elements of energy storage and dissipation, it is a site for future work.

*Change in Water Level*

The hoist on the barge ship controls the depth of the dredge head, which is measured by the length of the hoist rope. During dredging, however, water levels may change and effect the elevation of the barge ship relative the positioning winches. Therefore, a global positioning system (GPS) measures the ship's vertical elevation relative to each winch location. This elevation is used to correct the positioning error associated with the changing water level and rope lengths.

**System Boundary Conditions**

Understanding the boundary conditions and limitations of the cable-driven dredge will allow for improved system positioning. The dredge head may be manipulated over the working space by controlling its position and the applied forces. However, the dredge head's movement is bound by the limiting forces of the system components, such as the positioning winches. Within certain areas of the workspace, the winches will not be able to move the dredge head in the desired direction. Moreover, variations in the materials bed will affect the cutting forces within the workspace, resulting in a changing boundary condition. This next section explores the boundary conditions and limitations within the workspace.

Each of the positioning winches is constrained by the maximum and minimum system force capacity. The maximum force will be constrained by the maximum allowable torque of the winches or the maximum allowable rope tensile force. The minimum and maximum forces are defined as $\boldsymbol{f_{min}}$ and $\boldsymbol{f_{max}}$, respectively and constrain $\boldsymbol{f_{wi}}$.

$$\boldsymbol{f_{min}} \leq \begin{bmatrix} \boldsymbol{f_{w1}} \\ \boldsymbol{f_{w2}} \\ \boldsymbol{f_{w3}} \\ \boldsymbol{f_{w4}} \end{bmatrix} \leq \boldsymbol{f_{max}} \qquad (72)$$

As the dredge head approaches a workspace boundary, the angle between the two position winches and the dredge head increases. As a result, a smaller percentage of the applied winch force contributes to the motion along the dredge head path. This is illustrated in two dimensions in Figure 4.18.

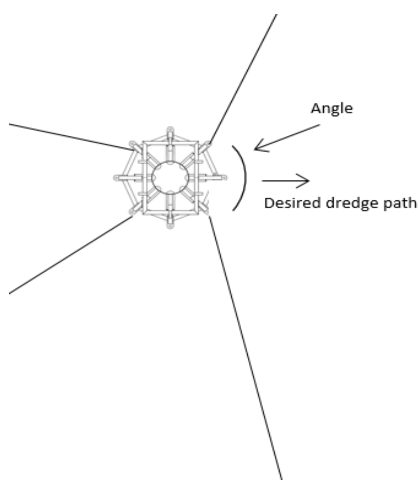


Figure 4.18: Winch Pulling Angle

To assess the workspace boundary conditions, we ran a simulation of the dredge system that uses a static force balance where the external forces are combined into a vector, $\boldsymbol{w}$ and a structured matrix $\boldsymbol{A}$ is combined with the winch forces $\boldsymbol{f}$, as shown Eq. (73).

$$\boldsymbol{Af} + \boldsymbol{w} = 0 \qquad (73)$$

where,

$$\boldsymbol{A} = \begin{bmatrix} \eta_{1x} & \eta_{2x} & \eta_{3x} & \eta_{4x} \\ \eta_{1y} & \eta_{2y} & \eta_{3y} & \eta_{4y} \\ \eta_{1z} & \eta_{2z} & \eta_{3z} & \eta_{4z} \end{bmatrix}$$

$$\boldsymbol{f} = \begin{bmatrix} \boldsymbol{f}_{w1} \\ \boldsymbol{f}_{w2} \\ \boldsymbol{f}_{w3} \\ \boldsymbol{f}_{w4} \end{bmatrix}$$

$$\boldsymbol{w} = \begin{bmatrix} \boldsymbol{f}_{bx} \\ \boldsymbol{f}_{by} \\ \boldsymbol{f}_{bz} \end{bmatrix}$$

The simulation uses a constant dredge head weight, and a constant net force (cutting force and hydrodynamic forces) applied in the direction of dredge head motion. The required force to move the dredge head was simulated from the central origin between the four winches, straight towards the perimeter formed by the winches. The simulated dredge head forces within the workspace are shown in Figure 4.19.

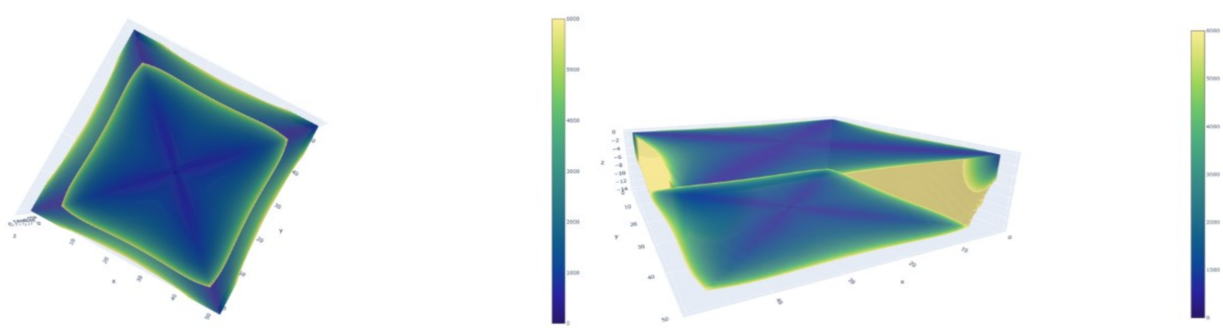

Figure 4.19: Simulation of Dredge Head Workspace

The simulations showed the formation of a star shape boundary within the workspace. Increased depth limits the conditions in which the dredge head can work. This shrinking boundary condition is a result of the constant dredge head weight. As the dredge head approaches the positioning winches, a larger fraction of the applied force is distributed in the upward, $z$, direction and less force is applied along the desired path.

Likewise, as we increase the constant cutting force and hydrodynamic force applied to the dredge head, the available workspace diminishes. This effect is shown in Figures 4.20 and 4.21, as the force increases by three times and six times, respectively.

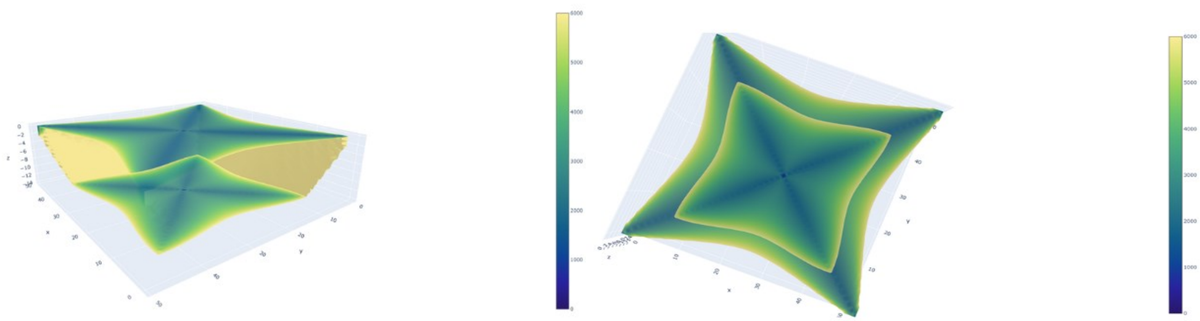

Figure 4.20: Simulation, Workspace based on Three Times Constant Force

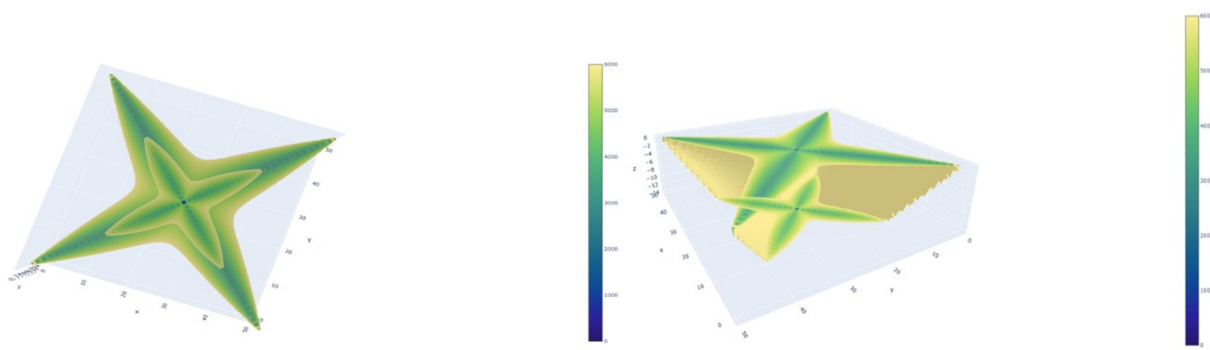

Figure 4.21: Simulation, Workspace based on Six Times Constant Force

One method to improve access to the boundary conditions and workspace is through improved path planning. If the planned dredge path is mapped to manage the winch pull angles, the trajectory may be achieved while staying below $\boldsymbol{f_{max}}$. This improved path planning provides the dredge access to the bounded areas in the workspace after the system has mapped the physical environment conditions. Moreover, as the cable-driven dredge hits the physical limitation of the available winch forces, the barge ship may reduce the weight of the dredge head. This will reduce the cutting force and provide the system more access to the boundary conditions. Intelligent path planning and optimization weight control simulations of the boundary conditions are recommended for future work.

Another way to improve the dredge head movement at the boundary conditions is by adding positing winches at shore. The addition of shore winches to the system, reduces the angle formed between any two adjacent position winches, improving the working space. However, the addition of winches to the cable-driven system has negative practical implications and economic impacts. Furthermore, the increase in dredging area realized by adding winches to the system has diminishing returns, as illustrated in Table 4.1.

Table 4.1: Effective Work Area by Winch

| Number Winches with equal rope length | Shape formed by perimeter of winches | Area formed by perimeter winches | Area Per Winch |
|---|---|---|---|
| 3 | Triangle | 1.00 | 0.33 |
| 4 | Square | 1.66 | 0.42 |
| 5 | Pentagon | 1.96 | 0.39 |
| 6 | Hexagon | 2.12 | 0.35 |

### Overall Dredge System Control

#### *System Goals*

Every dredge application is unique and often the desired results are based on many factors. For most dredge designs, the main goal is the optimization of solids production while minimizing energy input. For most organizations the goal is maximizing profit through safe operation. To develop the overall control system and optimization techniques in future work, we must first start by defining a desired result.

The simplified control scheme for the cable-driven dredge is shown in Figure 4.22.

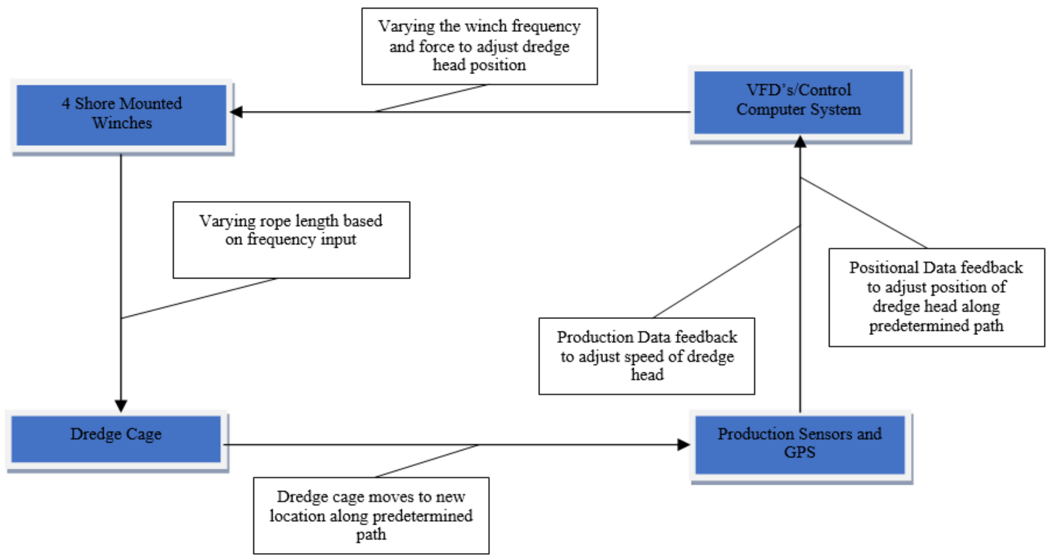


Figure 4.22: Generalized Control Scheme

*Influence of Parameters*

If the dredge head moved too fast or at a cutting depth set too low, the dredge system may exceed the upper boundary condition of the production capacity. This may result in too high a concentration of solids entering the system, resulting in line plugging. Moreover, if the excavation rate exceeds the fluid capacity to move the solids, then the system will see spillage resulting in multiple passes and reduced efficiency. Therefore, we look at three parameters and their effects on the dredge system production: dredge head velocity; cutting depth; and dredge pump speed.

*Production Rate*

To control the production rate of the system, we look to measure the instantaneous production rate of the dredge process through the measurement of the dredge pump power draw and pressure recording. As the mixture density and production rate increase, the input energy of the pump increases due to the additional hydraulic mass and resulting system losses. As a result of the increased system power, the amperage for the dredge pump increases.

## Conclusion

In this chapter the simplified dynamics of the dredge system subsystem components are presented. Considering a two-dimensional plane, the barge ship is evaluated along with key parameters which are thought to influence the system. The barge ship dynamics are not further explored in this chapter, as empirical data will be collected when testing the barge ship in a tow tank in a future study. Using the key parameters, a simplified analysis of the barge ship's interaction with the dredge head is considered. This is applied using an ideal transmission between the barge ship and dredge head. Like the barge ship, the dredge head dynamics are considered on a two-dimensional plane. Key parameters thought to influence the dredge head subsystem are identified. The forces applied to the dredge head, including the interaction with four positioning winch cables, are evaluated using a simplified analysis. Lastly, the winch dynamics are considered as a part of the system component dynamics.

A secondary evaluation is completed on the dredge system using a planar analysis of the cable driven system. This further simplification of the dredge system allows us to identify aspects of the system which contribute significantly to the governing equations. Further component analysis and simplified models are considered for the dredge excavation, dredge pump and pipeline. A brief overview of the dredge head control is explored along with some of the advantages and disadvantages posed by a force control method versus a trajectory-based control method. The controls overview presented in this chapter is limited as the system dynamics and thus controllability of the system is also limited. Moreover, the control for the dredge system is not the focus of this work but is an area for further study. Lastly, the limitations and sources of measurement are explored, where areas of the system may present potential risks due to uncertainty. Further testing will be required for the aspects identified that cannot be predicted through engineering analysis due to areas of uncertainty.

# Chapter 5: Prototype Experiments

## Introduction

One goal of this study is to verify if the simplified models developed behave close enough to the dredge system that these models can be used in system development or if additional more comprehensive model development is required. In addition, we aim to identify key system parameters that have significant impacts on the dredge model behavior and make the model sensitive to change. The models verified and key parameters identified from this study will be used in future, more comprehensive studies of the dredge system and its development. Since the models developed here are simplified, it is necessary to complete some experiments on aspects of the models which could not be predicted through engineering analysis, due to the uncertainty in the physics.

A scaled-down version of the cable-driven dredge was designed to test several of the simplified dredge models developed and the effects of system parameters on the models. We designed the scaled model to operate in a two-dimensional vertical plane, under the assumption that testing in two dimensions would capture the dominant system effects which could then be applied to the three-dimensional system in a future study. The following section describes the models that were tested and how they were included in the experimental design or not.

### *The Barge Ship Dynamics*

The barge dynamics were not tested or verified as part of the experimental setup. However, the experimental setup is designed with a load cell that measures the tension in the rope which connect the dredge head and barge ship. It is assumed that the forces generated by the ship dynamics will be translated to the connecting rope and measured by the load cell. This measured tension force will be used as an input for the dredge head dynamics.

For the experimental setup, the dredge head was suspended from a gantry with a roller trolley attached to the gantry beam. As the trolley traversed the gantry beam, we assume that the trolley will behave with similar resistive force characteristics to those produced by the ship's dynamics. Additional testing in a future study will be required to verify these assumptions. In the future study, the ship dynamics and total resistance force can be empirically determined using a tow tank.

*Winch and Cable Dynamics*

The winch and cable dynamics were not tested as part of the experimental setup as field testing of the dredge system completed outside this study had already shown adequate system control. However, two winches with controllers and synthetic rope were used in the experimental setup to move the dredge head along a linear path within the sediment holding tank.

*Dredge Head Dynamics*

The dredge head dynamics were included in the experimental design and testing. Experimental testing of the dredge head dynamics was required due to the uncertainty in the nature of the physics when the dredge head moved through the fluid and saturated bed of material. Several aspects and resulting forces applied to the dredge head were uncertain. More specifically, the dredge head's surface and overall shape is complex, and the total resistance forces as the system moved through water were unknown. In addition, we did not know the force of the interactions of both the cutting and friction forces between the cutting ring and the sediment bed. This unknown was due to the uncertainty around the physics associated with the excavation rate of the sediment bed, which is thought to be closely tied to (1) the dredge head speed, (2) cutting head depth, and (3) the turbulent fluid action at the dredge head inlet which is related to the pump's rotational speed.

*Discharge Pipe Model*

Because of the complex nature of slurry flow and uncertainty in the model predictions as the system parameters change, the discharge pipeline model was tested with the experimental setup. The discharge pipe model was tested in the experimental design as a secondary measure for predicting the estimated losses over the discharge pipeline when transporting a solid-water mixture. However, the primary measure of pressure change in the discharge pipe was through a pressure sensor installed at the discharge of the dredge pump. It was thought that if a predictive model could be verified for the pipeline pressure drop, this model would be a more robust measure than the use of a pressure gauge in dredge environments.

*Pump Production Model*

The pump production model was tested in the experimental setup. This model was tested in the experimental setup for several reasons. First, the basis of the pump and production model uses the pump characteristics that are developed through manufacturer's empirical data and testing. Manufacturer's empirical data is used due to the complex physics associated with the turbulent behavior of fluid flow within the pump. Adjustments to the water curve to a water-solid curve is also based on empirical data due to the complex physics associated with pumping a water-solid mixture. Secondly, it was unknown how the adjustment of the dredge head speed, pump speed and cutting depth parameters would influence the water-solids concentration. Lastly, it was unknown whether the algorithm developed here could predict the solids production rate based on the instrumentation used to measure the inputs and sensitivity of the model.

*Excavation Model*

The excavation model was tested with the experimental setup to determine the amount of material that would be excavated around the dredge head based on the cutting ring speed, cutting head depth, and pump speed. The physics associated with the rate of excavation and the change in the parameters were uncertain due to the turbulent action of the fluid and rate at which the sediment would be entrained in the surrounding fluid flow. Therefore, experimental testing was required to verify whether the simplified excavation model could reasonably predict the rate at which the sediment bed was removed or if additional modeling was required in a future study.

In conclusion, the experimental design was completed in this study as an initial high-level check of the simplified physics models developed which could not be predicted through engineering analysis, due to the uncertainty in the nature the physics. The anticipated outcome of this experimental testing were the verification of simplified models, identification of models that require more comprehensive modeling and identification of parameters which make the system model output sensitive to change. Due to the lean nature of this study, the experimental design does not follow the standard design of experiments structure. This initial testing is only intended to provide initial insight into model behavior and sensitive parameters which can be used to develop a more comprehensive system model. Further, it is intended that the results of this study will be used to develop a base for verification of the more comprehensive model through a standard design of experiments structure.

**Materials and Method**

The experimental setup consisted of five main subsystems.

1. Dredge head with discharge pipe
2. Two holding tanks
    a. Sediment holding tank and
    b. Discharge collection tank
3. Linear positioning system

a. Two winches, winch controllers and synthetic rope

4. Instrumentation (sensors and monitoring hardware)

5. Supervisory Control and Data Acquisition (SCADA) system

**Test Setup**

Figure 5.1 illustrates an overview of the test setup. Figure 5.2 shows the arrangement of the dredge head in the sediment tank. Figure 5.3 shows the test setup and Figure 5.4 shows the test sediment tank.

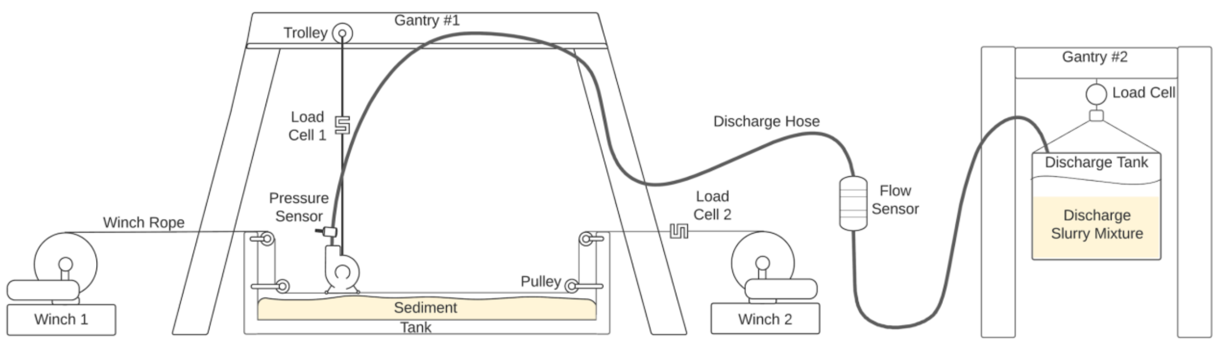


Figure 5.1: Experimental Test Setup

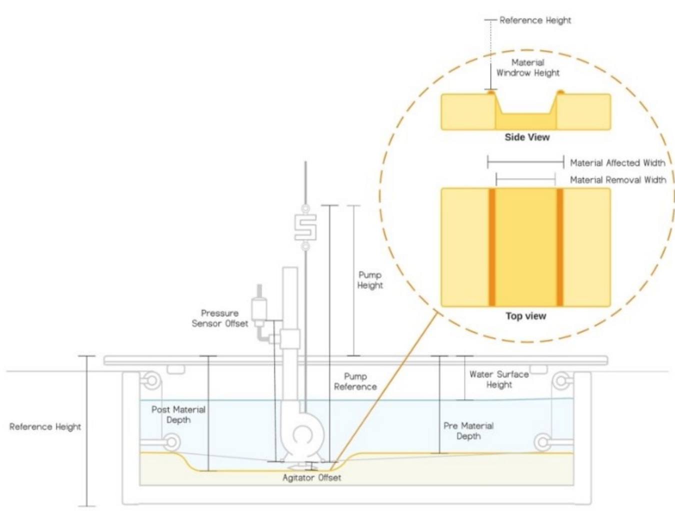


Figure 5.2: Experimental Setup, Path

Figure 5.3: Test Setup

Figure 5.4: Sediment Tank, Test Setup

**Experimental Design**

The centrifugal submersible dredge pump used for this setup was a 3-inch Flygt model 3085. The pump motor controller was a Yaskawa V1000 variable frequency drive (VFD). 35 meters of 3" EDPM discharge piping ran from the test pump to the discharge tank. Two ¼-turn isolation valves were installed along the discharge line, one at the discharge connection of the pump and the other at the discharge tank. The two isolation valves were installed to prevent air from entering the discharge hose when the pump was lifted out of the water during trial runs. The discharge hose was suspended along a gantry crane beam and trolly, directly in line with the system's movement. The weight of the hose and slurry was supported by the gantry and setup to minimize the resistance associated with the discharge hose.

The sediment holding tank was sized to contain a 120 mm thick test bed of sediment and the level of water required to submerge the pump for the duration of each trial. The apparatus size was selected based on the availability of the test pump. The travel distance of the dredge was limited by the internal dimensions of the holding tank, approximately 1.4 meters in length. The discharge collection tank was suspended from a separate gantry structure. The weight of the collection tank and resulting slurry was measured by a load cell. The discharge tank has a maximum volumetric capacity of 1000 L, which allowed for approximately 75 seconds of pump runtime at the maximum system flow rates. The discharge tank was adjacent to the holding tank and elevated, allowing the slurry to drain into the holding tank at the end of each trial.

Due to the limitations of the holding tank, test trial durations varied depending on either the travel distance or discharge tank capacity. The various test trial periods were based on the system travel speeds. A range of 15 Hz and 5 Hz winch frequencies were used, resulting in test periods ranging from 30 to 110 seconds, respectively. At low travel speeds, the test trials ended when the discharge tank was full, which occurred before the dredge travelled the total available distance. At high travel speeds, trial duration was limited and ended due to the dredge reaching the maximum available distance before the tank's capacity was reached.

The linear positioning system moved the dredge along a straight path through the sediment holding tank. The dredge was suspended from a trolley travelling along a beam placed above the sediment holding tank. Winches were placed at each end of the holding tank in alignment with the ends of the beam. The winch cables were connected to the sides of the dredge head through a series of pulleys. The winch configuration provided the forward motion of the dredge head along a two-dimensional plane. A series of pulleys were setup to route the winch cables over the rim of the holding tank and down to a level height with the dredge head, which provides the horizontal pulling force.

Sensors were placed at specific locations in the system to measure and log the real-time status and outputs of the system through the trial run. A 0-15 psi digital pressure transducer was connected to the discharge hose 0.2 m downstream of the volute discharge to provide the pump discharge pressures. A 6” magnetic flowmeter was installed in the discharge hose 9.5 m downstream from the pump. To reduce the effects of solids settling and influence on flow measurements, the flow meter was oriented vertically with the flow direction. To measure the suspended weight of the dredge head, a load cell was installed between the beam trolley and the dredge. We recorded the force applied to the bed of solid materials using the known weight of the dredge. To provide the measured pull force required to advance the dredge through the sediment bed, we installed a second load cell between the dredge and the forward pulling winch. We used a digital readout crane scale to measure the suspended discharge collection tank and to obtain the post-test weight of the slurry and collected solids. The VFDs for the dredge and winches provide the speed, amperage, power consumption, and other measures, for each of the motors to be recorded by the datalogger. The supervisory control and data acquisition (SCADA) host managed the sensors and VFDs. Each of the peripheral devices were connected to the network through a serial device server, or to a signal converter, which was connected to the nearest ethernet hub.

**Variables**

The solids material selected for this initial test setup was grade SIL-4 DS2000 [156]. This selection was based on readily available materials for test setup. SIL-4 DS2000 has an average specific gravity of 2.65 and $d_{50}$ of 425 μm [156].

The SCADA host logs system hardware status and sensor measurements at a rate of 50 ms per sample. This averages approximately 1300 data samples per trial run. Each experiment trial captures the parameters listed in Table 5.1.

Table 5.1: Hardware and Sensor Parameters

| PARAMETERS | DESCRIPTION |
|---|---|
| Sample | Sample ID |
| Time | Timestamp (ms) |
| Trial | Trial ID Name |
| Speed, Manipulated Var | Travel Speed (m/s) |
| Distance, Controlled Var | Distance Travelled (m) |
| Flow Rate, Responding Var | Flow rate through the system (L/s) |
| Down Force, Manipulated Var | Force applied onto the sediment (kg) |
| Pull Force, Responding Var | Force applied onto the dredge (kg) |
| Slurry Weight, Responding Var | Weight of the discharge collection tank (kg) |
| Pressure, Responding Var | Pressure at dredge discharge (psi) |
| Pump Status | Pump operating status |
| Pump Amperage, Responding Var | Pump current (A) |
| Pump Power, Responding Var | Pump power (kW) |
| Pump Reference Frequency, Manipulated Var | Desired impeller frequency (Hz) |
| Pump Output Frequency, Responding Var | Actual impeller frequency (Hz) |
| Pump BUS Voltage, Responding Var | DC BUS Voltage (V) |
| Winch 1 Status | Winch 1 operating status |
| Winch 1 Amperage, Responding Var | Winch 1 current (A) |

| | |
|---|---|
| Winch 1 Power, Responding Var | Winch 1 power (kW) |
| Winch 1 Reference Frequency, Manipulated Var | Desired spool frequency (Hz) |
| Winch 1 Output Frequency, Responding Var | Actual spool frequency (Hz) |
| Winch 1 BUS Voltage, Responding Var | DC BUS Voltage (V) |
| Winch 2 Status | Winch 2 operating status |
| Winch 2 Amperage, Responding Var | Winch 2 current (A) |
| Winch 2 Power, Responding Var | Winch 2 power (kW) |
| Winch 2 Reference Frequency, Controlled Var | Desired spool frequency (Hz) |
| Winch 2 Output Frequency, Responding Var | Actual spool frequency (Hz) |
| Winch 2 BUS Voltage | DC BUS Voltage (V) |

Further, for each trial, we recorded a collection of pre-trial and post-trial setup conditions describing the start and end conditions of the tests. These conditions are summarized in Table 5.2.

Table 5.2: Pre-Trial and Post Trial, Recorded Conditions

| PARAMETER | DESCRIPTION |
|---|---|
| Time | Timestamp (ms) |
| Trial | Trial ID Name |
| Solid Type | Sediment description |
| Particle Size | Solids particle size (μm) |
| Particle Distribution | Distribution of solid particles |
| Density (Dry) | Density of the sediment when dry (kg/m3) |
| Density (Wet) | Density of the sediment when wet (kg/m3) |

| | |
|---|---|
| Reference Height | Height from bottom of holding tank to top of guide bar (mm) |
| Pump Reference | Height from the pump intake to the top of the load cell (mm) |
| Agitator Offset | Height from the bottom of the agitator to the pump intake (mm) |
| Gross Weight | Suspended weight of the pump and discharge hose (kg) |
| Discharge Height | Height of the open end of the discharge hose relative to reference height (mm) |
| Pressure Sensor Offset | Height of pressure sensor relative to pump intake (mm) |
| Pre-Material Depth | Depth of material from reference height (mm) |
| Water Surface Height | Depth of water surface from reference height (mm) |
| Pump Height | Height to the top of the load cell relative to reference height (mm) |
| Slurry Total Volume | Total volume of slurry in discharge tank (L) |
| Slurry Total Weight | Total weight of slurry in discharge tank (kg) |
| Decanted Solids Weight | Weight after trial completed and water removed (kg) |
| Total Solids Weight | Weight after trial completed and hose lines flushed (kg) |
| Post-Material Depth | Depth of material after dredging relative to reference height (mm) |
| Material Affected Width | Total width of material distributed from dredging (mm) |
| Material Windrow Height | Top of disturbed material to reference height (mm) |
| Material Removal Width | Width of material removed by dredge (mm) |

**Design Matrix**

A design matrix (Table 5.3) was developed based on 15 permutations of parameter combinations. To reduce the number of test trials required, the complete set of all parameter combinations was not tested. This lean approach was structured around 15 parameter combinations which were thought to have results that would be useful in future study.

Table 5.3: Design Matrix

| Run | Frequency (F) | Speed (P) | Depth (D) |
|---|---|---|---|
| 1 | H | L | L |
| 2 | H | L | M |
| 3 | H | L | H |
| 4 | H | M | L |
| 5 | H | M | M |
| 6 | H | M | H |
| 7 | H | H | L |
| 8 | H | H | M |
| 9 | H | H | H |
| 10 | L | L | L |
| 11 | L | L | M |
| 12 | L | M | L |
| 13 | L | M | M |
| 14 | L | H | L |
| 15 | L | H | M |

where, F = Pump Frequency (L = 50 Hz, H = 60 Hz), P = Travel Speed (L = 5 Hz, M = 10 Hz, H = 15 Hz), and D = Dredge Depth into Material (L = 40 mm, M = 80 mm, H = 120 mm)

**Procedure**

1. First run
    1. Flush discharge hose.
        1. Run dredge pump in clean water for minimum 40 seconds to clear any residual sand from the discharge hose.
        2. Close 3” discharge valve on pump discharge and close 1/2" vent valve to prevent hose from draining when the dredge pump is lifted out of the water.
2. Test Reset
    1. Position the dredge pump at the start position.
        1. Ensure 3” discharge valve is closed and 1/2” vent valve is open.
        2. Hoist dredge upwards and clear of the guide rails.
        3. Disconnect forward winch rope from the dredge pump.
    2. Drain discharge tank and remove any solids.
        1. Close discharge tank drain valve.
    3. Evacuate water from holding tank.
        1. Use submersible pump to transfer water to discharge tank and auxiliary tank. Leave 10-15cm of water in the holding tank. This will ensure the sand is fully saturated when forming the test bed to prevent air entrapment, allow quick settling of the sand, and prevent the sand from drying and forming a crust.
    4. Prepare test bed of solids (sand)

1. Use shovel to scoop submerged sand from the edges of the holding tank and place in the test bed area. The approximate width of the test bed is the width of the guide rails.
    1. Following each two scoops of material, settle the solids by placing the shovel flat on the material surface and oscillate the shovel forth and back while providing a slight downwards pressure. Settling will be evident by the emergence of liquid water at the surface of the sand.
2. Use the screed tool on the guide rails to screed the sand to a consistent height. Fill any deficient areas with scoops of saturated materials. Remove air voids from any shavings produced by the screed by pouring water on the disturbed shavings and settling with the shovel.

3. Remove sand from the start area below the pump to the depth equal to the intended dredge start depth. This will allow the pump to be lowered to the desired initial depth without being held up by the sand.

4. Move dredge pump to start position
    1. Reconnect forward winch rope to dredge.
    2. Lower dredge into start position at desired initial depth, measuring from the guide rails up to the pump reference.
    3. Spool winches to take up slack in the winch ropes, ensure pump is positioned correctly in the start position.
    4. Hang excess hoist chain from hoist hook to prevent snagging on the holding tank.

5. Flood the holding tank

1. Drain the water from the discharge tank SLOWLY and use a diffuser to prevent waves and currents that will erode the bed of solids.
2. Pump water from the auxiliary tank into the discharge tank to utilize the diffuser. Wash any remaining solids out of the discharge tank using the water from the auxiliary tank.
3. Close the discharge tank drain valve. Remove the drain hose and any objects from the discharge tank.
4. Dredge pump load cell should read zero with the dredge pump fully suspended by the hoist at the test depth and the discharge hose fully primed. If not, ensure no other forces are acting on the pump and zero the display. It is important that air not be trapped in the volute or discharge hose, or the measured weight will be affected. As the test bed pushes upwards against the dredge pump, the load cell display will show and report a <u>negative</u> reading indicating the downward force on the load cell has decreased. The sign of this reading is changed by the computer interface to display the negative measurement from the load cell as a positive force exerted by the dredge pump directed vertically down. A negative value on the computer display indicates the suspended weight of the dredge pump has increased.

6. Prime dredge pump

    1. Purge air from dredge pump volute by opening the 1/2" vent valve. Close valve after 30 seconds, or when the air stops flowing. Air must be purged from the volute, or the pump will not prime, resulting in a failed test. This also minimizes the volume of the air bubble that will pass through the flow meter at the start of the test allowing for quicker reading stabilization.
    2. Open the 3” discharge valve on the dredge pump.

5. Tare the discharge tank load cell or crane scale.

3. Input test parameters, measurements, and material properties
4. Toggle devices to ‘ON’
    1. Winches, Dredge Pump
    2. Sensors – Flow meter, pressure sensor, load cell 1, load cell 2
5. Run automated test sequence
6. Post-test Measurements
    1. Measure and record post-test water surface height.
    2. Record discharge tank slurry weight.
    3. Record discharge tank slurry volume.
        1. Ensure discharge tank is hanging level, use measuring device to measure the water level between volume reference marks on the discharge tank. Interpolate the captured volume. Record the volume.
    4. Photos/measurements of dredged test bed
        1. Close 3” discharge valve on dredge pump.

2. Open the 1/2" vent valve to drain the pump volute.
3. Use submersible pump to remove remaining water from the holding tank and transfer into the auxiliary tank and the discharge tank if necessary.
4. Capture required photos.
5. Measure and record dredged channel dimensions.

5. Prepare dredge pump for flushing discharge hose.
    1. Use a shovel to remove all remaining solid materials in the start area of the holding tank; the dredge pump must not pick up additional solids when flushing the discharge hose.
    2. Raise dredge pump using hoist until pump inlet is at least 200mm above holding tank bottom.
    3. Use the reverse winch to return the dredge pump to the start position.

6. Measure collected slurry solids weight.
    1. Use shovel to clear solids away from the drain opening inside the discharge tank.
    2. Connect drain hose to the discharge tank drain.
    3. Drain water from discharge tank slowly. Tilt the discharge tank as necessary to decant the visible water from the solids.
    4. Close the drain valve.
    5. Remove the drain hose.
    6. Record the measured weight of the decanted solids.

7. Flush residual solids from the discharge hose.

    1. Transfer water from auxiliary tank to holding tank (if necessary) until there is sufficient water depth to provide 30-40 seconds of runtime; use caution to prevent sand from being eroded and deposited below the dredge pump.
    2. Close 1/2" vent valve on pump discharge.
    3. Open 3” discharge valve on dredge pump.
    4. Run dredge pump for 40 seconds.
    5. Close 3” discharge valve on dredge pump and open the 1/2" vent valve; the discharge hose is now flushed and primed for the next test.

8. Measure the total dredged solids weight (collected slurry solids + residual solids).

    1. Use shovel to clear solids away from the drain opening inside the discharge tank.
    2. Connect drain hose to the discharge tank drain.
    3. Drain water from discharge tank slowly. Tilt the discharge tank as necessary to decant the visible water from the solids.
    4. Close the drain valve.
    5. Remove the drain hose.
    6. Record the measured weight of the decanted solids.

7. Post-test cleanup

    1. Install drain hose to discharge tank and open drain valve.
    2. Place the submersible pump in the holding tank and use the hose to wash the solids out of the discharge tank back into the holding tank.

3. Tilt the discharge tank as necessary to guide the solids to the outlet drain; trace solids can be cleaned out later when the holding tank is being filled for a test.
4. Close drain valve.
5. Proceed to Step 2 to start a new test.

**Limitations of Experimental Designs**

Four main groups of experimental limitations were identified during setup and commissioning of the test system: general system limitations; procedural limitations; hardware and sensors limitations; and software and controls limitations.

**General System Limitations**

Given the small size of the test tank, it was difficult to assemble a model large enough to represent the full system. The size of the tank also made sufficient runtimes difficult. Test sequences therefore had to minimize dredge travel time and pumping time during start up and shutdown. We minimized the ramp-up and ramp-down time of the pump and winches between zero speed and full speed. The ramp time of the pump and winches was set to the shortest time available that did not result in excessive torque on the dredge pump or tension on the winch rope.

**Post-Trial Procedural Considerations**

To capture and verify the system’s production results for changes to the dredge speed and material depth, we measured the quantity of solids collected in the discharge tank and the quantity of solids removed from the sediment holding tank. The removal of the pump required specific procedures to preserve the condition of the test bed while also recovering the residual solids from the discharge hose that were deposited when the system stops at the end of a test. For example, to minimize the amount of time to recalibrate the test setup, it was advantageous to flush the discharge hose prior to draining the holding tank as this allowed for easier depth and width measurements of the test bed post trial.

The sequence of steps to record post-trial were as follows.

1. Close dredge isolation valves.

2. Measure and record water level in holding tank.

3. Record weight and volume of collected slurry.

4. Decant remaining water from the holding tank into auxiliary storage.

5. Measure and record the profile of the removed material from the bed of solids.

6. Remove all solids from the dredge start area.

7. Elevate dredge and return to start position.

8. Decant water from discharge tank to holding tank.

9. Record weight of collected solids.

10. Adjust height of dredge in water to provide 40 seconds of run time.

11. Open dredge isolation valves.

12. Run dredge for 40 seconds.

13. Close dredge isolation valve.

14. Decant water from discharge tank to holding tank.

15. Record weight of collected solids.

This sequence was necessary because hoisting and discharge hose components made it difficult to remove the pump from the holding tank. All flushing water was from the water cap in the holding sediment tank.

**Hardware**

Our biggest hardware issues related to setup, aligning and position of the equipment. We reconfigured the discharge collection tank to drain it more effectively and to better clean the solids before returning them to the holding tank. Figure 5.5 shows the discharge collection tank relative to the holding tank.

Figure 5.5: Discharge Tank, Test Setup

We installed a permanent crane scale to allow easy measurement of the discharge tank. The discharge tank was also further elevated to enable better draining of the water and solids.

**Software and Controls**

Data was difficult to acquire during development and commissioning of the control software and hardware integration due to the limited reach and transmission of the hardware sensors. For dredge applications in the field, the software and controls are remote to the sensors gathering the data. To simulate this remoteness during data collection, the sensors reported to remote software and control centres. Because of their locations, cable lengths and communication protocols made it difficult to integrate sensors with the rest of the system.[6] Three serial device servers were used for testing due to convenience and proximity to the test apparatus however the number of serial servers could have been reduced to one. CAT 5e shielded cables with four twisted pairs were used to transmit data over the network.

Data acquisition samples were recorded on a 50 ms intervals. This sample rate was selected to capture granular detail of the dredging process without overloading the hardware. The acquisition rate was selected so they could be reproduced with economical and commercial grade hardware and sensors available on the market. Additionally, observations from the field indicate that dredging applications typically have longer transient time windows where meaningful changes in dredge production can be observed.

**Trial Identification**

Each trial was given a unique identification number. After the dataset was collected, it was processed by the data analysis tool; post trial calculations, graphing, and model development were performed for each trial dataset. Figure 5.6 highlights a segment of the post-trial calculations.

[6] Initially, a central serial hub was to be used for collecting the data of all the sensors. However, when attempting to establish communication with the flow sensor, significant signal loss was observed due to cable length and the positioning of the serial hub was not feasible.

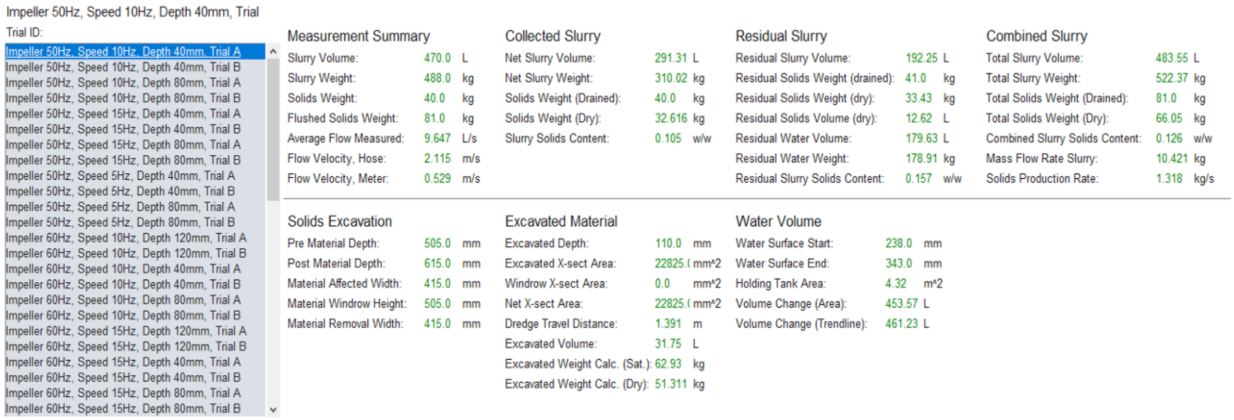


Figure 5.6: SCADA Data, Post Trial

**Verification of Published Data**

*Pumps Curve*

Prior to verifying the production model, we verified the manufacturer's pump characteristics. Figure 5.7 shows results using water as the test fluid and the pump speed set at 60 and 50 Hz across the range of flows tested in this experimental setup.

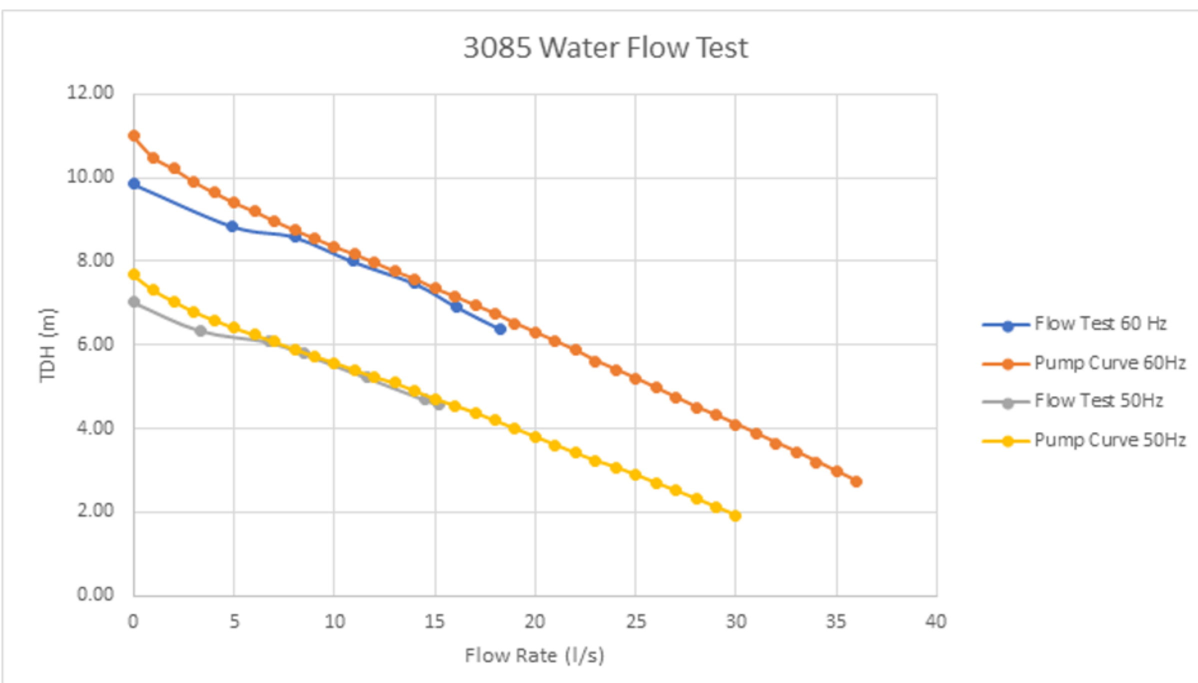


Figure 5.7: Verification of Published Curves, Model 3085

The results of the test aligned with the manufacturer pump characteristics for the pump model flow and head. Comparing the test data with the manufacturer published pump characteristics data a maximum of 3% error was calculated for the range of flows (8 l/s at to 15 l/s) at corresponding pressures, recorded during the test trial. This error was calculated using Eq. (74).

$$Q_{Err_1} = 100\% * \left(\frac{|Q_{man} - Q_{test}|}{Q_{man}}\right) \tag{74}$$

where, $Q_{man}$ is the manufacturer published flow at specified pressure, $Q_{test}$ is the recorded flow rate at specified pressure, and $Q_{Err_1}$ is the error between test data and manufacturer published data.

When testing the production model, we used the power draw on the dredge pump to estimate the solids mixture concentration and flow rate of the dredge system. Combining the solids mixture concentration with mixture flow rate provides the estimated dredge production as it moves through a sediment bed. Using the predicted production rate from the model, the cable-driven dredge controller can adjust system parameters to optimize production. The effects of changing parameters such as hose length, $d_{50}$ sediment and many others involved in dredging were not part of this study. However, these affects are of interest for future work.

*Estimated Solids Effect for 152 mm Impeller*

The generalized solids-effect diagram for pumps of various sizes sourced from Wilson et. al. does not provide curve data for impellers sized below 200 mm. An estimated solids-effect curve was developed for the 152 mm diameter impeller used in the experimental setup. The developed solids-effects curve is based on extrapolation of the curve data shown in Figure 5.8. Starting with an impeller diameter of 200 mm, the curves appear to follow a quadratic curve until reaching 410 mm, at which point the curves transition to nearly linear with increasing impeller size. For each particle diameter, a second order polynomial regression was applied to the data points for 200, 300, and 410 mm impeller sizes, followed by the 152 mm diameter substituted to calculate the estimated $R_H$. Reading the estimated 152 mm impeller curve for the experiments $d_{50}$ particle size of 0.425 mm, $R_H$ is estimated to be 15%.

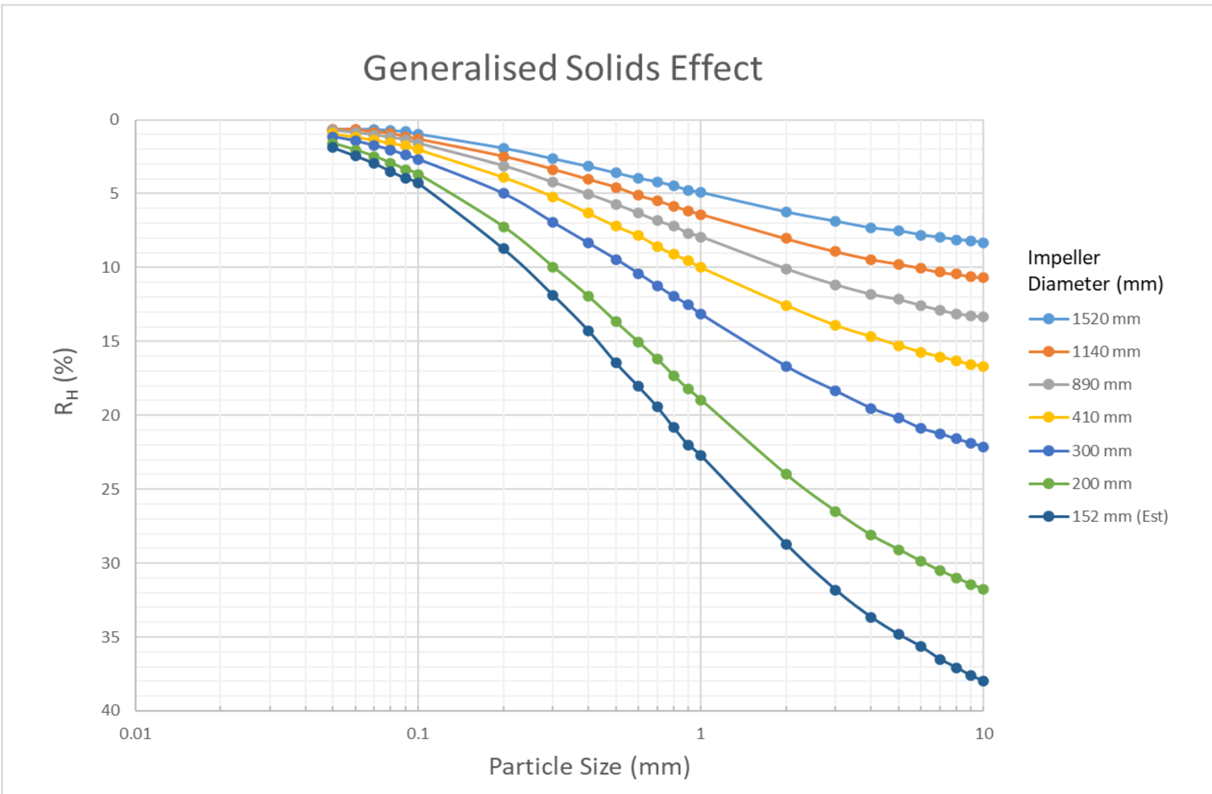


Figure 5.8: Generalized Solids Effects [148]

*Pump Power*

With the pump speed set to 60 hz, two test runs were conducted on pure water to verify that the equipment and sensor readings were behaving as expected and to verify the manufacturers power curve data.

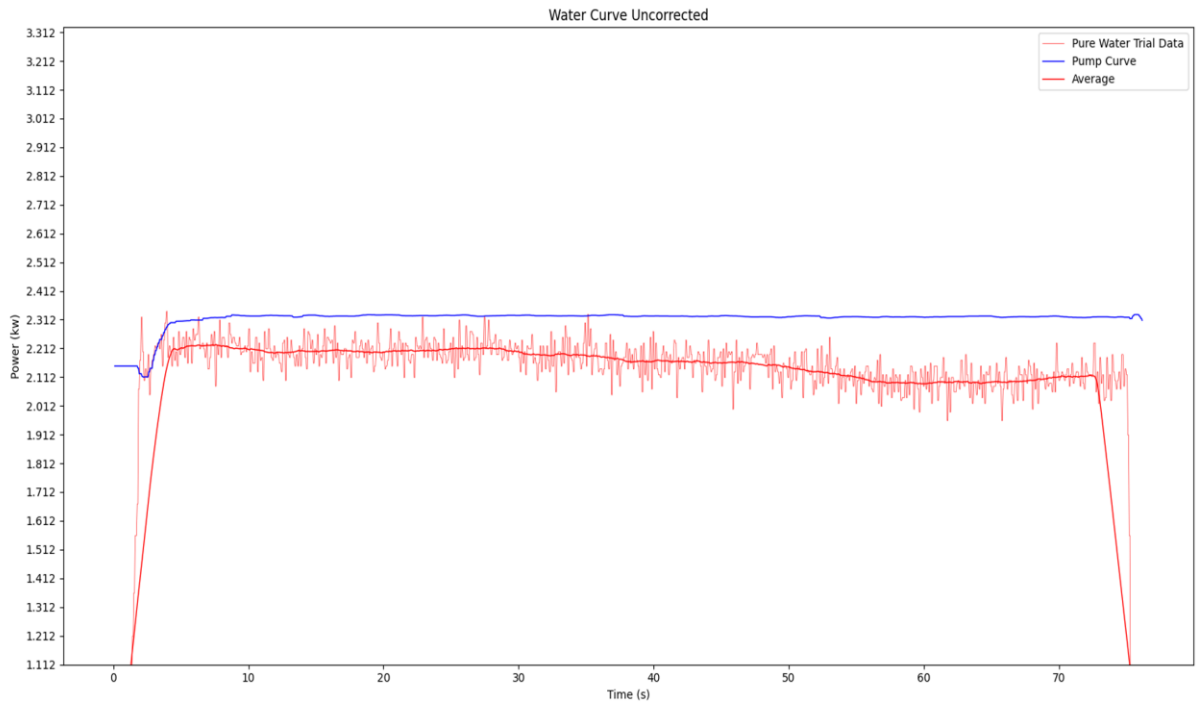


Figure 5.9: Manufacturer Pump Power Curve vs Pump Power Recorded, Clean Water, Pump Speed 60 hz

In the results shown in Figure 5.9, the power recorded by the pump was slightly under the manufacturer's published data. Therefore, the sensor outputs were adjusted by a scaling factor to calibrate the clean water trial results to the published pump curve values. The resulting corrections required were a 4.4% increase to flow rates, an 11.7% increase to pressure, and an 8.3% increase to input power. After applying the calibration correction factors, the Manufacturer Pump Power Curve vs Pump Power Recorded is shown in Figure 5.10.

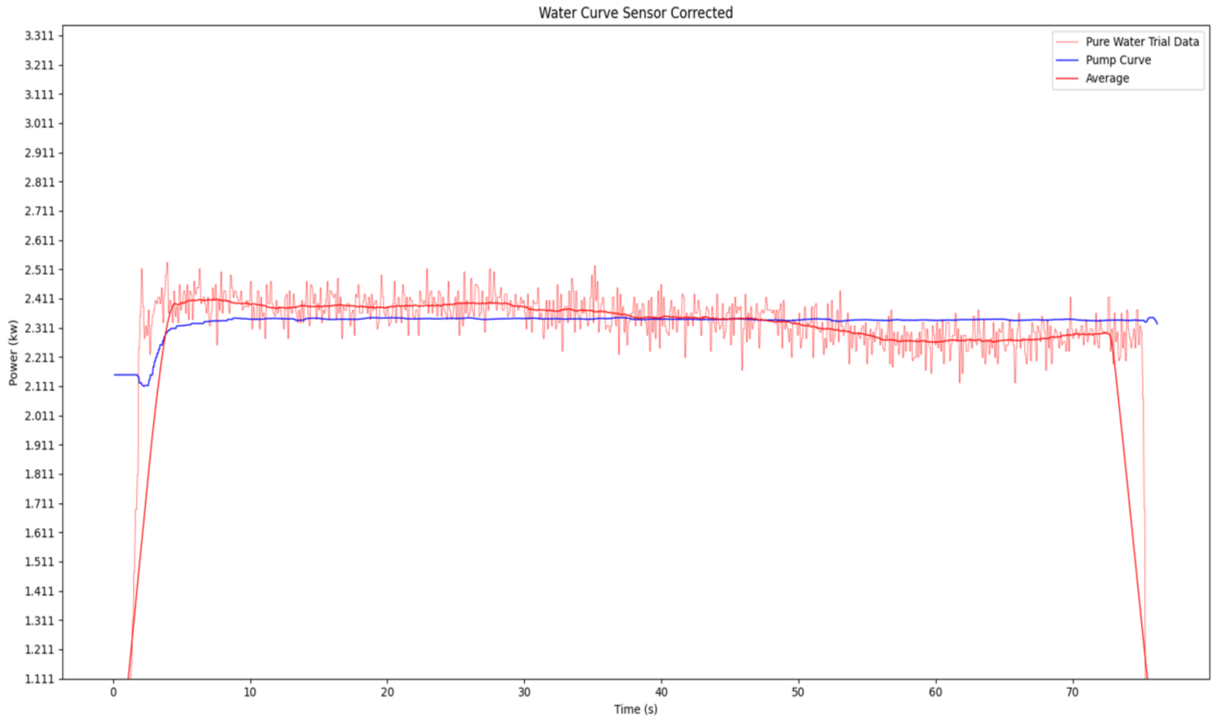


Figure 5.10: Manufacturers Pump Power Curve vs Pump Power Recorded, Corrected, Pump Speed 60 hz

The average power draw shown in Figure 5.10 does show a slight decrease in power over the period. One potential explanation for this is that the initial power draw was the result of a cold start-up. As the run time increased, the system's resistance gradually reduces as the wiring heats up, resulting in less power input. This result requires further investigation in future study to determine why there is a decreasing power input for the test setup.

# Chapter 6: Results and Discussion

In this section each of the models are verified and the coefficients further developed based on the test data gathered. Specifically, models of production, excavation, pipeline, and dredge head are further developed and analyzed. The barge ship model is not specifically verified as the component influence on the dredge system is represented by the gantry in this experimental setup. The overall control model of the cable-driven dredge in three dimensions is not studied as it is already considered to have sufficient dynamic control through full scale industrial test applications and not the focus of this study.

### Model Verification

Each of the trial data sets were run through the production model and plotted with corresponding trial measurements for comparison. Four of the trial data sets are discussed in the following section as they cover the range of results over all data sets. The data sets discussed are: (1) Impeller 60 Hz, Speed 15Hz, Depth 120 mm, Trial A; (2) Impeller 60 Hz, Speed 5Hz, Depth 40 mm, Trial A; (3) Impeller 50Hz, Speed 15Hz, Depth 80 mm, Trial A; and (4) Impeller 50Hz, Speed 5Hz, Depth 40 mm, Trial A.

The "Residual $C_v$" is the concentration of the sample collected in the discharge line at the end of each trial. The collection process included draining the residual sediment from each of the discharge hose sections which introduced error as one hundred percent of the residual sediment could not be gathered. The "Collected $C_v$" is the average concentration of the sample gathered in the collection tank from the trial period. The "Average Predicted $C_v$" trend line is based on an average of ten adjacent "Predicted $C_v$" values from the algorithm model, forming a moving average. The "Input Power" is the measured power over the trial period.

It is important to note that the test tank allows for a maximum dredge travel distance of 1.4 m. Therefore, the trials at low travel speed have a period three times longer than the trials at high speed. In practice, because the collection tank became full, the low travel speed trials had to be stopped before the pump traveled the full 1.4 m. The approximate trial time durations by travel speed are as follows: low speed, 75 seconds; medium speed, 50 seconds; high speed, 35 seconds.

Figure 6.1 shows that the Average Predicted $C_v$ starts the trial near the value for the Collected $C_v$ and gradually trends closer to the Residual $C_v$. Ideally, the trial would end with the Predicted $C_v$ on the Residual $C_v$ line. However, for the purposes of this initial testing, this data provides sufficient results of responding variables that can be used later to investigate why the predicted and actual values differ.

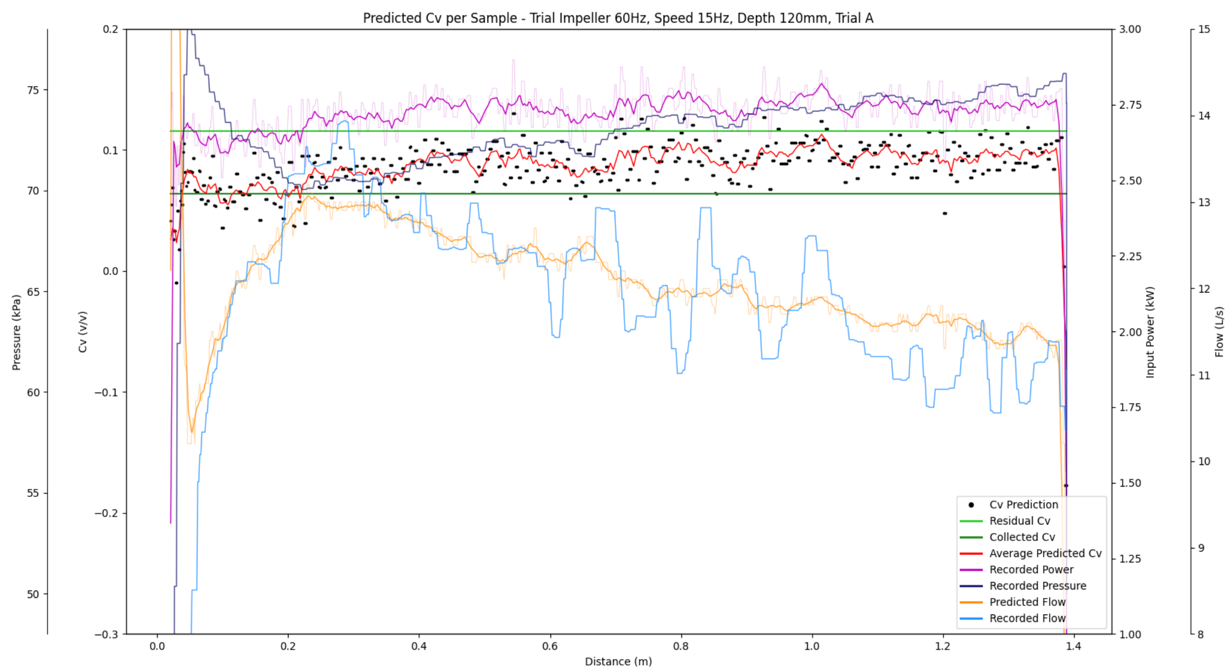


Figure 6.1: Production Model Predictions - Impeller 60 Hz, Speed 15Hz, Depth 120 mm, Trial A

A notable difference between the Collected $C_v$ and Residual $C_v$ lines indicates that the concentration of solids in the pipe is higher than the concentration of solids deposited in the collection tank. Since the flow velocity and Average $C_v$ for this trial are above the predicted Deposition Limit Velocity, we expect that slippage rates account for the increased Residual $C_v$ compared to the Collected $C_v$. The results from Impeller 60 Hz, Speed 15Hz, Depth 120 mm, Trial A, shown in Figure 6.1, has an average flow rate of 12.1 litres/second, which required a minimum of 16.4 seconds for a complete fluid change inside the pipe. If slippage rates impact the system, the time required to stabilize the system would increase. For short trial durations, with the greatest materials depths, as shown in Figure 6.1, system stabilization may not have been fully achieved. This prediction is based on the difference between the Residual $C_v$ and Collected $C_v$. Further study should involve longer trial runs to help determine if the cause of this difference between the Residual $C_v$ and Collected $C_v$ is due to system stabilization.

Figure 6.1 shows that the recorded pressure drops after initial system ramp up, then steadily increases over the remainder of the trial. This gradual increase in pressure is an expected result because the concentration of the slurry mixture increases in the pipeline, causing discharge pipe losses. As the concentration increases, the predicted flow trends downwards, in alignment with the recorded flow.

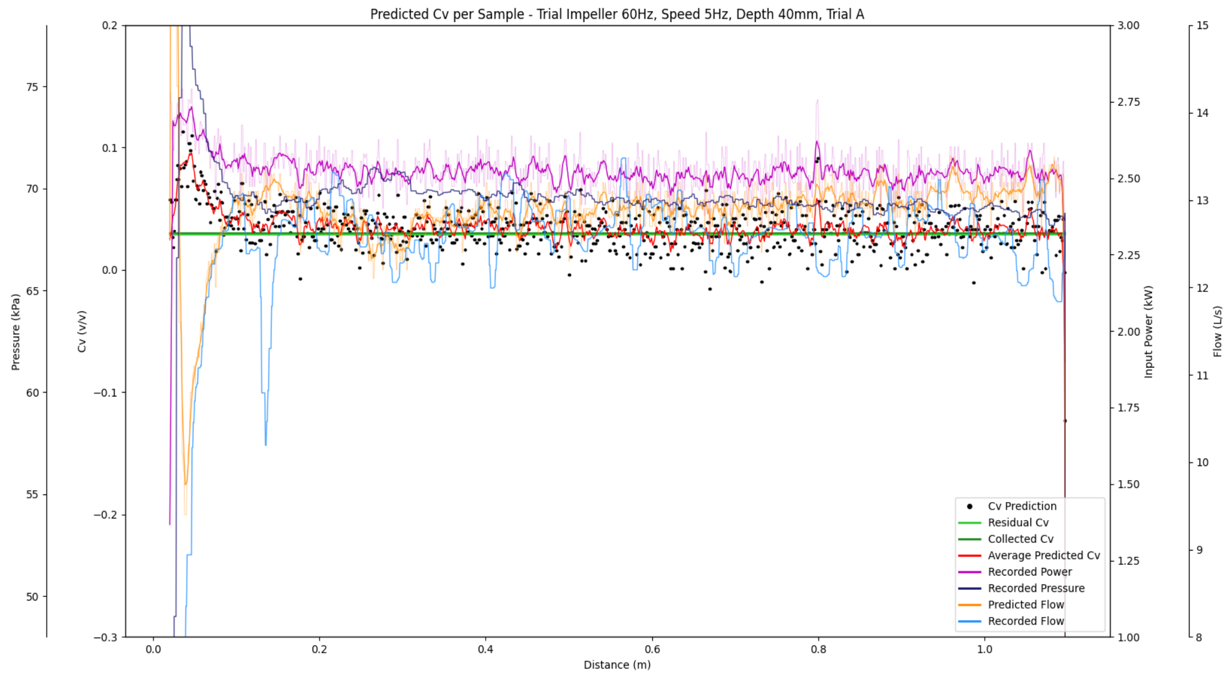


Figure 6.2: Production Model Predictions - Impeller 60 Hz, Speed 5Hz, Depth 40 mm, Trial A

Analysis of the data collected for trial Impeller 60 Hz, Speed 5Hz, Depth 40 mm, Trial A is shown in Figure 6.2. Unlike the previous set of data, trial Impeller 60 Hz, Speed 5Hz, Depth 40 mm, Trial A shows a strong alignment with the residual $C_v$ and collected $C_v$ as both values mirror one another. This result indicates that there is little slippage or deposition of the solids within the discharge pipeline.

The average predicted $C_v$ oscillates along the residual $C_v$ and collected $C_v$ trendlines showing agreement with the trial averages. The recorded power and average predicted $C_v$ also follow similar trends for this data set. As shown in Figure 6.2, the predicted flow is a near mirror image to the recorded pressure curve indicating a strong flow/head correlation as would be expected based on dynamic system losses. The recorded flow and recoded pressure remain relatively constant over the trial. However, the recorded pressure does have a slight negative trend.

Shortly after start-up the recorded pressure lowered to a value approximately equal with the pressure near the end of the trial before sharply rising and then starting its slight negative trend. We think this pressure trend is due to either residual solids in the discharge hose, or a large quantity of solids entering the system at start-up. Either situation would result in a sudden increase in the local slurry density, causing a larger static pressure and power draw at the pump. As flow continued, the slurry density slowly reduced, resulting in less static pressure at the pump. There is a noticeable valley in the recorded flow graph coinciding with the sharp rise in recorded pressure, which would also support this assumption. Another result shows that the average collected $C_v$ (3.4%) was slightly larger than the residual $C_v$ (3.0%), which indicates an impossible negative slip. A complete error analysis was not done as part of this lean approach as the intent was to get an initial understanding of the influencing variables on the system. However, it is predicted that this difference may be the result of error associated with the test setup and this should be further investigated in future experiments.

Figure 6.3 and Figure 6.4 show the analysis of the data gathered over Impeller 50Hz, Speed 15Hz, Depth 80 mm, Trial A and Impeller 50Hz, Speed 5Hz, Depth 40 mm, Trial A. Figure 6.3 shows a decreasing pressure trend and increasing flow for as far as 0.4 meters, after which the pressure steadily increases while the flow decreases to the end of the trial. Figure 6.4 Impeller 50Hz, Speed 5Hz, Depth 40 mm, Trial A also displays a similar decreasing pressure trend over the same time interval. We expect that the initial deposition of solids in the line influence the discharge pressure. Impeller 50Hz, Speed 15Hz, Depth 80 mm, Trial A did not reach the minimum deposition velocity to maintain solids in suspension (see Figure 6.3). We think the wide deviation in the "Residual $C_v$" and the "Collected $C_v$" lines indicate a high rate of solids' slippage (or lag) and potential settling in the discharge hose.

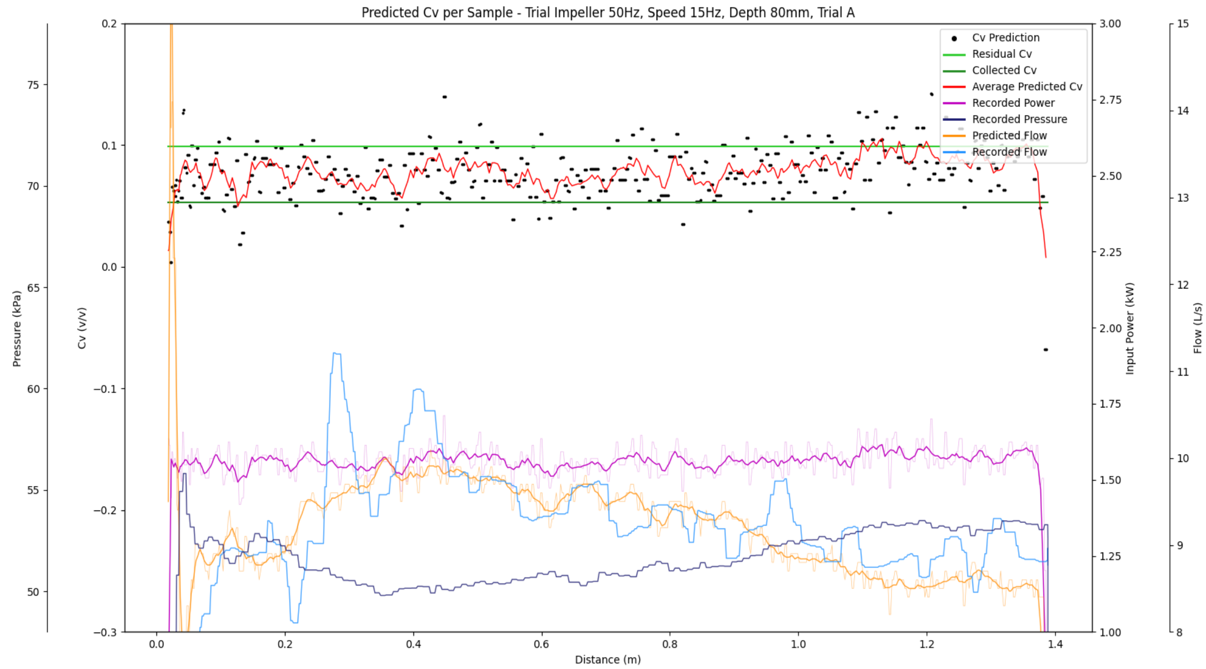


Figure 6.3: Production Model Predictions – Impeller 50Hz, Speed 15Hz, Depth 80 mm, Trial A

Figure 6.4 was one of two 50 Hz trails that exceeded the deposition limit by a small margin. The narrow separation between the "residual $C_v$" and the "collected $C_v$" lines indicate low slippage rates and heterogeneous slurry flow. However, the predicted production does see a slight negative trend over the operating period. This slight negative trend is also shown in the measured pressure results while the flow increased slightly.

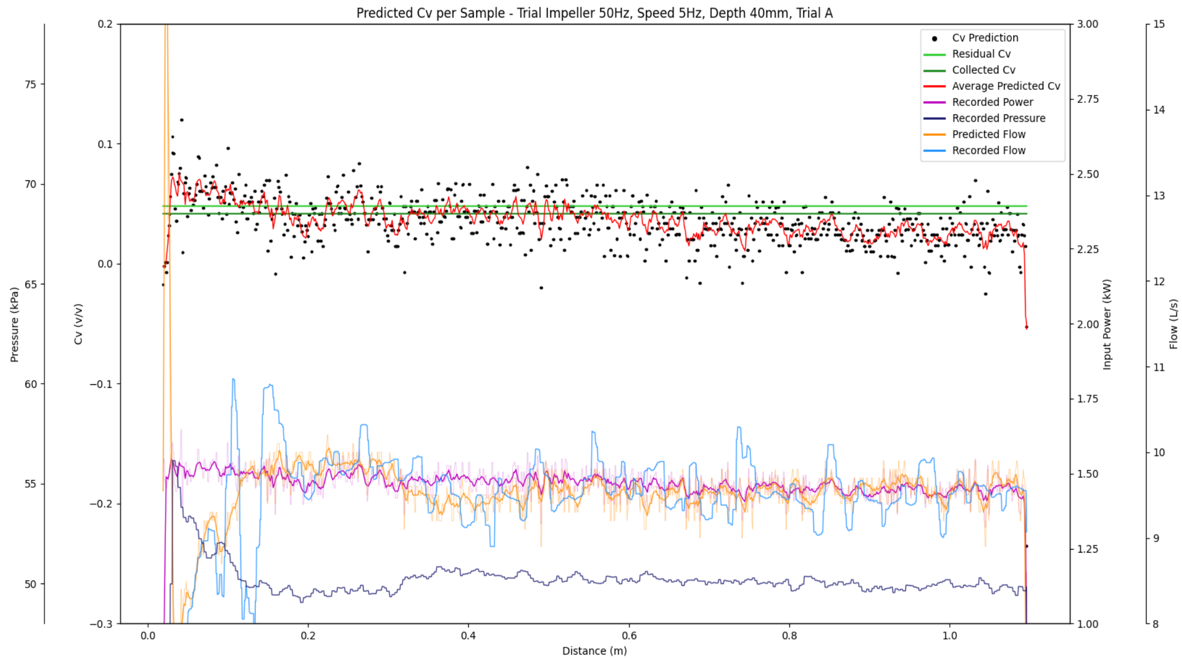


Figure 6.4: Production Model Predictions – Impeller 50Hz, Speed 5Hz, Depth 40 mm, Trial A

As with all trials, and shown in Figures 6.1 – 6.4, there is a strong correlation between the "input power" and corresponding measured $C_v$. This indicates the significance of measuring the pump power to estimate the concentration of solids entering the pump. However, based on the limited test durations and initial trial results, additional investigation in future study is required to determine if steady state operation was reached for each of the trials.

Figure 6.5 shows that for all but two of the 50 Hz trials, the critical deposition velocity of conveyed solids was not met.

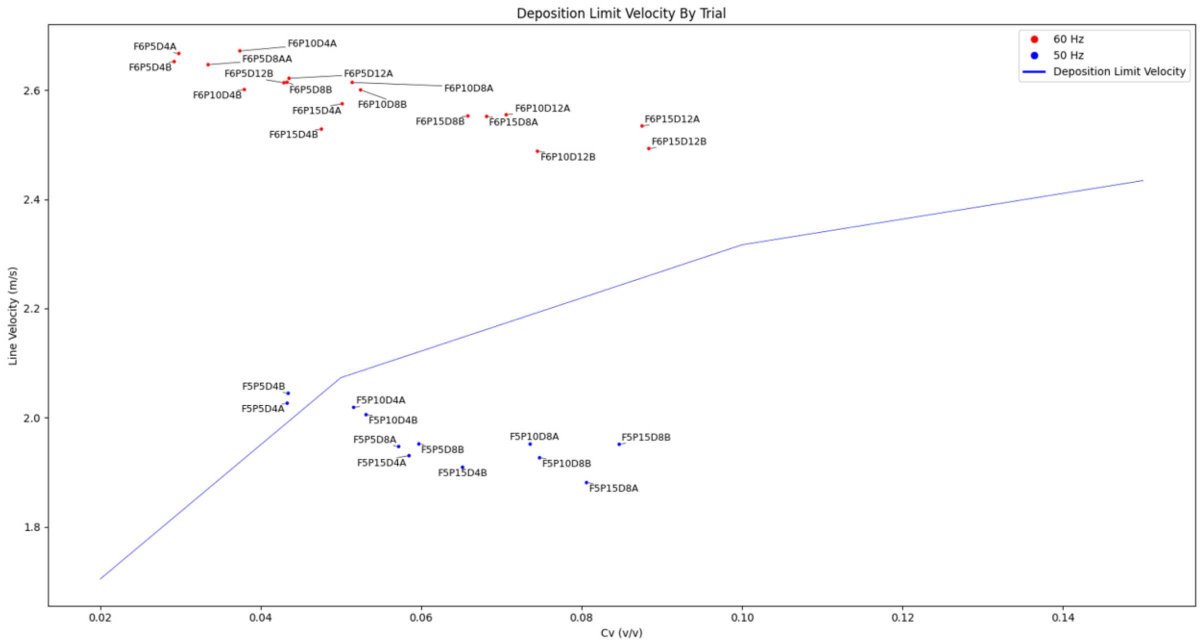


Figure 6.5: Deposition Limit Velocity, By Trial

The effects of settling and slippage are further highlighted in the trials where the dredge pump rotational frequency was set to 50 Hz. This deviation of “average residual $C_v$” and the “average collected $C_v$” for the 50 Hz and 60 Hz trials is shown in Figure 6.6.

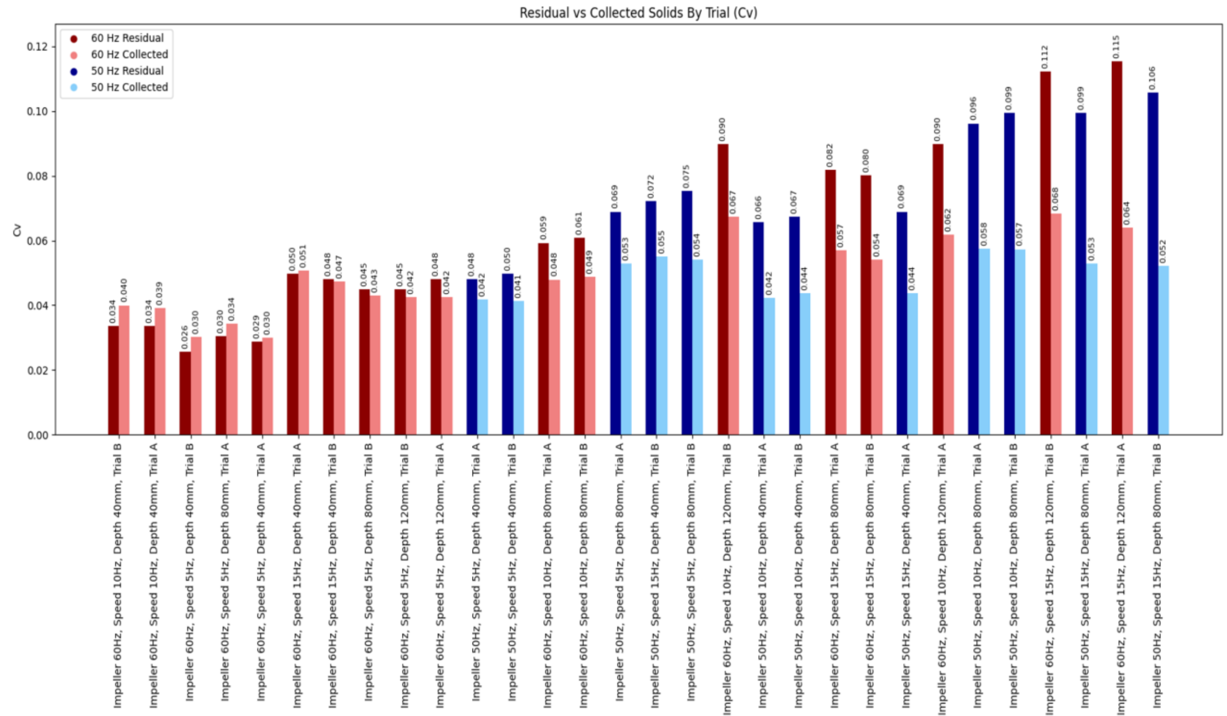


Figure 6.6: Residual vs Collected Solids, by Trial

As shown in Figure 6.6, the higher performance 60 Hz trials, specifically those with a travel frequency of 10Hz and 15Hz and a depth of 80mm and 120mm, also indicate slipping or deposition even though the line velocity exceeds the minimum deposition velocity shown in Figure 6.5. It is assumed that because of the trending pressure and flow readings, the trials with higher $C_v$ had not reached a steady state operating point by the end of the trial. This assumption requires further verification.

Trials were analyzed based on the predicted $C_v$ and measured $C_{v,}$, as well as the predicted and measured flow. Outlier data from ramp up and ramp down were removed for analysis over all data sets. In addition, the 50 Hz trials were removed for the analysis since all but two of the trials fell outside the critical deposition limit. Table 6.1 and Table 6.2 show the comparison of the measured and recorded flow and solids concentrations during the trials.

Table 6.1: Production Model, Flow Results, 60 Hz Trials

| ***Trial*** | ***Samples*** | ***Average Flow (L/s)*** | ***Predicted Flow (L/s)*** | ***Diff. (L/s)*** |
|---|---|---|---|---|
| *Impeller 60Hz, Speed 10Hz, Depth 120mm, Trial A* | 952 | 12.2 | 12.2 | 0.0 |
| *Impeller 60Hz, Speed 10Hz, Depth 120mm, Trial B* | 951 | 11.9 | 12.1 | -0.2 |
| *Impeller 60Hz, Speed 10Hz, Depth 40mm, Trial A* | 951 | 12.8 | 12.9 | -0.1 |
| *Impeller 60Hz, Speed 10Hz, Depth 40mm, Trial B* | 953 | 12.4 | 12.9 | -0.4 |
| *Impeller 60Hz, Speed 10Hz, Depth 80mm, Trial A* | 950 | 12.5 | 12.5 | -0.1 |
| *Impeller 60Hz, Speed 10Hz, Depth 80mm, Trial B* | 947 | 12.4 | 12.6 | -0.2 |
| *Impeller 60Hz, Speed 15Hz, Depth 120mm, Trial A* | 654 | 12.1 | 12.0 | 0.1 |
| *Impeller 60Hz, Speed 15Hz, Depth 120mm, Trial B* | 654 | 11.9 | 12.2 | -0.2 |
| *Impeller 60Hz, Speed 15Hz, Depth 40mm, Trial A* | 657 | 12.3 | 12.7 | -0.4 |
| *Impeller 60Hz, Speed 15Hz, Depth 40mm, Trial B* | 655 | 12.1 | 12.7 | -0.6 |
| *Impeller 60Hz, Speed 15Hz, Depth 80mm, Trial A* | 656 | 12.2 | 12.4 | -0.2 |
| *Impeller 60Hz, Speed 15Hz, Depth 80mm, Trial B* | 656 | 12.2 | 12.5 | -0.3 |
| *Impeller 60Hz, Speed 5Hz, Depth 120mm, Trial A* | 1471 | 12.5 | 12.4 | 0.1 |
| *Impeller 60Hz, Speed 5Hz, Depth 120mm, Trial B* | 1474 | 12.5 | 12.6 | -0.1 |
| *Impeller 60Hz, Speed 5Hz, Depth 40mm, Trial A* | 1470 | 12.7 | 12.8 | -0.1 |
| *Impeller 60Hz, Speed 5Hz, Depth 40mm, Trial B* | 1474 | 12.7 | 13.1 | -0.4 |
| *Impeller 60Hz, Speed 5Hz, Depth 80mm, Trial A* | 1471 | 12.6 | 12.8 | -0.2 |
| *Impeller 60Hz, Speed 5Hz, Depth 80mm, Trial B* | 1474 | 12.5 | 12.7 | -0.2 |

Table 6.2: Production Model, Concentration Results, 60 Hz Trials

| ***Trial*** | ***Samples*** | ***Average Measured Cv (%)*** | ***Predicted Cv (%)*** | ***Net Diff. (%)*** |
|---|---|---|---|---|
| *Impeller 60Hz, Speed 10Hz, Depth 120mm, Trial A* | 952 | 7.1 | 6.3 | 0.8 |
| *Impeller 60Hz, Speed 10Hz, Depth 120mm, Trial B* | 951 | 7.5 | 7.4 | 0.1 |
| *Impeller 60Hz, Speed 10Hz, Depth 40mm, Trial A* | 951 | 3.7 | 6.3 | -2.5 |
| *Impeller 60Hz, Speed 10Hz, Depth 40mm, Trial B* | 953 | 3.8 | 5.3 | -1.5 |
| *Impeller 60Hz, Speed 10Hz, Depth 80mm, Trial A* | 950 | 5.1 | 4.6 | 0.5 |
| *Impeller 60Hz, Speed 10Hz, Depth 80mm, Trial B* | 947 | 5.2 | 6.2 | -0.9 |
| *Impeller 60Hz, Speed 15Hz, Depth 120mm, Trial A* | 654 | 8.8 | 8.4 | 0.4 |
| *Impeller 60Hz, Speed 15Hz, Depth 120mm, Trial B* | 654 | 8.8 | 8.7 | 0.1 |
| *Impeller 60Hz, Speed 15Hz, Depth 40mm, Trial A* | 657 | 5.0 | 6.8 | -1.8 |
| *Impeller 60Hz, Speed 15Hz, Depth 40mm, Trial B* | 655 | 4.8 | 4.7 | 0.1 |
| *Impeller 60Hz, Speed 15Hz, Depth 80mm, Trial A* | 656 | 6.8 | 6.3 | 0.6 |
| *Impeller 60Hz, Speed 15Hz, Depth 80mm, Trial B* | 656 | 6.6 | 6.4 | 0.2 |
| *Impeller 60Hz, Speed 5Hz, Depth 120mm, Trial A* | 1471 | 4.4 | 4.7 | -0.3 |
| *Impeller 60Hz, Speed 5Hz, Depth 120mm, Trial B* | 1474 | 4.3 | 5.1 | -0.8 |
| *Impeller 60Hz, Speed 5Hz, Depth 40mm, Trial A* | 1470 | 3.0 | 3.3 | -0.3 |
| *Impeller 60Hz, Speed 5Hz, Depth 40mm, Trial B* | 1474 | 2.9 | 4.5 | -1.6 |
| *Impeller 60Hz, Speed 5Hz, Depth 80mm, Trial A* | 1471 | 3.3 | 4.6 | -1.3 |
| *Impeller 60Hz, Speed 5Hz, Depth 80mm, Trial B* | 1474 | 4.3 | 5.3 | -1.0 |

The maximum difference in flow, shown in Table 6.1, during the trials was 0.6 l/s, which is within 5% of the measured flow using Eq. (75).

$$Q_{Err_2} = 100\% * \left(\frac{|Q_{Avg} - Q_{pred}|}{Q_{Avg}}\right) \tag{75}$$

where, $Q_{Avg}$ is the average measured flow rate for the trial, $Q_{pred}$ is average predicted flow rate for the trial, $Q_{Err_2}$ is the error between the measured and predicted flow rates per trial.

The maximum net difference in Predicted $C_v$ and Measured $C_v$ was 2.5% which indicates that the preliminary predictive model provides some insight into solids being produced. However, the relative deviation of the predicted concentration from the measured concentration was calculated to be up to 70% using Eq. (76). This large deviation is due to the sensitivity of the data at small ranges which makes small changes in concentration show as large deviation in the prediction model versus the measured result.

$$C_{v(Err)} = 100\% * \left(\frac{|C_{v(Trial)} - C_{v(pred)}|}{C_{v(Trial)}}\right) \tag{76}$$

where, $C_{v(Trial)}$ is the average measured concentration for the trial, $C_{v(pred)}$ is average predicted concentration for the trial, and $C_{v(err)}$ is the error between the measured and predicted concentrations per trial.

Further testing is required to determine if the predicted model maintains a difference within 2.5% of the measured result. For the purposes of this baseline study, the production model and associated power trends provides some initial insight into the influence of the adjusted parameters. However, as expected future work is required to reproduce and verify these results in a controlled laboratory environment.

*Pipeline Model*

The pipeline model provides a secondary measure for predicting the estimated losses over the discharge pipeline when transporting a slurry. The pipeline model verification compared the measured discharge pressure of the test setup with the model described by Furboter [98]. In calculation of the pressure loss across an incremental length of discharge pipe, the relative effect of Furboter's [98] model coefficient $a_p$ (water effect) and $b_p$ (solids effect) components are important. Figure 6.7 shows the theoretical pressure loss caused by the water effect and solids in Furboter's [98] model when using a solids concentration of 5% by volume. As shown, the solids effect becomes less significant as the flow velocity increases.

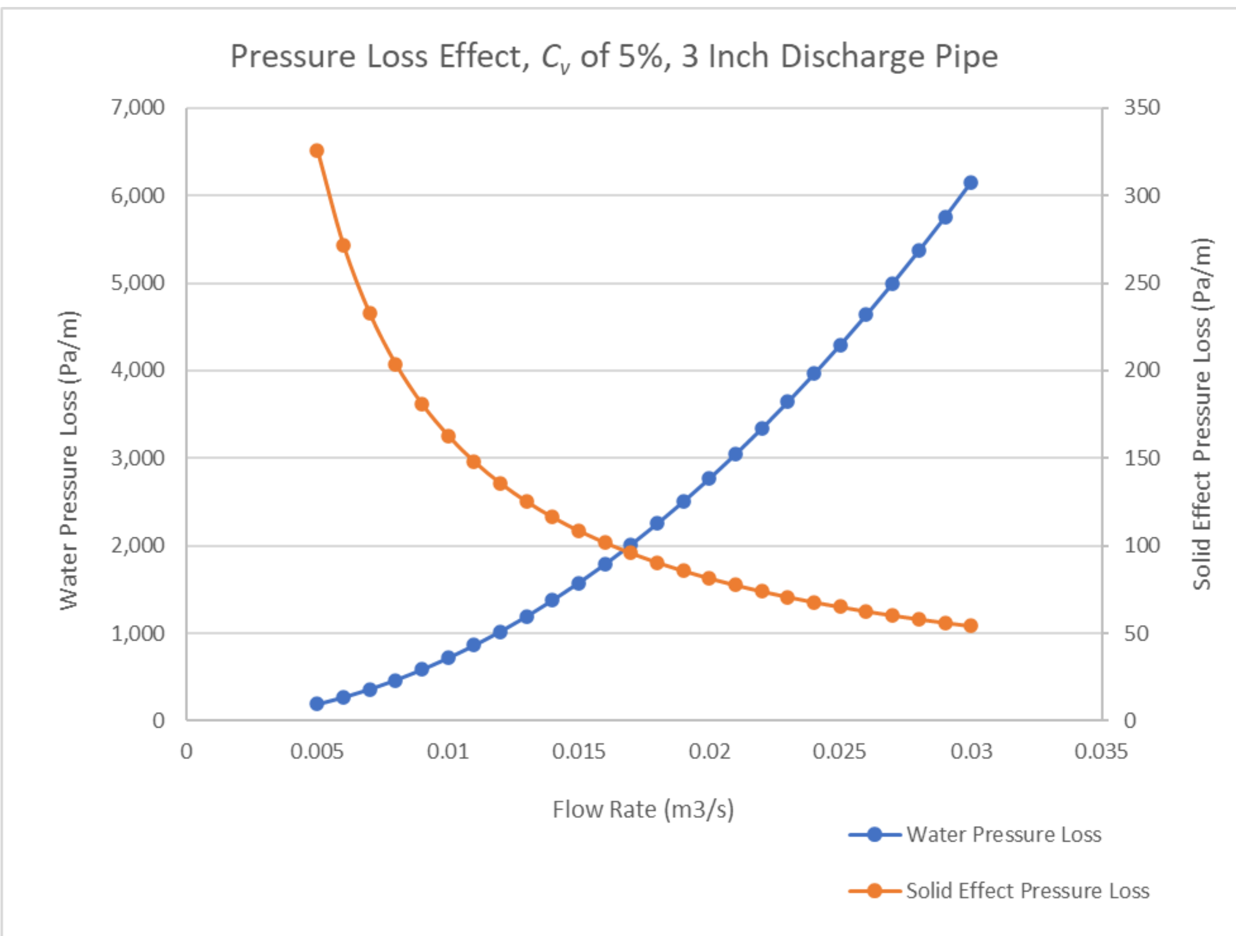


Figure 6.7: Pipeline Pressure Loss [98], Solids Vs Water, $C_v$ of 5%, 3 inch Discharge Pipe

The dynamic viscosity of the mixture used to determine the Reynolds number was calculated using three different methods, as shown in Figure 6.8.

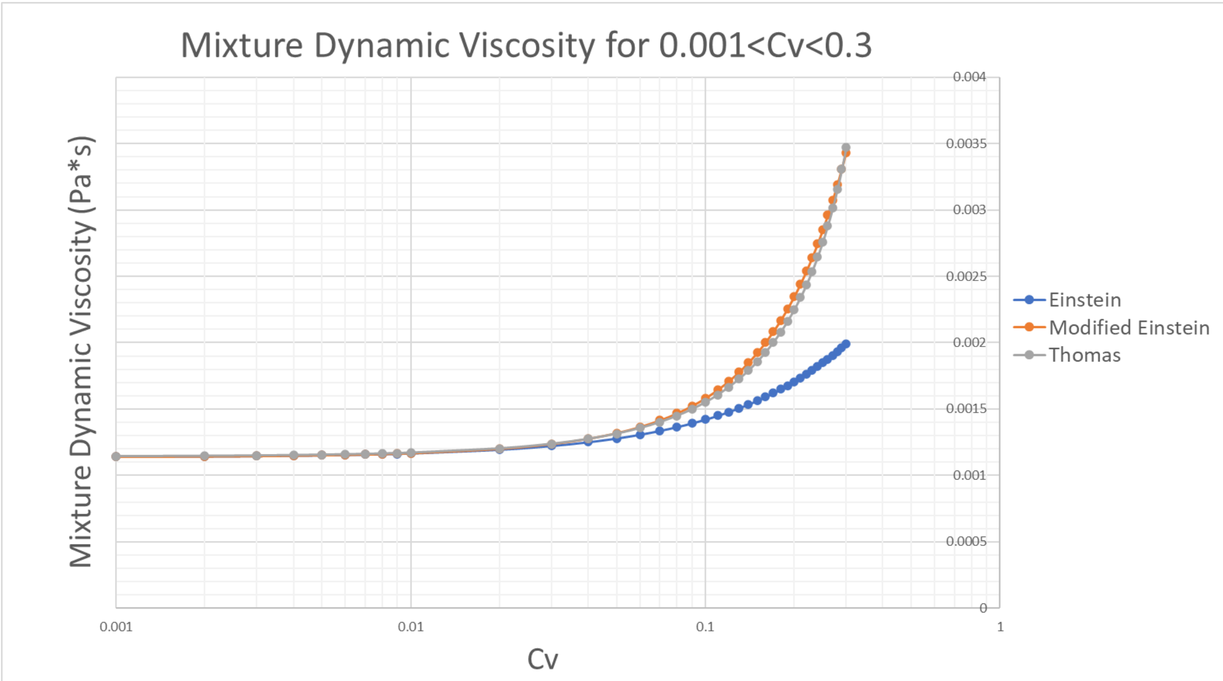


Figure 6.8: Mixture Dynamic Viscosity for $0.001<C_v<0.3$ [157]

The Modified Einstein and Thomas equations [157] produce similar viscosities for low solids concentrations ($C_v$ less then 0.05). For solids concentrations above 0.05, and up to 0.3, the Modified Einstein equation [157] produces a higher viscosity, which will produce a smaller Reynolds number and in turn produce a more conservative friction factor by the Swamee-Jain formula [158] used in Furboter's model [98]. From the three methods considered, the Modified Einstein [157] equation was selected for determining the dynamic viscosity of the mixture. Figure 6.9 compares the pressure effect when using the dynamic viscosity of water versus the pressure effect when adjusting for the dynamic viscosity of solids using the Modified Einstein equation [157].

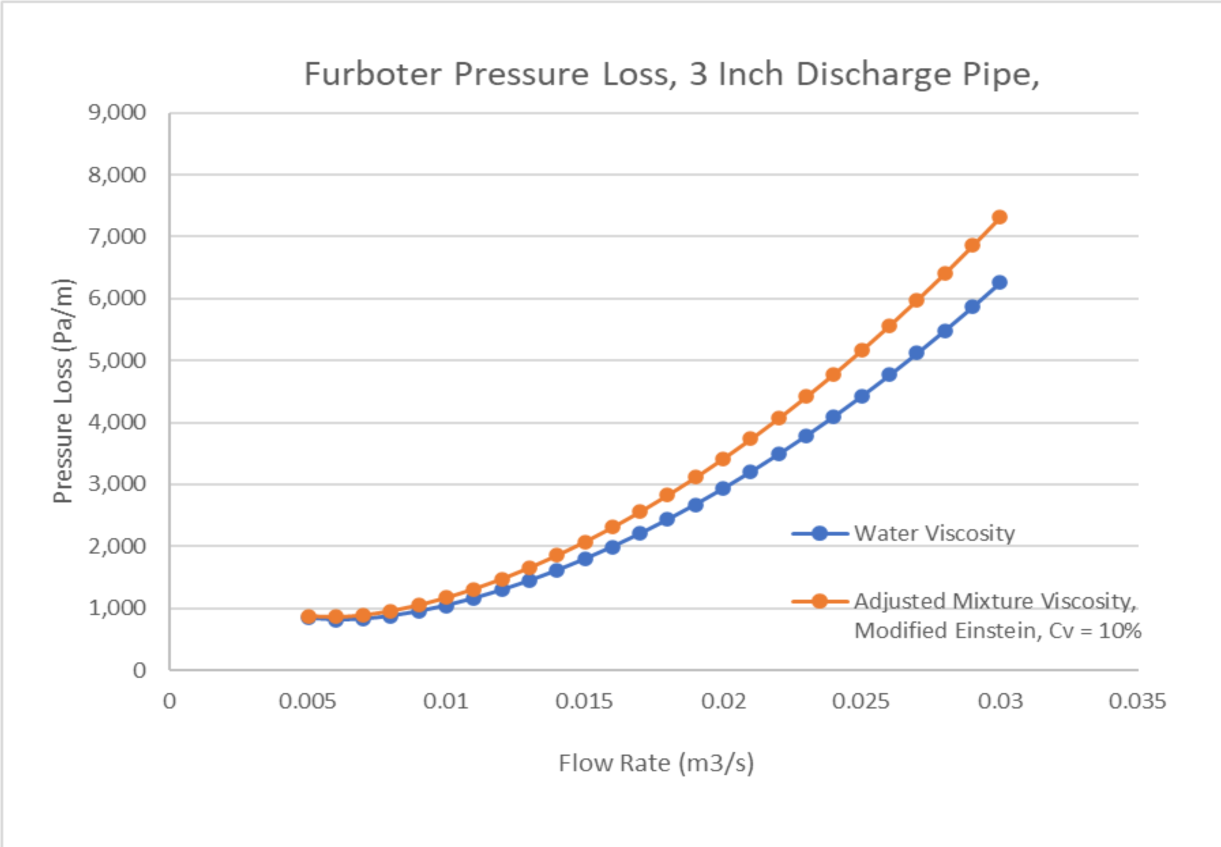


Figure 6.9: Pressure Loss, Furboter $C_v$ at 10% [98]

For each of the trials, the predicted TDH losses were calculated by substituting the average measured values of flow rate and $C_v$ into the equations for dynamic viscosity, Reynolds number, friction factor, and pressure loss. The predicted TDH is shown in comparison to the measured TDH in Figure 6.10. As shown, the adjusted Furboter model [98] underpredicts the TDH of the 50 Hz and 60 Hz pump trials by an average of 2% and 6%, respectively. The TDH values for the predicted head are inclusive of the head loss, elevation gain, and dynamic head. The measured TDH values include the pressure sensor values converted to head based on the average slurry density, pressure sensor elevation offset from the water surface, and dynamic head for the average trial slurry density and flow rate.

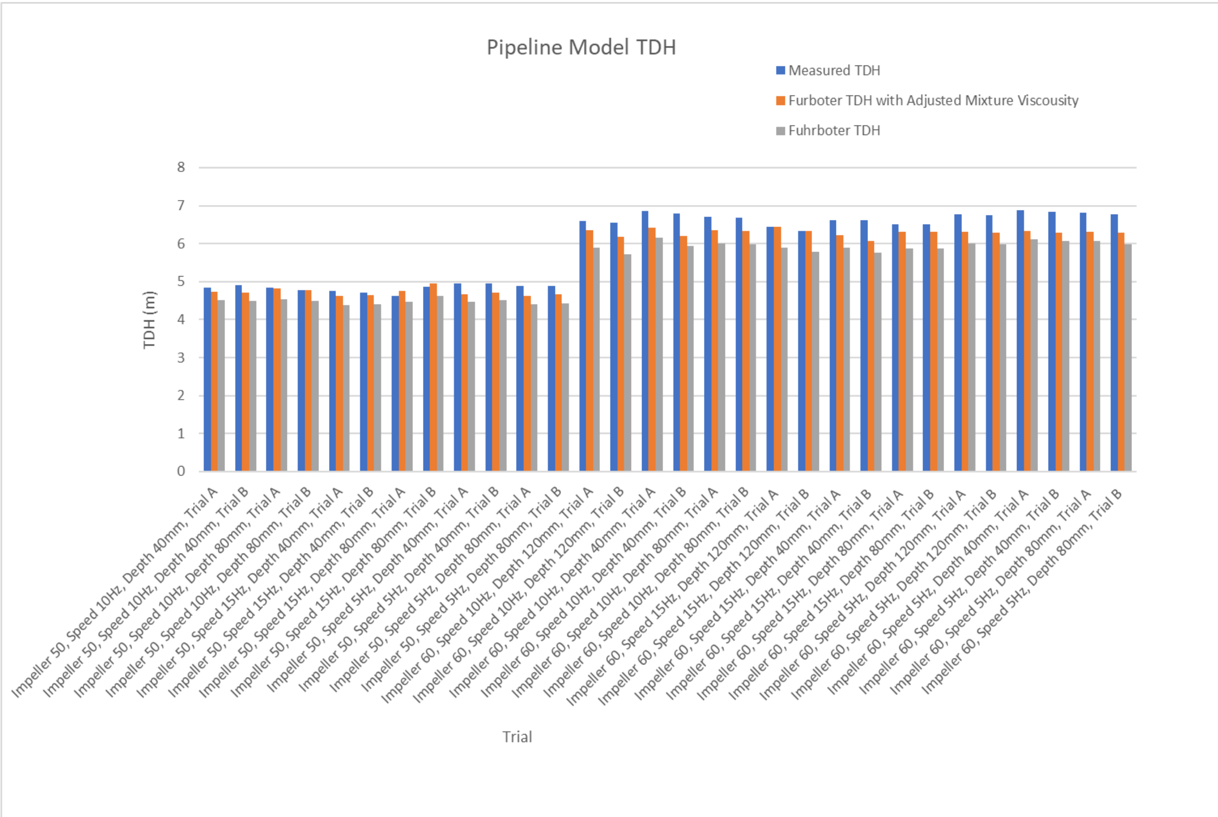


Figure 6.10: Pipeline Model TDH, by Trial

The calculated pipeline losses per trial with both the modified viscosity and water viscosity are shown for comparison in Figure 6.11. Using the dynamic viscosity of water is expected to produce a lower predicted TDH since the pipeline model predicts the TDH using a mixture dynamic viscosity that is greater than that of water, for $0 < C_v < 10\%$.

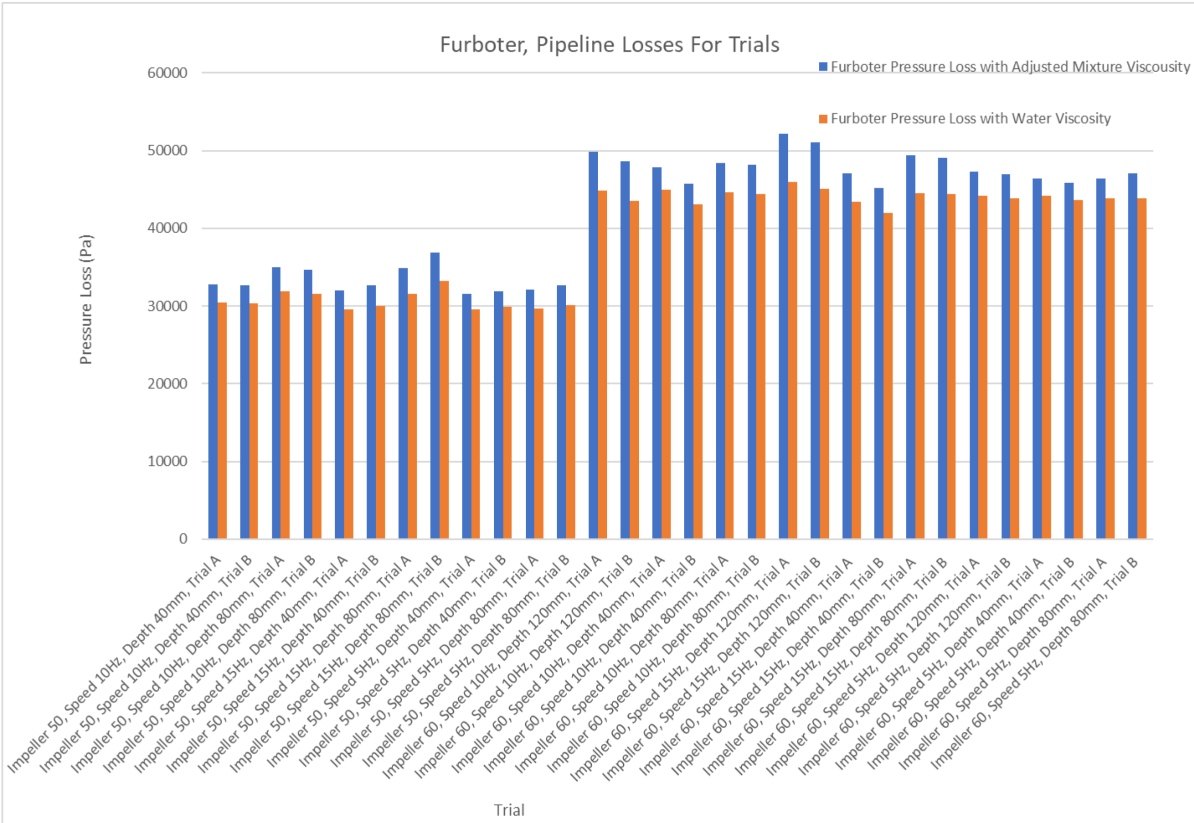


Figure 6.11: Pipeline Losses, by Trial

The comparison shows that the TDH may be scalable to produce a close match in TDH for a system. However, the scale factor used would not hold for different pipe sizes and types or different solid particle sizes and distributions. Therefore, to use the model for each setup would require specific calibration over a range of solids, which is not practical for working dredge applications.

It is challenging to calculate predicted pressure loss across a length of pipe, even when the input flow, particle size, distribution, and slurry density are known. This is due to the many possible flow regimes, and their different behaviours and effects on system losses. Even a pipeline with a fixed flow rate may have sections operating in different flow regimes due to a varying input $C_v$, changing particle size and distribution, and elevation changes along the pipeline length. At best, the calculated pressure loss for a set of known slurry flow conditions should be considered an estimate and requires further testing. In the case of an unknown flow rate and $C_v$, the model is expected to be sensitive to small changes in the inputs which lead to inaccurate predictions. We therefore do not recommend using the predictive pipeline model to determine system total dynamic head. Instead, we suggest using a pressure sensor in combination with the production model to estimate concentration and flow.

*Slip Ratio*

Furboter's model [98] did not accurately predict the discharge pressure and deviated by up to 18%. Another potential reason for this large deviation is that the model assumes an $S_{kt}$ factor based on the median particle size, most often approximated by the $d_{50}$. The $S_{kt}$ factor accounts for the effects of the particles in the flow [79, 141], and provides a convenient method to calculate pressure loss due to the presence of solids in a mixture. However, the $S_{kt}$ factor assumes a constant slip ratio of 0.35 in all flow conditions, regardless of particle size or fluid velocity. We expect that this assumed constant slip ratio contributes to the associated error over the trials. Figures 6.12 and 6.13 illustrate the pressure gradients produced by various solids concentrations at increasing slippage rates. For a fixed $C_v$, the pressure gradient becomes greater as the slip increases. Miedema agrees that a constant slip ratio for all flow condition regardless of particle size and fluid velocity is not acceptable [100].

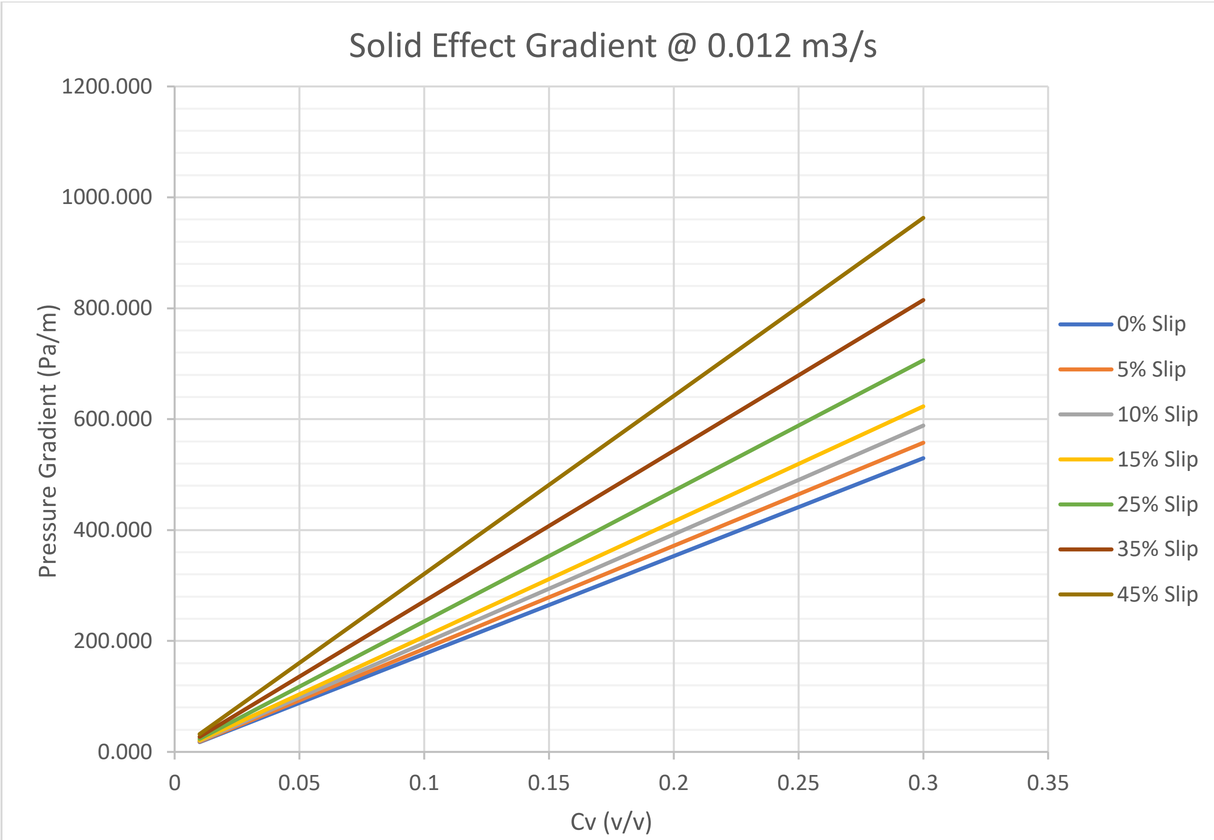


Figure 6.12: Solids Effect Gradient @ 0.012 m3/s [100]

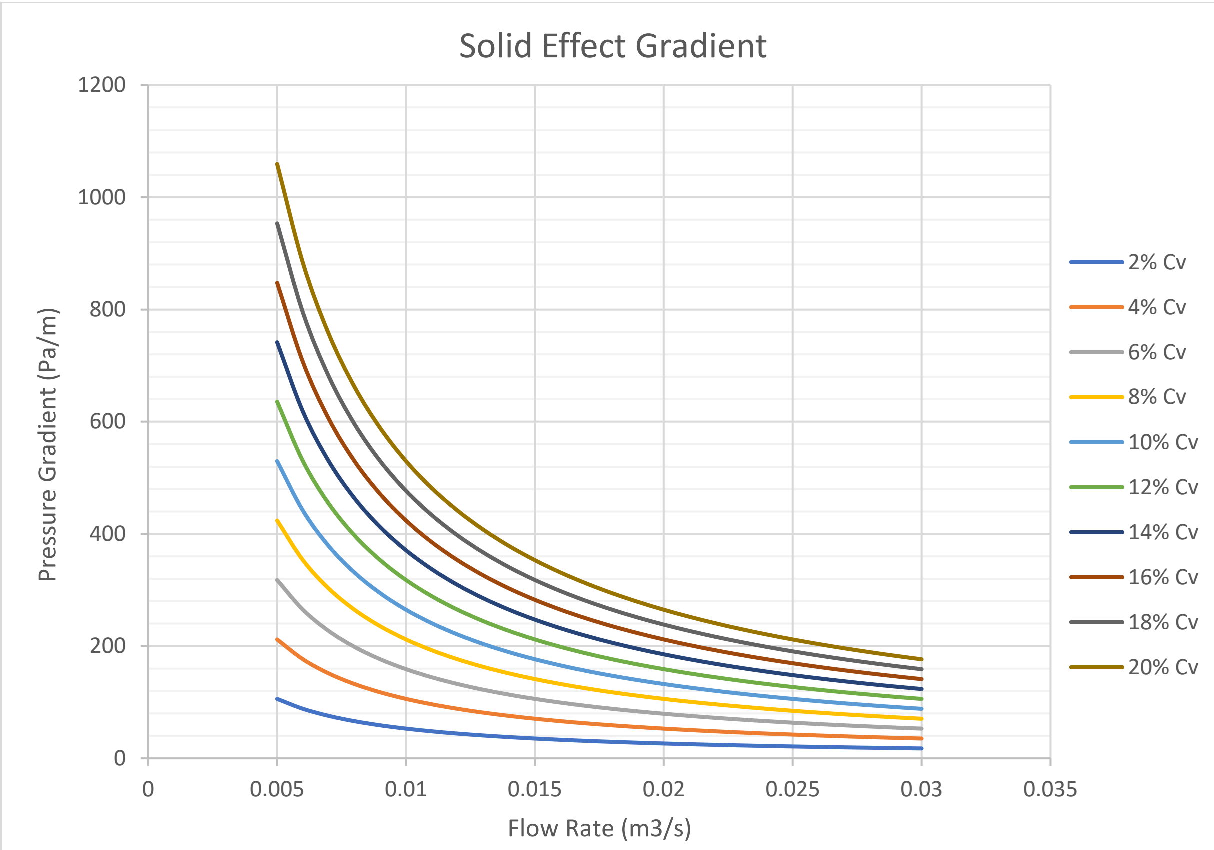


Figure 6.13: Solids Effect Gradient, by Solids Concentration, Slip 20% [100]

Another potential source of error for this model is the vertical section of discharge pipe associated with the test setup. The test apparatus discharge pipe included 6 meters of positive vertical elevation and 2 meters of negative vertical elevation, 23% of the overall pipe length. This change in elevation influences the slippage by causing an increase in the local solids' concentration in the ascending vertical sections, and a decrease of the solids' concentration in the descending vertical sections.

Through further analysis of the results and data, we observed Furboter's model [98] consistently underpredicts the slurry head losses relative to the measured pressure. Therefore, if the model is to be used, we suggest abandoning a constant $S_{kt}$ factor in favour of an adjusted $S_k$ factor which varies depending on slip velocity which is based on the solids being transported.

Over the trials, the slip factor was investigated by comparing the residual $C_v$ and the collected $C_v$ results. As shown in Table 6.3, the average slip ratio over all trials is 44%, which is 9% higher than the assumption in the Furboter model [98]. However, it is important to note that the residual $C_v$ is based on the slurry left in the hose at the end of the trial, which is only a snapshot of the concentration at the end of the trial and is not necessarily representative of concentrations during any other time during the trial. On the other hand, the collected $C_v$ results are based on the average mixture concentration discharged into the collection tank over the entire trial period. This snapshot of residual concentration versus the average collected concentration over the trial is one explanation why some of the slip values shown in Table 6.3 are negative.

Table 6.3: Estimate of Slip Factor by Trial

| Slip % by Trial | | | |
|---|---|---|---|
| Trial | Residual *Cv* | Collected *Cv* | Slip % |
| *Impeller 50Hz, Speed 10Hz, Depth 40mm, Trial A* | 6.6% | 4.2% | 36% |
| *Impeller 50Hz, Speed 10Hz, Depth 40mm, Trial B* | 6.7% | 4.4% | 35% |
| *Impeller 50Hz, Speed 10Hz, Depth 80mm, Trial A* | 9.6% | 5.8% | 40% |
| *Impeller 50Hz, Speed 10Hz, Depth 80mm, Trial B* | 9.9% | 5.7% | 42% |
| *Impeller 50Hz, Speed 15Hz, Depth 40mm, Trial A* | 6.9% | 4.4% | 37% |
| *Impeller 50Hz, Speed 15Hz, Depth 40mm, Trial B* | 7.2% | 5.5% | 24% |
| *Impeller 50Hz, Speed 15Hz, Depth 80mm, Trial A* | 9.9% | 5.3% | 47% |
| *Impeller 50Hz, Speed 15Hz, Depth 80mm, Trial B* | 10.6% | 5.2% | 51% |
| *Impeller 50Hz, Speed 5Hz, Depth 40mm, Trial A* | 4.8% | 4.2% | 13% |
| *Impeller 50Hz, Speed 5Hz, Depth 40mm, Trial B* | 5.0% | 4.1% | 17% |

| | | | |
|---|---|---|---|
| *Impeller 50Hz, Speed 5Hz, Depth 80mm, Trial A* | 6.9% | 5.3% | 23% |
| *Impeller 50Hz, Speed 5Hz, Depth 80mm, Trial B* | 7.5% | 5.4% | 28% |
| *Impeller 60Hz, Speed 10Hz, Depth 120mm, Trial A* | 9.0% | 6.2% | 31% |
| *Impeller 60Hz, Speed 10Hz, Depth 120mm, Trial B* | 9.0% | 6.7% | 25% |
| *Impeller 60Hz, Speed 10Hz, Depth 40mm, Trial B* | 3.4% | 3.9% | -16% |
| *Impeller 60Hz, Speed 10Hz, Depth 40mm, Trial A* | 3.4% | 4.0% | -19% |
| *Impeller 60Hz, Speed 10Hz, Depth 80mm, Trial A* | 5.9% | 4.8% | 19% |
| *Impeller 60Hz, Speed 10Hz, Depth 80mm, Trial B* | 6.1% | 4.9% | 20% |
| *Impeller 60Hz, Speed 15Hz, Depth 120mm, Trial A* | 11.5% | 6.4% | 44% |
| *Impeller 60Hz, Speed 15Hz, Depth 120mm, Trial B* | 11.2% | 6.8% | 39% |
| *Impeller 60Hz, Speed 15Hz, Depth 40mm, Trial B* | 5.0% | 5.1% | -2% |
| *Impeller 60Hz, Speed 15Hz, Depth 40mm, Trial A* | 4.8% | 4.7% | 2% |
| *Impeller 60Hz, Speed 15Hz, Depth 80mm, Trial B* | 8.2% | 5.7% | 30% |
| *Impeller 60Hz, Speed 15Hz, Depth 80mm, Trial A* | 8.0% | 5.4% | 32% |
| *Impeller 60Hz, Speed 5Hz, Depth 120mm, Trial B* | 4.8% | 4.2% | 12% |
| *Impeller 60Hz, Speed 5Hz, Depth 120mm, Trial A* | 4.5% | 4.2% | 5% |
| *Impeller 60Hz, Speed 5Hz, Depth 40mm, Trial B* | 2.9% | 3.0% | -4% |
| *Impeller 60Hz, Speed 5Hz, Depth 40mm, Trial A* | 2.6% | 3.0% | -18% |
| *Impeller 60Hz, Speed 5Hz, Depth 80mm, Trial A* | 3.0% | 3.4% | -13% |
| *Impeller 60Hz, Speed 5Hz, Depth 80mm, Trial B* | 4.5% | 4.3% | 4% |

*Excavation Model*

$$\dot{E}_D = k_s \, w_{cr} \boldsymbol{v} \, h_d \rho_{si}$$

The excavation model is the fundamental component of the dredge system and effects the overall rate of production. Excavation rate for future controllers is expected to increase through parameter adjustments such as dredge head depth, velocity of dredge head or pump rotational speed.

Figure 6.14 shows the difference in the measured production rate compared to the estimated production rate of the excavation model without a $k_s$ factor. In this case, because the experimental trials all include the same material and cutting ring, the density and cutting ring terms are removed from the equation. Measurements of the material removed were taken along the dredge path during each trial. These measurements were compared with the excavation model over the set of trial data, and the $k_s$ factor was developed through a regression model to minimize the difference in the prediction and the measured results.

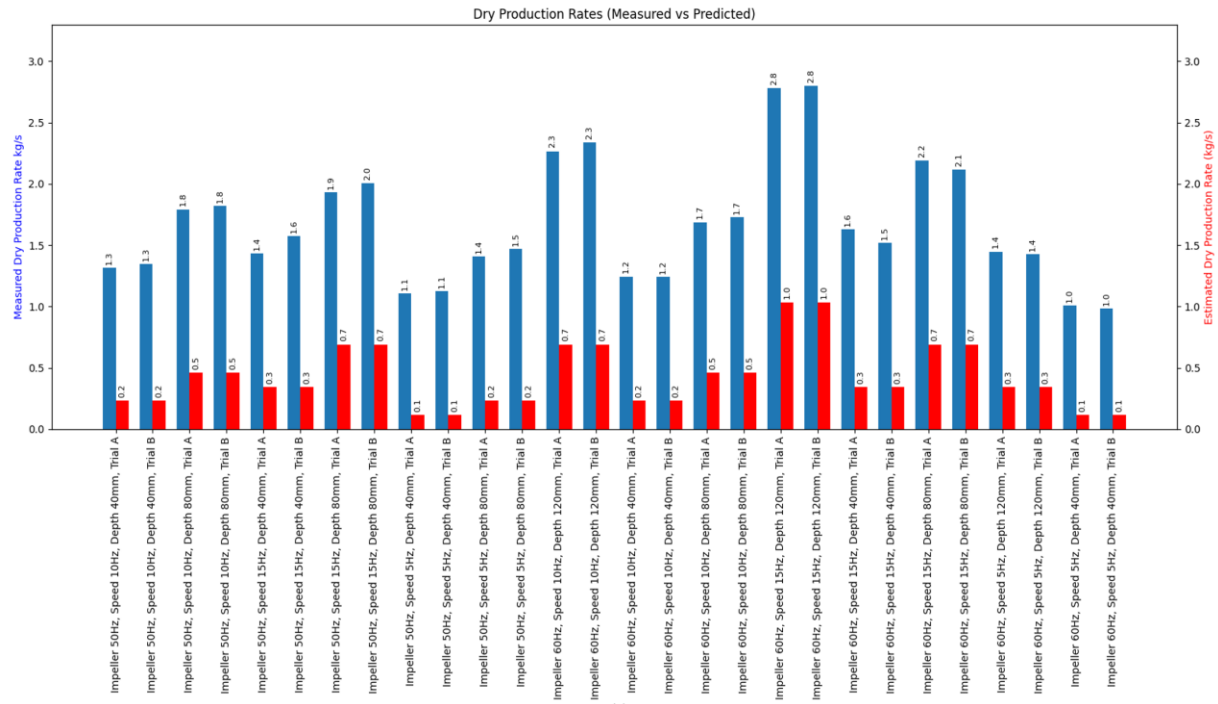


Figure 6.14: Dry Production Rates Per Trial

The $k_s$ factor model was implemented using linear regression with the following terms: F, P, and D, are the trial parameters where, F = pump impeller speed, Hz (50,60); P = pump travel speed, Hz (5,10,15); and D = depth into material, mm (40,80,120). The $k_s$ factor for the excavation models was developed using two-thirds of the trial data, this data was assumed to be training data for the model. Once the initial $k_s$ factor was created based on the training data, we input the remaining one-third of the trial data that the model had never seen to check if the output result aligned with the measured results.

The coefficients for the model were as follows:

a = -0.466;

b = 3.12;

c = 2.24;

d = 0.811;

e = 0.840;

f = 2.81;

g = -0.465;

h = -8.10;

i = -7.30;

j = 9.49.

The variation in the $k_s$ values indicate a disproportionate impact that each of the tested parameters has on the final production results. Or alternatively, there is a missing/hidden variable not included in our equation that bridges this gap. For example, the pump rotational speed, travel speed, and depth calculation does not have a linear relationship to production which results in the $k_s$ factor not being a constant value.

Figure 6.15 shows the predicted $k_s$ factor with the measured $k_s$ factors from each trial.

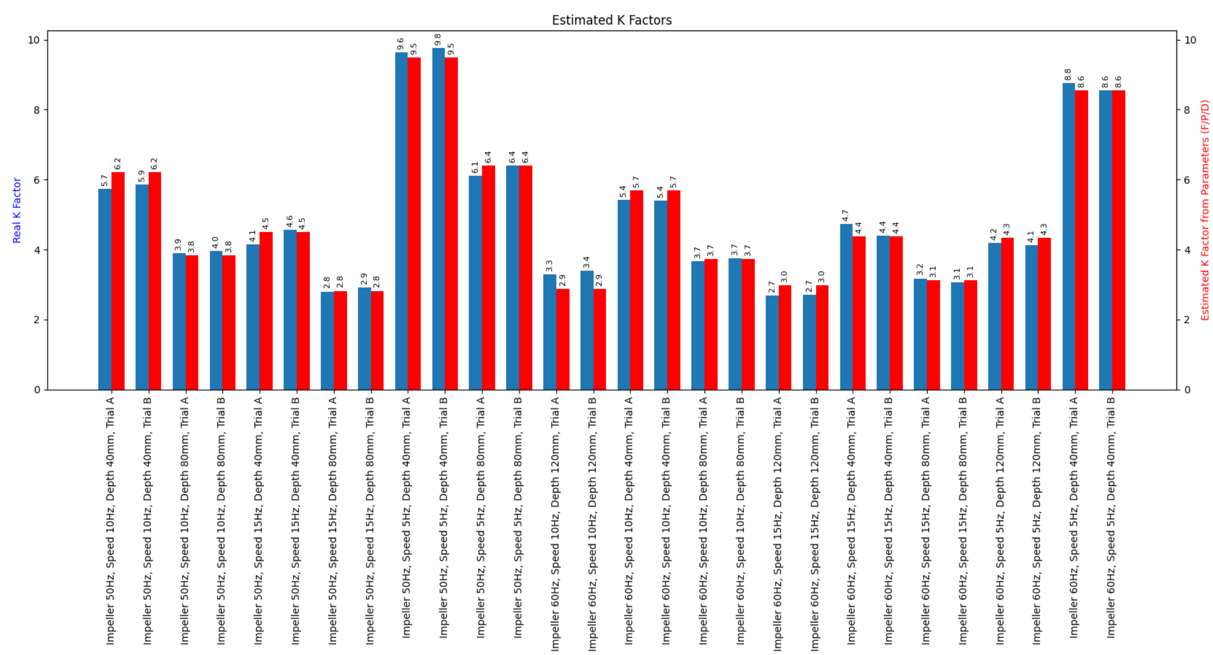


Figure 6.15: Predicted $k_s$ factors, by Trial

The regression model $k_s$ factor fits the data with an $R^2$ value of 0.985 and has a mean absolute percentage error of 4.5% using Eq. (77),

$$K_{(err)} = \frac{1}{n}\sum_{t=1}^{n}\left|\frac{k_{(meas)_t} - K_{(pred)_t}}{K_{(meas)_t}}\right| \tag{77}$$

where, $k_{(meas)}$ is the measured $k_s$ factor for the trial; $k_{(pred)}$ is predicted $k_s$ factor for the trial; and $K_{(err)}$ is the mean absolute percentage error.

As shown in Figure 6.15, the $k_s$ factors are reasonably accurate to predict the excavated materials for the soil conditions. However, due to the limited number of trials available to fit the model, we investigated overfitting of the data to determine whether the model could be applied to a broader range of test setups. The model was trained independently five times on uniquely partitioned datasets. The performance of each model is shown in Table 6.4.

Table 6.4: Partitioned Data Sets

| **PARTITION** | **TRAINING MEAN ABSOLUTE ERROR** | **TESTING MEAN ABSOLUTE ERROR** |
|---|---|---|
| **1** | 0.151 | 0.621 |
| **2** | 0.180 | 0.252 |
| **3** | 0.187 | 0.524 |
| **4** | 0.178 | 0.285 |
| **5** | 0.191 | 0.255 |
| **AVERAGE** | **0.184** | **0.329** |

Based on these results, the excavation model has a consistent performance on average. Therefore, the model is unlikely to be overfitting the data but does result in a slightly higher variance than previously predicted. When the production rate estimation is multiplied by the corresponding predicted $k_s$ factor, the resulting accuracy of the model was found to be within 0.082 kg/s on average. These results are shown in Table 6.5.

Table 6.5: Excavation, Error

| **TRIAL** | **PREDICTED (KG/S)** | **MEASURED COLLECTION TANK (KG/S)** | **MEAN ABSOLUTE ERROR (KG/S)** |
|---|---|---|---|
| Impeller 50Hz, Speed 10Hz, Depth 40mm, Trial A | 1.379 | 1.318 | 0.062 |
| Impeller 50Hz, Speed 10Hz, Depth 40mm, Trial B | 1.379 | 1.347 | 0.033 |
| Impeller 50Hz, Speed 10Hz, Depth 80mm, Trial A | 1.783 | 1.793 | 0.010 |
| Impeller 50Hz, Speed 10Hz, Depth 80mm, Trial B | 1.783 | 1.821 | 0.039 |
| Impeller 50Hz, Speed 15Hz, Depth 40mm, Trial A | 1.487 | 1.432 | 0.055 |
| Impeller 50Hz, Speed 15Hz, Depth 40mm, Trial B | 1.487 | 1.573 | 0.086 |
| Impeller 50Hz, Speed 15Hz, Depth 80mm, Trial A | 1.957 | 1.933 | 0.024 |

| | | | |
|---|---|---|---|
| Impeller 50Hz, Speed 15Hz, Depth 80mm, Trial B | 1.957 | 2.007 | 0.050 |
| Impeller 50Hz, Speed 5Hz, Depth 40mm, Trial A | 1.072 | 1.109 | 0.037 |
| Impeller 50Hz, Speed 5Hz, Depth 40mm, Trial B | 1.072 | 1.123 | 0.051 |
| Impeller 50Hz, Speed 5Hz, Depth 80mm, Trial A | 1.507 | 1.407 | 0.100 |
| Impeller 50Hz, Speed 5Hz, Depth 80mm, Trial B | 1.507 | 1.471 | 0.036 |
| Impeller 60Hz, Speed 10Hz, Depth 120mm, Trial A | 2.004 | 2.266 | 0.263 |
| Impeller 60Hz, Speed 10Hz, Depth 120 mm, Trial B | 2.004 | 2.339 | 0.336 |
| Impeller 60Hz, Speed 10Hz, Depth 40mm, Trial A | 1.303 | 1.245 | 0.058 |
| Impeller 60Hz, Speed 10Hz, Depth 40mm, Trial B | 1.303 | 1.241 | 0.062 |
| Impeller 60Hz, Speed 10Hz, Depth 80mm, Trial A | 1.711 | 1.688 | 0.023 |
| Impeller 60Hz, Speed 10Hz, Depth 80mm, Trial B | 1.711 | 1.726 | 0.014 |
| Impeller 60Hz, Speed 15Hz, | 3.046 | 2.781 | 0.265 |

| | | | |
|---|---|---|---|
| Depth 120mm, Trial A | | | |
| Impeller 60Hz, Speed 15Hz, Depth 120mm, Trial B | 3.046 | 2.798 | 0.248 |
| Impeller 60Hz, Speed 15Hz, Depth 40mm, Trial A | 1.521 | 1.631 | 0.110 |
| Impeller 60Hz, Speed 15Hz, Depth 40mm, Trial B | 1.521 | 1.519 | 0.002 |
| Impeller 60Hz, Speed 15Hz, Depth 80mm, Trial A | 2.147 | 2.191 | 0.044 |
| Impeller 60Hz, Speed 15Hz, Depth 80mm, Trial B | 2.147 | 2.117 | 0.030 |
| Impeller 60Hz, Speed 5Hz, Depth 120mm, Trial A | 1.553 | 1.448 | 0.105 |
| Impeller 60Hz, Speed 5Hz, Depth 120mm, Trial B | 1.553 | 1.425 | 0.128 |
| Impeller 60Hz, Speed 5Hz, Depth 40mm, Trial A | 0.984 | 1.008 | 0.023 |
| Impeller 60Hz, Speed 5Hz, Depth 40mm, Trial B | 0.984 | 0.985 | 0.001 |
| | | **AVERAGE** | 0.082 |

We recommend further studies for different soil types, compaction rates and excavation tools to further verify and develop $k_s$ factors associated with unique soil conditions.

Additionally, other regression models such as random forest [159] may prove to be a more effective approach to lower both the error and the variance of the model.

*Dynamic Model*

The dredge head dynamic model is not directly verified in the experimental setup. Instead, the pull forces associated with moving the dredge head through water only versus the pull forces associated with excavating are measured and compared. To develop a baseline for the viscous pull forces associated with unspooling the opposing positioning winch, we ran an initial trial with the rope only, no dredge. A secondary test was completed with the pump moving through water only. This test removed the sediment from the holding tank while keeping the other parameters the same. An increase in pull force between these two trials, is shown in Figure 6.16.

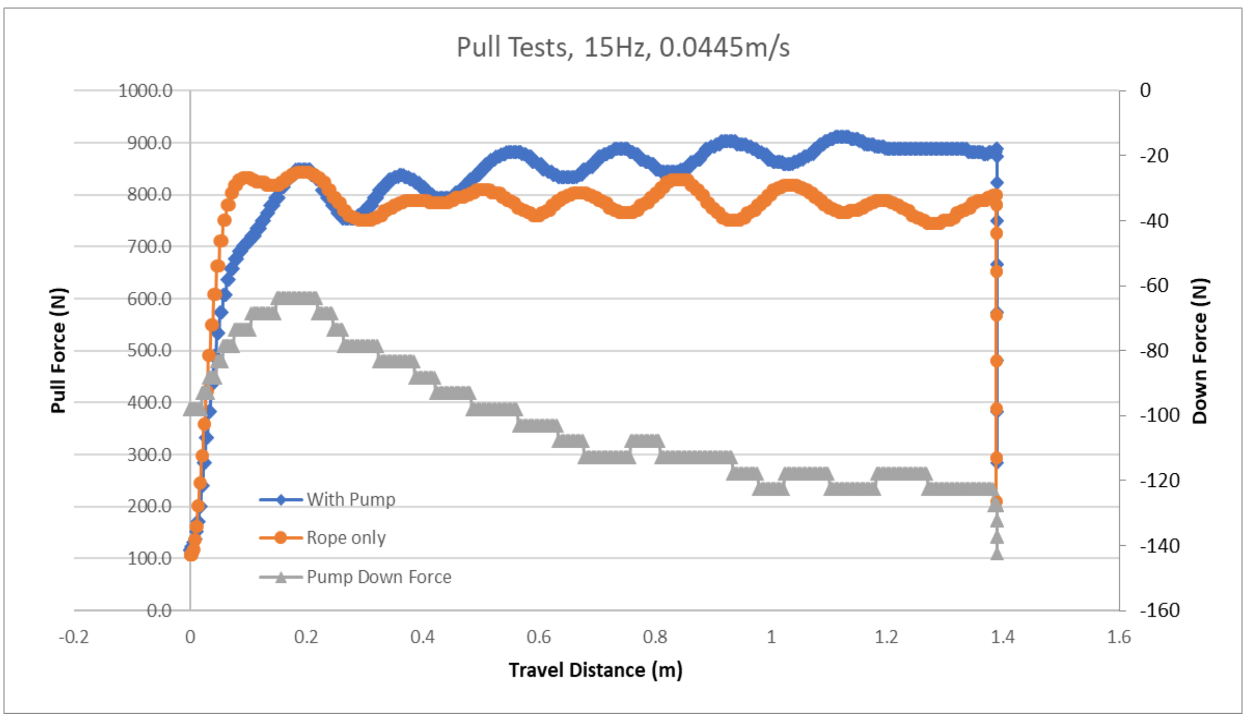


Figure 6.16: Dredge Pull Force

Figure 6.16 shows an oscillating wave pattern of the pull force. We think this may be the result of frictional resistance of the system, such as the trolley resistance and corresponding winch resistance. For the “rope only” test, the average value oscillates around 800 N whereas the “with pump” test oscillates with an increasing pull force trend. As the pump travels, the “pump down force” gradually decreases, indicating an increasing suspended load, which coincides with the increase in pull force. We think this relationship may be caused by a difference in elevation between the pulley and the rope attachment point on the pump, creating a vertical component of the pull force as the pump approaches the pulley. Additionally, the resistance forces from the gantry trolley may act on the pump, resulting in a moment or slight tipping of the dredge pump as it travels.

The test dredge moved at very slow speeds (0.9 to 2.7 m/min), which we think produced drag forces that would be negligible when compared to other forces: the rolling resistance of the overhead trolley; the friction of the pulleys used to route the winch rope underwater; the elastic effect of the flexing discharge hose; and the drag of the unspooling winch. We think the hydrodynamic forces associated with the dredge head’s slow movement will be negligible for system control, but this will need to be verified in future work.

**Pull Force vs Production**

The excavation rate is dependent upon the system’s ability to fluidize a layer of sediment along the dredge head path. We assume that the system’s ability to disturb the sediment layer is related to the pull force of the positioning winches. The relationship of the pull force (shown as mass in KG) to the overall production rate is shown in Figure 6.17.

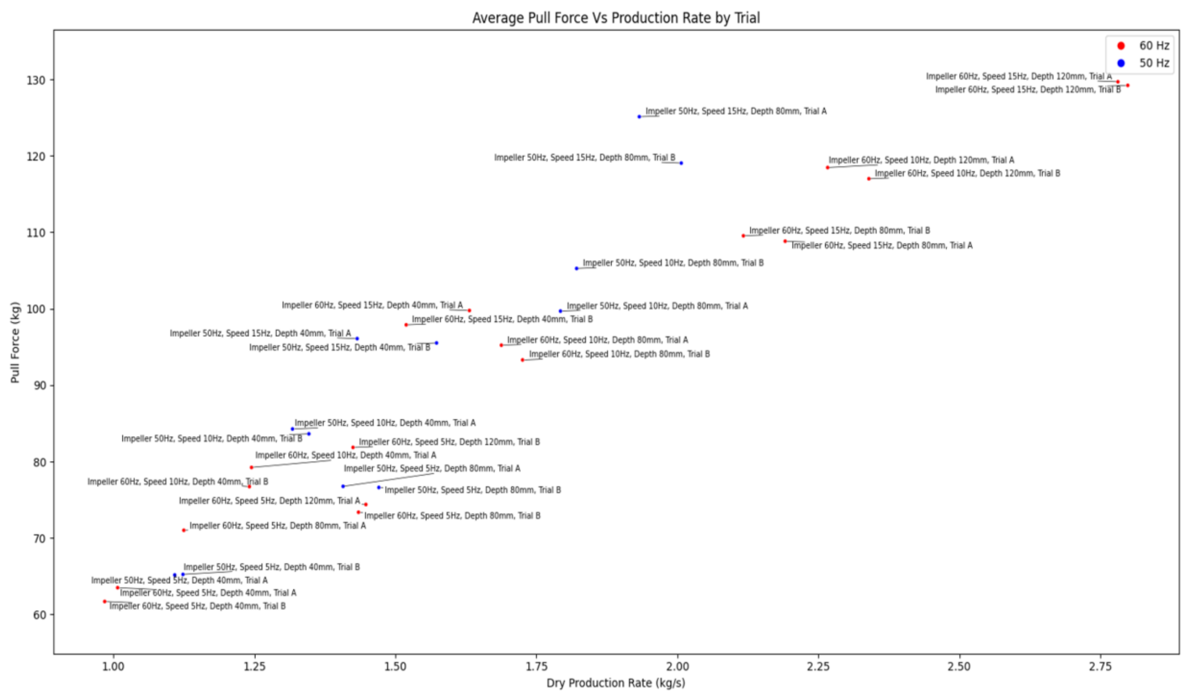


Figure 6.17: Average pull force (shown as mass in KG) vs production rate by trial

As seen in Figure 6.17, the pull force has a positive correlation to production rate. This is expected as the forces associated with pulling the pump through the test bed are related to the rate at which the solids are disturbed and introduced to the surrounding flow. However, not all the pull force is applied to sediment agitation. Independent tests were performed to identify the effect of changing travel speed on the pull force of the system. This was done by pulling the pump through clean water at each travel speed, unimpaired by sediment.

To better understand the relationship between pull force and production rate, each trial was normalized by the pull force required to only move the pump at each speed. The inherit pull force required at each travel speed is summarized in Table 6.6.

Table 6.6: Pull Force by Travel Speed

| Parameter (P) | Mass (KG) | Force (N) |
|---|---|---|
| 5 | 59.0 | 578.6 |
| 10 | 73.6 | 721.8 |
| 15 | 86.7 | 850.2 |

The result of each trial, corrected by their respective inherit pull forces (shown as mass in KG), is shown in Figure 6.18.

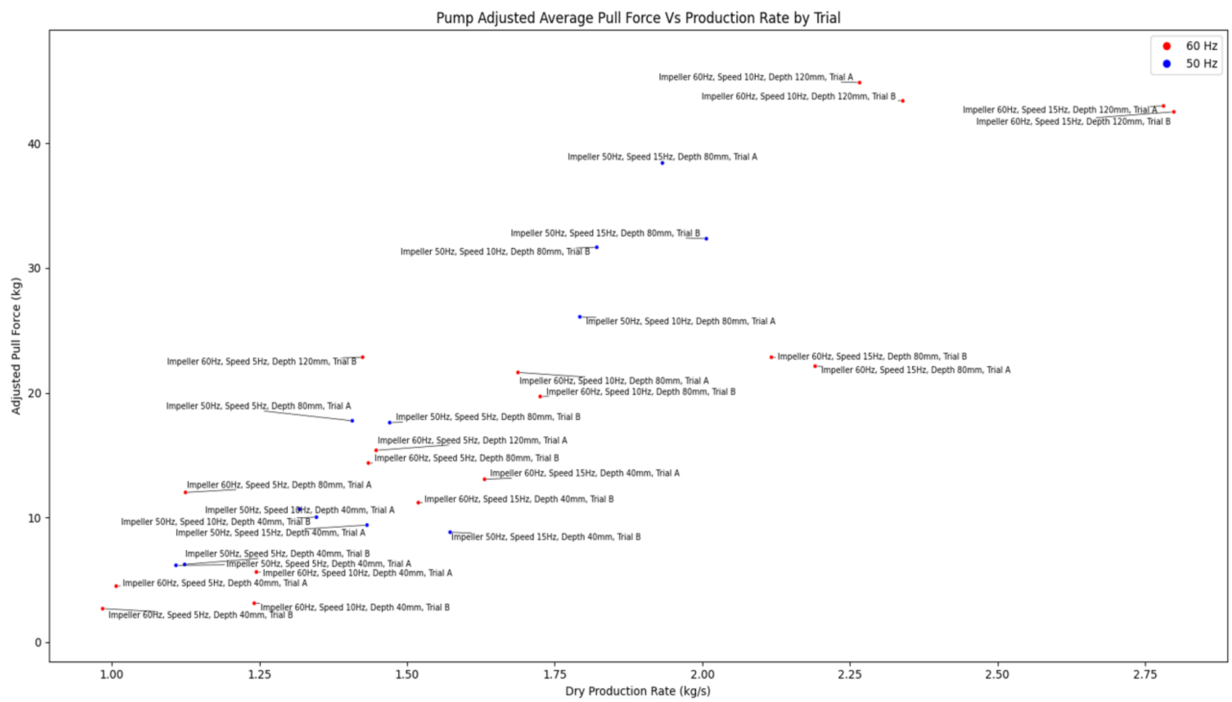


Figure 6.18: Adjusted Average Pull Force (shown as mass in KG) vs Production Rate, by Trial

**Efficacy of Pump Three Parameters**

In this section, three parameters and their influence on the production rate are investigated. These parameters include the depth of the dredge head into the material, the dredge pump rotational speed, and the speed at which the dredge head travels through the material. A total of 33,940 data points were collected with an average of 1000 data samples recorded per test trial run. Each combination of parameters was performed twice with the results differentiated as A or B. The goal of the double test runs was to provide a training dataset and a test data set for each set of parameters. An additional 31,052 data points were collected as a baseline to capture forces acting on the system, such as pull forces of the winches without a load.

Figure 6.19 and Figure 6.20 show the influence that each of the three test parameters had on the production rate and the concentration of solids, respectively.

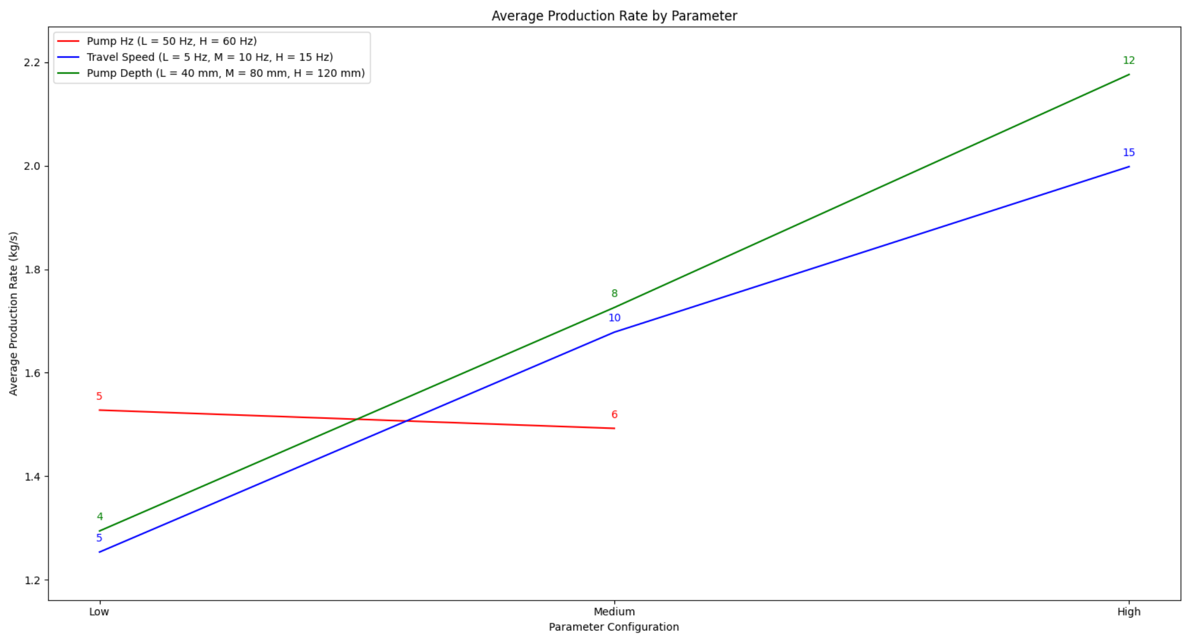


Figure 6.19: Efficacy of Parameters on Average Production Rate

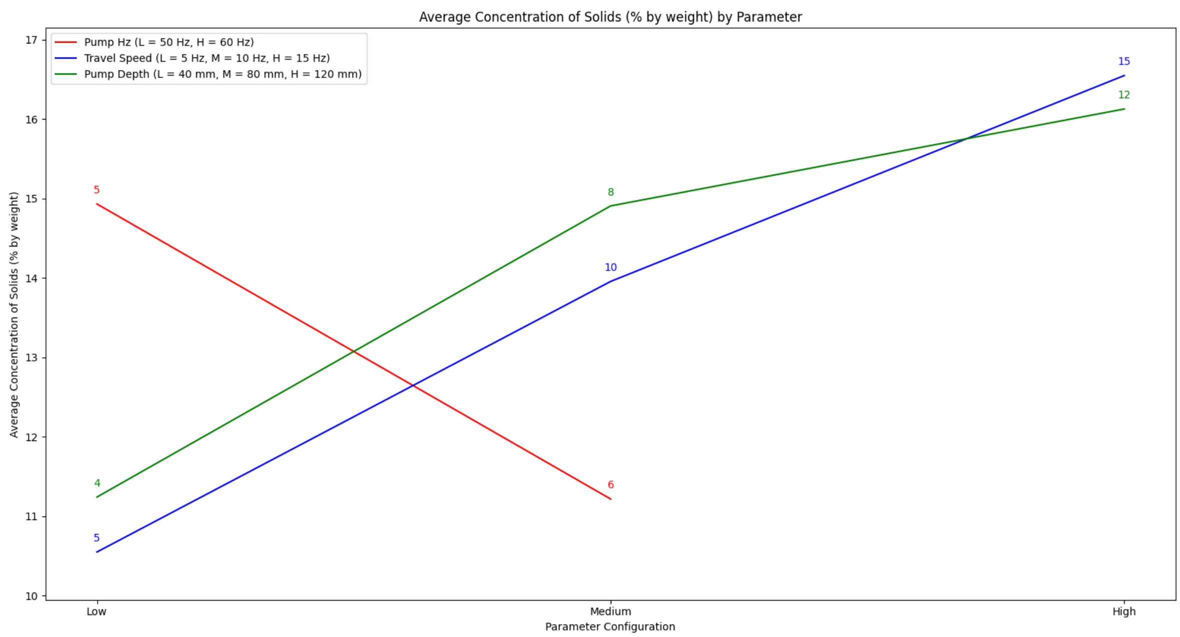


Figure 6.20: Efficacy of Parameters on Average Concentration of Solids (% by weight)

An increase to each of the three parameters tested resulted in a positive or neutral impact on production. For example, as pump depth increases the rate of production increases. Likewise, the pump travel speed has a positive relationship with production, but the slope of the relationship reduces beyond a certain point, perhaps indicating that a limit has been reached. Due to the critical velocity limit and the potential for settling solids in the discharge line, we only tested two pump impeller speeds. As a result, other than a potential negative impact between the low and medium parameter configuration, there are not enough sample points to determine the degree of relationship for impeller speed with respect to production rate.

Figure 6.19 shows that increasing the impeller speed has little impact on the overall production rate. Instead, the impeller speed was found to mainly determine whether a combination of the other two parameters produced a viable production rate for the system based on the minimum solids deposition velocities.

Figure 6.20 shows that increasing impeller speed has a negative impact on the concentration of solids. However, all but two 50 Hz trials fell below the calculated deposition limit velocity, and it is suspected that the sand in the hose affected these results. Additionally, the decrease in the concentration of solids of the 60 Hz trials are proportionally increased by the flow rate of the system to a point where the difference in total production rate is negligible.

Figure 6.21 shows the relationship with the parameters on the average solids weight by parameter.

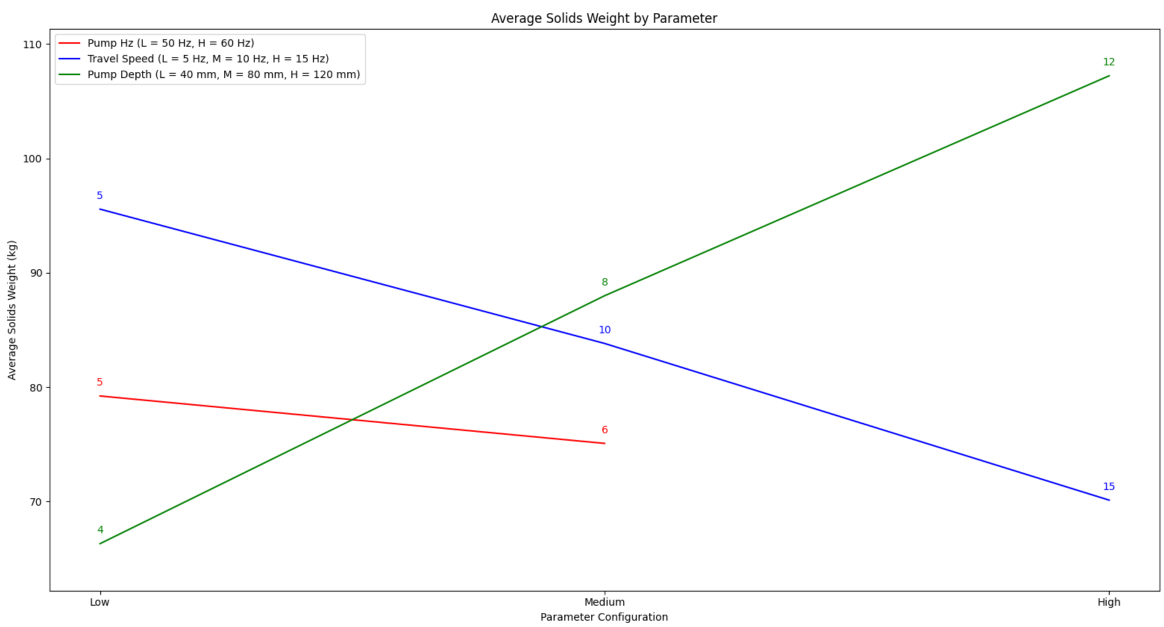


Figure 6.21: Efficacy of Parameters on Average Solids Weight

A positive relationship is shown with pump depth into the material, while a negative relationship is shown with travel speed. This negative trend is expected because as the travel speed increased, the trial time was limited by the available travel bed distance. Like the production rate, the impeller speed has less of an effect on the amount of material collected.

Figure 6.22 shows the relationship between the pulling force and the three parameters tested. The dredge head's travel speed and depth both increase the pulling force. The increased speed is predicted to increase the disturbance of solids along the system path. Likewise, the depth of the dredge head into the material results in additional material being excavated and shows an increase in pull or digging force.

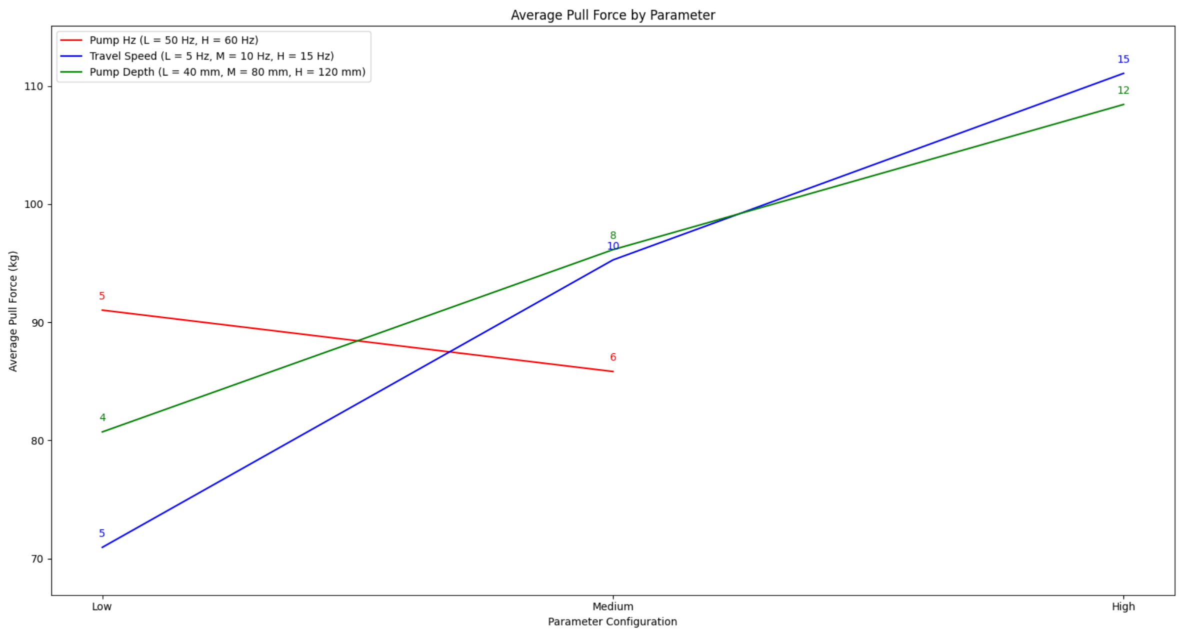


Figure 6.22: Efficacy of Parameters on Average Pull Force

Figure 6.22 also shows that as the pump rotational speed is increased, pull force decreases. This reduction may be due to increased flow rate causing increased erosion. We think this increased erosion in front of the dredge path results in reduced pull force.

### Concentration of Solids (% by weight) Results

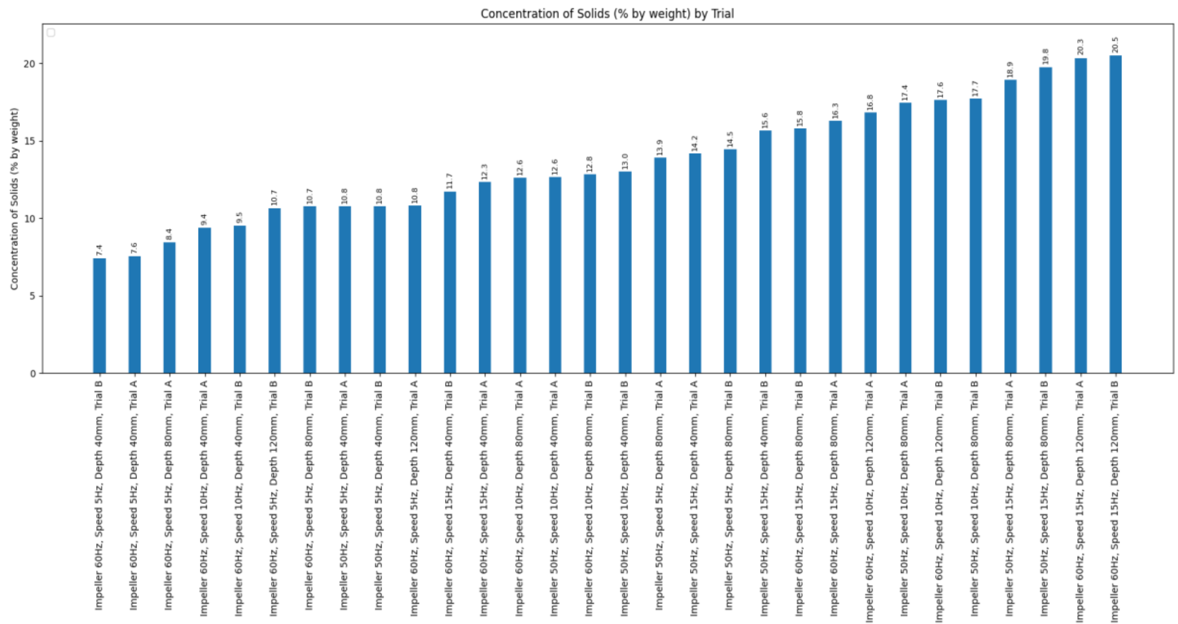


Figure 6.23: Concentration of Solids by Trial

Figure 6.23 shows the approximate concentration of solids for each trial from lowest to greatest. Generally, trials containing the 50 Hz impeller speed dominate the top half of the graph with a greater concentration of 60 Hz impeller speed at the lower end. We think this is because the 60 Hz impeller speed trials have an increased flow rate, which offsets the lower concentration of solids to maintain the production rate. The increased flow rate can dilute the concentration of solids entering the pump during excavation.[7]

### Production Rate

Figure 6.24 provides the measured production rate of dry solids by trial. One observation is that the maximum combination of parameters, travel frequency and depth, have a

---

[7] 120mm depth trials were not performed for the set of 50Hz pump speed, so these results are excluded from the comparison.

disproportionate impact when compared to the rest of the datasets. This leap may indicate that there is a significant correlation between pump depth into material and pump travel speed to provide the most efficient operating point. That is, increasing these two parameters together by a moderate amount may improve production more significantly than by only increasing one parameter by a greater amount and the other parameter by a lesser amount. One example of this result is shown by travel frequency of 10 Hz and depth of 80 mm resulting in a greater production rate than travel frequency of 15 Hz and depth of 40 mm.

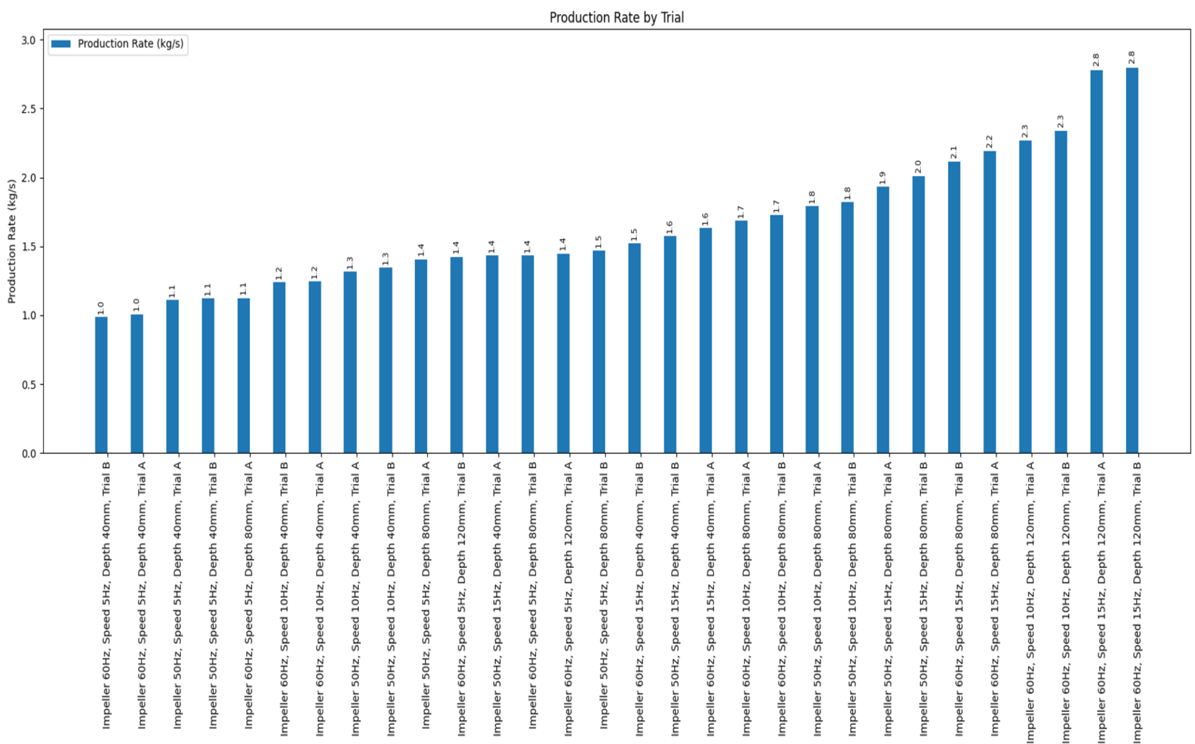


Figure 6.24: Production Rate by Trial

**Production vs Concentration of Solids (% by weight)**

Plotting the average concentration of solids and average production rate by trial further reveals the effects of the pump impeller frequency. As shown in Figure 6.25, the 50 Hz impeller trials show a larger increase to concentration of solids, but the overall production rate remains consistent. We think that the flowrate of the 50 Hz trials would need to proportionally decrease to keep the production rates equivalent to the 60 Hz counterpart.

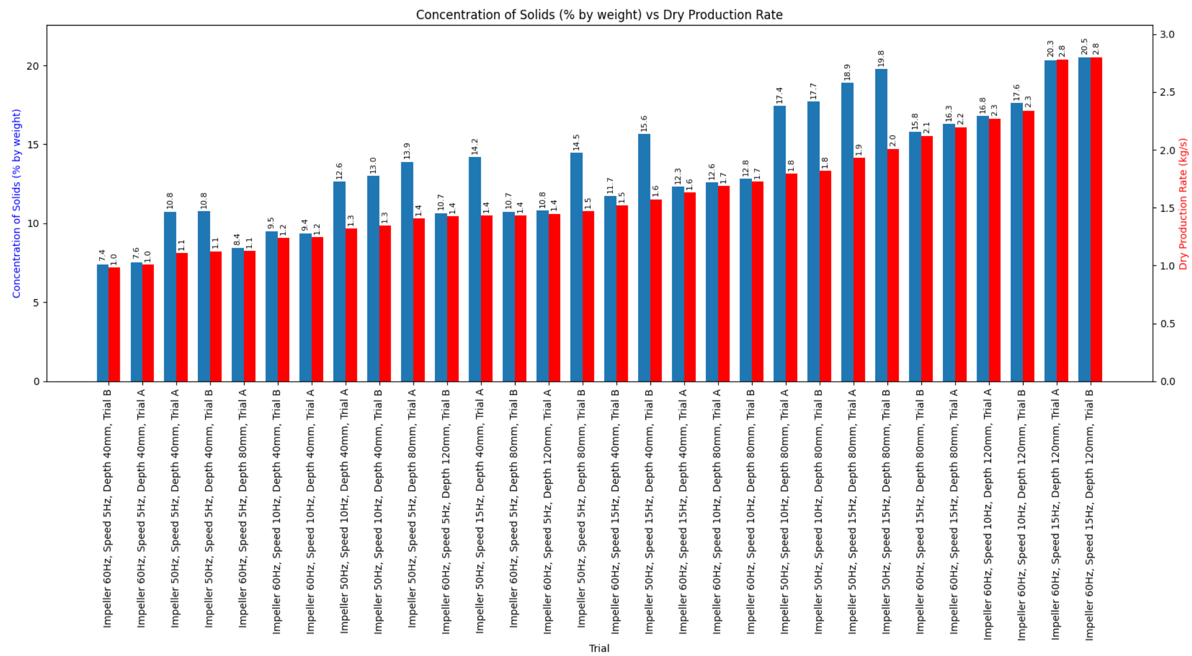


Figure 6.25: Concentration of Solids vs Production Rate

**Solids Weight**

Figure 6.26 compares the total dry weight of all material collected in the discharge tank versus the dry weight of material removed based on the calculated volume of the excavated trench in the test bed. This comparison provides relative confidence that the collected weight results are accurate. Measurements of the excavated area were taken at the centre of the test bed to calculate an approximate volume. The comparison indicates that the calculated weights can be relied upon as an accurate metric for determining the performance of each trial.

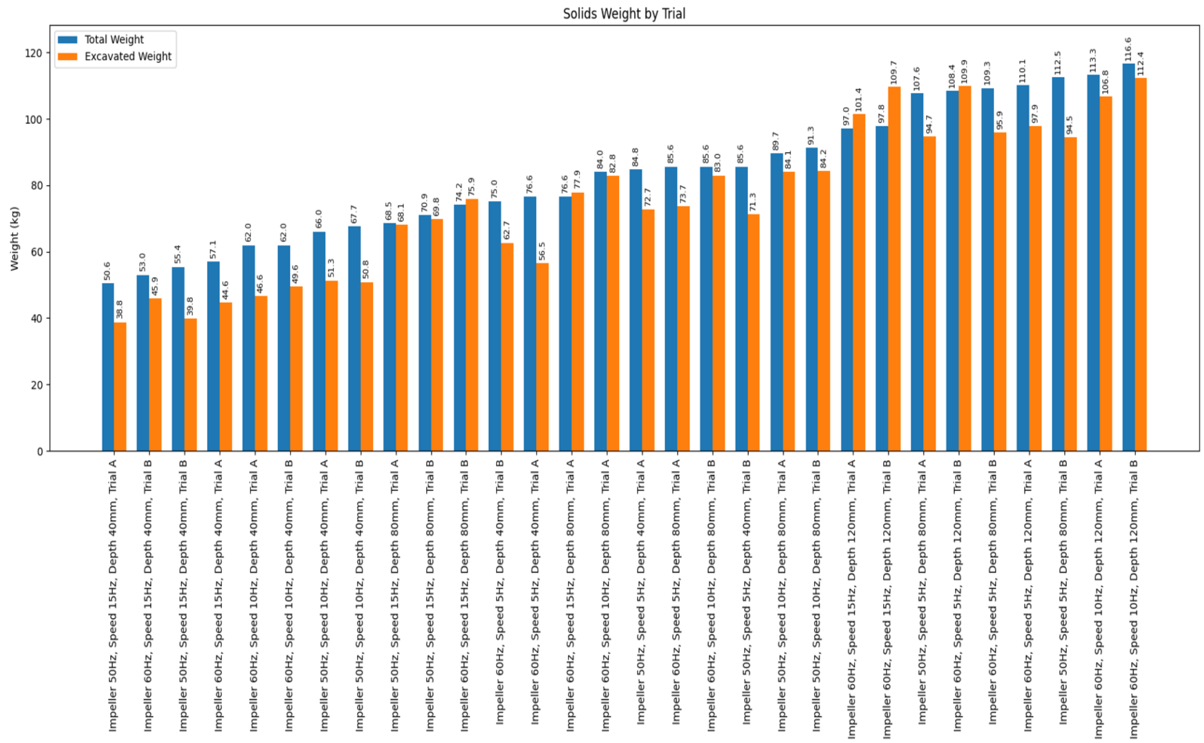


Figure 6.26: Total Solids Weight, by Trial

**Flow Rate**

Figure 6.27 plots the recorded flow from the flow sensor with the measured flow at the end of the trial by comparing the total volume of slurry moved with the elapsed run time of the experiment. There is a consistent offset error in the measurements, which can be offset in further calculations to reduce the impact it may have on the results. Applying the same correction factor of 4.4% determined by the pump curve for pure water results in the flow rates shown in Figure 6.28.

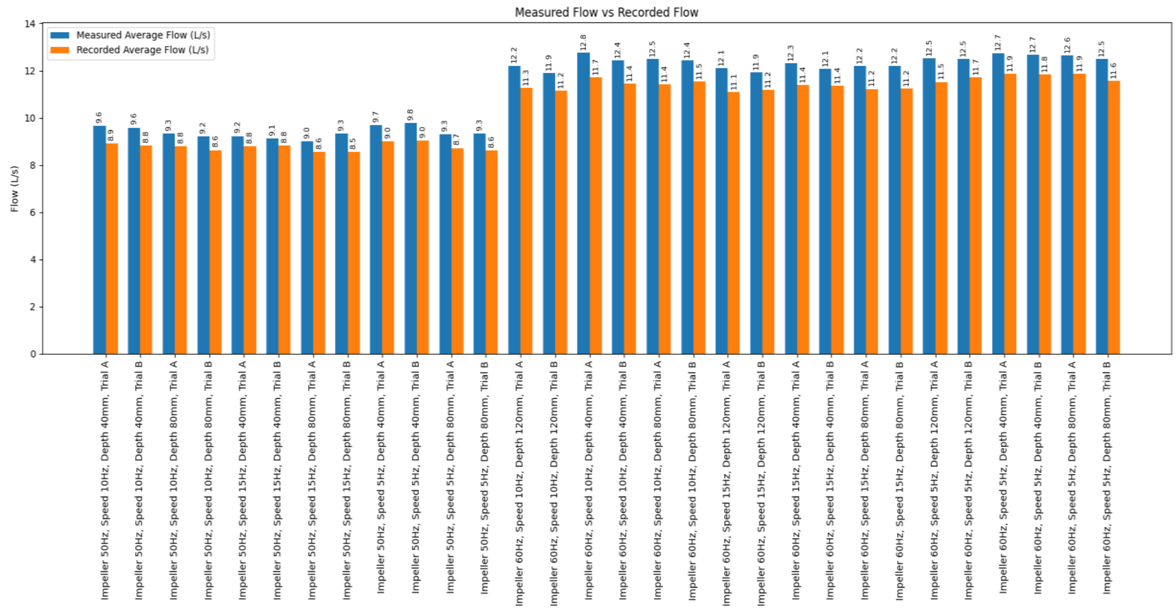


Figure 6.27: Flow by Trial

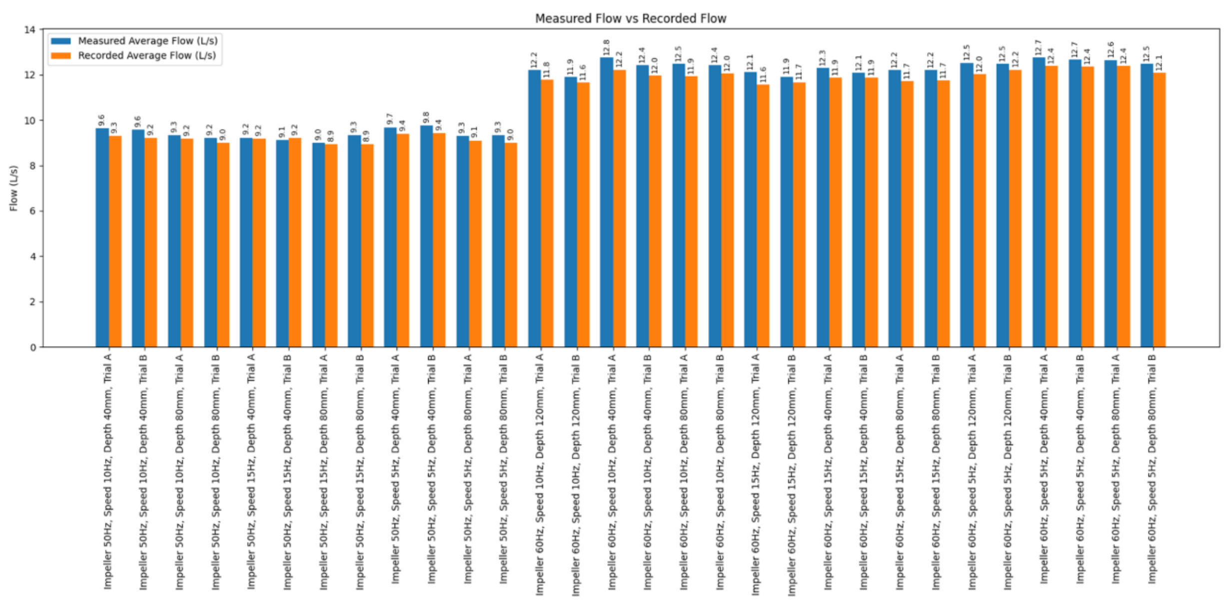


Figure 6.28: Flow by Trial, with scaling factor

Figure 6.29 and Figure 6.30 compare the flow, power, and amperage of the pump for two trials. Impeller 50Hz, Speed 5Hz, Depth 40mm, Trial A (Figure 6.29) indicates a consistent flow rate over the duration of the test. Impeller 50Hz, Speed 15Hz, Depth 80mm, Trial A (Figure

6.30) instead shows a gradual decline in flow rate over the duration of the trial. We think that the decrease in flow rate is due to an increasing solids concentration in the mixture. Because of the short test duration, it is unclear whether the flow rate would eventually stabilize or if the trend would continue until the pipeline is plugged.


Figure 6.29: Flow vs Power vs Amperage (No drop in flow)

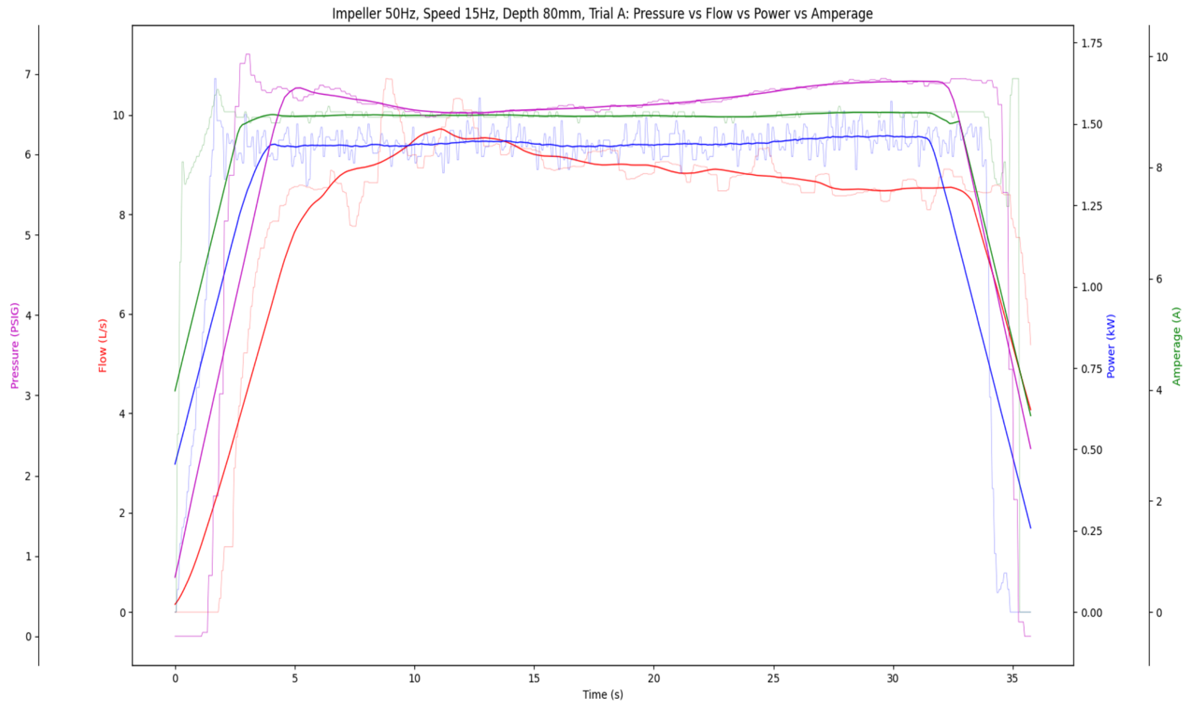


Figure 6.30: Flow vs Power vs Amperage (Drop in flow)

Further analysis shows that Impeller 50Hz, Speed 5Hz, Depth 40mm, Trial A lies above the deposition limit velocity line while the remaining trials, including Impeller 50Hz, Speed 15Hz, Depth 80mm, Trial A, lie below the line. These results further support the assumption that solids were settling in the pipeline due to the deposition limit velocity. Further investigation into the relationship amongst flow, solids concentration and the deposition limit velocity for the mixture are recommended. Such results could help a predictive controller maintain production without plugging the discharge line.

**Production Rate Versus Travel Speed**

Figure 6.31 shows the effects of the three parameters tested on the production rate. As shown, the production rates increase over the travel speeds tested. One interesting result shows that the 50 Hz pump speed results in higher production rates than the 60 Hz pump speed when the dredge head is traveling at speed up to 0.03 m/s. This result indicates that future work could assess optimization points for the dredge system's travel speed and the rotational speed for the pump.

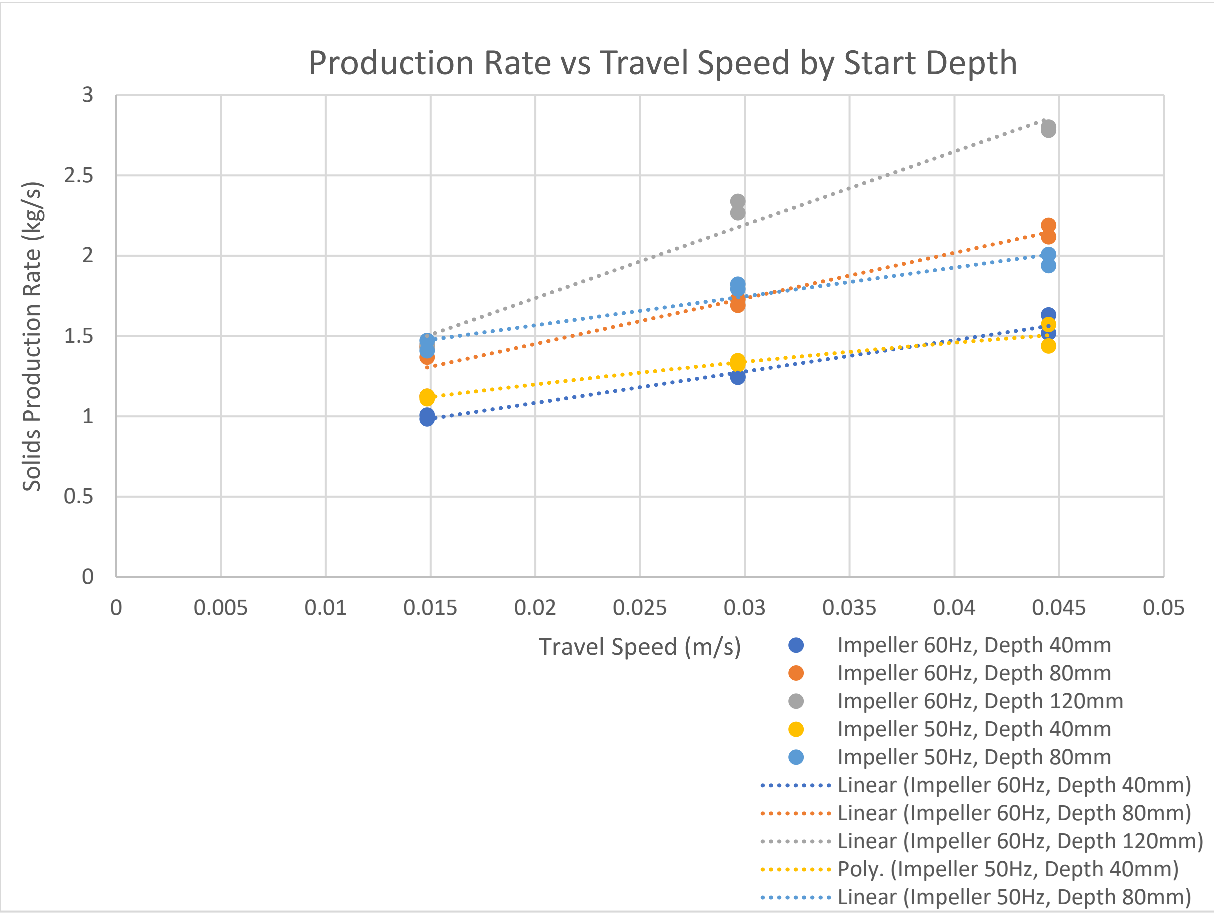


Figure 6.31: Production Rate Vs Travel Speed by Start Depth

**Excavation Depth Versus Travel Speed**

Figure 6.32 shows the measured excavation depth versus travel speed by starting depth. The results show that the 50 Hz pump speed resulted in a greater excavation depth than the 60 Hz pump speed for both 40 mm and 80 mm material start depths. However, at 120 mm start depth, the 60 Hz pump speed penetrated further into the material bed. For 50 Hz pump speed, the plotted excavation depth is more linear with a steeper slope than for the 60 Hz pump speed. This suggests that the favourable inlet flow characteristics at 50 Hz pump speed are less effective at higher travel speeds compared to the increased flow rate provided by the 60 Hz pump speed.

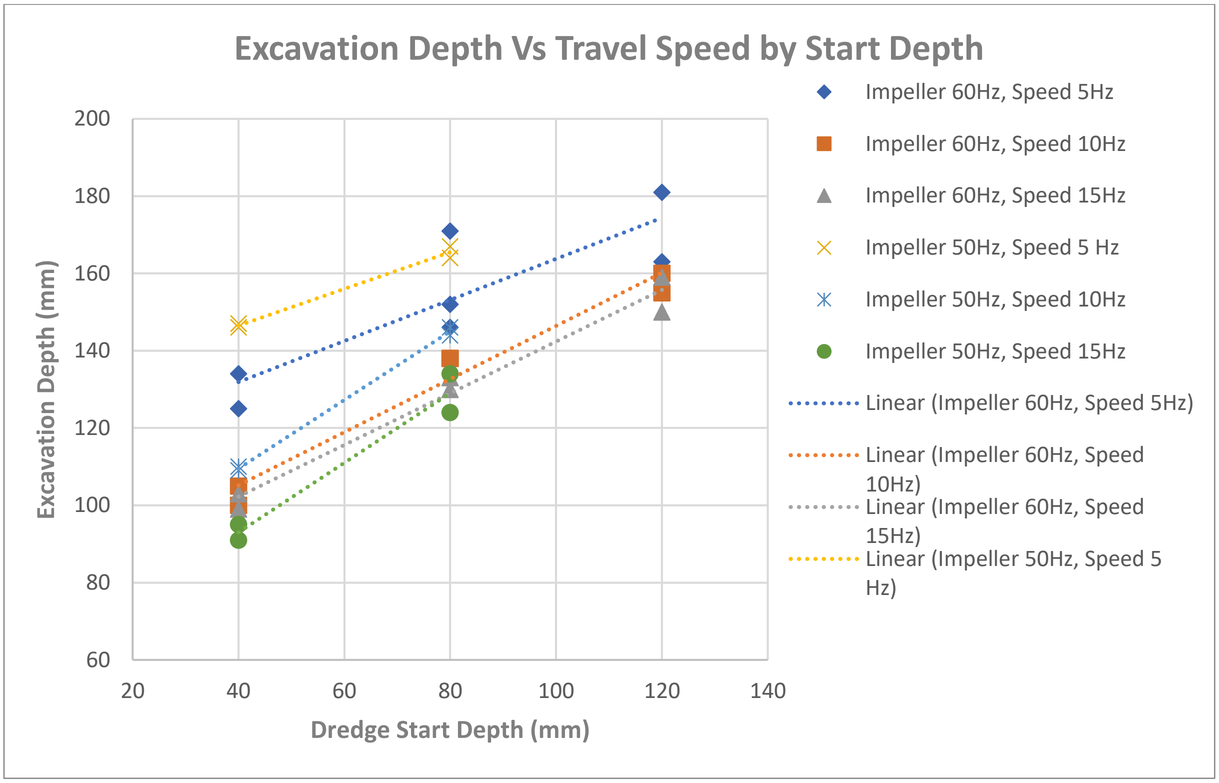


Figure 6.32: Excavation Depth Vs Travel Speed by Start Depth

In all the test trials, increasing the dredge start depth resulted in increased production. Based on the start depths tested, the trend indicates that further increases in start depth would result in increased production. However, we expect to encounter an upper limit for production once the dredge head increases to a depth where the pump inlet cannot physically handle the feed rate, or the line plugs because of a high solids concentration. We recommend that the production versus depth be further investigated over a wider variety of soil conditions to determine the optimal and upper limit depths as they relate to production.

**Production Rate Versus Travel Speed and Start Depth**

Figure 6.33 shows that maximum production occurred when all three input parameters were at their maximum values. The trendlines of the production rate charts indicate that additional solids production is possible. However, the best fit second order polynomial trendline for the 60 Hz and 120 mm start depth trials, shown in Figure 6.33, suggest that a maximum production rate of 2.91 kg/s would be achieved at a travel speed of 0.0564 m/s. Although the results show that an increased material start depth would result in increased production, based on the trend of the 120mm start depth trials, it is unknown if this would result in a greater maximum production rate compared to the test case of lesser material depth at higher travel speed.

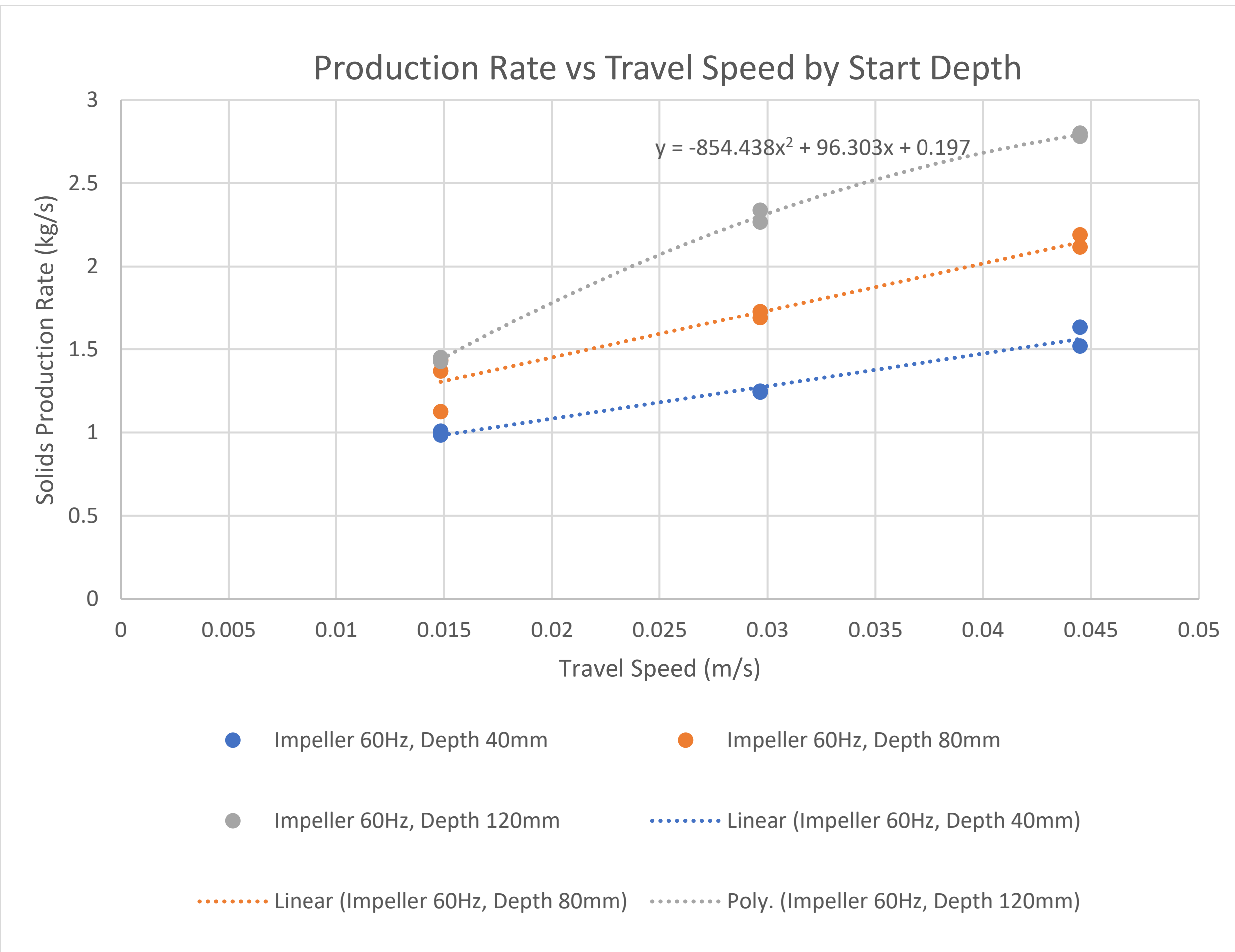


Figure 6.33: Production Rate vs. Travel Speed by Start Depth

The increased production rate at low travel speeds for the 50 Hz pump speed could optimize energy and water usage. For example, for the 50 Hz pump speed, a maximum average specific production rate of 1.44 (kg/s/kW) at the maximum average production rate of 1.97 kg/s was observed. This is in comparison to the pump at 60 Hz with a maximum average production of 2.79 kg/s and an average specific production of 1.27 (kg/s/kW). Water consumption was inversely proportional to the concentration of solids where the 50 and 60 Hz pump speeds produced a concentration of solids of 8.3% and 8.8%, respectively.

**Limitations due to Simplifying Assumptions**

The results of this lean experimental approach have provided a general system understanding and highlighted key parameters which influence the cable-driven dredge system. However, there are several simplifying assumptions used in the model developed and applied in this study. Therefore, the results from the testing completed here are limited at best and not conclusive. Because the system behaves in three dimensions, along with the potential for rotation, one of the main limiting assumptions of the model is the consideration of the system in a two-dimensional plane. A second limiting assumption is the consistent nature of the mixture in the discharge pipeline and the limited effects of the vertical sections of pipe. Further study may find that sections of the discharge pipe experience complex, multi-phase flow, which will have an impact on the production results. Lastly, the experimental setup was completed in a manner that leaves a great deal of room for experimental error in the setup and testing which limits the reproducibly of results. These major simplifying assumptions, and many others used within this study, mean that the results of this study may be significantly different than those in a later study that applies a more comprehensive model that is tested and verified in a more controlled experimental design and system analysis. Therefore, the results of this work must only be used for the basis in which they were intended; that is to provide a general system understanding and provide some general insight into parameters which must be focused on in future modeling and experimental design.

# Chapter 7: Knowledge Capture & Future Work

Because it involves several overlapping disciplines, the art of dredging remains highly specialized, and the number of companies performing the work remains relatively small. One of the main challenges associated with dredging is effectively estimating, and efficiently controlling, production. This is due to of the number of interlinked operation and application-specific parameters [160]. Historically, successful dredging has relied heavily on operational experience and knowledge.

Many companies rely on veteran dredge operators who have developed methods and techniques for high production rates without process interruptions. Dredge operators have relied on the equipment and process cues [74, 161] to manage high levels of production. More recently, dredgers and their operators have begun to rely on condition monitoring sensors and computational systems to improve production. Even so, dredge companies continue to rely on experienced operators for consistent production. It's therefore desirable to develop an intelligent control solution for production modeling that can utilize the operator's experience and learn from operations [162]. A few dredge companies are working on or have developed new innovative dredge technology that does not rely so heavily on operator experience. This study considers one such technology, which utilizes a computer and sensors without an operator to operate and control a cable-driven dredge system.

Once the operator sets the initial input parameters based on the application conditions, the cable-driven dredge operates through an automated controller. The system is therefore heavily reliant on the path planning and condition monitoring systems. Sensors and instrumentation in the process logic controls maintain and optimize production outputs without operating interactions. The automated control system must be optimized to behave like an experienced operator.

Dredge companies hope that automated controllers can adjust the system to deal with changing application conditions and provide a consistent, normalize production throughput. As an additional by-product of developing an improved system controller, the dredge is expected to optimize system production while reducing downtime due to line plugging. This is expected to reduce the number of human-machine interactions, making the dredge safer and more efficient.

This thesis is a case study and descriptive system design of this novel dredge technology. During this study, empirical data and operator feedback were gathered to understand relationships between operating parameters, operator knowledge and system production. Significantly, dredge operators used dredge input power as the main predictive method for controlling the dredge system parameters and production rates. Based on this study, and operator input, it was determined that dredge head velocity and applied force and depth of the dredge head are positively related to dredge production.

**Lessons from this Study**

We developed a dredge system process diagram showing interaction between the dredge system components and their influence on production. These parameters included the system power, discharge pressure, flow rate, speed of the dredge head, applied dredge head force, depth of the dredge head into the material and speed of the dredge pump. As part of this study, a scaled prototype of the cable-driven dredge system has been developed based on the industrial model. The scaled prototype was used with the simplified dynamic equations as a lean approach to investigate the component models and the overall influence on system production when adjusting three system parameters: dredge head speed; applied force and depth into the material; and the dredge pump rotational speed.

*Control*

Because the positioning controller for the cable-driven system already provides adequate dynamic system control in the field, the verification of this control model was not included as part of this study. However, the cable-driven dredge position control techniques were briefly discussed. The control scheme for the cable-driven dredge uses a trajectory-based control framework. This control solution has provided adequate positioning of the end effector within the operational space and along a predetermined path.

Simplified dynamical equations for dredge system components were developed. Using these equations, we investigated the components and their influence on one another and the system's production. A simplified two-dimensional experimental test setup was developed and used to investigate the model components and test the influence of three control parameters on production. We tested the following component models: production model; discharge pipe model; and excavation model.

*Production Model*

The production model is based on an algorithm which predicted the concentration of solids within the slurry mixture based on the dredge pump power draw. These preliminary test results indicate a strong relationship between the power draw and the solids concentration. The simplified production algorithm predicts the mixture flow rate within a 5% range over the set of trials. For the measured concentration during the trials, the predicted concentration deviated by up to 70%. However, this deviation is not unexpected, as the data is highly sensitive due to the low range in solids concentration. Reviewing the datasets and comparing the differences between average *Cv* and predicted *Cv*, the largest error was found to predict concentration within 2.5% of the measured average concentration. Although the accuracy of the production model could be improved, the result of the preliminary testing completed in this case study indicate strong production trends based on the amperage draw. Additional testing using design of experiments will need to be completed to determine if the algorithm is able to predict within the same accuracy for model verification.

*Excavation Model*

The excavation model was also developed and tested in the scaled test setup. The excavation model developed was based on the dredge head velocity and area of the dredge cut. Using experimental data and a linear regression model, a spillage factor was developed and verified over partitioned datasets. The resulting accuracy of the excavation model was found to be within 8%. Further studies are required to validate the findings and to be completed on different soil types, compaction rates and excavation tools to validate and develop $k_s$ factors associated to unique soil conditions. Additionally, it is recommended that other algorithms such as random forest [159] with bootstrapping [163] be investigated as potential alternatives as these may provide a more effective approach to lower both the error and the variance of the excavation model.

*Pipeline Model*

A pipeline model developed by Furboter [79, 98] was tested in the experiment setup. However, it was found that the pipeline model underpredicted the system's measured results. Therefore, the pipeline model was adjusted based on the dynamic viscosity of a mixture when solids are present. The adjusted model improved the predicted losses, but still underpredicted the measured data.

Results indicate that the model may be scalable to produce a close match in TDH for the test setup. However, the scale factor used is not expected to hold for different pipe sizes and pipe materials, or different solid particle sizes and distributions. Therefore, this is an area that requires further study. Moreover, the pipeline model that we studied would require specific calibration over a range of solids, which is not practical for working dredge applications. Therefore, based on these initial results, it is not recommended to determine system operating conditions using the predictive pipeline model. Instead, we suggest that a pressure sensor should be used in combination with the production model to estimate concentration and flow.

*Cutting Forces*

The cutting forces of the dredge system along the dredge path were also investigated. Through small scale lab testing, the cutting forces were found to have a positive influence on the production rate. However, this is unique to the test bed material and is predicted to have less impact on production as the compaction of the soil increases. Further work is recommended in the study of the dredge head force as it relates to the system production.

*Production Parameters*

In addition, three parameters and their effects on production were tested. These parameters included the following: the dredge head travel speed; dredge head cutting depth, and associated force on the material; and the dredge pump speed. The results show that an increase to each of the three parameters resulted in a positive or neutral impact on production. The depth of the dredge pump into the material, and the travel speed showed positive relationships with the rate of production, however, the slope of the relationship decreases as the travel speed increases, indicating that a limit may be reached. Results indicate there may be an optimization point that needs to be further investigated based on the dredge head depth and dredge pump rotational speed.

Two variations of the pump impeller speed, 50Hz and 60Hz, were tested. However, in the 50Hz trials, the flow rate in the discharge pipe that was not sufficient to keep the flow above the minimum solids' deposition velocity. Therefore, the overall impacts of impeller speed on dredge production were inconclusive but useful data were extracted through moments of what we believed to be line plugging.

**Future Work**

The simplified system model developed here for this complex, multi-physics cable-driven dredge system provides a basic understanding and identifies parameters with high sensitivity. This study and its results provide the framework for future work, where a more comprehensive model and robust experimental design are completed. Moreover, this study identified parameters that make the models sensitive, and will need to be handled with particular care in future design and more comprehensive testing.

Although the simplified models, and the lean approach, used here provides a general system understanding, and identify parameters with high sensitivity, this approach does come with many limitations. Specifically, the results from this study are not the standard reproducible scientific results typically found in a structured design of experiments methodology. Therefore, it is expected that many of the results may have large errors associated with them and conclusions for a full-scale system cannot be made. This uncertainty can be dealt with in future studies by a complete experimental design process that will include increasing the number of experimental trials along with an error analysis. Moreover, the system component models, and their interactions are a simplification of the complex dredge system. Significant error may be introduced as a result, which may hide aspects of the true system behavior. The future development of a full parametric model and design of experiment testing will provide more insight into the complete system behavior and is the focus of future work.

The goal of this lean approach was to develop simplified models for a complex system to provide the engineer with insight into areas of the system that require additional modeling work in further studies. As a result, we identify key areas of the system models that require additional investigation and experimental testing prior to designing a robust system controller. This study provides one streamlined approach for identifying key areas of uncertainty, early on, in complex system design when resources and time are limited. The knowledge acquired by this approach provides key insights into model behavior, which can be used to better manage, plan, develop, and reduce major risks associated with uncertainty and gaps in knowledge.

Future development of a robust dredge controller will enable the cable-driven dredge system to work in a larger range of inland dredge applications while improving system efficiency and reliability. The system model and controls developed in this work are the initial framework for the development of an improved controller. Future work will involve a full parametric system model with three-dimensional analysis. Moreover, the model will need to be validated over a variety of test beds with varying compactness and solids properties. Further study is recommended on the effects of agitation methods or attachments on the excavation rate in a variety of test beds. This is critical when dealing with dredge application that contain compacted sediment, which are not easily fluidized by the process of erosion alone.

Future work will need to include modifying and testing of a full parametric model and the control system with a variety of mixtures and soils and test beds. As well, many dredge environments involve changing sediment beds due to deposit areas and settling rates. Therefore, the future development of the cable-driven dredge controller must involve changing solids size, particle distribution and solid density throughout the application. To deal with such a diverse control solution, a multivariable controller, or a more comprehensive advanced adaptive controller, such as machine learning, or artificial intelligence, may be required.

Future studies should investigate the optimization of the dredge path planning for a variety of applications. The optimization work needs to include dredge head path planning based on winch configuration, optimization of dredge head velocity based on production rate of various applications, and control for changing slurry applications. Due to the complexity of the boundary conditions of ponds, a variety of dredge patterns may be required to optimize the dredge path. In addition, the optimization of path planning at the boundary conditions will need to be considered and investigated in future work.

Most dredge applications involve several practical challenges not explored in this study. A few of these challenges include vegetation, large solids, and foreign obstacles. The initial cable-driven dredge does not consider all these factors, but they may influence the system. Future work needs to consider these variables and their effects on the performance of the dredge system. Developing a robust predictive controller that can deal with a variety of changing parameters will have the large impact on the dredge system's effectiveness.

This study considers a relatively flat, homogeneous, isotropic bed of material for dredge testing. However, many dredge applications have non-uniform sediment profiles which consisting of low valleys, high peaks, and abrupt ridges. Moreover, some dredge applications have objects which impact the mobility of the dredge head and may impact the network of the cables which span between the dredge head and winch. These foreign objects affect dredge production and overall system movement. Additional work on the controller will allow for adaptive path planning, which will enable the dredge system to not only look at the original dredge application conditions but also adapt as the environment changes. This is important as many dredge applications have inconsistent sediment buildups, where the median solid size, density and compaction continuously change. Developing an adaptive controller will provide the system with data to adjust the path planning, system speed or applied force to optimize production.

**Summary**

When resources and time are limited, project management must consider the tradeoffs between schedule, cost, scope, and quality [30]. Here, a lean approach was taken to modeling and experimental design to develop a basic understanding of the complex cable-driven dredge system and parameters which make the model sensitive. This lean approach simplifies the dynamic system to develop a basic system model. Using the simplified models developed, a lean approach for industrial experimental testing is completed. The focus of this study was not to produce the same level of scientific results expected in standard design of experiments, but instead to create new knowledge about influencing parameters, especially those with high sensitivity. A more comprehensive model, and experimental design, can be developed in future work with the understanding we have gained of the influence of these parameters on this complex system. This approach provides organizations, working with limited resources and time, insight into a complex system, the influencing parameters and knowledge of where care must be taken when evaluating the system.

Understanding the dredge system and overall performance characteristics has been a primary focus for many companies that employ dredges. One of the main difficulties with developing automated dredgers with high production and efficiency is related to the complexity of the dredge working environment [75]. The relationship between the sensor signals and operator actions are highly complicated and not easily captured with mathematical models [74]. The use of empirical knowledge is one feasible solution for developing an automated dredge controller [73]. Developing intelligent control solutions which use the operator's experience as the control framework and can learn from operations is desirable [75].

Developing dredge equipment with high production and high system efficiency is difficult. Dredge efficiency is closely related to the extremely complicated working environment of dredging operations [162]. The cable-driven dredge technology studied is a new technology that takes a different approach to conventional human-operated dredge systems. The cable-driven dredge is controlled through a remote logic-based controller which does not require a designated operator. This automated system makes the dredge safer and less expensive to operate than conventional dredges and does not rely on the operator's experience. Moreover, the dredge system moves in continuous patterns through sediment, maintaining production throughout the dredge project. This makes the dredge system more efficient than conventional dredge equipment, which require reposition water cycles.

As a result of this work, new knowledge is developed around simplified dredge component models. The lessons provided within this study form the basis for further investigation and development of a full parametric system model which will lead to an improved automatic dredge controller. The test results provide preliminary insight into three pre-set condition parameters which influence the system's production output.

This lean approach in combination with further, comprehensive model development and protype testing, will lead to a robust adaptive controller that can be used in a wide variety of dredge applications. Ultimately, the controller developed will be used as the framework for optimizing the dredge technology production rate. Further studies are anticipated to enable the system to detect and predict line blockages and adjust system parameters to reduce the negative impacts of these occurrences.

Managing projects with a high degree of uncertainty and limited resources is a challenge. There is a constant balancing act and many trade-offs between scope, quality, schedule, and costs that must be considered to provide the decision maker with a good enough understanding to begin and plan design work. The project manager or technology developer must choose carefully where they are going to spend time and money to get the best understanding within the constraints.

When resources are limited, and uncertainty is high, a lean approach to investigate system behavior and modeling may be used to reduce uncertainty and the associated risks. We do not conclude based on the results of this lean approach but observe trends associated with the data which can lead us to areas of further investigation and were to narrow our focus for planning and future work. This allows us to deal with uncertainty and retire some of the major risks due to uncertainty early in the design. Like the Agile project management framework, we may focus on areas we are most concerned about, test these areas as simply as possible and in short iterations, to get some reasonable confidence that we understand the implications to design and control. We acknowledge and accept that the results are not going to be as precise as we may desire however directionally it is going to be an improvement.

Using the results of this lean approach and the knowledge gained, risks due to uncertainty can be better managed early and upfront. Some of the results show that there is a lot more to investigate and we are not able to capture all aspects with the simplified dynamics. However, we are better informed and have gained enough of an understanding to move on to the next phase of design. Fortunately, the results from this lean approach tell us where we need to focus on in future study which we think will lead to an improved project plan, improved risk management and ultimately a better design.

# References


[1] J. Taalbi, "What drives innovation? Evidence from economic history," *Research Policy,* vol. 46, no. 8, pp. 1437-1453, 2017.

[2] M. Jackson, S. Ekman, A. Wikström, and M. Wiktorsson, "Innovation and design inspired product realization," in *DS 58-3: Proceedings of ICED 09, the 17th International Conference on Engineering Design, Vol. 3, Design Organization and Management, Palo Alto, CA, USA, 24.-27.08. 2009*, 2009.

[3] M. A. Stanko, F. J. Molina-Castillo, and J. L. Munuera-Aleman, "Speed to market for innovative products: blessing or curse?," *Journal of Product Innovation Management,* vol. 29, no. 5, pp. 751-765, 2012.

[4] G. L. Urban, T. Carter, S. Gaskin, and Z. Mucha, "Market share rewards to pioneering brands: An empirical analysis and strategic implications," *Management Science,* vol. 32, no. 6, pp. 645-659, 1986.

[5] J. C. Mankins, "Technology readiness levels," *White Paper, April,* vol. 6, no. 1995, p. 1995, 1995.

[6] F. B. Dovichi Filho, Y. C. Santiago, E. E. S. Lora, J. C. E. Palacio, and O. A. A. del Olmo, "Evaluation of the maturity level of biomass electricity generation technologies using the technology readiness level criteria," *Journal of Cleaner Production,* vol. 295, p. 126426, 2021.

[7] J. P. Messina, T. P. Evans, S. M. Manson, A. M. Shortridge, P. J. Deadman, and p. H. Verburg, "Complex system models and the management of error and uncertainty," *Journal of Land Use Science,* vol. 3, no. 1, pp. 11-25, 2008.

[8] C. E. Hmelo, D. L. Holton, and J. L. Kolodner, "Designing to learn about complex systems," *The journal of the learning sciences,* vol. 9, no. 3, pp. 247-298, 2000.

[9] H. Tasalloti, H. Eskelinen, P. Kah, and J. Martikainen, "An integrated DFMA–PDM model for the design and analysis of challenging similar and dissimilar welds," *Materials & Design,* vol. 89, pp. 421-431, 2016.

[10] N. Dahmani, A. Belhadi, K. Benhida, S. Elfezazi, F. E. Touriki, and Y. Azougagh, "Integrating lean design and eco-design to improve product design: From literature review to an operational framework," *Energy & Environment,* vol. 33, no. 1, pp. 189-219, 2022.

[11] J. Braaksma, "Model based control of hopper dredges," Doctoral thesis, Mechanical Maritime and Materials Engineering, Delft University of Technology 2008. [Online]. Available: https://repository.tudelft.nl/islandora/object/uuid:c39f031e-4b1a-448f-b33a-41a2679fd15c?collection=research

[12] NOAA. "What is Dredging?" https://oceanservice.noaa.gov/facts/dredging.html (accessed 2022).

[13] S. A. Miedema and S. Becker, "The Use Of Modelling And Simulation In The Dredging Industry In Particular The Closing Process Of Clamshell Dredges," 2007.

[14] H. Andersen and B. Hepburn, "Scientific method," 2015.

[15] M. Tovey, "Styling and design: intuition and analysis in industrial design," *Design studies,* vol. 18, no. 1, pp. 5-31, 1997.

[16] B. H. Reich and S. Y. Wee, "Searching for Knowledge in the PMBOK® Guide," *Project Management Journal,* vol. 37, no. 2, pp. 11-26, 2006.

[17] J. M. Juran and J. Juran, *Juran on quality by design: the new steps for planning quality into goods and services*. Simon and Schuster, 1992.
[18] J. Heagney, *Fundamentals of project management*. Amacom, 2016.
[19] D. W. Parker, N. Parsons, and F. Isharyanto, "Inclusion of strategic management theories to project management," *International Journal of Managing Projects in Business,* 2015.
[20] F. Marle and L.-A. Vidal, "Project management traditional principles," in *Managing Complex, High Risk Projects*: Springer, 2016, pp. 1-52.
[21] S. J. Cicmil, "Critical factors of effective project management," *The TQM magazine,* vol. 9, no. 6, pp. 390-396, 1997.
[22] A. Rolstadås, I. Tommelein, P. M. Schiefloe, and G. Ballard, "Understanding project success through analysis of project management approach," *International journal of managing projects in business,* 2014.
[23] T. Hanif, "A new approach to project management based on a combination of predictive and adaptive thinking," Kingston University, 2011.
[24] A.-T. Chang, J. Shih, and Y. Choo, "Reasons and costs for design change during production," *Journal of Engineering Design,* vol. 22, no. 4, pp. 275-289, 2011.
[25] R. G. Cooper, "Stage-gate systems: a new tool for managing new products," *Business horizons,* vol. 33, no. 3, pp. 44-54, 1990.
[26] A. A. Adenowo and B. A. Adenowo, "Software engineering methodologies: a review of the waterfall model and object-oriented approach," *International Journal of Scientific & Engineering Research,* vol. 4, no. 7, pp. 427-434, 2013.
[27] H. K. Aroral, "Waterfall Process Operations in the Fast-paced World: Project Management Exploratory Analysis," *International Journal of Applied Business and Management Studies,* vol. 6, no. 1, pp. 91-99, 2021.
[28] D. J. Fernandez and J. D. Fernandez, "Agile project management—agilism versus traditional approaches," *Journal of Computer Information Systems,* vol. 49, no. 2, pp. 10-17, 2008.
[29] T. Dilger, C. Ploder, W. Haas, P. Schöttle, and R. Bernsteiner, "Continuous Planning and Forecasting Framework (CPFF) for Agile Project Management: Overcoming the," in *Proceedings of the 21st Annual Conference on Information Technology Education*, 2020, pp. 371-377.
[30] S. C. Dwyer, "Agile design project methodology for small teams developing mechatronic systems," 2017.
[31] R. Ranjan, "Adaptive Project Management," *International Research Journal of Modernization in Engineering Technology and Science,* vol. 3, no. 11, pp. 120-123, 2021.
[32] J. A. Highsmith and J. Highsmith, *Agile software development ecosystems*. Addison-Wesley Professional, 2002.
[33] S. Costantini, J. G. Hall, and L. Rapanotti, "Using complexity and volatility characteristics to guide hybrid project management," *International Journal of Managing Projects in Business,* 2021.
[34] E. Papadakis and L. Tsironis, "Hybrid methods and practices associated with agile methods, method tailoring and delivery of projects in a non-software context," *Procedia computer science,* vol. 138, pp. 739-746, 2018.
[35] A. M. C. Barbosa and M. C. P. Saisse, "Hybrid project management for sociotechnical digital transformation context," *Brazilian Journal of Operations & Production Management,* vol. 16, no. 2, pp. 316-332, 2019.

[36] I. Craig, "THE ENGINEERING DESIGN PROCESS (2nd Edn.), by Atila Ertas and Jesse C. Jones, John Wiley, Chichester, UK, 1996, 614 pages, including index and four appendices and bibliographies (Hardcover,£ 29.95)," *Robotica,* vol. 16, no. 1, pp. 119-121, 1998.
[37] L. J. Robertson, R. Abbas, G. Alici, A. Munoz, and K. Michael, "Engineering-based design methodology for embedding ethics in autonomous robots," *Proceedings of the IEEE,* vol. 107, no. 3, pp. 582-599, 2019.
[38] J. Rothman, *Agile and lean program management: Scaling collaboration across the organization*. Practical Ink, 2016.
[39] G. Dieter and L. Schmidt, 5, Ed. *Engineering Design*. 2009.
[40] E. H. Kessler and P. E. Bierly, "Is faster really better? An empirical test of the implications of innovation speed," *IEEE Transactions on engineering management,* vol. 49, no. 1, pp. 2-12, 2002.
[41] N. Chiriac, K. Hölttä-Otto, D. Lysy, and E. S. Suh, "Three approaches to complex system decomposition," in *DSM 2011: proceedings of the 13th international DSM conference*, 2011.
[42] C. W. Johnson, "What are emergent properties and how do they affect the engineering of complex systems?," *Reliability Engineering and System Safety,* vol. 91, no. 12, pp. 1475-1481, 2006.
[43] C. L. Beck, J. Doyle, and K. Glover, "Model reduction of multidimensional and uncertain systems," *EEE Transactions on Automatic Control,* vol. 41, no. 10, pp. 1466-1477.
[44] Y. Yue, L. Feng, and P. Benner, "Reduced-order modelling of parametric systems via interpolation of heterogeneous surrogates," *Advanced Modeling and Simulation in Engineering Sciences,* vol. 6, no. 1, pp. 1-33, 2019.
[45] B. Lightsey, "Systems engineering fundamentals," DEFENSE ACQUISITION UNIV FT BELVOIR VA, 2001.
[46] A. Kossiakoff, W. N. Sweet, S. J. Seymour, and S. M. Biemer, *Systems engineering principles and practice*. John Wiley & Sons, 2011.
[47] B. Curtis, H. Krasner, and N. Iscoe, "A field study of the software design process for large systems," *Communications of the ACM,* vol. 31, no. 11, pp. 1268-1287, 1988.
[48] M. E. Kreye, Y. M. Goh, L. B. Newnes, and P. Goodwin, "Approaches to displaying information to assist decisions under uncertainty," *Omega,* vol. 40, no. 6, pp. 682-692, 2012.
[49] Y. Chen, J. Shi, and X.-J. Yi, "Design Improvement for Complex Systems with Uncertainty," *Mathematics,* vol. 9, no. 11, p. 1173, 2021.
[50] S. Lasso, M. Kreye, J. Daalhuizen, and P. Cash, "Exploring the link between uncertainty and project activities in new product development," *Journal of Engineering Design,* vol. 31, no. 11-12, pp. 531-551, 2020.
[51] P. Cash and M. Kreye, "Exploring uncertainty perception as a driver of design activity," *Design Studies,* vol. 54, pp. 50-79, 2018.
[52] M. Blauth, R. Mauer, and M. Brettel, "Fostering creativity in new product development through entrepreneurial decision making," *Creativity and Innovation Management,* vol. 23, no. 4, pp. 495-509, 2014.
[53] M. J. Chalupnik, D. C. Wynn, and P. J. Clarkson, "Comparison of ilities for protection against uncertainty in system design," *Journal of Engineering Design,* vol. 24, no. 12, pp. 814-829, 2013.

[54] S. O. Schmitt, M. Scheitza, and P. Groche, "A model for improving the applicability of design methodologies to mechanical engineering design routines," *Journal of Engineering Design,* vol. 26, no. 10-12, pp. 302-320, 2015.
[55] R. Neufville, "Real options: dealing with uncertainty in systems planning and design," *Integrated Assessment,* vol. 4, no. 1, pp. 26-34, 2003.
[56] J. Dejean and G. Blanc, "Managing uncertainties on production predictions using integrated statistical methods," in *SPE Annual Technical Conference and Exhibition*, 1999: OnePetro.
[57] B. López-Mesa, G. Thompson, and M. Williander, "Managing uncertainty in the design and development process by appropriate methods selection," in *DS 30: Proceedings of DESIGN 2002, the 7th International Design Conference, Dubrovnik*, 2002.
[58] R. Doctor, D. P. Newton, and A. Pearson, "Managing uncertainty in research and development," *Technovation,* vol. 21, no. 2, pp. 79-90, 2001.
[59] W. F. Wright and G. H. Bower, "Mood effects on subjective probability assessment," *Organizational behavior and human decision processes,* vol. 52, no. 2, pp. 276-291, 1992.
[60] D. F. Cooper, S. Grey, G. Raymond, and P. Walker, *Project risk management guidelines*. Wiley, 2005.
[61] M. A. Mustafa and J. F. Al-Bahar, "Project risk assessment using the analytic hierarchy process," *IEEE transactions on engineering management,* vol. 38, no. 1, pp. 46-52, 1991.
[62] D. Hillson, *Effective opportunity management for projects: Exploiting positive risk*. Crc Press, 2003.
[63] M. Radujković and I. Burcar, "Risk breakdown structure for construction projects," in *3rd International Conference on Construction in the 21st Century, CTIC-III, Atena, Greece*, 2005, pp. 164-169.
[64] R. S. Kaplan and A. Mikes, "Managing risks: a new framework," *Harvard business review,* vol. 90, no. 6, pp. 48-60, 2012.
[65] K. Grebici, Y. Goh, and C. McMahon, "Uncertainty and risk reduction in engineering design embodiment processes," in *DS 48: Proceedings DESIGN 2008, the 10th International Design Conference, Dubrovnik, Croatia*, 2008.
[66] R. M. Becker, "Lean manufacturing and the Toyota production system," *Encyclopedia of world biography,* 1998.
[67] J. P. Womack, D. T. Jones, and D. Roos, *The machine that changed the world: The story of lean production--Toyota's secret weapon in the global car wars that is now revolutionizing world industry*. Simon and Schuster, 2007.
[68] H. Soltan and S. Mostafa, "Lean and agile performance framework for manufacturing enterprises," *Procedia Manufacturing,* vol. 2, pp. 476-484, 2015.
[69] T. V. Stern, *Lean and agile project management: how to make any project better, faster, and more cost effective*. Productivity Press, 2017.
[70] H. B. Wang, J. Kinugawa, and K. Kosuge, "Exact Kinematic Modeling and Identification of Reconfigurable Cable-Driven Robots With Dual-Pulley Cable Guiding Mechanisms," (in English), *Ieee-Asme Transactions on Mechatronics,* Article vol. 24, no. 2, pp. 774-784, Apr 2019, doi: 10.1109/tmech.2019.2899016.
[71] P. Eskerod, M. Huemann, and C. Ringhofer, "Stakeholder inclusiveness: Enriching project management with general stakeholder theory1," *Project Management Journal,* vol. 46, no. 6, pp. 42-53, 2015.

[72] A. Albar, R. E. Randall, B. Dwibarto, and B. L. Edge, "A bucket wheel dredge system for offshore tin mining beyond the 50m water depth," *Ocean Engineering,* vol. 29, no. 14, pp. 1751-1767, 2002/11/01/ 2002, doi: https://doi.org/10.1016/S0029-8018(02)00003-3.
[73] J. Tang, Q. Wang, and T. Zhong, "Automatic monitoring and control of cutter suction dredger," *Automation in Construction,* vol. 18, no. 2, pp. 194-203, 2009/03/01/ 2009, doi: https://doi.org/10.1016/j.autcon.2008.07.006.
[74] J.-Z. Tang, Q.-F. Wang, and Z.-Y. Bi, "Expert system for operation optimization and control of cutter suction dredger," *Expert Systems with Applications,* vol. 34, no. 3, pp. 2180-2192, 2008/04/01/ 2008, doi: https://doi.org/10.1016/j.eswa.2007.02.025.
[75] S. A. Miedema, "Automation of a Cutter Dredge, Applied to the Dynamic Behaviour of a Pump/Pipeline System (Adobe Acrobat 4.0 PDF-File 254 kB)," *Proc. WODCON VI,* 2001.
[76] K. Law, "Integrated Dredging Automation."
[77] J. P. Martin and L. J. Mauriello, "Dredge Automation: The State-of-the-Art," ASCE, pp. 514-525.
[78] R. E. Randall, A. C. Drake, and W. A. Cenac, "Improvements for dredging and dredged material handling," 2011, vol. 8.
[79] J. B. Klaassens, C. de Keizer, J. Braaksma, and R. Babuska, "Model predictive control for optimizing the overall dredging performance of a trailing suction hopper dredger," presented at the WODCON XVIII, Orlando, Florida, USA, 2007.
[80] A. Loginov, A. Proskurnikov, E. Ambrosovskaya, and D. Romaev, "DP systems for track control of dredging vessels," *IFAC Proceedings Volumes,* vol. 45, no. 27, pp. 453-458, 2012.
[81] D. G. Mamunts, S. A. Morozov, V. D. Gaskarov, A. V. Sauchev, and Y. N. Tsvetkov, "Development of an automated system for managing and optimizing management decisions in the design, organization and production of dredging," 2018: IEEE, pp. 73-76.
[82] J.-S. Chou and C.-H. Liu, "Automated sensing system for real-time recognition of trucks in river dredging areas using computer vision and convolutional deep learning," *Sensors,* vol. 21, no. 2, p. 555, 2021.
[83] L. Jingui, L. Jinjun, Y. Jianhua, and D. Shuyou, "Technical research on the precise dredging of contaminated sediment," 2007.
[84] S. A. Miedema, "Calculation of the Cutting Forces when Cutting Water Saturated Sand," TU Delft, 1987.
[85] V. Matousek, "Flow Mechanism Of Sand-Water Mixtures in Pipelines," TU Delft, 1997.
[86] A. Albar, *Modeling of a Bucket Wheel Dredge System for Offshore Sand and Tin Mining*. Texas A & M University, 2001.
[87] T. A. Wilson, "Offshore Mining Paves the Way to Ocean Mineral Wealth," *Engineering and Mining Journal,* vol. 166, no. 6, pp. 124-166, 1965.
[88] C. van Rhee, "On the sedimentation process in a Trailing Suction Hopper Dredger," 2002.
[89] R. Tarodiya and B. K. Gandhi, "Hydraulic performance and erosive wear of centrifugal slurry pumps-A review," *Powder Technology,* vol. 305, pp. 27-38, 2017.
[90] L. C. Fairbank Jr, "Effect on the characteristics of centrifugal pumps," *Transactions of the American Society of Civil Engineers,* vol. 107, no. 1, pp. 1564-1575, 1942.
[91] W. Wiedenroth, "Experimental Work on the Transportation of Solid-Liquid Mixtures through Pipeline and Centrifugal Pumps," in *Fifth International Conference on the*

*Hydraulic Transport of Solids in Pipes, May 8th-11th, Bedford, England, Paper A*, 1978, vol. 2.
[92] J. Vocadlo, J. Koo, and A. Prang, "Performance of centrifugal pumps in slurry service," 1974.
[93] K. Burgess and J. Reizes, "The effect of sizing, specific gravity and concentration on the performance of centrifugal slurry pumps," *Proceedings of the Institution of Mechanical Engineers,* vol. 190, no. 1, pp. 391-399, 1976.
[94] K. Kazim, B. Maiti, and P. Chand, "A correlation to predict the performance characteristics of centrifugal pumps handling slurries," *Proceedings of the Institution of Mechanical Engineers, Part A: Journal of Power and Energy,* vol. 211, no. 2, pp. 147-157, 1997.
[95] T. Engin and M. Gur, "Comparative evaluation of some existing correlations to predict head degradation of centrifugal slurry pumps," *J. Fluids Eng.,* vol. 125, no. 1, pp. 149-157, 2003.
[96] d. Bree, "Centrifugal dredgepumps," *Ports and Dredging,* vol. 2, no. 27, p. 45, 1977.
[97] R. Durand and E. Condolios, "Transport Hydraulique et decantation des materiaux solids, Deuxiemes Journees de l'Hydraulique," ed, 1952, pp. 27-55.
[98] A. Furboter, "About the transport of sand-water mixture in pipelines, Communications from Franzius Institute," ed, 1961, pp. 163-166.
[99] K. Wilson and A. Sellgen, "Hydraulic Transport of Solids,," in *Pump Handbook*, 3rd ed.: McGraw Hill Education, 2001, ch. 9.321-9.349.
[100] S. A. Miedema, *Slurry Transport: Fundamentals, A Historical Overview & The Delft Head Loss & Limit Deposit Velocity Framework*, 2 ed. 2019.
[101] D. M. Newitt, J. Richardson, and C. Shook, "Hydraulic conveying of solids in horizontal pipes. Part II: Distribution of particles and slip velocities," in *Proceedings: Interaction between fluids and particles, IChemE, London*, 1962, pp. 87-100.
[102] K. Wilson, "A unified physically-based analysis of solid-liquid pipeline flow," in *Proc. Hydrotransport*, 1976, vol. 4: BHRA Fluid Engineering Cranfield, UK, pp. 1-16.
[103] K. Wilson, "Evaluation of interfacial friction for pipeline transport models," in *Proceedings 11th Conference on the Hydraulic Transport of Solids in Pipes*, 1988, pp. 107-116.
[104] K. Wilson and F. Pugh, "Dispersive-force modelling of turbulent suspension in heterogeneous slurry flow," *The Canadian Journal of Chemical Engineering,* vol. 66, no. 5, pp. 721-727, 1988.
[105] Y. Televantos, C. Shook, M. Streat, and A. Carleton, "Flow of slurries of coarse particles at high solids concentrations," *The Canadian Journal of Chemical Engineering,* vol. 57, no. 3, pp. 255-262, 1979.
[106] M. Roco and C. Shook, "Turbulent flow of incompressible mixtures," 1985.
[107] F. L. Hsu, R. M. Turian, and T. W. Ma, "Flow of noncolloidal slurries in pipelines," *AIChE journal,* vol. 35, no. 3, pp. 429-442, 1989.
[108] R. C. Worster and D. F. Denny, "Hydraulic transport of solids materials in pipelines, *Proceedings of Institute of Mechanical Engineering*.," ed, 1955, pp. 49, 166.
[109] P. Doron and D. Barnea, "A three-layer model for solid-liquid flow in horizontal pipes," *International Journal of Multiphase Flow,* vol. 19, no. 6, pp. 1029-1043, 1993.

[110] T. Nabil, I. El-Sawaf, and K. El-Nahhas, "Computational fluid dynamics simulation of the solid-liquid slurry flow in a pipeline," in *Proc. 17th International Water Technologies Conference IWTC17*, 2013, vol. 57.
[111] K. S. Davidson and L. Schiff, "Turning and course keeping qualities of ships," 1946.
[112] K. Nomoto, T. Taguchi, K. Honda, and S. Hirano, "On the steering qualities of ships," *International Shipbuilding Progress,* vol. 4, no. 35, pp. 354-370, 1957.
[113] M. Zhu, A. Hahn, Y.-Q. Wen, and W.-Q. Sun, "Optimized support vector regression algorithm-based modeling of ship dynamics," *Applied Ocean Research,* vol. 90, p. 101842, 2019.
[114] M. A. Abkowitz, "Lectures on ship hydrodynamics--Steering and manoeuvrability," 1964.
[115] D. J. Yeo and K. P. Rhee, "Sensitivity analysis of submersibles' manoeuvrability and its application to the design of actuator inputs," *Ocean engineering,* vol. 33, no. 17-18, pp. 2270-2286, 2006.
[116] X.-g. Wang, Z.-j. Zou, Z.-l. Yang, and F. Xu, "Sensitivity analysis of the hydrodynamic coefficients in 4 degrees of freedom ship manoeuvring mathematical model," *Journal of Shanghai Jiaotong University (Science),* vol. 20, no. 5, pp. 584-590, 2015.
[117] R. R. Shenoi, P. Krishnankutty, and R. P. Selvam, "Sensitivity study of hydrodynamic derivative variations on the maneuverability prediction of a container ship," in *International Conference on Offshore Mechanics and Arctic Engineering*, 2015, vol. 56550: American Society of Mechanical Engineers, p. V007T06A008.
[118] T. Pérez and M. Blanke, *Mathematical ship modelling for control applications*. Ørsted-DTU, Automation Lyngby, Denmark, 2002.
[119] J. P. Hooft, "The cross-flow drag on a manoeuvring ship," *Ocean engineering,* vol. 21, no. 3, pp. 329-342, 1994.
[120] A. Alikhani, S. Behzadipour, A. Alasty, and S. A. Sadough Vanini, "Design of a large-scale cable-driven robot with translational motion," *Robotics and Computer-Integrated Manufacturing,* vol. 27, no. 2, pp. 357-366, 2011/04/01/ 2011, doi: https://doi.org/10.1016/j.rcim.2010.07.019.
[121] A. Pott, C. Schenk, C. Masone, and H. H. Bulthoff, "Application of a differentiatorbased adaptive super-twisting controller for a redundant cable-driven parallelrobot," in *Cable-Driven Parallel Robots*: Springer, 2018, pp. 254–267.
[122] A. B. Alp and S. K. Agrawal, "Cable suspended robots: design, planning and control," in *Proceedings 2002 IEEE International Conference on Robotics and Automation (Cat. No.02CH37292)*, 11-15 May 2002 2002, vol. 4, pp. 4275-4280 vol.4, doi: 10.1109/ROBOT.2002.1014428.
[123] S. Rezazadeh and S. Behzadipour, "Workspace Analysis of Multibody Cable-Driven Mechanisms," (in English), *Journal of Mechanisms and Robotics-Transactions of the Asme,* Article vol. 3, no. 2, p. 10, May 2011, Art no. 021005, doi: 10.1115/1.4003581.
[124] J. P. Merlet, *Parallel robots* (Solid Mechanics and Its Applications). Springer, Dordrecht, 2001, p. 402.
[125] J. Radojicic, D. Surdilovic, and J. Krüger, "Application challenges of large-scale wire robots in agricultural plants," *IFAC Proceedings Volumes,* vol. 46, no. 4, pp. 77-82, 2013/01/01/ 2013, doi: https://doi.org/10.3182/20130327-3-JP-3017.00021.

[126] H. D. Taghirad and M. Nahon, "Kinematic Analysis of a Macro–Micro Redundantly Actuated Parallel Manipulator," *Advanced Robotics,* vol. 22, no. 6-7, pp. 657-687, 2008/01/01 2008, doi: 10.1163/156855308X305263.
[127] J. Y. Zhang, D. G. Cao, and Y. Q. Wu, "Kinematic Analysis and Motion Planning of Cable-Driven Rehabilitation Robots," (in English), *Applied Sciences-Basel,* Article vol. 11, no. 21, p. 19, Nov 2021, Art no. 10441, doi: 10.3390/app112110441.
[128] R. Bostelman, J. Albus, N. Dagalakis, A. Jacoff, and J. Gross, "Applications of the NIST Robocrane," *Robotics and Manufacturing,* vol. 5, 01/01 1994.
[129] A. Riechel, P. Bosscher, H. Lipkin, and I. Ebert-Uphoff, "Cable driven robots for use in hazardous environments.," in *10th International Conference on Robotics and Remote systems for Hazardeous Envirомnments*, ed. Gainesville, 2004.
[130] A. Ghasemi, M. Eghtesad, and M. Farid, *Workspace Analysis for Planar and Spatial Redundant Cable Robots*. 2008, p. 044502.
[131] R. Caverly and J. Forbes, *Maintaining positive cable tensions during operation of a single degree of freedom flexible cable-driven parallel manipulator*. 2015, pp. 1205-1210.
[132] C. Jin and R. Randall, "The Estimation of Production and Location of Pumps for a Cutter Suction Dredge using a Long Distance Pipeline," *Journal of Dredging,* vol. 16, 04/30 2018.
[133] F. Xu, H. Wang, K. W. S. Au, W. Chen, and Y. Miao, "Underwater Dynamic Modeling for a Cable-Driven Soft Robot Arm," *IEEE/ASME Transactions on Mechatronics,* vol. 23, no. 6, pp. 2726-2738, 2018, doi: 10.1109/TMECH.2018.2872972.
[134] Y. Wang, J. Chen, K. Zhu, B. Chen, and H. Wu, "Time-Delay Control of Cable-Driven Robots With Adaptive Fractional-Order Nonsingular Terminal Sliding Mode," *IEEE Access,* vol. 6, pp. 54086-54096, 2018, doi: 10.1109/ACCESS.2018.2871611.
[135] O. Jacobsen, "Autonomous underwater cable suspended dredging system: a method to combat the eutrophication of the baltic sea.," Electrical Engineering Masters thesis, Computer Science, KTH, 2015. [Online]. Available: https://go.exlibris.link/mcdMXB8d
[136] T. R. Camp, "Sedimentation and the design of settling tanks," *Transactions of the American Society of Civil Engineers,* vol. 111, no. 1, pp. 895-936, 1946.
[137] L. Lennart, "System identification: theory for the user," *PTR Prentice Hall, Upper Saddle River, NJ,* vol. 28, p. 540, 1999.
[138] J. Sjöberg *et al.*, "Nonlinear black-box modeling in system identification: a unified overview," *Automatica,* vol. 31, no. 12, pp. 1691-1724, 1995.
[139] J. A. Suykens, J. Vandewalle, and J. P. Vandewalle, *Nonlinear Modeling: advanced black-box techniques*. Springer Science & Business Media, 1998.
[140] W. J. Vlasblom, "The Breaching Process," ed: Delft University of Technology, 2003.
[141] H. Hussein, J. C. Santos, J. B. Izard, and M. Gouttefarde, "Smallest Maximum Cable Tension Determination for Cable-Driven Parallel Robots," (in English), *Ieee Transactions on Robotics,* Article vol. 37, no. 4, pp. 1186-1205, Aug 2021, doi: 10.1109/tro.2020.3043684.
[142] P. Gallina and A. Rossi, "Planar Cable-Direct-Driven Robots, Part II: Dynamics and Control," *Proceedings of the ASME Design Engineering Technical Conference,* vol. 2, 01/01 2001, doi: 10.1071/ASEG2001ab148.
[143] F. Inel, M. M. Noor, and I. O. P. Publishing, "3D cable-based parallel robot simulation using PD control," in *5th International Conference on Mechanical Engineering Research*

*(ICMER)*, Kuantan, MALAYSIA, Jul 30-31 2019, vol. 788, BRISTOL: Iop Publishing Ltd, in IOP Conference Series-Materials Science and Engineering, 2020, doi: 10.1088/1757-899x/788/1/012069. [Online]. Available: <Go to ISI>://WOS:000594058000068

[144] M. A. Kökpinar and M. Gogus, "Critical Flow Velocity in Slurry Transporting Horizontal Pipelines," *Journal of Hydraulic Engineering,* vol. 127, pp. 763-771, 2001.

[145] T. M. Turner, *Fundamentals of hydraulic dredging*, 2 ed. American Society of Civil Engineering Press, 1996.

[146] S. A. Miedema, *Slurry Transport Fundamentals, A Historical Overview and The Delft Head Loss and Limit Deposit Velocity Framework*, 1 ed. (Institutional Repository). Delft, The Netherlands: SA Miedema/ Delft University of Technology, 2016.

[147] M. Pérez-Sánchez, P. A. López-Jiménez, and H. M. Ramos, "Modified affinity laws in hydraulic machines towards the best efficiency line," *Water resources management,* vol. 32, no. 3, pp. 829-844, 2018.

[148] K. Wilson, G. Addie, A. Sellgreen, and R. Clift, *Slurry Transport using Centrifugal Pumps*. New York: Springer Science, 2006.

[149] T. Bruckmann, L. Mikelsons, T. Brandt, M. Hiller, and D. Schramm, "Wire Robots Part II: Dynamics, Control & Application," 2008.

[150] A. S. Niyetkaliyev, E. Sariyildiz, and G. Alici, "Kinematic Modeling and Analysis of a Novel Bio-Inspired and Cable-Driven Hybrid Shoulder Mechanism," (in English), *Journal of Mechanisms and Robotics-Transactions of the Asme,* Article vol. 13, no. 1, p. 12, Feb 2021, Art no. 011008, doi: 10.1115/1.4047984.

[151] N. Mortensen, J. A. Johnson, and A. J. Shturmakov, "Precision cable winch level wind for deep ice-coring systems," *Annals of Glaciology,* vol. 55, no. 68, pp. 99 - 104, 2014, doi: 10.3189/2014AoG68A013.

[152] M. H. Korayem, M. Bamdad, and M. Saadat, "Workspace analysis of cable-suspended robots with elastic cable," in *2007 IEEE International Conference on Robotics and Biomimetics (ROBIO)*, 15-18 Dec. 2007 2007, pp. 1942-1947, doi: 10.1109/ROBIO.2007.4522464.

[153] X. Diao and O. Ma, "Vibration analysis of cable-driven parallel manipulators," *<i data-test="journal-title" style="box-sizing: inherit;">Multibody System Dynamics volume,* vol. 21, 2009, doi: https://doi.org/10.1007/s11044-008-9144-0.

[154] D. Gueners, B. C. Bouzgarrou, and H. Chanal, "Cable Behavior Influence on Cable-Driven Parallel Robots Vibrations: Experimental Characterization and Simulation," (in English), *Journal of Mechanisms and Robotics-Transactions of the Asme,* Article vol. 13, no. 4, p. 17, Aug 2021, Art no. 041003, doi: 10.1115/1.4049978.

[155] R. Vafapour, M. R. Gharib, M. Honari-Torshizi, and M. Ghorbani, "ON THE APPLICATIVE WORKSPACE AND THE MECHANISM OF AN AGRICULTURE 3-DOF 4-CABLE-DRIVEN ROBOT," (in English), *International Journal of Robotics & Automation,* Article vol. 36, no. 2, pp. 103-109, 2021, doi: 10.2316/j.2021.206-0366.

[156] S. I. M. Inc. "Sil Blasting Sands." Wallace Construction Specialties, LTD. https://www.wallace.sk.ca/public/plugins/products/15/1491587113FILE0.pdf (accessed.

[157] A. Lozhechnikova, "Determination of slurry's viscosity using case based reasoning approach," 2011.

[158] P. K. Swamee and A. K. Jain, "Explicit equations for pipe-flow problems," *Journal of the hydraulics division,* vol. 102, no. 5, pp. 657-664, 1976.

[159] D. Guo, H. Chen, L. Tang, Z. Chen, and P. Samui, "Assessment of rockburst risk using multivariate adaptive regression splines and deep forest model," *Acta Geotechnica,* vol. 17, no. 4, pp. 1183-1205, 2022.
[160] M. W. Miertschin and R. E. Randall, "Costs and Production Estimation for a Cutter Suction Dredge.[Master's Thesis]," *Ocean Engineering Program, Civil Engineering Department, Texas A&M University,* 1997.
[161] S. Bai, M. C. Li, Q. R. Lu, H. J. Tian, and L. Qin, "Global Time Optimization Method for Dredging Construction Cycles of Trailing Suction Hopper Dredger Based on Grey System Model," (in English), *Journal of Construction Engineering and Management,* Article vol. 148, no. 2, p. 19, Feb 2022, Art no. 04021198, doi: 10.1061/(asce)co.1943-7862.0002239.
[162] S. A. Miedema, *Automation of a cutter dredge, applied to the dynamic behavior of a pump/pipeline system.* Kuala Lumpur, Malaysia, 2001.
[163] N. Musmeci, S. Battiston, G. Caldarelli, M. Puliga, and A. Gabrielli, "Bootstrapping topological properties and systemic risk of complex networks using the fitness model," *Journal of Statistical Physics,* vol. 151, no. 3, pp. 720-734, 2013.
[164] E. Dredges. "Series 370 Dragon Dredge." https://www.dredge.com/series-370-dragon-dredge/#:~:text=Ellicott%20Dredges%20is%20one%20of,suction%20dredges%20in%20the%20industry. (accessed.
[165] J. Suttwill, "Alluvial mining grows in popularity " *Engineering and Mining Journal* vol. 190, no. 11, pp. 42-47, 1989.
[166] R. H. Charlier and C. C. Charlier, "Environmental, economic, and social aspects of marine aggregates' exploitation," *Environmental Conservation,* vol. 19, no. 1, pp. 29-38, 1992.
[167] S. E. Alter, L. Tariq, J. K. Creed, and E. Megafu, "Evolutionary responses of marine organisms to urbanized seascapes," (in English), *Evolutionary Applications,* Review vol. 14, no. 1, pp. 210-232, Jan 2021, doi: 10.1111/eva.13048.
[168] R. IHC. https://www.royalihc.com/-/media/royalihc/products/dredging/hopper-dredging/trailing-suction-pipe-systems/d4-dredging-equipment-tshd.jpg (accessed.
[169] L. W. Technology. "LWT Dredging Systems." https://d3pcsg2wjq9izr.cloudfront.net/files/1051/download/473847/011515_LWT_Brochure_FINAL.pdf (accessed.
[170] I. Dredges. "MODEL 7012 HP VERSI-DREDGE." https://www.imsdredge.com/ims-model-7012-hp-versi-dredge/#:~:text=%C2%AE,%2C%20light%20clays%2C%20and%20salt. (accessed.
[171] H. Yoda, K. Uranishi, C. Takahashi, and Y. Handa, "A Study of Efficiency Corrections for Centrifugal Pumps Handling Viscous Liquids in ISO/TR 17766: 2005," *International Journal of Fluid Machinery and Systems,* vol. 14, no. 3, pp. 270-279, 2021.
[172] H. T. Kazerooni, W. Fornari, J. Hussong, and L. Brandt, "Inertial migration in dilute and semidilute suspensions of rigid particles in laminar square duct flow," *Physical Review Fluids,* vol. 2, no. 8, p. 084301, 08/08/ 2017, doi: 10.1103/PhysRevFluids.2.084301.
[173] R. G. Gillies, C. A. Shook, and K. C. Wilson, "An improved two layer model for horizontal slurry pipeline flow," *The Canadian Journal of Chemical Engineering,* vol. 69, no. 1, pp. 173-178, 1991, doi: 0.1002/cjce.5450690120.
[174] G. Anthony, A. Roudnev, and K. Burgess, "Slurry Pumping Manual," ed. January 2002: Weir Slurry Group Technology, 2002.

[175] "6 - Flow of Settling Slurries," in *Solid-Liquid Two Phase Flow*, S. M. Peker, Ş. Ş. Helvacı, H. B. Yener, B. İkizler, and A. Alparslan Eds. Amsterdam: Elsevier, 2008, pp. 329-383.
[176] G. R. R. A. S. Addie and A. Sellgren, "The new ANSI/HI centrifugal slurry pump standard," *Journal of the Southern African Institute of Mining and Metallurgy,* vol. 107, no. 6, pp. 403-409, 2007.
[177] H. Plattner, C. Meinel, and L. Leifer, *Design thinking: understand–improve–apply*. Springer Science & Business Media, 2010.
[178] K. Thoring and R. M. Müller, "Understanding design thinking: A process model based on method engineering," in *DS 69: Proceedings of E&PDE 2011, the 13th International Conference on Engineering and Product Design Education, London, UK, 08.-09.09. 2011*, 2011, pp. 493-498.
[179] T. Brown, "Design thinking," *Harvard business review,* vol. 86, no. 6, p. 84, 2008.
[180] T. Brown, *Change by design: how design thinking transforms organizations and inspires innovation*. Harper Business, 2009.
[181] H. Plattner, C. Meinel, and U. Weinberg, *Design-thinking*. Springer, 2009.
[182] V. Taajamaa, S. Kirjavainen, L. Repokari, H. Sjöman, T. Utriainen, and T. Salakoski, "Dancing with Ambiguity Design thinking in interdisciplinary engineering education," in *2013 IEEE Tsinghua International Design Management Symposium*, 2013: IEEE, pp. 353-360.
[183] R. Razzouk and V. Shute, "What Is Design Thinking and Why Is It Important?," *Review of Educational Research,* vol. 82, no. 3, pp. 330-348, 2012, doi: 10.3102/0034654312457429.
[184] K. Dorst, "The core of 'design thinking'and its application," *Design studies,* vol. 32, no. 6, pp. 521-532, 2011.
[185] R. G. Cooper, S. J. Edgett, and E. J. Kleinschmidt, "Optimizing the stage-gate process: what best-practice companies do—I," *Research-Technology Management,* vol. 45, no. 5, pp. 21-27, 2002.
[186] R. S. Adams and C. J. Atman, "Cognitive processes in iterative design behavior," in *FIE'99 Frontiers in Education. 29th Annual Frontiers in Education Conference. Designing the Future of Science and Engineering Education. Conference Proceedings (IEEE Cat. No. 99CH37011*, 1999, vol. 1: IEEE, pp. 11A6/13-11A6/18 vol. 1.
[187] C. L. Dym and P. Little, *Engineering design: A project-based introduction*. John Wiley and sons, 1999.
[188] Y. Haik, S. Sivaloganathan, and T. M. Shahin, *Engineering design process*. Cengage Learning, 2015.
[189] NASA. "NASA Procedural Requirements." https://nodis3.gsfc.nasa.gov/displayDir.cfm?t=NPR&c=7123&s=1B (accessed September 17, 2022).
[190] H. J. Thamhain, "Can innovative R&D performance be managed," presented at the Portland International Conference on Management of Engineering and Technology, Portland, 2002.
[191] A. Kleyner and A. Nebeling, "Applying automotive robustness validation to reduce the number of unplanned reliability testing cycles," in *2016 Annual Reliability and Maintainability Symposium (RAMS)*, 25-28 Jan. 2016 2016, pp. 1-7, doi: 10.1109/RAMS.2016.7448049.

# Appendix A: Further Information on Dredging

## Dredging Overview

Dredging is a centuries-old technology, and involves a set of skilled, experienced personnel. There are three common dredge methods: hydraulic dredging; dewatering followed by open excavation and hauling; mechanical dredging. The most effective method for specific applications often depends on the application conditions, including the type and compaction of solids, rheology of the slurry, discharge location relative to the excavation site, and the abundance of the carrier fluid. Hydraulic dredgers can perform excavation and transportation work at the same time which makes them an efficient system as long as there is a carrier fluid available.

## The Dredge Cycle

Figure A1.1 represents  the conventional dredge cycle using a centrifugal pump as points A-B-C-D-E [145].

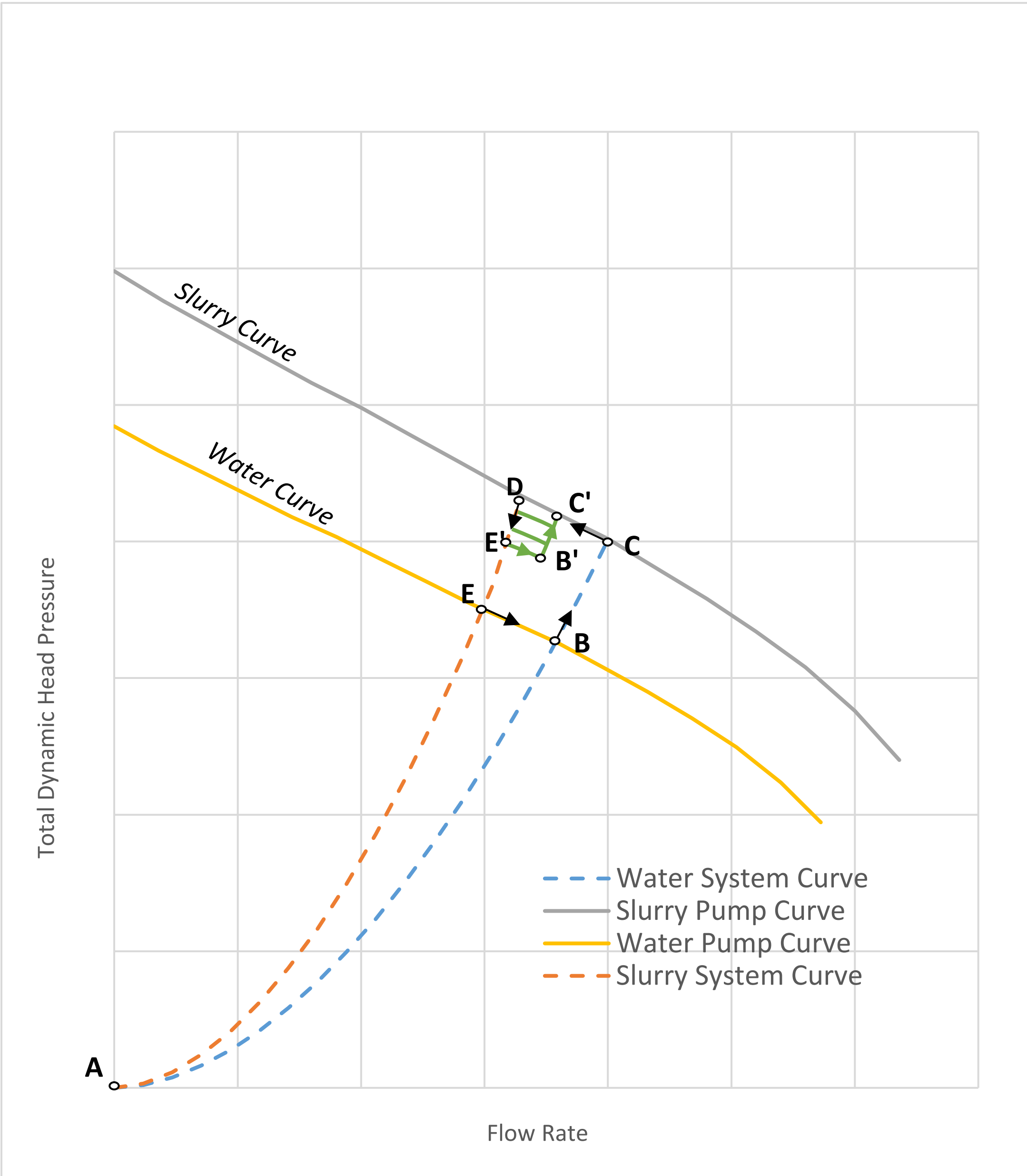


Figure A1.1: Dredge Cycle [146]

Turner [145] describes the dredge cycle as starting at point A, where the dredge pump is inactive. Once the dredge pump is turned on, the pump and discharge pipe fill with water, and follow the water system curve until the operating point is reached. As the dredge head is lowered into the sediment bed, solids begin to enter the system, which shifts the operating point to C. As a result, the power draw on the dredge pump and the system's total pressure increases.

As the mixture enters the discharge pipeline, dynamic slurry losses cause the operating point to shift from C to D. If the excavation rate of the dredge is kept constant, the operating point will be maintained at position D. However, most hydraulic dredgers must be repositioned to gain access to new material. During this repositioning process, the dredge head and cutter are removed from the sediment bed. As a result, water re-enters the system which reduces the density of the slurry and shift the operating point from D to E. As the discharge line shifts from mainly slurry to mainly water the operating point moves from position E to B. As the dredge head moves back into the material, the operating point once again shifts back along the path of B to C and then again to D.

As the system reaches maximum solids' concentration, we also reach the power limit. At this power limit, flow may be decreased and settling in the discharge line may occur. Since an optimal operating point is unique to the system layout and application conditions, dredge systems often utilize instrumentation to provide details on slurry density, flow, pressure, and horsepower conditions. Once an optimal point for a given system is established, dredge operators work to maintain this optimal point by manipulating the position of the dredge head within D, E', B', and C'.

A dredge pump's performance characteristics are affected by many factors, from the solid particle size, solids' specific gravity, concentration of solids, and the ratio of particle size, to impeller diameter. Likewise, the friction losses in the discharge pipe due to moving a slurry are dependent on the mixture velocity, concentration, pipe roughness, as well as solid's size distribution, shape, and density. Understanding how these parameters influence the pump's performance and losses is key to planning successful dredge jobs and developing an automated production controller.

**Dredge Methods & Applications**

In general, most dredge systems fall into two general categories: hydraulic, or mechanical. Hydraulic dredgers consist of a floating platform which carries pumps, agitators, propulsion system, power source, anchoring system, dredge head, ladder, hoist, instrumentation, and control system. Hydraulic dredgers, or suction dredgers, use pressurized water to break up in-situ material, and a suction pipe to access sediment layers. Suspended solids, or slurry are then transported to the discharge site. Hydraulic dredgers use hydraulic systems such as centrifugal pumps to fluidize materials which can be transported as a slurry through a pipeline.

Mechanical dredgers use conventional earthworks (truck and shovel) to excavate solids found below the waterline. Mechanical dredgers are affixed to work barge platforms which support the activity. The spoils of the mechanical dredge work are often transported by barges, ships, trucks, or some combination of these three. Barges are typically equipped with draglines, grabbers, clamshells, and excavators. When there is not enough carrier fluid to support hydraulic dredging, dewatering followed by open excavation may be necessary. Because of the different equipment required, and the time to organize each stage, excavation and mechanical dredges are generally less efficient than hydraulic dredges.

The selection of the right dredge method for each application is complex and depends on many factors, such as the depth and volume of available water, sediment characteristics, rheological properties of the mixture, amount of material to be removed and distance to the deposit area. Dredge projects often have the goal of maximizing or maintaining consistent production output for the least input energy or input cost. To accomplish this goal there are a variety of dredge systems on the marketplace today. Most of these systems include specialized features that allow them to improve their performance in specific applications.

Depending on the application and system requirements, dredging equipment can significantly range in complexity and size. For example, ocean dredgers involve large capacity ships with storage hoppers which separate the solids from the mixture to optimize capacity. These large dredge vessels are built to travel vast distances, with large payloads and deal with a variety of weather conditions. In comparison, inland dredgers are significantly smaller and designed with modularity. Inland dredgers modularity provides flexibility for transport as these systems are more commonly transported by truck and trailer.

**Applications**

*Environmental* applications require a dredge to remove contaminated sediments to a processing or disposal area.

*Aggregate and Mining* applications remove sand, gravel, precious metals, coal, phosphates, wastewater, and various other minerals to process.

*Tailings and Reclamation* dredging removes sediments from tailings' storage areas to create more capacity. Sediment typically goes through a water separation process so that it can be utilized to reclaim previously mined land.

*Overgrowth* applications remove deposits and overgrown vegetation from oceans, lakes, river ways and ponds that have become shallower over time.

*Port, Harbor, Lake and Reservoir and Maintenance* applications remove sediments and overgrown vegetation that reduces water depth.

*Beach Restoration and Land Development* projects move sediment from various locations to restore beaches or develop new land masses.

## Dredge Phases

Excavation and erosion break up the cohesive bonds of the in-situ sediment. Dredge excavation can be done through mechanical or hydraulic means. Mechanical excavation loosens the sediment so that it is more readily suspended in passing fluid.

For large dredge ships, transportation of solids consists of storing and moving them in the ship's hopper. For inland dredgers, hydraulic transport conveys the solids in a carrier fluid through a pipeline. Finally, materials must be redistributed at the discharge location. Often between the excavation, transport, and redistribution activities, there are activities such as separation of precious minerals. For applications that involve extraction or separation of ore, process plants are involved prior to the redistribution step. The processing plant may even be mobile and follow the dredge path. This allows the dredge to feed the processing plant and then redistribute the material back at the original excavation area once the ore has been extracted.

## Operation and Operators

Historically, the control of any dredge system has been heavily reliant on the experienced dredge operator. The operator must balance several system parameters to improve production output. In author interviews we identified several important parameters: system power, discharge pressure, flow rate, speed of the dredge head, applied dredge head force, depth of the dredge head into the material, and speed of the dredge pump. Dredge production is also governed by the available dredge power and deposition of solids in the pipe which is specific to the solid-fluid mixture being transported.

Controlling the dredge system requires lowering the dredge head into the material so that a dense mixture of solids and fluid enters the pump. This results in increased system pressure and additional power draw. As the mixture is transported through the discharge pipe, system pressure, power draw and fiction losses increase, due to sediment in the pipe. As a result, there is a reduction in mixture flow and line velocity. As the dredge operator adjusts parameters to improve the concentration of the solids-fluid mixture, the dredge flow tends to decrease. The upper limit for the dredge production rate is met as the solids concentration increases to the point where the conveyed solids begin to deposit and plug the discharge line.

For most inland dredgers, the dredge system performs dredge cuts. The system must be repositioned between each cut. This repositioning of the dredge involves lifting the dredge head out of the sediment bed which allows clean water to enter the dredge and pipeline. This process, known as the dredge water cycle, decreases the dredge efficiency by up to 50%.

**Hydraulic Dredge Structure**

Most hydraulic dredgers consist of a floating platform that supports multiple pieces of equipment. The main dredge components are: booster pump(s); a surface or submersible dredge pump; agitator; propulsion system; power source; anchoring system; dredge head; ladder; hoist; instrumentation; and control system. An example of an Ellicott 870 suction dredge is shown in Figure A1.2.

Figure A1. 2: Elliott 870 Dredge [164][72]

### Hydraulic Dredge Types: Ocean and Inland

There are two common classifications of hydraulic dredges: ocean, and inland. Both dredgers use a pump to induce a velocity water stream through a pipeline, in which solids are entrained and transported to the deposition area [145]. Both systems are commonly designed with the following components: a ship or barge platform; positioning system; dredge pump(s); agitation method; power source; a ladder with hoist (or swell compensator); instrumentation and operator's control station.

### Dredge Ship and Barges

Ocean dredgers, the largest dredgers, are built for deep water applications outside coastal waters [87, 165]. Ocean dredgers store slurry in the ship's storage hopper. Once in the hopper, the dredge spoils settle, and clean water can be extracted and returned to the ocean, which maximizes the system's capacity. Once the dredge hopper reaches capacity, the solids are transported by the ship to a deposit site or offloading area. Because ocean dredgers dredge, store, and transport solids from the excavation site, their design includes a ship with built-in hydraulic dredge and storage hopper.

The most common ocean dredgers are trailing suction hopper systems, as shown in Figure A1.3, which have been used since the 1990s [166, 167]. A trailing suction hopper dredge drags, alongside the ship, a dredge head, which excavates material from the ocean floor and conveys the material to the hopper for transport. The trailing suction hopper dredge utilizes an ocean swell compensator which adjusts the depth of the dredge head as the ocean profile changes or as the dredge ship moves up and down with the wave action.

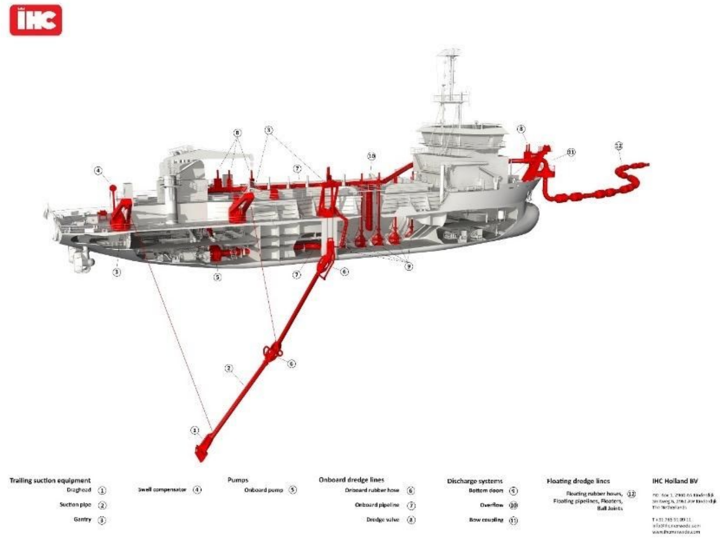


Figure A1.3: Suction Hopper Dredge [168]

Ocean dredgers are sometimes utilized in river applications, typically near the mouth of the river with access to the ocean. This provides the dredger access to the area without being removed from the water.

Inland dredgers are designed to work in shallow, calm water applications common to lakes, rivers, and ponds. For most applications, solids are transported from the site to a discharge area through a connecting discharge pipe. As a result, inland dredgers are smaller and lighter when compared to ocean dredger. Most inland dredge systems use a configuration of modular barges to support the dredge equipment. These modular barges allow the system to be more effectively assembled, disassembled, and shipped to various inland applications.

Typically, this transport process occurs within a discharge pipeline, where the system's terminal elevation and system losses are unique to the dredge and application setup. To deal with long distances and high terminal discharge elevations, hydraulic dredgers often include a series booster pumps which increase the fluid's energy along the discharge line while conveying the solids to the discharge location. A hydraulic dredger's production is heavily dependent on the net positive suction head available versus the net positive suction head required. For dredge applications with high suction lift, submersible dredge pumps are commonly used which moves the pump closer to the mixture, thus improving the systems net positive suction head available.

Inland hydraulic dredgers mainly consist of a dredge pump, ladder system with weight compensator, operators' station, power source and positioning system. The positioning mechanism between dredgers varies widely depending on the application but in general dredge position systems involve a propeller system, spud walker system, Starwheel™ drive, or a winch positioning system. Each of the conventional positioning systems are typically controlled by an operator's station aboard the dredger. The operator's station provides the operator access to dredge pump, positioning system, instrumentation readings and equipment which are all used to monitor and control the dredge production.

For small inland applications, remote operated dredge systems exist. These systems are controlled remotely by an operator at shore. To manage these remote-controlled dredge systems, the operator mainly relies on several visual cues from a distance and sensor data which is relayed from the instrumentation to the operator.

## Dredge Operations

Historically, the dredge operator has been the most important component of the dredge system, as the dredge's efficiency mainly depends on the operators and their experience; most hydraulic dredgers have an operator's station located on the dredge ship or barge [3]. The complexity of the dredging process has been studied by scholars around the world for years [25]. This research has found that when dredge operators are inexperienced, the dredge control is not optimized as the operator does not fully understand the impacts of the system adjustments [11]. Over the last century there has been technological improvements in dredge monitoring, instrumentation, and data collection. As a result of this monitoring and data collection, empirical data have been gathered which has led to a better understanding of the dredge processes. Additionally, there have been recent improvements in remote monitoring and wireless technologies that has led to the emergence of remote operated dredge systems. More recently, autonomous dredge equipment has been developed by a select few companies, however, predicting the dredging process remains a challenge [73].

**Remote Operated Dredgers**

Several remote-operated inland dredge systems exist. The crawler dredge, shown in Figure A1.4, pulls the dredge system along a traverse line that spans the length of the application area. Since the dredge moves along a fixed traverse line, the system operation is linear motion.

Figure A1.4: Remote Operated – Mudcat Dredge [169]

Each time the dredge finishes a cut, the system is repositioned for additional cuts, as illustrated in Figure A1.5. This continuous repositioning reduces the overall dredge efficiency.

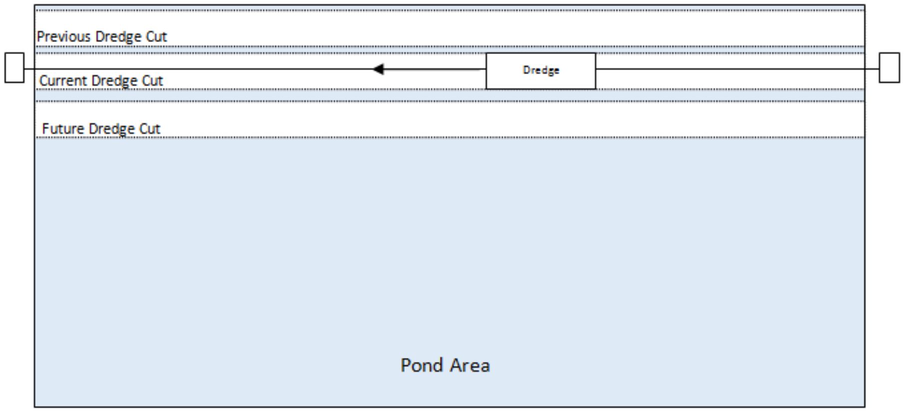


Figure A1.5: Remotely Operated, Dredge Path

Control of the crawler dredge is done by an operator with a handheld remote, typically from shore. This remote operation makes the system inherently safer. However, it also negatively impacts the operator's ability to maintain the dredge process through equipment observation. As a result, remote-operated crawler dredgers, and their operators, are heavily reliant on their system instrumentation.

Another example of a remote-operated dredge is a track system, which is a remote operated vehicle (ROV) dredger, as shown in Figure A1.6. This dredger eliminates the conventional dredge ship and operator station, making these dredgers compact and easier to transport, assemble and operate in tight spaces. The ROV dredger uses a track system to position the dredge head within the application workspace. Like the crawler dredge, the ROV dredger is controlled by a shore-based remote controller. However, because the entire system is submerged, the exact location of the dredger is difficult to determine in low visibility applications. The lack of visual data makes the ROV dredger challenging to maneuver and control.

Unlike the crawler dredge, the ROV dredge can position itself and perform continuous dredge cuts. However, the system is limited in many applications due to its maneuverability. Since the ROV does not have a ship or barge system, the ROV dredger is unable to control the applied weight of the dredge on the material bed. As a result, the dredge must operate in applications with stable materials beds which support the system's weight. If the material bed cannot support the dredger, it is prone to getting stuck. In addition, many dredge applications involve saturated soils, which are not well suited to support the weight or force of the system's positioning tracks. Due to these limitations, the ROV dredger are only deployed in limited applications.

Figure A1.6: Example of Under Water Crawler Dredge [169]

**Dredger Positioning Systems**

There are various methods to move and position hydraulic dredgers. Ocean dredgers commonly use a propeller system connected to the stern of the ship. Inland dredgers have three common positioning methods: spud walking; paddlewheel, or Starwheel$^{TM}$; and cable system. Inland dredgers can use a combination of the three positioning systems, which provides them with more versatility and movement within an application.

Spud walking dredge systems, as shown in Figure A1.7, use a systematic method of picking up one or multiple spuds attached to the dredge to pivot or "walk" the dredge forward. Spud walking dredges often use a combination of winching systems along with the spuds to move the dredge and position the dredge head.

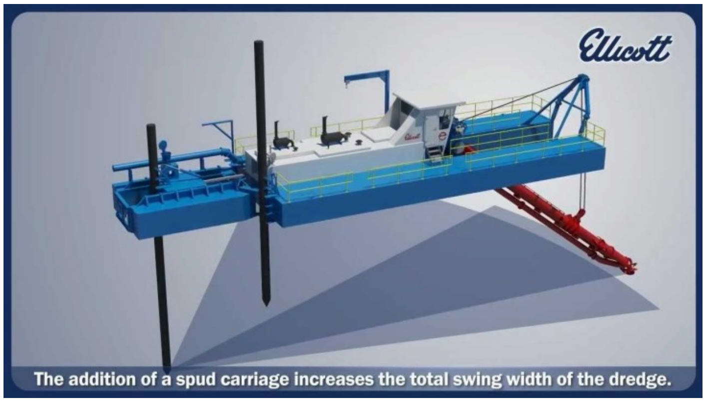


Figure A1.7: Spud Walking Dredge [72]

Alternatively, a Starwheel$^{TM}$ dredge, as shown in Figure A1.8, uses a wheel at the stern of the dredge which is lowered into the material bed. These Starwheel$^{TM}$ dredges push against the bed of material to move the system forward or backward.

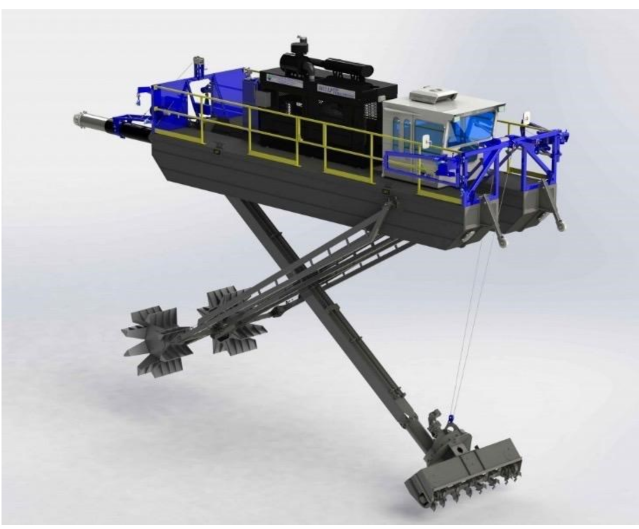

Figure A1.8: Starwheel$^{TM}$ Dredge [170]

The third common method of dredge movement is through a winch and anchoring system. For these dredgers, anchors are pre-set within the dredge application. Using these anchor points, on-board winches can pull the dredge system towards the anchor points.

**Ladder and Hoist System (or swell compensator)**

For most dredgers, the dredge head is lowered into a material bed below the hull through a ladder and hoist control system. The hoist is responsible for managing the weight of the dredge head against the bed of material while adjusting the vertical position of the dredge head. For some dredge systems, especially ocean dredgers in wave action, the adjustment of the dredge head is automated through a swell compensator system.

**Agitation System**

Hydraulic dredgers operate by lowering the dredge head into a layer of sediment. If the solids to be dredged are loosely compacted, the inlet velocity turbulence, and lift force, fluidizes the solids through the process of erosion. However, for many applications, the solids have formed cohesive bonds with one another which make these solids more difficult to break up and transport by erosion alone [11]. Therefore, many dredge systems use a means of agitation to breakup these bonds during the dredge process. One example of an agitator is a rotating cutter head which is shown in Figure A1.9 and Figure A1.10.

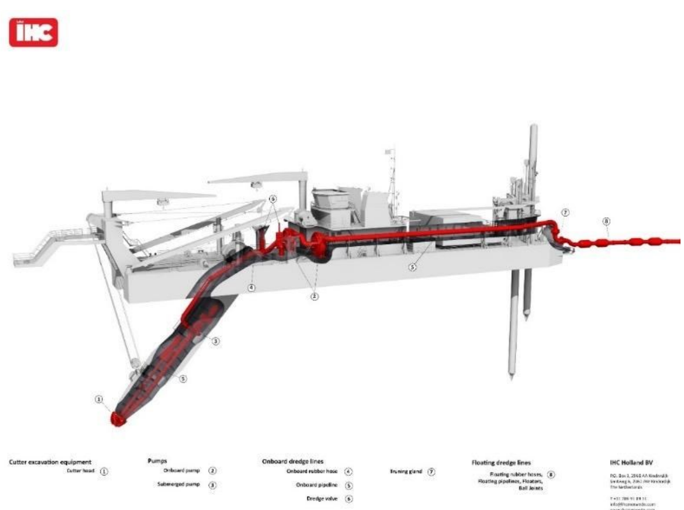


Figure A1.9: Cutter Dredge [168]

Figure A1.10: Cutter Dredge Teeth [168]

**Agitators**

Dredgers are often outfitted with a mechanical or hydraulic agitator which assist in the breakup of packed sediment beds. There are a variety of dredge agitators a few of which are summarized in the following section.

*Rotating cutter head*

These agitators dig up compact materials such as cemented clays. Cutter heads include teeth that can be changed out depending on the material harness. Hydraulic dredgers with a rotating cutter head are commonly referred to as a cutter suction dredge.

*Auger head*

Augurs, enclosed in a shroud, feed loose, often suspended, materials to the inlet of a dredge pump. Hydraulic dredges with an auger head are commonly referred to as auger dredges.

*Bucket Wheel*

Bucket wheel dredge attachments consist of a series of buckets along a wheel that excavates sediment layers. Hydraulic dredges with a bucketwheel are commonly referred to as a bucketwheel dredge.

*Drag head*

Drag heads contains teeth which drag along a sediment bed and break up the sediment. Drag heads are commonly used on trailing suction hopper dredgers used in ocean applications.

*Jetting Head*

Jetting heads use high-pressure water jets to break up loosely packed sediment, such as sands.

**Dredger Pumps**

Hydraulic dredgers may include one or multiple dredge pumps, depending on their purpose. The first pump in a dredge system is known as the primary pump, and subsequent pumps in series with the primary system are referred to as booster pumps. Ocean dredgers often include more than one submersible dredge pump. For these deep-water applications, the submersible dredge pumps are required to move the solids from the ocean floor to the hopper at sea level. Likewise, inland dredge systems may have multiple pumps in series. However, these booster pumps are typically installed aboard the dredger or along the discharge pipe at shore.

Depending on the system's intended digging depth, inland dredgers may or may not include a submersible primary pump. A dredger's available hydraulic dredging depth is limited by the net positive suction head requirements (NPSHr) of the primary pump and the net positive suction head available (NPSHa). To maximize the NPSHa, and available digging depth, many dredger designs include either a submersible primary pump or have the primary dredge pump semi-submerged in the hull of the dredger.

## Effects of Slurry on Pump Performance and Slurry Transport

### Dredge Pumps

A pump system's efficiency is defined by its performance characteristics, which are determined by the manufacturer's empirical test data. In their efforts to design efficient pumps, manufacturers maintain tight clearances in their pump design. However, because of the abrasive nature of slurry, once the pump is in service, these clearances are quickly eroded. Dredge pumps are therefore designed with easy-to-replace, sacrificial components, protected with wear-resistant coating. Dredge pumps are also designed to rotate at lower speeds resulting in less wear and larger clearances which make them better suited for low head, slurry applications.

### Effects of Slurry on Pump Performance

Because it is impossible to test all slurry mixtures, dredge pump manufacturers use clean water as the standard test medium to generate a pump's performance characteristics. Once a pump's standardized water performance is known, a pump-and-system curve may be adjusted to adequately estimate the new characteristics' curve for the given solids-fluid mixture. As the mixture becomes more viscous, the internal friction makes it more difficult for the fluid to deform[8] and the dredge pump requires more input shaft power to overcome the shear forces. As a result, the head and flow rate normally decrease while the power usage and the net positive suction head (NPSH) increase with viscosity [171]. The power, and NPSH required, increase with an increase in a fluid viscosity [171]. ANSI/HI has developed correction factors [80] that can be applied to the standard water curve to estimate the performance of a centrifugal pump with different viscous liquids.

---

[8] The ANSI Hydraulic Institute uses four factors to adjust the head and efficiency of a centrifugal pump. These four factors include solid particle size, solid specific gravity, solid concentration in slurry, and the ratio of particle size divided by the impeller diameter.

## Slurry Transport

In the dredging process, the fluid energy within the discharge pipe keeps the solids partially or fully suspended in the flow. When a slurry mixture is homogeneous, solids travel at the velocity of the carrier fluid. In heterogeneous slurries, the solids move slower than the carrier fluid, causing lag in delivery [148]. The main factors that influence the hydraulic transport process are the pressure drop along the pipeline length and the solid-fluid velocity. The total pressure drop for a system is due to the static head and dynamic system losses. The static head is based on the elevation change while dynamic losses are dependent on friction losses. Friction losses are produced by the friction between the pipe wall and the slurry as well as the interaction and resulting friction of the solids being transported. The total pressure loss of a system is unique and closely connected to the nature of the solids conveyed.

A fluid's rate of flow through a pipe is characterized by its Reynolds Number. Similarly, a particle moving in a fluid can be characterized by the particle Reynolds Number, which characterizes the ratio of inertial force to the viscous force, a key parameter when determining particle inertial migration [172]. When transporting fine particles with a Reynolds Number between $10^{-6}$ and 0.1, the flow tends to be homogeneous, and the fine particles are fully suspended in the flow. A pseudo-homogeneous flow tends to be the most economical flow due to the balance of flow velocity and solid transport; these flows occur with particles with Reynolds Numbers between and 0.1 and 2 [145].

There are two categories of slurry transport: non-settling, and settling [173]. Within the dredging industry, it is generally agreed thought that non-settling slurries tend to form a homogeneous mixture and have a particle size that is less than 40 um [174]. Settling slurries may form a pseudo-homogeneous, heterogeneous partially stratified, and heterogeneous fully stratified. Pseudo-homogeneous flows tend to occur with a particle size greater than 40 um that are sufficiently turbulent to keep the solids in suspension. If the flow is not sufficiently turbulent, or the particle size is greater than 100 um [174], a heterogeneous partially stratified ,or heterogeneous-fully stratified flow will occur. Some flows are a combination of homogenous and heterogenous mixtures. These flows are called complex flow [173] and involve two or more phase flows. Complex flows are not covered in detail here.

Dredge systems typically use a floating discharge pipeline on the water's surface. However, as the slurry discharge pipe transitions to land, the topography may include a steep vertical slope. When the vertical section of slurry flow becomes too steep, the solids begin to build up at the bottom of these pipe sections. For system control, it is important to understand the influence of these sections on the system as they are the most vulnerable to plugging.

**Slurry, Friction, and Energy Losses**

As a fluid moves through a pipe, there are energy losses due to the friction between the fluid and pipe wall. As the velocity of the flow increases, the losses increase as a function of the fluid velocity squared. Where the system curve intersects the water pump curve, the flow and head are at an operating equilibrium for the system conditions. The point where this intersection occurs is known as the operating point. Figure A1.11 illustrates a generic pump curve and the system curve which defines a system's operating point (point B).

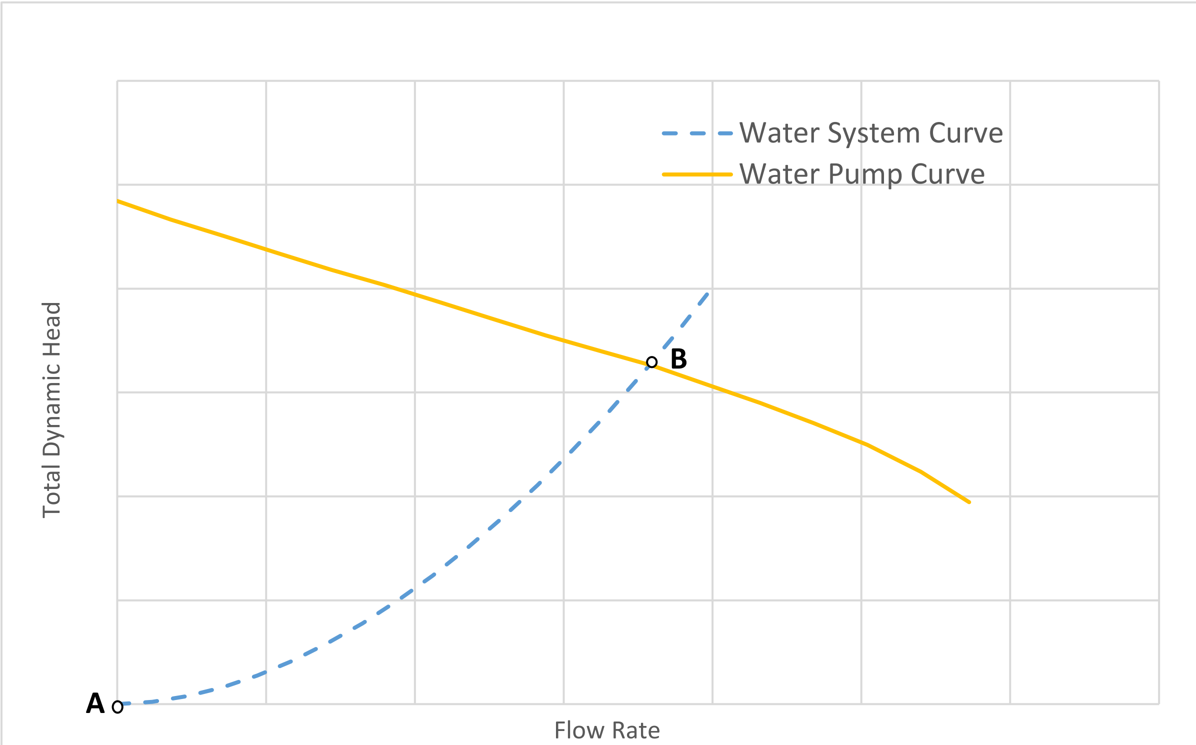

Figure A1.11: Generic Pump Curve with Operating Point

To prevent a line blockage requires the system to operate above the minimum deposition velocity for the slurry; the pump must have sufficient power to meet these energy demands. When moving water at a fixed pump RPM, the operating point for a fixed system does not change. A pump's RPM is directly proportional to its head pressure and flow. The adjustment of RPM and the effects on head pressure and flow is defined by affinity laws. When there is enough input power, increasing the pump RPM produces more head and flow. When increasing the RPM of a pump, increased flow results in increased dynamic system losses.

Systems containing solid-fluid mixtures experience additional losses due to friction. If the mixture density increases as solids are introduced, the static head pressure also increases due to increased density. The difference between the water curve and equivalent slurry-water curve is illustrated in Figure A1.1. The difference between the slope of the slurry system curve and the water system curve is the result of additional friction losses when dredging a mixture.

**Hydraulic Gradient**

The hydraulic gradient is different for settling and non-settling slurries in a pipeline [173]. To illustrate this, generic performance characteristics for settling, non-settling, and a combination of settling and non-settling slurries are shown in Figures A1.12 - A1.14 [175].

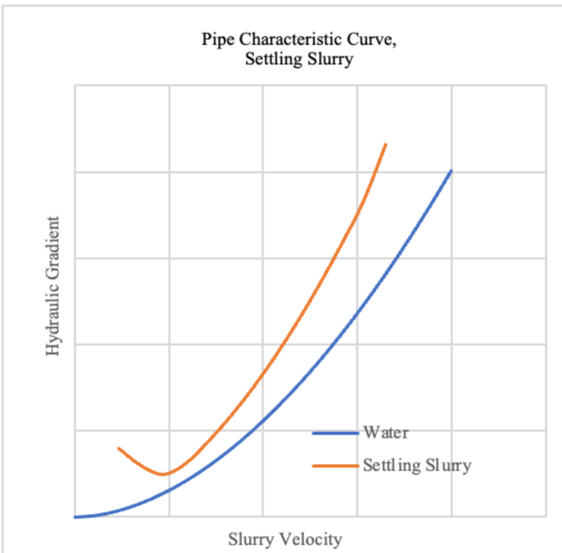


Figure A1.12: Settling Slurry - Pipe Characteristic Curve [175]

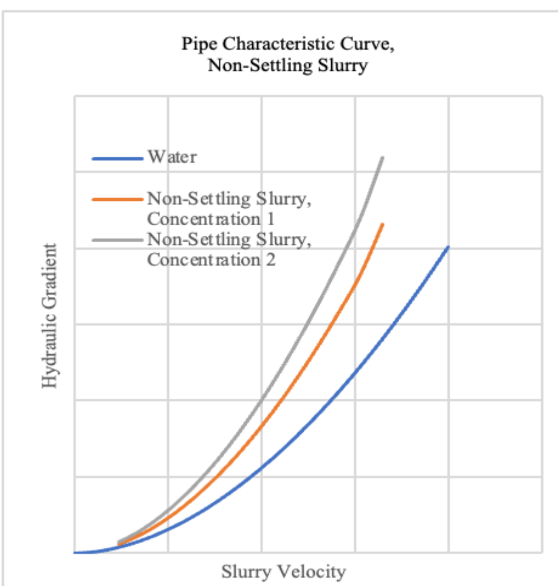


Figure A1.13: Non-Settling Slurry - Pipe Characteristic Curve [175]

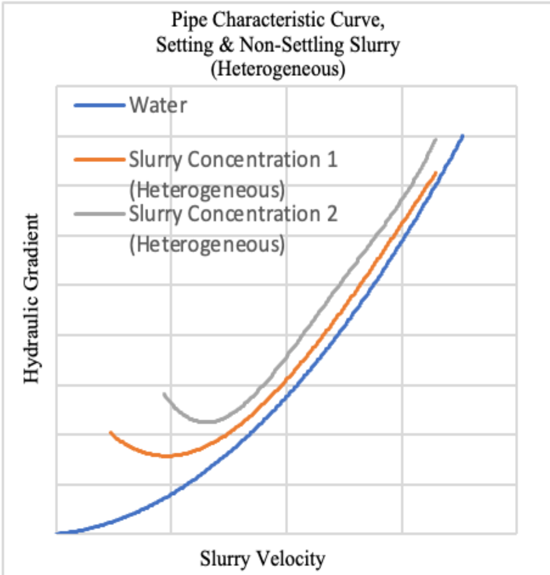


Figure A1.14: Non-Settling & Settling Slurry - Pipe Characteristic Curve [175]

**Slurry Types**

ANSI/HI Standard 12.1-12-2005 [176] categorizes slurry mixtures as follows: Class 1 (light slurries); Class 2 (medium slurries); Class 3 (Heavy slurries); and Class 4 (very heavy slurries). Class 1 slurries typically comprise of $d_{50}$ particles size of less than 50 µm. Due to the relatively small median particle size, compared to Class 2, 3 and 4 slurries, Class 1 slurries are often non-settling and tend to form a homogeneous mixture. Class 2, 3, and 4 slurries, on the other hand, are almost always a settling slurry and form a heterogeneous mixture.

**Production Rates**

The dredge system's production rate is heavily dependent on the excavation rate, the hydraulic capacity of the dredge pump, the input power, and the rheology of the mixture being transported. The excavation rate in the dredge process depends on the position and speed of the dredge head, the solids characteristics (such as density, shape, and diameter), the compaction of the bed of material, and the carrier fluid's velocity. Available agitation also affects the excavation rate [145]. The hydraulic capacity and efficiency of any pump is dependent on its characteristics, which are unique to the pump's design.

**Various Limits**

**NPSH Limits**

Hydraulic dredgers are governed by the net positive suction pressure available, and the net positive suction pressure required. The net positive suction pressure available at the inlet of the dredge pump depends on atmospheric pressure, inlet dynamic losses, static head pressure and the mixture's vapour pressure. The difference between the suction pressure of the pump and the saturation pressure of fluid must be kept larger than the net positive suction pressure required by the pump to avoid cavitation [74, 161]. If there is not enough pressure on the fluid at the inlet of the dredge pump, the fluid will begin to form a vapour. Cavitation occurs as the vapour is reintroduced to high pressure zones within the pumping system. As vapour changes back to liquid in these high-pressure zones, there is a violent collapse of the vapour and the release of energy forms pits and cavities in the dredge pump materials. In addition, the release of energy creates excess vibrations in the pumps shaft, which leads to premature seal and bearing pump failure. The net positive suction head required (NPSHr) is a pump characteristic determined by pump manufacturer empirical testing. For most centrifugal pumps, as the flow increases the net positive suction pressure required also increases which makes the dredge production heavily dependent on the available pressure at the inlet of the dredge pump.

**Power Limits**

If the dredge system flowrate stays constant, and the mixture density increases due to higher solids concentration, the system's static and dynamic losses increase. As a result of this additional energy demand, the input energy required from the power source increases. Therefore, the production of a dredger is also governed by the available power input.

**Solid Deposition Limits**

Another factor which governs the dredger's production and the ability to transfer solids in a pipe is the critical settling velocity. The critical settling velocity depends on internal pipe diameter, particle diameter and relative density [174]. If the critical settling velocity for the solids is not maintained in a dredge system, the solids tend to settle in the pipe which may lead to plugging. The dredge system's mixture velocity is dependent on the pipe diameter and flow rate. As the pipeline velocity increases, turbulent flow increases which helps maintain solids suspension. However, as the fluid velocity increases, the friction losses increase which results in an increase demand for power and increased wear on the pipe. Therefore, the hydraulic dredge system design, including the discharge pipeline, must balance the critical deposition velocity for the mixture and the fluid velocity rate, which is economical.

**Dredge Head Travel Speed**

For ocean dredgers and inland dredgers, the feed rate of material to the dredge head is heavily dependent on the dredge head velocity. For ocean dredgers, such as the trailing suction hopper dredge, the dredge head velocity is coupled to the ship's propulsion velocity [11]. For inland dredgers, the dredge head velocity is often decoupled from the dredge system positioning velocity. For example, inland dredgers often pivot the dredge head from side-to-side, as illustrated in Figure A1.7. This motion creates a cutting arc in front of the dredge while the dredge position remains fixed. The velocity of the arc regulates the dredge head speed and influences the system's production rate. Once the material is excavated along the cutting arc, the dredge repositions the entire dredge forward to reach more material.

# Appendix B: Further Information on Engineering Design Processes

As illustrated in Figure 1.1 [177], the design thinking and the engineering design process has five main stages, although other variations of similar framework exist for the design thinking process [178-181].

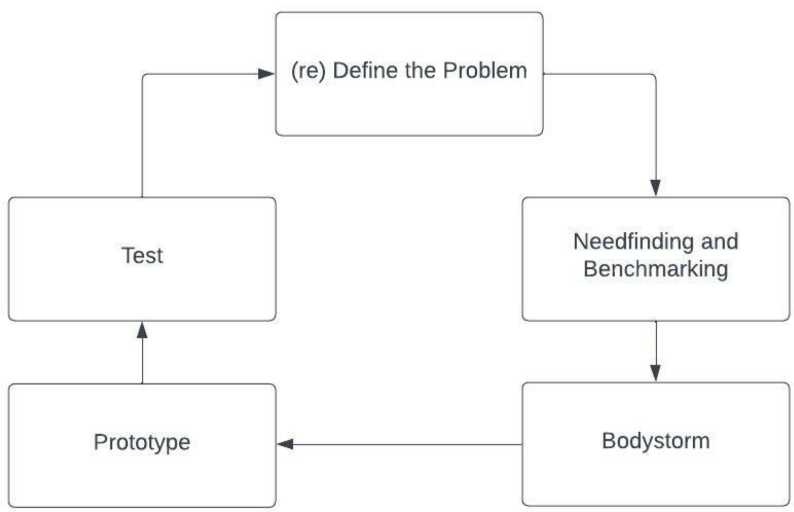


Figure B1.1: Design Thinking Process [177]

In this figure, each of these five stages appears to occur independently and happen sequentially. After the first cycle, subsequent iterations of the redesign cycle occur which leads to an ever-improving system model or design. What's more, researchers have found that design thinking tends to take a less structured approach and seems to have someone arbitrary choices between each iterative steps [178].

The engineering design process involves developing governing equations, parameters that influence a system, boundary conditions, and system constraints. Understanding a complex system's structure, behavior and fusion considers multiple perspectives, and the system analysis may conflict with, or extend beyond, everyday experience [8]. Complex systems are studied and observed, models developed, and then tested for verification. This model verification process is often iterative and continues until a model behaves close enough to the observed system that design work or modification of the design may begin.

For complex, multi-physics systems, this experimental design and verification is often completed with scaled-down prototype models in controlled laboratory environments. This approach provides repeatable experimental results. To fully understand and describe a complex system's behavior, teams of design engineers and scientists from different fields are required to participate in the modeling and design process. The design thinking and engineering design process can be somewhat ambiguous [182]. This process involves a combination of creativity and analysis which require experimentation, creation and prototyping of models, gathering feedback, and redesigning [183]. However, often these complex systems, and their associated experimental results, are difficult to understand and require significant time plus a great deal of organizational resources. In organizations and instances of limited time and resources, this approach is simply not feasible.

Engineering design considers the addition of the *how* (working principles) plus the *what* (thing) to determine a *result* (observed) or in business applications a *value* [184]. Using design thinking, an engineer solves for one of the unknowns: deduction, which determines the *result* from knowing the *what* and *how;* induction, which determines the *how* from knowing the *results* and the *what*; and abduction, which determines the *what* from the *how* and *result* [184]. However, in some cases, engineering design is more open and deals with complex problems or systems of two or sometimes three simultaneous unknowns. In these situations the engineer designs paradoxes, where parallel creation is required [184]. These complexities are one reason that design thinking tends to be more fluid than rigorously structured.

Due to the complex nature of parallel creation in the engineering design process, it can be difficult to know how an innovation is progressing and when a technology is ready to be introduced to the market. To help guide engineers in the design process, many organizations use a gate approach [185]. This approach frames criteria at various stages throughout the design project and does not allow the project to progress unless a threshold has been met. This provides some structure for the design engineer to focus on specific areas and provides the organization with some level of assurance that a design project is worth continuing and supporting with organizational resources.

All engineering design, and the development of a system model, involves some level of associated risk. These risks include, but are not limited to, technical design risks, market risks, project management risks, financial risks, resource risks, organizational risks, and safety risks. The engineering design process also allows for identification of design limitations that may pose risks in production and deployment. A tolerance for these risks is assumed within the modeling and at different stages in the design process. Even basic models involve some level of risk-based assumptions, which are verified through standard experimental design processes. With multi-physics design, the risks due to uncertainty in system behaviour increase due to the sheer number of assumptions and the complexity of physical interactions amongst technical elements of the design. Moreover, the first iteration of multi-physics system designs are often too big and too complex to result in a complete understanding of the system and an optimized model [186].

Other variations exist such as Ertas and Jones [36] that use process steps similar to the traditional waterfall model but includes some iterative, agile philosophies and practices.

Alternatively, Dym and Little [187] have built on the traditional waterfall method using both a descriptive and prescriptive design process model. They focus on a linear framework but emphasize an iterative refinement of the design through feedback. Haik and Shahin [188] identify five design process steps with feedback loops which include: requirements, product concept, solution concept, embodiment and detailed design which are then further divided into tasks. Dieter [39] also implement similar process ideas and tools for engineering design. Although each of these approaches tend to follow a linear waterfall approach, they each include some aspects of the iterative feedback throughout the engineering design process.

NASA [189] has developed a structure for complex system design which can be applied to their small and large projects. According to NASA, a "system" as a collection of different elements, which together produce results that one element could not produce alone [189]. NASA's *Systems Engineering Processes and Requirements* describes systems' engineering with three common technical processes which are iterative and recursive during a project [189]. The three higher level process are system design, product realization and technical management.

The System Design Process involves defining the baseline for the stakeholder expectations, technical requirements and converting the defined technical requirements into design solutions which satisfy the stakeholder expectations. This approach uses logical decomposition to develop a system hierarchy and elements. Developing design solutions that meet the technical requirements and stakeholder expectations is then applied from the top of the system structure to the bottom until all elements at each level can be built, bought, or reused. The remaining products in the system structure are then realized through element integration.

The product realization process involves several sub-processes including technical planning, technical control, technical assessment, and technical decision analysis. In the product realization process, design solutions are created, verified, and validated for each element that makes up the system structure. This approach starts at the lowest level and, working back up through the elements, integrates the design solutions while confirming that both technical and stakeholder definitions are met.

The technical management process directs the project's technical plans, communication and evaluate project progress against plans. This process involves three sub-processes: product transition; evaluation; and design realization. The technical management process is intended to control the project execution from the start to the end while helping in decisions making throughout.

# Appendix C: EQUIPMENT LIST

1. Centrifugal Pump 3-phase, 230V, Model 3085 Flygt Submersible pump
2. Pump Controller, Variable Frequency Drive, Model Yaskawa V1000
3. 3” EDPM Discharge Hose, Length 35 Meters
4. 3” ¼-Turn Isolation Valves:
    a. Valve #1 - located at pump discharge outlet.
    b. Valve #2 – located 25 meters past pump discharge outlet.

Note: The isolation valves prevent air from entering the discharge hose when the pump is lifted out of the water during testing resets and calibration.

1. Holding Sediment Tank, Capacity 1000 L
2. Gantry with trolly
3. Load Cell #1, Dredge Head Weight, Model 5000 lb S type loadcell
4. Pressure Transducer, Model Modbus RS485
5. Winches: #1 and #2, Model Jeamar NHT1900
6. Winch Controllers, Variable Frequency Drive, Model Yaskawa V1000
7. Load cell #2, Dredge Head Movement, Model 5000 lb S type loadcell
8. 6” Inline Magnetic Flow Sensor, Model Krohne
9. Fittings:
    a. Two, Steel Reducers, 3” x 6”
    b. One, 6” Spool, 1.5 meters in length
    c. One, 6” Spool, 1 meter in length
10. Load Cell #3, Discharge Tank Weight, Model Model XZ-GLE

11. Holding Discharge Tank, 1000 L

# Appendix D: Prototype, Testing and Product Development

### Project Initiation, Planning, and Development

Product development and innovation are important aspects for many businesses as they compete for market share. This section captures lessons from the development of the cable-driven dredge, discusses the practical challenges faced in each phase of product development and dredge testing, and includes takeaways from realization, planning, prototyping, and various stages of product testing. Acknowledging these challenges, and developing techniques and solutions to deal with them, are key factors which contribute to a product's success. Lastly, this Appendix provides insight into the controllability of the cable-driven dredge in real working environments.

### Product Realization

Canada Pump and Power (CPP) is an innovative industrial company that provides services and products in four key areas: dive; pump; barge; and dredge. From start-up, CPP focused on providing services and selling products to Canada's oil and gas sector in Northern Alberta. However, since entering the market and securing a presence, CPP has quickly expanded its service and products offerings throughout Canada. Canada Pump and Power's main goal is to provide the best and easiest solution to their existing and future clients. CPP invests a portion of its resources in research and development to improve safety, cost, and efficiency. Ideas for new products are driven by the leadership team in response to clients' needs and operational challenges. Product development has focused on a collaborative work effort between technical and experienced operations groups. This study used CPP's product development process to build, prototype, and test the cable-driven dredge. The next section briefly reviews the company process and identifies the lessons from this approach.

Product development and realization at CPP involves three distinct stages, illustrated in Figure D1.1. At the end of each stage, a gate analysis is completed which involves a go or no-go decision based on a matrix evaluation and the project's current state.

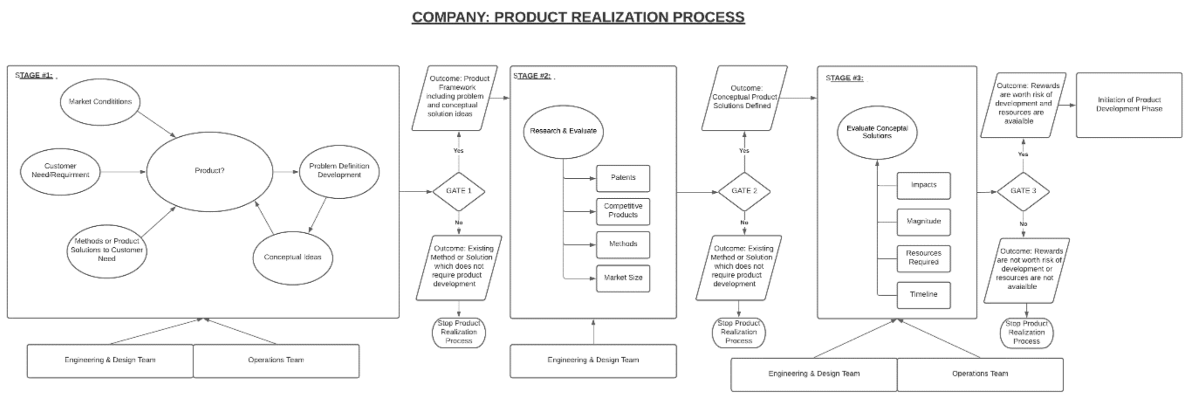


Figure D1.1: Product Realization Process at Canada Pump and Power

The first stage of the product development process, product realization, narrows the project requirements, objectives, and conceptual ideas. This stage, which arises due to a client need or operational challenge, involves a careful and in-depth review of market conditions, and existing products, to gain a clear understanding of the problem. Then the framework for the problem statement can be developed. Using the problem statement, ideas are developed that may fully or partially satisfy the problem. At CPP, stage one is highly iterative to ensure the problems, concepts and solutions are well understood. During these iterations, the company uses both its engineering and operations group, which brings numerous and diverse perspectives, experience, and knowledge to the product realization process. As an outcome and deliverable of this initial stage, the conceptual framework and product attributes are developed.

The second stage in the product realization process involves extensive research. This research focuses on competitive products which are emerging or available in the market. This involves researching patents, competitive products and other methods or techniques which may provide solutions to the problem identified or similar problem. Most of the work in this second stage is completed by the company's engineering and design team. This stage results in conceptual product methods or solutions or a report on current products that address the need. If a product exists, additional evaluation is completed to determine whether CPP should develop or purchase products.

The third and final stage of the product realization process for the company involves the evaluation of conceptual solutions developed in stage two. This stage includes estimating the impacts and magnitude of the product as a solution and evaluates the resources required to meet the project delivery. Following the process above, the cable-driven dredge product was realized which initiated the project planning and development.

**Project Planning & Development**

This cable-driven dredge plan focused on ten standard knowledge areas: integration; scope; schedule; cost; quality; procurement; resources; communication; risk and stakeholder management. Project scope was explored in the early stages of development. Because dredger systems are designed in a variety of configuration, and sizes, and are often unique to specific applications, it was important to define and manage the project scope throughout product development.

Once a strong scope statement was developed, we created the project work structure, along with the project schedule and milestones. A risk registry was generated that identified the major and minor risks associated with the work, as well as strategies to mitigate each. One of the main risks in any new product development, and identified for the cable-driven dredge project, was a competitor developing a similar product to market first. To mitigate this risk, we applied a two-prong approach. First, we applied for a patent, which provided some protection from the competitor, who was operating in the region protected by the patent. Second, we devised a strategy of concurrent design and development, to bring the product to market faster. This strategic approach included concurrent work in the areas of design, simulation, prototyping, and testing of the cable-driven dredge from the start of the project to the introduction to market.

The process of product realization and the subsequent product development required alignment and significant company resources [190]. To reduce the resource loading, in the early stages of product design, the Company utilized its operational team to test products at client-based service applications. Cross-functional integration also relieved a significant portion of the financial burden and provided direct operator feedback, which aided in the development of a robust and practical product solution. The field-test of prototypes also reduced the number of validation cycles involved in prototyping, testing, modifying, a new prototype before narrowing down a product design [191].

However, if not carefully managed, speed-to-market has disadvantages. One of the risks of this approach is prototype or testing failure in the field, which may negatively impact the relationship with the client. Moreover, field operators may misreport failure modes of the prototype based on a lack of understanding and knowledge or because of environmental conditions unrelated to the prototype. Understanding these risks, the company utilized a combination of experienced operators, along with a designated engineering team to test the prototype in the field. In addition, adequate spare equipment was provided in case the prototype failed.

**Project Objectives & Project Structure**

At the onset of the cable-driven dredge project, major system requirements were to develop a shore-based positioning system which used a network of winch cables to position and move a dredge head throughout an application area.

**System Control, Communication and Power Distribution**

a. System control will be remote from the workspace.
b. System control will be capable of executing patterns, pre-sets, and circuits without continuous operator input.
c. The positioning system will include a network of electrical cables which run to one or multiple power distribution centres.
d. System controls will be capable of connecting to an external network and report system progress on a scheduled basis. This network will allow access to monitor and adjust system parameters.
e. The system controller will measure production and adjust parameters to maintain a target production rate.

**System Hardware**

a. The dredge system hardware will consist of inter-connected components to form one product.
b. The main system components will be interchangeable with spare or alternate components allowing for efficient changes to the system when required.
c. The hardware system components will be deployed and removed from an application without the use of cranes.

## Project Structure

Product development structure progressed through four development phases.

## Phase 1: Prototype Development and Simulation

In phase 1 we developed a working prototype of the positioning system. Once a positioning system prototype was developed, it was coupled with a dredge head and tested. Most of the dredge testing was completed in the field. This field testing provided input on the practical challenges associated with the working environment.

## Software Development - Prototype

For the initial software prototype simulations, an idealized force control system was developed. A systematic approach was taken to understand the basic system control, this was done through simulations using a constant force representing the dredge head weight and associated dynamic forces. Several simulations were trialed using this basic simulation. The constant dredge head force was gradually increased with each simulation to understand the system's behavior within the workspace. These simulations also provided insight into the initial path planning in two dimensions. One of the initial simulations is shown in Figure D1.2.

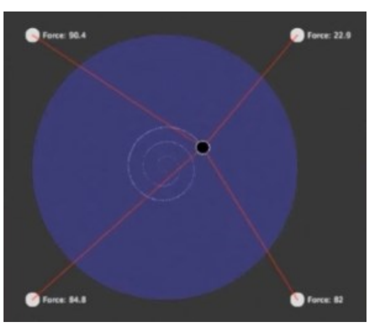


Figure D1.2: Software Testing

## Prototype Hardware Development

Hardware selection for the initial product development was based on criteria of scalability, communication, modularity, and connectivity of the dredge components. Initially, the forces required to move the dredge head through a sediment bed were not well understood. As a baseline, a prototype dredge head, shown in Figure D1.3, was pulled through a bed of material with a controlled pull force. Using the results of this trial, the initial positing winch hardware was selected.

Figure D1.3: Example Dredge Head

**Software & Hardware Integration**

After the initial control system was developed, and the hardware selected, the software and hardware system were integrated with a communications network. We used a single winch and controller for the initial testing of this communication network. After the commands and controls were verified using the single controller, the three additional winch systems were added to the cable-driven dredge system.

**Positioning System Prototype Testing – Land Based**

The initial software protypes focused on dynamic force control, however, the control approach was adjusted to a kinematic position control after initial land-based trials. This strategic decision change for system control happened because the team did not fully understand the associated forces that influence the system dynamics. Moreover, it was thought that this approach would be more efficient in producing the initial product and it would provide sufficient control for an initial working prototype. Using the prototype for testing, along with sensors, a dynamic controller may be developed later. The following section describes the prototype testing using a kinematic control method.

Two of the four winches were spaced in line with one another, on a flat plane. Each of the two winches were unspooled and connected at a centre connection point. This initial testing did not incorporate a load at the connection point. Position testing began by spooling-in one winch line while the other unspooled at an equivalent frequency. The results were positive; the controller was able to move the centre point back and forth between the winch systems with little error.

Based on the positive initial testing, a third winch system was connected to the central point. However, after multiple trials, it was observed that positioning error propagated as the system moved throughout the control space. Further observation and investigation into the error indicated that the rope stretch, and inconsistent winch cables spooling were contributing factors. To correct for this error, a global positioning system (GPS) was introduced at the centralized connection point between the three winches. The introduction of the GPS provided a feedback mechanism to locate the position of the dredge head. In addition to the introduction of the GPS, the winch hardware was modified with fairleads, which improved the consistency and reliability of cable spooling. The GPS, and modifications to the hardware resulted in adequate control of the three-winch system. During this phase, several software adjustments were required to incorporate the global positioning feedback information. With gradual prototype testing, and software adjustments, an initial control solution was developed for the three-winch system.

Once the control system for the three-winch system provided suitable control, a fourth winch was added. To test and validate the four-winch positioning system, the winches were set up in a square configuration. Each of the winch ropes were once again connected at the centralized connection point with a GPS module. Initial positioning of the end effector showed promising results. However, as dynamic movement and patterns were examined, the testing resulted in winch rope slack and controllability issues. As a result of this cable slack, each of the spooling winches had to first spool in slack line before the dredge head could move. This effected the smooth motion of the control point which had many frequent starts and stops as a result.

The positioning error was handled through a passive control method.[9] This method released the brake for any position winches that had no positive contribution to the end effector's forward motion. This allowed the spooling winch systems to apply tension to the dredge head and maintain tensions in the free spooling winches. This passive control improved the overall system motion while keeping tension in each of the connected winches. Once adequate software and hardware adjustments were developed with satisfactory control, the dredge head was added to the positioning system.

**Complete Water-Based System Prototype Testing**

Once land-based testing provided sufficient control, a dredge head and discharge pipe was added to the system for aquatic testing. The complete prototype (four positioning winches, dredge head and discharge pipe) was deployed in a square configuration around a test bed. We found that the dredge environment introduced forces not observed during land trials. These additional forces resulted in rope stretch which affected control beyond an acceptable threshold. To improve control, data from the GPS was reported to the controller at a higher rate. This

[9] One of the methods considered to improve the tension in the network of cables was to add springs to each of the control winches so that excess slack in the system could be managed. However, this concept was not pursued as it was predicted to result in other practical challenges once applied in working dredge applications.

adjustment resulted in moderate control improvements, but negatively impacted the continuous motion of the system.

During the aquatic testing, it was also observed that a large catenary would form between the winch position and dredge head. The catenary negatively affected the system in two ways. First, it resulted in a positioning error, as each winch had to spool-in excess rope before the dredge head moved in the intended direction. Second, the catenary resulted in rope being dragged on the pond floor which increased wear on the ropes and left them prone to snagging on application debris. To deal with these concerns, the wire ropes were changed out to synthetic rope, which had a major impact on the system's control. The synthetic rope was buoyant and so their mass was supported over the span between winches and dredge head. This removed most of the error associated with the catenary. Because the synthetic rope had less stretch than the previously tested wire rope, it also positively affected the system's control.

The second major challenge in prototype testing was the system's control at the boundary conditions. As the dredge attempted to move towards the perimeter formed by the position winches, the angle of approach made it difficult for the dredge head to move. Several software logic modifications to the dredge head path and angle of approach to the boundary were developed to better handle the control at the system boundary conditions. After several iterations of software adjustments and testing, the system's controllability at the specified boundaries was acceptable. Figures D1.4 through D1.13 show test dredge application setup and discharge.

Figure D1.4: Overview of Test Dredge and Application

Figure D1.5: Gantry with Discharge Pipe

Figure D1.6: Positioning Winch

Figure D1.7: Dredge Head Gantry

Figure D1.8: Fairlead Snatch Block

Figure D1.9: Overview of Test Dredge and Application

Figure D1.10: Application Settled Slurry

Figure D1.11: Discharge Area

Figure D1.12: Pumping Water

Figure D1.13: Pumping Slurry

**Phase 2: Scaling the Prototype, Industrial Model**

As a prototype was tested which provided adequate control in the test pond, a scaled-up version of the dredge system was rapidly developed for testing in commercial applications.

**Phase 2: Commercial Model Testing & Application with Operator Supervision**

Although the prototype testing of the cable-driven dredge system had positive results, it was expected that industrial applications would introduce new practical system challenges. To handle the unknowns during commercial testing, we planned to have the cable-driven dredge system under continuous supervision during each of the pilot tests. The first pilot project took place at one of the wastewater ponds in the Alberta Oilsands. The area was approximately 150 meters in length by 100 meters in width, with a pond depth ranging from 3 to 5 meters. The application consisted of settled material with specific gravity between 1 and 1.07. The pilot test setup is illustrated in Figure D1.14. The main goal of the pilot project was to identify system challenges for the cable-driven dredge in a commercial application, including cold weather conditions. Observations from the pilot testing were applied in the system design.

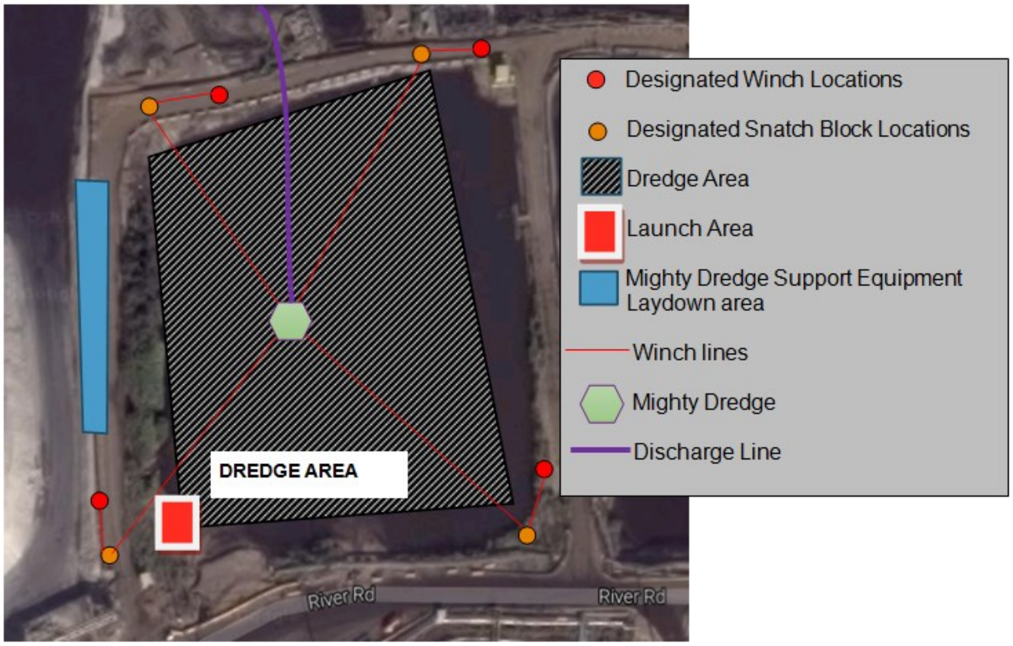


Figure D1.14: Dredge Pilot, Test Bed Overview

The pump used in the initial pilot was a Mighty Pump, model MPR8220. The MPR8220 is a 31 hp electric slurry pump, fitted with an agitator. The MPR8220 slurry pump is designed to pick up settled pond material; it is not designed to dig or change the pond bottom profile beneath the loose slurry material. The pump was installed approximately four inches above the bottom of the dredge cage. This setup allowed the system to remove loose material while preventing the dredge head from digging into or significantly altering the clay bottom. The prototype dredge head used is shown in Figure D1.15. To measure the system's overall production, pre-work and post-work hydrographic surveys were completed to estimate the volume of sediment removed from the wastewater pond. To study the instantaneous production, a nuclear density meter and flow meter were installed on the dredge system discharge line.

Figure D1.15: Dredge Head with Pump and Agitator

As anticipated, new challenges arose during the test application: the effects of cold weather on the system; foreign debris in the application; and pockets of slurry with high viscosity.

**Cold Weather**

One of the main challenges was ice build-up on the system components, especially the network of winch cables. As each of the positioning winch ropes entered and exited the application, a layer of ice formed along the wetted rope surface area. The weight of this ice resulted in a catenary effect like the one previously observed. The rope with ice buildup sagged, which affected the system's continuous movement. During the pilot project, personnel manually cleared ice that built up on system components.

**Pond Debris**

Foreign pond debris was caught on the dredge head electrical umbilical, causing cable damage. The electrical cord umbilical was initially fastened to the top of the discharge pipe out of the water. As the system repositioned the dredge head through the application, the electrical cable spun to the bottom of the pipe because of its weight. As the discharge pipe moved past the debris the electrical cable caught on the debris and broke the securing straps. Figures D1.16 and D1.17, highlights the foreign debris encountered during the pilot project.

Figure D1.16: Foreign Debris 1, System Trial #1

Figure D1.17: Foreign Debris 2, System Trial #1

**High Viscosity Slurry**

During the pilot project, we observed several occurrences of what was thought to be highly viscous slurry pockets. These pockets of slurry blocked the dredge and reduced or stopped flow, affecting the hydraulics and output production of the system. An image of the discharge during the pilot project is shown in Figure D1.18.

Figure D1.18: Discharge, System Trial #1

Daily production results from the nuclear density meter and flow meter during the pilot project were tabulated and shown in Table D1.1.

Table D1.1: Average Daily Production, Pilot Project

| Date | Run (Hrs) | $SG_{SL}$, Avg | $SG_{SL}$, Max | Flow, Avg (US gpm) | Slurry Density, Avg ($kg/m^3$) | Est. Solids Removed (kg) |
|---|---|---|---|---|---|---|
| 05-Nov-16 | 9 | - | - | 1130 | - | - |
| 06-Nov-16 | 8 | 1.07 | 1.18 | 1150 | 1070 | 62,603 |
| 07-Nov-16 | 10 | 1.00 | 1.052 | 1100 | 1000 | 42,472 |
| 08-Nov-16 | 24 | 1.022 | 1.062 | 960 | 1022 | 272,752 |

| | | | | | | |
|---|---|---|---|---|---|---|
| 09-Nov-16 | 23 | 1.074 | 1.12 | 970 | 1074 | 266,664 |
| 10-Nov-16 | 24 | 1.067 | 1.103 | 950 | 1067 | 248,643 |
| 11-Nov-16 | 23.5 | 1.077 | 1.18 | 970 | 1077 | 200,734 |
| 12-Nov-16 | 22 | 1.074 | 1.161 | 940 | 1074 | 216,914 |
| 13-Nov-16 | 22 | 1.05 | 1.074 | 990 | 1050 | 247,759 |
| 14-Nov-16 | 12 | 1.065 | 1.103 | 950 | 1078 | 113,517 |
| 18-Nov-16 | 8 | 1.02 | 1.351 | 711 | - | - |
| 19-Nov-16 | 24 | 1.03 | 1.30 | 705 | - | - |
| 20-Nov-16 | 24 | 1.03 | 1.15 | 712 | - | - |

Overall, the dredge technology performed effectively during the pilot project. We learned several lessons to improve the final product design and process. These are briefly summarized below.

Lesson #1 An initial application survey was completed by a third party that did not identify foreign objects in the pond that could interfere with dredge operations. In future projects, a pre-dredge pond survey is recommended to identify foreign objects in the application that could interfere with the system's control.

Lesson #2 The electrical cable from the dredge head along the discharge pipe needs to be better secured. The securement straps need to withstand commercial service applications and potential obstacles and to mitigate resulting slack in the cable. Improving the strength and protection of the electrical cable will improve the system's reliability.

Lesson #3 Although the dredge head performance was acceptable, a more robust dredge pump is recommended for future applications. The dredge head must be suitable for commercial applications with highly abrasive solids and changing slurry viscosities. We also recommended that the dredge head cage be redesigned so that it can break up a layer of material in the dredge path.

**Phase 3: Commercial Product Testing with Client Supervision**

As part of the next phase in product development, the cable-driven dredge was tested in a commercial application supervised by a client rather than CPP personnel. In addition to operators supplied by the client, the company provided personnel responsible for mobilization, setting up and training of the client with the new technology. The main goal of this phase was to collect feedback based on the client's supervision experience. The test site was a closed harbour, ocean application, illustrated in Figure D1.19.

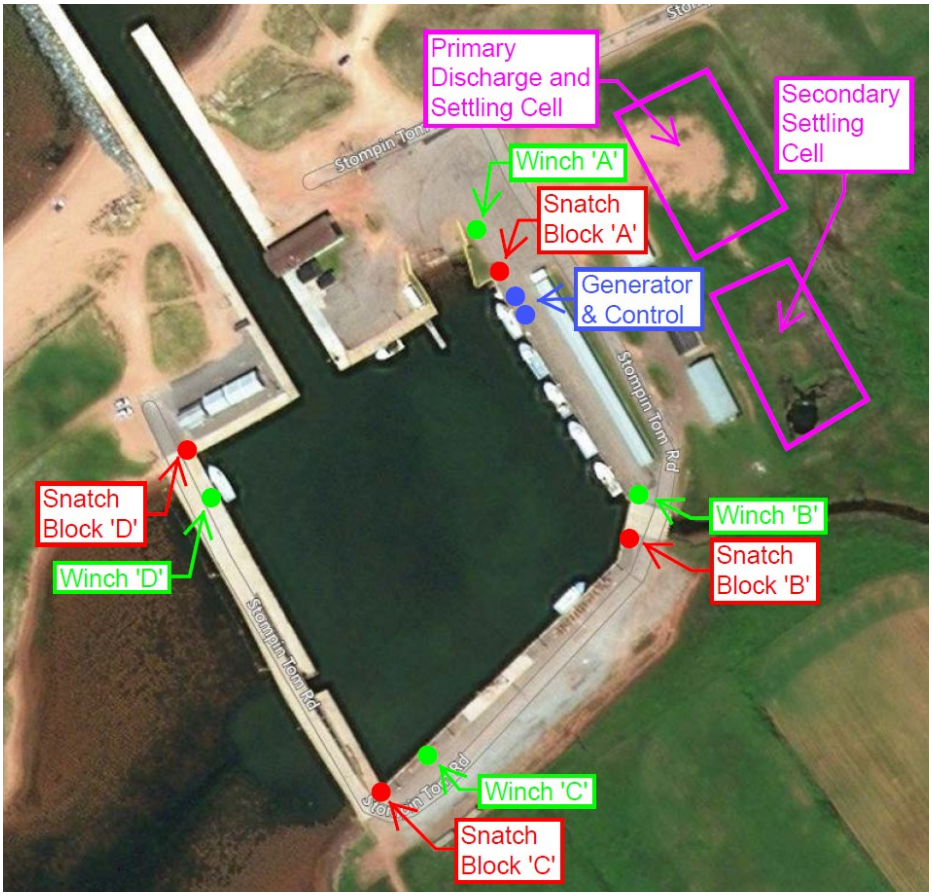


Figure D1.19: Closed Harbour, Test Trial #2

As part of the monitoring program, several dredge production measurements were recorded: production rates; power draw; application water quality during dredging; system performance; downtime; water and fuel usage. The data was collected using a combination of sensors and physical measurements. During the second pilot, the cable-driven dredge system operated continuously in a variety of environmental conditions including sun, moderate winds, rain, and sub-zero temperatures, with no effect on the system's operation. Various operational interruptions occurred, ranging from minor, easily cleared, pipe clogs to more severe blockages that required system shutdown for several hours.

Figure D1.20: Foreign Debris, System Trial #2

Clogging of the dredge system dredge head were observed throughout the test period as shown in Figure D1.20. The first and second passes through the new operating area caused the most frequent clogs which were mainly due to foreign debris entering the dredge head.

While moving clear water, the nominal pump load ranged between 28 to 37 amps with a weighted average of 32.9 amps. When the system was sampled and observed to be pumping slurry, the pump loads ranged between 28 to 50 amps with an increased average load of 33.2 amps corresponding to a load increase of less than 1%. However, slurry sample measurements and flow rates indicated that the slurry was 3.1% more dense than clear harbour water. It is predicted that the density increase resulted in more dredge pump amperage draw. However, the resulting friction in the discharge pipe resulted in reduced system flow. This balanced to a negligible increase in amperage draw. The amperage draw shows indications of clogging in advance of the event through a gradual or sharp decrease in pump loading. Most clog events were cleared by stopping the dredge system and dredge pump for 30 to 180 seconds, which allowed the existing discharge column in the pipe to backflush through the dredge head. On four occasions, clog events were not cleared by stopping and backflushing and the pump. To clear the debris, the dredge head was lifted out of the water and set onshore to manually remove the blockages.[10]

The dredge system effectively operated in all weather conditions during the test period and was only negatively affected by high winds. Sustained winds of more than 50 km/h caused several operational issues, and in severe cases, required the cessation of automated movement entirely. High winds applied a tension force to the discharge piping. As shown in Figure D1.21, high winds resulted in drifting of the discharge pipe and an applied force on the dredge head, affecting the system's movement.

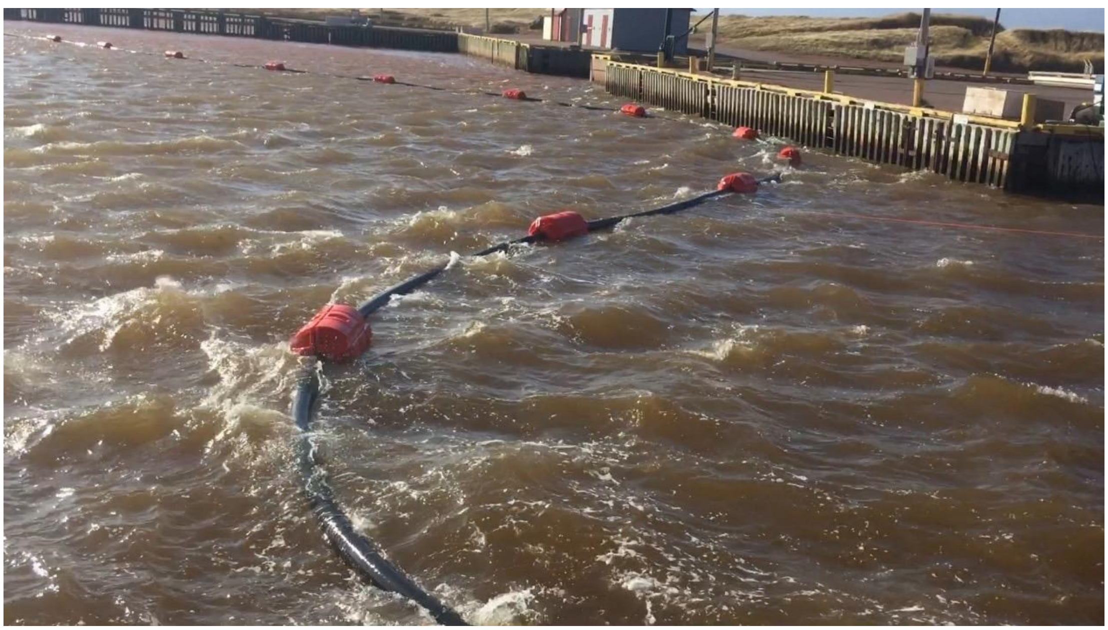

Figure D1.21: High Winds, System Trial #2

The system operated for 12 consecutive days, 24 hours per day. The dredge removed sediment from the shallowest areas of the harbour before moving to deeper areas. Based on pre-work and post-work hydrographic surveys, the system increased the harbour depth by up to 0.8

[10] Two instances were debris lodged in the dredge head pump: one instance being a clump of netting while the other a section of tree root 60 millimetres in diameter and approximately 1 metre in length. The other two blockages consisted of wood and netting lodged in the flexible connection between the pump and discharge pipe.

metres in some areas and removed a total estimated volume of 4,627.2 cubic metres of material. The estimated discharge flow rate of the test dredge pump was 125 cubic metres per hour, based on pump curve data and estimated operating points. We recorded a maximum flow rate of 160 cubic metres per hour during clear water flow.

A flow meter instrument measured the actual flow rates. As the slurry density increased, the flow velocity at the discharge point visibly reduced, indicating a reduction of flow rate. The system logged 140.2 hours of production time, an average solids production rate of 33 cubic metres per hour, as shown in Table D1.2. The results shown in Table D1.2 were calculated using the surveyed production quantities. The production rate and percent solids by volume calculated based on field samples are 30 cubic meters per hour and 24%, respectively, with a difference of 9% relative to the production quantities derived from the survey quantities. This suggests agreement between two independently obtained production rates.

Table D1.2: Dredging Performance Summary

| Performance Metrics | Quantity | Units |
|---|---:|---|
| Dredged Volume | 4627 | $m^3$ |
| Production Time | 140.2 | h |
| Total Run Time | 201.3 | h |
| Solids Production Rate | 33.0 | $m^3/h$ |
| Slurry Flow Rate | 125 | $m^3/h$ |
| % Solids v/v | 26.4 | % |
| Water Usage (Water per Solids) | 2.8 | $m^3/m^3$ |
| Fuel Economy (Diesel per Solids)* | 0.30 | litre/$m^3$ |
| Energy Economy* | 3.2 | kWh/$m^3$ |

* Fuel and Energy economy are calculated based on active Production Time only. Average Fuel and Energy economy for the Total Run Time of the test period are 0.49 litre/m$^3$ and 5.2 kWh/m$^3$, respectively.

Slurry samples were taken from the discharge pipe sample port and weighed on site or bottled for further analysis. There was a discrepancy between the density of the samples weighed on site and those taken for analysis. The slurry density of the samples weighed at site was approximately 1027 kg/m3 versus the bottled samples that measured 1006 kg/m3, with a corresponding slurry % by volume of 24% and 7.5%, respectively. The slurry flowed at an estimated 2.0 m/s; at this flow rate some dense particles may have settled to the bottom of the discharge pipe and form a stratified flow. The sample port was positioned at the side (three o'clock position) of the pipe, as shown in Figure D1.22. The location of the sample port may have allowed the heavier settled solids to pass the port without sufficient capture.

Figure D1.22: Sample Port, System Trial #2

Several potential improvements were noted during the test period, which can be grouped into two categories, are summarized below.

**Production Improvements**

For this project, the pump took in material from the dredging surface through a 100-millimetre diameter full port opening located at the bottom of the pump. The pump is designed to pass solids up to a 100mm sphere. However, debris such as sticks, netting, rope, and fibrous plants can buildup and restrict flow through the pump or cause a sudden blockage.

Grating could prevent large objects from entering the pump. This would prevent large debris, rocks, or blocks of wood from entering the pump, but would be less effective for preventing long slender objects such as sticks, rope, or netting that can fit through the grate openings. A small grating area would likely become clogged with fibrous weeds, grasses, netting, and cordage and reduce the effectiveness of backflushes. Focusing on improvements to the handling of sludge and fibrous weeds would save more downtime than would a focus on protecting against large objects.

Fluidized, or suspended, solids are readily ingested by the dredge pump. However, viscous sludges or mixtures may clog the pump intake and discharge piping. At the test site, the dredge cage sank into the soft harbour bottom and produced a wave of viscous sludge at least 0.8 metres high as it moved, as evidenced by sludge deposits on the pump and cage. We think the sludge, composed of decaying organic materials, fibrous seaweed, sediment, and sand, engulfed the pump intake to such a depth that clear seawater could not reach the pump inlet, resulting in thick slurry and reduced flow rates. The installation of a jetting agitator located near the pump inlet would provide agitation to help break up clumps of material for easier pumping.

Figure D1.23: Snatch Block, System Trial


Figure D1.24: Winch Setup, System Trial

**Positioning System Improvements**

The major mechanical components of the positioning system are the four winch and snatch block sets, shown in Figures D1.23 and D1.24, which pull the dredge pump on a defined path within the dredging area. A winch and snatch block set must remain in close alignment during operation so that the winch rope is properly spooled onto the winch drum. To hold the winch in position, the base skids of the winches are typically chained to concrete ballast blocks.

Removable ballast cradles pinned or bolted to the winch skids would provide a stable and scalable ballast system that would provide increased stability to the winch, while still retaining the compact size of the existing skid and remove the requirement for chains and load binders.

**Conclusion**

The lessons learned from the initial project stages to the final pilot project have been used to improve the overall cable-driven dredge system and to better understand the system control. Since the completion of the final pilot with client-based supervision, the cable-driven dredge system has been used in multiple commercial application. During each of these projects, the system controllability and production continue to be monitored and improved.

---

[1] Mechanical dredges use a single mechanical bucket or a series of buckets or teeth to excavate soil from the dredge area. As material is excavated, the dredgeate produced is hydraulically transported, or shipped via trucks or barges.

[2] Ocean dredgers must store slurry in the ship's storage hopper. Once in the hopper, the dredge spoils settle, and clean water can be extracted and returned to the ocean, which maximizes the system's capacity. Once the dredge hopper reaches capacity, the solids are transported by the ship to a deposit site or offloading area.

[3] The dredge pump VFD is not submersible. Therefore, it is housed within the dredge system's main control station located at shore.

[4] However, existing literature does model a variety of other dredge technologies and systems. The CLAMSHELL program uses field experience, mathematical modeling, and physics research in a systematic approach to the development of simulation models [13].

[5] Only velocity is shown in each of the control diagrams.

[6] Only the velocity input is shown as the adjustment and control of the dredge head velocity is the main control goal. However, it should be noted that position, velocity, and acceleration are all inputs.

[7] Velocity is shown because this is the primary focus of the pump.

[8] This is different from the winch motor controllers, which are connected to the motors.

[9] Fast moving currents do exist in small and large bodies of water due to various factors such as wind, temperature, and hydraulic gradients. One of the external factors influencing the drag and lift force is the relative velocity of the surrounding water, or the application current. For the purposes of this model, however, it is assumed that the body of water is calm, and the current is negligible.

[10] Correction factors for the above conditions have been provided by Wilson et. al. However, these corrections were not used in this model verification.

[11] The rate at which the solids are excavated may be influenced by a form of agitation. However, agitation methods on production are not considered in this work.

[12] The fleet angle is the angle formed by the unspooled winch rope and centreline of the winch drum, as shown in Figure 4.17.

[13] This model neglects the effects of the catenary since the system uses a synthetic rope with a specific gravity similar to that of water.

[14] Initially, a central serial hub was to be used for collecting the data of all the sensors. However, when attempting to establish communication with the flow sensor, significant signal loss was observed due to cable length and the positioning of the serial hub would not be feasible.

[15] 120mm depth trials were not performed for the set of 50Hz pump speed, so these results are excluded from the comparison.

[16] The ANSI Hydraulic Institute uses four factors to adjust the head and efficiency of a centrifugal pump. These four factors include solid particle size, solid specific gravity, solid concentration in slurry, and the ratio of particle size divided by the impeller diameter.

[17] One of the methods considered to improve the tension in the network of cables was to add springs to each of the control winches so that excess slack in the system could be managed. However, this concept was not pursued as it was predicted to result in other practical challenges once applied in working dredge applications.

[18] Two instances were debris lodged in the dredge head pump, one instance being a clump of netting while the other a section of tree root 60 millimetres in diameter, and approximately 1 metre in length. The other two blockages consisted of wood and netting lodged in the flexible connection between the pump and discharge pipe.

[19] The various styles and shapes of concrete blocks can present a challenge to secure the concrete blocks to the winch skid and can result in poor geometry of the anchoring chains, often reducing the effectiveness of the ballast or allowing the winch skid to pitch or rotate under high loads.